University of Szeged

Faculty of Pharmacy

Institute of Pharmaceutical Technology and Regulatory Affairs

Head: *Prof. Dr. habil. Ildikó Csóka Ph.D.*

PhD Thesis

DEVELOPMENT OF LIPID- AND POLYMER-BASED NANOCARRIERS FOR INTRANASAL APPLICATION

By

Hussein Akel

Supervisor:

Prof. Dr. habil. Csóka Ildikó Ph.D.

SZEGED
2022

PUBLICATIONS RELATED TO THE SUBJECT OF THE THESIS:

1. Akel, H., Csóka, I., Ambrus, R., Bocsik, A., Gróf, I., Mészáros, M., Szecskó, A., Kozma, G., Veszelka, S., Deli, M.A., Kónya, Z., Katona, G. In Vitro Comparative Study of Solid Lipid and PLGA Nanoparticles Designed to Facilitate Nose-to-Brain Delivery of Insulin. International Journal of Molecular Sciences, 22, 13258 (2021). doi:10.3390/ijms222413258
   IF:5.924 (D1 Journal)
2. Akel, H., Ismail, R., Katona, G., Sabir, F., Ambrus, R., Csóka, I. A comparison study of lipid and polymeric nanoparticles in the nasal delivery of meloxicam: Formulation, characterization, and in vitro evaluation. International Journal of Pharmaceutics, 604, 120724 (2021). doi: 10.1016/j.ijpharm.2021.120724.
   IF:5.875 (D1 Journal)
3. Akel, H., Ismail, R., Csóka, I. Progress and perspectives of brain-targeting lipid-based nanosystems via the nasal route in Alzheimer's disease. European Journal of Pharmaceutics Biopharmaceutics 148, 38-53 (2021). doi: 10.1016/j.ejpb.2019.12.014.
   IF:5.571 (Q1 Journal)

PRESENTATIONS RELATED TO THE THESIS

1. Hussein Akel, Ildikó Csóka. Nanocarrier based systems for nose to brain delivery of antineurodegenerative medicines. 2019. I Symposium of Young Researchers on Pharmaceutical Technology, Biotechnology and Regulatory Science. doi: 10.14232/syrptbrs.2019.op6

2. Hussein Akel, Ildikó Csóka. Lipid based nanosystem designed for nose to brain delivery of Alzheimer disease drug. 2020. II Symposium of Young Researchers on Pharmaceutical Technology, Biotechnology and Regulatory Science. doi: 10.14232/syrptbrs. 2020.op22

3. Hussein Akel, Ildikó Csóka. Formulation and In Vitro Comparison Study between Lipid-Based and Polymeric-Based Nanoparticles for Nose-to-Brain Delivery of a Model Drug for Alzheimer's Disease. 2021. The 1st International Electronic Conference on Pharmaceutics. doi: https://doi.org/10.3390/IECP2020-08680

4. Hussein Akel, Ruba Ismail, Gábor Katona, Ildikó Csóka. 2021. III Symposium of Young Researchers on Pharmaceutical Technology, Biotechnology and Regulatory Science. doi: 10.14232/syrptbrs.2021.op9

5. Hussein Akel, Gábor Katona, Ildikó Csóka In vitro quantitative comparison study of insulin SLNs and PLGA NPs as potential carriers for the brain delivery of intranasal insulin. 2022. IV Symposium of Young Researchers on Pharmaceutical Technology, Biotechnology and Regulatory Science. doi: https://doi.org/10.14232/syrptbrs.2022.24

ABBREVIATIONS

CNS	central nervous system	**MEL**	meloxical
FRDA	Friedreich ataxia	**Ins**	Insulin
SMA	Spinal muscular atrophy	**COX-2**	cyclooxygenase-2
AD	Alzheimer's disease	**QbD**	Quality by Design
PD	Parkinson’s disease	**API**	active pharmaceutical ingredient
HD	Huntington’s disease	**NIRKO**	neuron-specific insulin receptor knockout
ALS	Amyotrophic lateral sclerosis	**CSF**	cerebrospinal fluid
LBD	Lewy body dementia.	**RA**	risk assessment
BBB	blood-brain barrier	**QTPP**	quality target product profile
SLNs	solid-lipid nanoparticles	**CPPs**	critical process parameters
PLGA	Poly lactic-co-glycolic acid	**CMAs**	critical material attributes
NPs	Nanoparticles	**CQAs**	critical quality attributes
C-NPs	chitosan coated nanoparticles	**SEM**	scanning electron microscopy
C-SLNs	chitosan coated SLNs	**FTIR**	Fourier transform infrared
C-PLGA NPs	chitosan coated PLGA NPs	**XRPD**	X-Ray Powder Diffraction
EMA	European Medicines Agency	**MBE**	mucin binding efficacy
FDA	U.S. Food and Drug Administration	**PDI**	poly dispercity index
NSAIDs	non-steroidal anti-inflammatory drugs	**ZP**	Zeta potential
APOE	ε4 apolipoprotein E	**EE**	encapsulation efficacy
DL	drug load	**HSA**	human serum albumin
IVIVC	in vitro in vivo correlation	**TEER**	transendothelial electrical resistance

LIST OF CONTENT

1. INTRODUCTION: 5

2. AIMS 6

3. LITERATURE BACKGROUND OF THE RESEARCH WORK 7

3.1. Neurodegenerative disorders and AD 7

3.2. Medical management of Alzheimer's disease 7

3.3. Why Meloxicam in AD? 8

3.4. Insulin as a cognitive enhancer 9

3.5. Nose to brain delivery 9

3.6. Nanoparticles to facilitate Nose to Brain delivery 10

3.7. Intranasal nanoscale therapeutics as an innovative brain-targeting strategy 11

3.8. Methods of preparation of SLNs and PLGA NPs 12

3.8.1. Emulsification solvent evaporation 13

3.8.2. Emulsification solvent diffusion 13

3.8.3. Emulsification reverse salting-out 14

3.8.4. Nanoprecipitation 15

3.9. Chitosan coating to improve nose to brain delivery 16

3.10. Quality by Design (QbD) approach 16

4. MATERIALS AND METHODS 17

4.1. Materials 17

4.1. Initial Risk Assessment (RA) as a part of QbD 17

4.2. Preparation of the nanoparticles (MEL SLNs, Ins SLNs, MEL PLGA NPs, and Ins PLGA NPs) 17

4.3. Chitosan coating of the SLNs and PLGA NPs 18

4.4. Characterization of NPs 19

4.4.1. Determination of mean particle diameter, polydispersity index and zeta potential 19

4.4.2. Determination of encapsulation efficacy (EE) and drug loading (DL) 19

4.4.3. Scanning Electron Microscopy (SEM) 21

4.4.4. Fourier-Transform Infrared Spectroscopy (FT-IR) 21

4.4.5. Raman Spectroscopy 21

4.4.6. X-ray Powder Diffraction (XRPD) 21

4.5. *In vitro* evaluation of the prepared nanosystems 21

4.5.1. *In vitro* drug release test 21
4.5.2. Mucoadhesion test 22
4.5.3. Permeability test 23
4.7. *In Vitro* Cell Line Studies 24
4.7.1. Human RPMI 2650 Nasal Epithelial Cell Culture 24
4.7.2. Human hCMEC/D3 Brain Endothelial Cell Line 24
4.7.3. Preparation of Insulin and Insulin-Loaded Nanoparticle Dilutions for Cellular Assays 25
4.7.4. Cell Viability Measurement 25
4.7.5. Permeability Studies 26
5. RESULTS AND DISCUSSION 27
5.1. Initial Risk Assessment (RA) as a part of QbD 27
5.2. Characterization of NPs 30
5.2.1. Mean particle diameter, size distribution, and zeta potential 30
5.2.2. Encapsulation efficiency and drug loading results 31
5.2.3. Scanning Electron Microscopy (SEM) 31
5.2.4. Fourier-Transform Infrared Spectroscopy (FT-IR) 32
5.2.5. X-ray Powder Diffraction (XRPD) 34
5.2.6. Raman spectroscopy 34
5.3 In vitro evaluation of the prepared nanosystems 35
5.3.1. Mucoadhesion test 35
5.3.2. *In vitro* drug release studies 37
5.3.3. *In vitro* Permeability test 39
5.4. *In vitro - in vivo* correlation (IVIVC) for Mel NPs 41
5.5. In Vitro Cell Line Studies for Ins NPs 42
5.5.1. Permeability Studies on Human RPMI 2650 Nasal Epithelial Cell Culture 42
5.5.2. Permeability Studies on Human hCMEC/D3 Brain Endothelial Cell Line 43
5.5.3. Cell Viability Measurement 44
6. CONCLUSIONS 47
7. Novelty and practical aspects 49
8. ACKNOWLEDGEMENTS 50
9. FINANCIAL SUPPORT 50
10. REFERENCES 51

INTRODUCTION:

Neurodegeneration is an umbrella term for a scope of disorders that primarily influence the neurons in the human central nervous system (CNS). It results in problems either with the movement, called ataxias, or with mental functioning called dementias. Dementias are considered the tremendous burden of neurodegenerative diseases, with Alzheimer's disease (AD) representing approximately 60-70% of the cases worldwide. All the available remedies for AD are of short-time efficacy accompanied by severe side effects. The intranasal route has emerged as an alternative pathway offering a non-invasive way for drug delivery to the CNS, enabling self-administration, good bioavailability, slow drug metabolism, and evading the first-pass metabolism. Nanotechnology is a revolutionary way of introducing the APIs intranasally for the brain delivery as they fulfill the requirements of bypassing the blood-brain barrier (BBB). Among the nanoparticles, Solid lipid nanoparticles (SLNs) and Poly lactic-co-glycolic acid (PLGA) are preferable for the N2B delivery of pharmaceutics as they are inert, non-toxic, submicron colloidal carriers with an ideal particle size range. Moreover, they control the drug release properties and are suitable for both the hydrophobic and hydrophilic APIs showing low toxicity and good biocompatibility& biodegradability. Since SLNs and PLGA NPs are sophisticated systems, relevant guidelines must be applied during all their manufacturing stages. Furthermore, the FDA has intensified the application of the Quality by Design (QbD) methodology, which can be remarkably useful for the novel, high-risk dosage forms, and administration routes for careful planning and development even at the early phase of the research.

This research was conducted to assess the potentiality of the above-mentioned two types of nanoparticles to ameliorate the brain delivery of meloxicam as a non-biological API and insulin as a biological one. The work adopted the QbD methodology to optimize the formulation materials and process parameters. Meloxicam was chosen because numerous epidemiological studies suggest that long-term use of non-steroidal anti-inflammatory drugs (NSAIDs) may protect subjects carrying one or more ε4 allele of the apolipoprotein E (APOE ε4) against the onset of AD. However, the high plasma protein binding and low apparent distribution volumes of MEL decrease its pharmacological effect. On the other hand, Insulin, as a biological molecule, showed an ameliorating effect of intranasal insulin in AD. It helps boosting memory performance as the brain insulin resistance tends to be pathophysiological factor in AD.

2. AIMS

The aim of this study was to develop two nanoformulations (SLNs and PLGA NPs) of meloxicam as a non-biological molecule and insulin as a biological one for the intranasal application and check their ability to directly deliver the encapsulated active pharmaceutical ingredient (API) to the brain. The research work was constructed according to the following steps:

- Screening the literature of the nose to brain delivery of pharmaceutics shows the high potential of SLNs and PLGA NPs to be the nanoparticles of choice for the direct delivery of pharmaceutical molecules to the brain following the intranasal application.
- The applicability of SLNs and PLGA NPs in a nasal formulation is considered a novel approach in pharmaceutical technology, thus, limited data for such systems are available up till the moment.
- QbD approach was employed to get the critical process and material parameters that impact the preparation of nanosuspensions ranked and prioritized.
- Four meloxicam/ insulin-containing nanoformulations were developed as freeze-dried formulations. Introducing nano encapsulated meloxicam/ insulin intranasally for the direct delivery to the brain via nanosystem-based formulations is a novel strategy that could ameliorate the brain bioavailability of both meloxicam and insulin with relatively high patient-acceptance. Then, the prioritized influential parameters were experimentally studied and optimized to finally get the nanosystems.

The main steps in the experiments were the following:

1. Implementation of the QbD approach for the research and development approach of the nanosystems as meloxicam/ insulin-containing preformulations as high potential choices to enhance the brain bioavailability.
2. Getting the optimized nanoformulations by performing the proper experiments.
3. Evaluation of the obtained nanosystems with regards to their physical, chemical, and characteristic properties.
4. Performing *in vitro* cell line studies, and *in vitro-in vivo* correlation studies of the nanoformulations.
5. -Assess the stability of the nanoparticles.

3. LITERATURE BACKGROUND OF THE RESEARCH WORK

3.1. Neurodegenerative disorders and AD

Neurodegenerative disorders are a heterogeneous group of disorders that are characterized by the progressive degeneration of the structure and function of the central nervous system or peripheral nervous system. They affect millions of people worldwide [1]. AD is the most prevalent neurodegenerative disorder worldwide. Although each individual is uniquely affected by AD, the disease is generally characterized by impairments of memory, cognition and behavior [2]. Memory loss certainly predominates and includes problems with recall of life events. Diagnosis is usually confirmed by assessments of behavior and cognition. As the disease progresses, confusion, irritability, aggression, mood swings and withdrawal become commonplace. The disease excludes individuals from maintaining normal life events and in the latter stages of disease often requires long-term care and institutionalization [3]. Pathologically, AD is characterized by loss of cortical, and to a lesser extent, subcortical neurons, and synapses [4-6]. There are two types of characteristic lesions: extracellular senile plaques and intracellular neurofibrillary tangles [7, 8]. Both are composed of abnormal aggregations of amyloid-β (Aβ). Tangles are composed of aggregates of hyperphosphorylated tau, a microtubule-associated protein [9, 10].

AD is highly prevalent and well characterized, with several potential therapeutic options, but regrettably, only few are currently available in the clinical practice. These include, but are not limited to, the clearance of aggregated Aβ, attenuation of neuroinflammatory activities, modulation of redox responses, and oxidative stress, halting the formulation of reactive oxygen species (ROS), cell-, tissue- and/or immune-based neurodegeneration, and/or protection and modulation of known biochemical responses [11-17]. Each of these would be improved substantively if drugs could be delivered specifically to affected brain areas. Direct applications could also improve diagnostics if plaques, tangles and/or neuropathological activities could be seen earlier in the disease course. Thus, in recent years there has been a significant effort researching the use of nanoformulations for diagnosing and treating AD [18].

3.2. Medical management of Alzheimer's disease

The increasingly progressive occurrence of AD worldwide generated great efforts to come up with new ways of managing this issue especially on the pharmaceutical field. Many investigations, research efforts, and clinical trials were conducted focusing on the discovery and development of

new medications that could enhance the life quality of the patients. Still, all the available therapies cannot completely cure the disease and are in a continuously developing situation on the way to get the optimal solution. Lately, the intranasal application attracted more attention in terms of brain-targeting therapeutics due to its potential to bypass the limitations facing the traditional oral medications available for AD. However, several drawbacks can lower the nose-to-brain delivery such as the poor drug permeability through the nasal mucosa, mucociliary clearance, enzymatic degradation, low drug retention time, and nasal mucosa toxicity [19]. **Table 1** presents the available choices of AD medication:

Table 1. The variety of potential therapies of AD

FDA approved medicines	Donepezil [20-23], Rivastigmine [24-26], Galantamine [27, 28], Memantine [29-31]
FDA non approved available supplements	Coconut oil [32-34], Coenzyme Q10 [35, 36], Ginkgo biloba [37-39], Huperzine A [40-42], Poly unsaturated fatty acids [43-45], Curcumin [46-48], Tramiprosate [49, 50]
Under-development medicines	Nilotinib [51-53], Insulin [54-64], GLP1 analogues [65-70], Monoclonal antibodiessuch as Aducanumab[71-74], Gantenerumab[75, 76], Serotonin Receptors Ligands: i.e. Intepirdine [77-79], BACE1 inhibitors: AZD3293[80, 81], Verubecestat [82, 83], Atabecestat [84, 85], EVP-0962[86], BMS-932481[87], Antiaggregation of Beta-Amyloid: Posiphen [88], ALZ-801 [89, 90], Tau Aggregation modulators: TPI-287 [91], Acetylcholine receptors ligands: Encenicline hydrochloride[92, 93],
Under-development medicines available on the market	Galantamine prodrug (Memogain®) [94-97]

3.3.Why Meloxicam in AD?

Oxidative stress is one of the affecting factors in AD, so, several antioxidants have been studied for the reduction of oxidative stress occurring during Alzheimer's disease [98]. Inflammation is a defense reaction against diverse insults, intended to remove damaging agents and to inhibit their detrimental effects [99]. Those agents were found to increase neuronal levels of cyclooxygenase 2 (COX-2) suggesting that the production of such inflammatory mediators can be triggered by the intracellular accumulation of abnormal proteins [100]. NSAIDs are the group of drugs which effectively interfere with the cyclooxygenase pathway, which is involved in generation of oxidative free radicals. Amongst the NSAIDs, MEL labors its pharmacological efficacy by inhibiting the enzymatic activity of cyclooxygenase-2 (COX-2) [101], which is linked with a neuroprotective action in Alzheimer’s disease [102-105]. However, the high rate of plasma protein binding and low apparent distribution volumes of MEL decrease its pharmacological effect [106].

Furthermore, MEL lipophilicity and its low water solubility [107] decrease its bioavailability following the conventional administration routes.

3.4. Insulin as a cognitive enhancer

Intranasal administration of insulin has been explored as a non-invasive method to decrease cognitive damage caused by brain insulin resistance [108-110]. Unlike peripheral administration, acute or chronic intranasal administration of insulin did not induce hypoglycemia and hyperinsulinemia in a mouse model of T2DM [111]. Importantly, intranasal administration of insulin improved long-term and short-term declarative memory in healthy patients [112]. Clinical trials have further pointed to cognitive improvement in amnestic patients with mild cognitive impairment (MCI) and Alzheimer's disease [113, 114]. Moreover, intranasal insulin was found to improve memory and significantly reduce AD-related tau-P181/Aβ42 ratio in the CSF of AD patients after two and four months of treatment. Additionally, the intranasally applied insulin was found to be safe and effective by improving the Aβ42/40 and Aβ42/tau ratios in the CSF of patients treated with intranasal insulin [115].

3.5. Nose to brain delivery

Nose to brain delivery of drugs have been experimented by several researchers around the globe to explore the merits of this route, such as circumvention of BBB, avoidance of hepatic first-pass metabolism, practicality, safety and convenience of administration, and non-invasive nature [116]. Although the precise mechanisms behind CNS targeting via intranasal administration is not entirely understood yet, many of the reported evidence demonstrates that integrated nerve pathways (olfactory and/or trigeminal nerve pathways) connecting nasal passages to brain and spinal cord, along with the pathways involving cerebrospinal fluid (CSF) and lymphatic systems, have been implicated in target-specific delivery of molecules from nasal cavity to the CNS [117].

A combination of these pathways is responsible, although one pathway may predominate. In the last few decades, major reports have emerged on the development of novel drug delivery systems to circumvent the BBB. This is due to the significant challenges faced the researchers, academicians and industrialists looking for effective treatment strategies for the increasing incidence of brain disorders in elderly population. There are still several challenges that remain, as most of the potent CNS acting drugs are hydrophilic in nature, which makes it difficult for them to cross the BBB. The below table (**Table. 2**) summarizes the advantages and disadvantages for the nose to brain delivery route:

Table 2 advantages and disadvantages for nose to brain delivery

Advantages
Safe, painless, and convenient method of drug delivery
Avoiding drug degradation in the gastrointestinal tract, particularly peptide drugs
Minimizing the first-pass effect and gut-wall metabolism, thus enhancing the brain bioavailability
Bypassing the BBB& ensuring CNS targeting and reducing systemic exposure of drugs
Better patient compliance as self-medication is possible with this route.
It is an alternative route for parenteral administration, especially for protein and peptide drugs
It shows excellent bioavailability for low molecular weight drugs
Mechanical loss of the dosage form could occur due to improper technique of administration
Disadvantages
Rapid elimination of drug substances from the nasal cavity due to mucociliary clearance
The small size of the human's olfactory region compared to that in rats 3–8% and 50%, respectively
Absorption enhancers used in these formulations may cause mucosal toxicity
The variability in the concentrations attainable in different regions of the brain and the spinal cord
High-molecular-weight drugs may result in decreased permeability across the nasal mucosa
Some therapeutic agents may cause irritation to the nasal mucosa or may be susceptible to enzymatic degradation and metabolism in the nasal milieu at mucosal surface
Frequent use of this route may cause mucosal damage like infection or anosmia
Nasal congestion due to the cold or allergy may interferes with this technique of drug delivery
Mechanisms of drug transport are still unclear

3.6. Nanoparticles to facilitate Nose to Brain delivery

Scanning the available literature shows that surface modification of drug carrier system would serve as one of the excellent approaches to circumvent this budding problem through enhanced direct nose to brain drug delivery. Nanoparticles have been classified as high-potential nose-to-brain carriers due to their notable improvement of drug delivery, since they are able to protect the encapsulated drug from biological as well as chemical degradation, and from extracellular transport by P-gp efflux proteins [118, 119]. One of the key considerations for their development as nasal dosage forms is the safety and toxicological assessment of the matrix [120]. Among colloidal carriers, polymeric and lipid nanoparticles are considered promising for nasal drug delivery, especially regarding their biocompatibility. They vary in diameter between 50 and 1000 nm. So far, when comparing the lipid nanoparticles to polymeric ones, they have been described as superior carriers as the following table (**Table 3**) shows:

Table 3. The advantages and disadvantages of the lipid and Polymeric nanoparticles.

	Lipid NPs	Polymeric NPs
Advantages	Production on a large industrial scale	Incorporation of hydrophilic and hydrophobic drugs
	Low toxicity due to their biocompatible and biodegradable components and absence of organic solvent(s) in their process	Tunable chemical and physical properties
	Incorporation of lipophilic and hydrophilic drugs	Use of biodegradable materials when desired
	Protecting drug from environmental conditions	Representing special properties when choosing the proper polymer
	Relatively low cost	Reproducible data when using synthetic polymers
	low toxicity Higher stability than lipid-based ones	Variety of the methods of preparation
	Good biocompatibility and biodegradability	Drug release in a controlled manner
	Relative high encapsulation efficiency and stability	Protecting drug from environmental conditions
	Simple and inexpensive manufacturing process	Increasing solubility of highly lipophilic drugs
	Enhanced penetration and permeation properties	
Disadvantages	Low drug-loading for SLNs	Insufficient toxicological assessment in the literature
	Poor stability& the risk of gelation for SLNs	Difficulty in their scale-up
	Drug expulsion during storage cause by lipid polymorphism for SLNs	Low drug-loading capacity
	Special requirements of storage	Not a good candidate carrier for hydrophilic drugs

Among the above mentioned two types of NPs, SLNs, which are made up of a solid lipid core matrix, and PLGA NPs, which consist of PLGA, a biocompatible and biodegradable polymer hold great promise for the nasal drug delivery directly to the brain due to their: (i) biocompatibility, (ii) biodegradability, (iii) enhancing penetration and permeation properties, (iv) modified drug release properties and (v) reduced drug toxicity [1, 121-125]. Moreover, their nanoscale size (up to 100 nm for lipid NPs and 220 nm for PLGA nanoparticles)[126], and further surface modification i.e., chitosan coating [127] are preferable for direct transport to the brain.

3.7. Intranasal nanoscale therapeutics as an innovative brain-targeting strategy

The use of nanoparticles as drug delivery systems allows controlled and site-specific delivery of therapeutic agents. Nanoparticles are able to protect the drug from biological or chemical degradation and help to evade drug-efflux mechanisms as P-glycoprotein transporter in the blood-

brain barrier, due to encapsulation of the drug [128]. To ensure the release of the content on the site of action, nanoparticles may be linked to specific targeting ligands [128, 129].

SLNs and PLGA NPs play a significant role in the efficient nose to brain delivery, and they demonstrate specific characteristics that placed them in the center of attention for this purpose namely: the non-toxic nature, biocompatibility, biodegradability, physical stability, cost-effective manufacturing process and scale-up, and finally the compatibility to link with small molecules, proteins, peptides, or nucleic acids. Furthermore, getting the drug molecules encapsulated into nanoparticles can improve their stability and reduce excipient-induced drug alterations to a minimum. Additionally, the controlled drug release profiles granted by the formulation of these nanosystems reduce the frequency of drug administration and improve patient compliance [128].

Amongst the various ways of tailoring nanoparticle uptake, three options are considered suitable for the nose to brain transport namely: a) enhancing the mucoadhesion behavior thus prolonging the interaction time of the nanoparticle with the nasal mucosa. This will intensify the chances of the drug molecules to permeate through the nasal epithelium and, finally, transported to the brain via either the olfactory or respiratory pathways, 2) the possibility of incorporating components that decrease the barrier function of tight junctions. These specialized particles would be able to transiently open tight junctions and thus, allow the drug to enter the nasal mucosa, 3) enhancing the chance of endocytosis of nanoparticles. Once endocytosed, the nanoparticles could release their drug content, which would be further delivered to the brain [130-133].

The use of nanoparticles for drug delivery brings along some benefits, such as a controlled and sustained drug release or by shielding the drug against environmental influences. This is in great importance when delivering proteins and peptides. Remarkably, particles can include ligands or molecular imprinting on their surface, which guide them to a targeted disease site [134, 135]. In conclusion, nanoparticles might thereby minimize the required dose of the drug, and as a result, provide lower toxicity and decreased adverse effects [130, 136]. The challenges are that nanoparticles should, on one hand, adhere to mucus to improve drug absorption but on the other hand, they should also penetrate mucus to avoid entrapping and clearance of the drug.

3.8. Methods of preparation of SLNs and PLGA NPs

A variety of preparation methods have been implemented successfully to prepare SLNs and PLGA NPs. Among them, there are four methods can be followed to get both the types of nanoparticles,

so the differences associated with the preparation technique are avoided. These methods include a) emulsification solvent evaporation; b) emulsification solvent diffusion; c) emulsification reverse salting-out, and d) nanoprecipitation.

3.8.1. Emulsification solvent evaporation

In case of this technique the lipid/polymer and the drug are first dissolved in a water-immiscible volatile solvent, then emulsified in an aqueous solution containing a stabilizer utilizing a high-energy shearing source, such as an ultrasonic device or homogenizer (**Figure 1**). The organic phase is evaporated under reduced pressure or vacuum, resulting in a fine aqueous dispersion of nanoparticles. The nanoparticles are collected by ultracentrifugation and washed with distilled water to remove stabilizer residues or any free drug, and then lyophilized for storage [137-139]. To entrap hydrophilic drugs, the double-emulsion technique is employed, which involves the addition of aqueous drug solution to organic polymer solution under vigorous stirring to form a water-in-oil emulsion. This water-in-oil emulsion is added into a second aqueous phase containing a stabilizer with stirring to form the water-in-oil in- water emulsion. The emulsion is then subjected to solvent removal by evaporation.

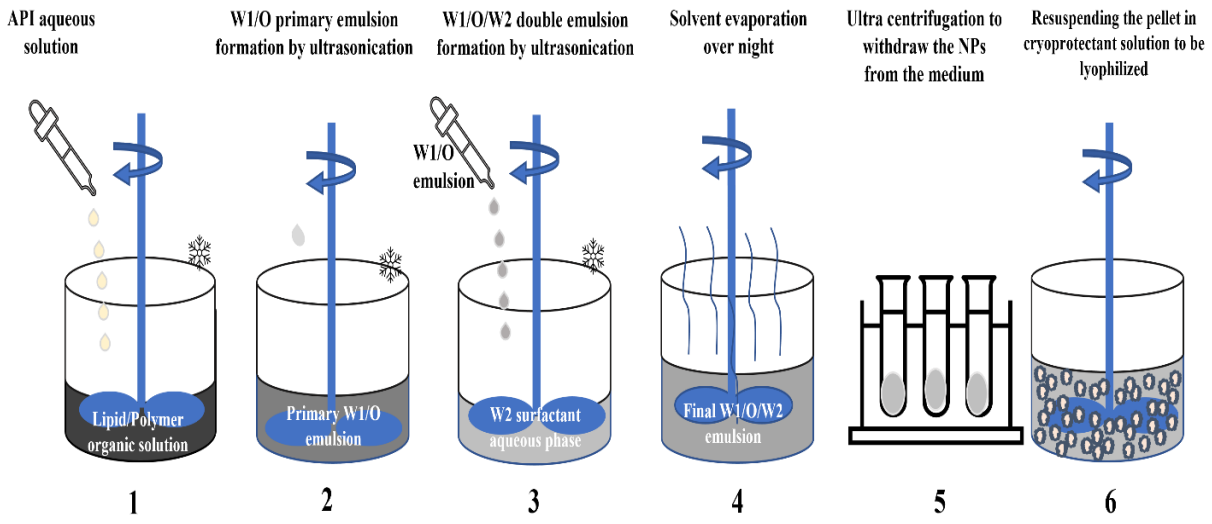

Figure 1. A diagram representing the sequential steps of the Emulsification solvent evaporation technique to prepare SLNs/PLGA NPs

3.8.2. Emulsification solvent diffusion

This method is also known as emulsification and solvent displacement. The solvent used to prepare the emulsion needs to be partly soluble in water [140]. The polymeric solution is added to an aqueous solution, containing stabilizer, under vigorous stirring [141]. Once the oil-in-water

emulsion is obtained, it is diluted with a large quantity of pure water (**Figure 2**). As a result of this dilution, additional organic solvent from the organic phase contained in the dispersed droplets can diffuse out of the droplets, leading to precipitation of the polymer. Suitable solvents include benzyl alcohol, propylene carbonate, ethyl acetate, isopropyl acetate, methyl acetate, methyl ethyl ketone, benzyl alcohol, butyl lactate, and isovaleric acid. This method has been used for PLGA nanoparticle preparation in many studies [142-145]. It should be noted that the solvent evaporation process is like this method, in the sense that the solvent must first diffuse out into the external aqueous dispersion medium before it can be removed from the system by evaporation [146].

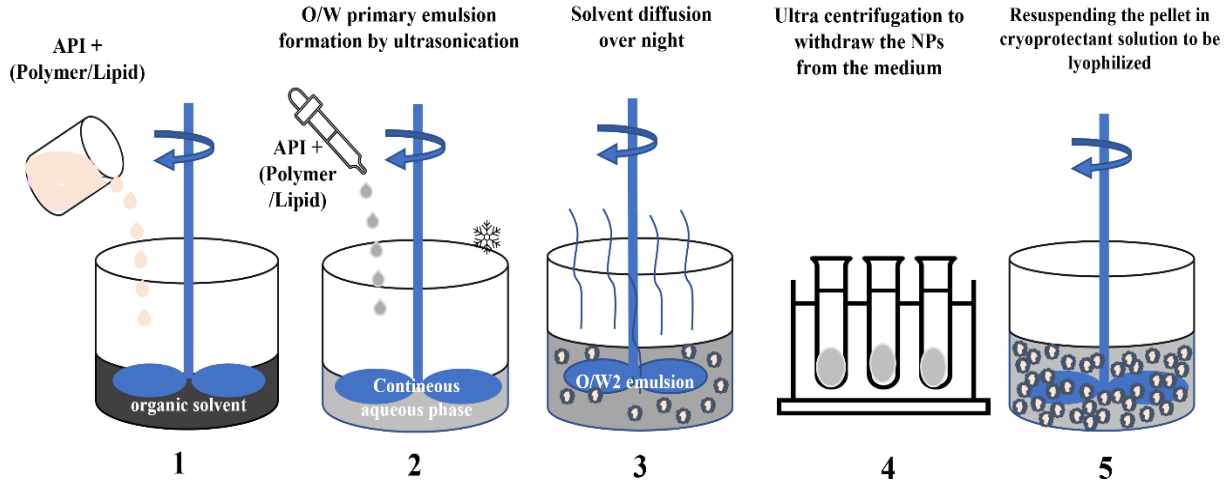

Figure 2. A diagram representing the sequential steps of the Emulsification solvent diffusion technique to get SLNs/PLGA NPs

3.8.3. Emulsification reverse salting-out

The emulsification reverse salting-out technique involves the addition of polymer and drug solution to a water-miscible solvent, such as acetone, and to an aqueous solution containing the salting-out agent, such as magnesium chloride, calcium chloride, and a colloidal stabilizer, such as polyvinyl pyrrolidone, under vigorous mechanical stirring (**Figure 3**). When this oil-in-water emulsion is diluted with a sufficient volume of water, it induces the formation of nanoparticles by enhancing the diffusion of acetone into the aqueous phase. The dilution produces a sudden decrease in the salt concentration in the continuous phase of the emulsion, inducing the polymer solvent to migrate out of the emulsion droplets. The- remaining solvent and salting-out agent are eliminated by cross-flow filtration [137, 147, 148]. Although the emulsification-diffusion method is a modification of the salting-out procedure, it has the advantage of avoiding the use of salts and thus eliminates the need for intensive purification steps [141]. Nanoprecipitation The

nanoprecipitation method is a one-step procedure, also known as the solvent displacement method [149]. It is usually employed to incorporate lipophilic drugs into the carriers based on the interfacial deposition of a polymer [150, 151].

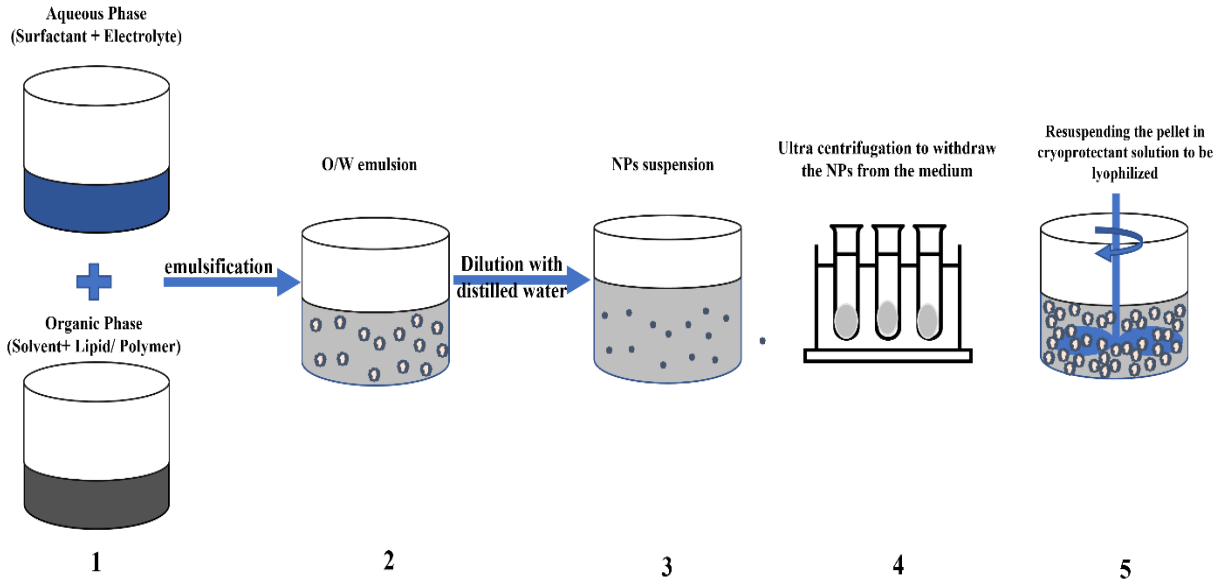

Figure 3. A diagram representing the sequential steps of the Emulsification reverse salting-out technique to obtain SLNs/PLGA NPs

3.8.4. Nanoprecipitation

This technique is performed using systems containing three basic ingredients, ie, the polymer, the polymer solvent, and the nonsolvent of the polymer (**Figure 4**). The solvent should be organic, miscible in water, and easily removed by evaporation. For this reason, acetone is the most frequently used solvent with this method [152]. Sometimes it exists as a binary blend of solvents, as acetone with a small amount of water, or as a blend of ethanol and acetone. Polymer, drug, and lipophilic surfactant (eg, phospholipids) are dissolved in a semipolar water miscible solvent, such as acetone or ethanol. The solution is then poured or injected into an aqueous solution containing stabilizer under magnetic stirring. Nanoparticles are formed immediately by rapid solvent diffusion. The solvent is then removed from the suspension under reduced pressure [141, 153].

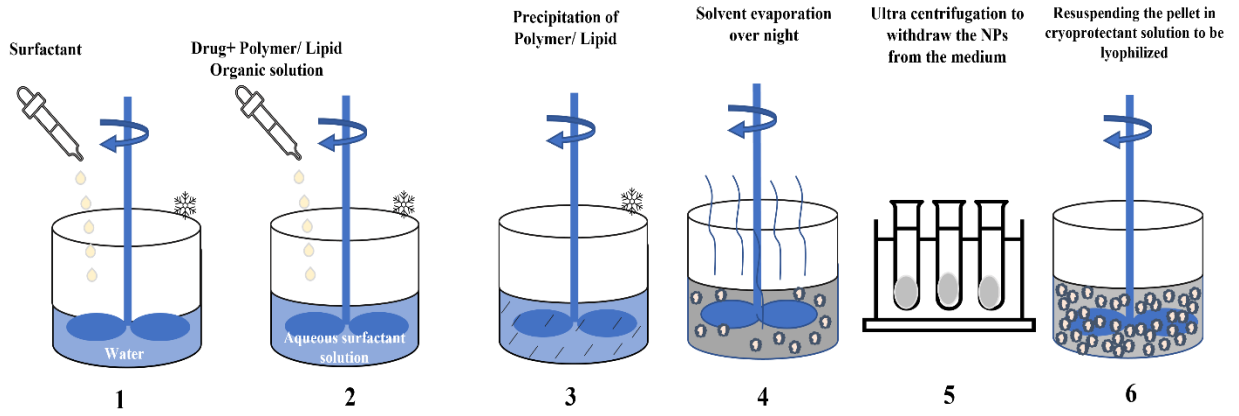

Figure 4. A diagram representing the sequential steps of the Nanoprecipitation technique to obtain SLNs/PLGA NPs

3.9. Chitosan coating to improve nose to brain delivery

A variety of strategies can be followed to promote the nose to brain transportation of therapeutics, such as i) incorporating permeation enhancers, enzyme inhibitors, or P glycoprotein inhibitors; ii) inhibiting mucociliary clearance; iii) implementing nanoparticles concept; iv) using prodrugs; v) incorporating cell-penetrating peptides; vi) adopting eutectic mixtures; and vii) employing vasoconstrictors.

These strategies can be adopted individually or more than one at once such in the case of this research. The main way was to formulate the SLNs and PLGA NPs to get the benefits they offer, then further promote their behaviour by chitosan coating which can happen due to many theories namely i) this polymer can alter the surface charge of the nanoparticles into positive values, which will result in a higher contact with the negatively charge nasal mucosa [127] ii) the mucoadhesive properties of this polymer help the coated nanoparticles to adhere more effectively to the nasal mucosa and resist the expelling effect of the mucociliary clearance [154]; iii) the interaction of negatively charged sites of the cell membranes and tight junctions of the mucosal epithelial cells with the positively charged amino group on chitosan stimulated the opening of the tight junctions [155]

3.10. Quality by Design (QbD) approach

Due to the sophisticated composition of SLNs and PLGA NPs that made them considered as complex systems, a variety of factors can influence their characteristics such as: lipid and polymer type and concentration [156-158], the surfactant type [159, 160], and concentration [161]. Therefore, implementing the QbD approach at the early stages of the research can be ideal to save

time, costs, and efforts [1]. This methodology starts by identifying the quality target product profile (QTPP), then moving to define the critical process parameters (CPPs) and critical material attributes (CMAs), which remarkably influence the critical quality attributes (CQAs) of the final output [162].

4. MATERIALS AND METHODS

4.1. Materials

Meloxicam (MEL) was obtained from Egis Pharmaceuticals Ltd. (Budapest, Hungary). Cholesterol was purchased from Molar Chemicals (Budapest, Hungary), while Insulin from the bovine pancreas, phosphatidylcholine (PCL), PLGA (poly (lactic-co-glycolic acid)) 75/25 Mw 4,000–15,000 Da, and poloxamer 188 were purchased from Sigma-Aldrich (Steinheim, Germany). Chitosan, trehalose dihydrate, and all the organic solvents (all are of analytical grade) and reagents were purchased from Merck (Darmstadt, Germany), unless otherwise indicated.

4.1. Initial Risk Assessment (RA) as a part of QbD

The QTPP of MEL-loaded NPs was defined as the first step of QbD. According to literature evaluation and preliminary experiments, after selecting double emulsion solvent evaporation as the method of preparation, CQAs, CPPs and CMAs were identified. RA tools were then used to rank CPPs and CMAs that significantly impact the quality (CQAs) of the final MEL loaded NPs. The initial RA was carried out using Lean QbD Software (Lean QbD® Software, QbD Works LLC. USA, CA, Fremont). The RA process results are presented in Pareto charts, which were obtained by the used software. These charts prioritize and rank the CQAs, CMAs, and CPPs based on their severity scores.

4.2. Preparation of the nanoparticles (MEL SLNs, Ins SLNs, MEL PLGA NPs, and Ins PLGA NPs)

First, it is worth mentioning that the used amount of MEL for the preparations (15 mg/ml) was chosen depending on the literature evaluation and our previous experience. In this concentration, MEL exhibited a protective effect against the oxidative stress in a mouse model of AD induced by Aβ peptide [102, 163].

Mel and Ins NPs were prepared following a modified double-emulsion solvent-evaporation technique [164], as shown in the following table, **Table 4**.

Table 4. Steps and conditions of the preparation techniques of the NPs

	MEL NPs	Ins NPs
Preparation method	Double-emulsion solvent-evaporation	
W/O/W emulsion	SLNs: 0.2ml MEL solution (15mg/ml)/1ml PhC in cyclohexane (45mg/ml) or cholesterol in ethanol (60mg/ml)/ 2% poloxamer solution Polymeric NPs: 0.2ml MEL solution/ 1ml (12 mg/ml) PLGA in ethyl acetate or 12 mg/ml PCL in chloroform / 2% poloxamer solution	SLNs: 0.35 ml Ins solution (2mg/ml)/1ml PhC solution in cyclohexane (45mg/ml)/ 1.6 mL of 2% w/v poloxamer solution PLGA NPs: 0.35 ml Ins solution/ 1ml (12 mg/ml) PLGA in ethyl acetate solution in cyclohexane/ 1.6 mL of 2% w/v poloxamer solution
Homogenizing condition	0.5 cycles with 75% amplitude	
Solvent evaporation technique	Stirring over the night at ambient temperature using a magnetic stirrer	

The water-in-oil-in-water ($W_1/O/W_2$) emulsion was prepared as follows: 0.2 ml of meloxicam aqueous solution (15 mg/ml) was added dropwise to the oily phase, which was prepared by dissolving either 9 mg of phosphatidylcholine in 1 ml of cyclohexane or 9 mg of cholesterol in 1 ml ethanol, using a homogenizing mixer (Hielscher, Germany) (0.5 cycles with 75% amplitude) for 1 min. The resultant nanoemulsion was then added dropwise into 1.6 ml of 2% poloxamer 188 aqueous solution (W_2) using the homogenizing mixer (0.5 cycles with 75% amplitude) for another 1 min. The final mixture was left under stirring over the night using a magnetic stirrer to allow the organic solvent evaporation, thus forming the SLNs.

MEL polymeric NPs were produced by following another modified double emulsion solvent evaporation technique [165]. First, the primary water in oil emulsion (W_1/O) was prepared by adding MEL aqueous solution (15 mg/ml) to the polymer organic solution (PLGA in ethyl acetate or PCL in chloroform (12 mg/ml)) under sonication (0.5 cycles with 75% amplitude) for 1 min. The primary emulsion was then dispersed in the external aqueous solution of poloxamer 2% under sonication. Finally, the organic solvent was evaporated by leaving the mixtures stirred over the night, thus forming the PLGA NPs.

4.3. Chitosan coating of the SLNs and PLGA NPs

Equal volumes of the NPs suspensions and chitosan solution were mixed and kept under the magnetic stirring for two continuous hours to ensure the successful formulation of C-SLNs, which

was checked by measuring the surface charge of the SLNs before and after the coating process [166-168]. The acquired positive charge of the negatively charged and freshly prepared SLNs confirms the successful coating. As the last step, NPs were harvested by centrifugation (16,000 rpm for 1 h at 4° C) (Hermle Z323, Hermle AG, Germany) and washed with deionized water. The NPs were resuspended in 1.5 ml of 5% (w/v) trehalose aqueous solution and then freeze-dried (Scanvac Coolsafe, Labogene, Lynge, Denmark) at – 40° C for 72h under a pressure of 0.013 mbar [127].

4.4. Characterization of NPs

4.4.1. Determination of mean particle diameter, polydispersity index and zeta potential

The mean particle diameter (Z-average), polydispersity index (PDI), and surface charge (zeta potential) of the NPs were analyzed in folded capillary cells, using Malvern Nano ZS zeta sizer instrument (Malvern Instruments, Worcestershire, UK). The temperature and refractive index of the apparatus were set at 25 ◦C and 1.755, respectively, with a total number of scans of 17. For the analysis, a sample of the NPs suspensions was withdrawn before and after the incubation with chitosan to compare size and PDI, then dispersed in ultrapure water (1:200 v/v) and placed in a cuvette for the analysis. The measurements were repeated three times, data was presented as mean±SD [127].

4.4.2. Determination of encapsulation efficacy (EE) and drug loading (DL)

The EE and DL are two essential parameters in developing drug delivery systems, especially nanotechnology-based ones, following the NPs characterization regarding size, PDI, and ZP.

In case of MEL-NPs the obtained NPs were withdrawn from the preparation medium by centrifugation at 16,000 rpm for 1 h, washed with deionized water, and centrifuged to obtain NPs pellets. The pellet was then immersed in a precise amount of chloroform, which can dissolve both the MEL and the lipid; then, a calculated volume of 0.1 M NaOH was added to extract only the used drug quantity and separate it from the organic solution. After vortexing the mixture, it was moved to a separatory funnel, and the aqueous phase was withdrawn to determine its drug content. The encapsulated MEL was analyzed by high-pressure liquid chromatography (HPLC) following the method developed by Sipos et al. (2020), as follows: an accurately weighed amount of formulation was tested utilizing the Agilent 1260 HPLC system (Agilent Technologies, Santa Clara, CA, USA). A C18 column (Kinetex® (5 μm, 150 mm × 4.6 mm)) was used as the stationary phase (Phenomenex, Torrance, CA, USA). 10 μl aliquots of the samples were then introduced to

determine the concentration of MEL with the temperature adjusted to 30 ◦C. The mobile phases used were 0.065 M KH2PO4 solution adjusted to pH 2.8 with phosphoric acid (A) and methanol (B). The gradient elution was employed in two steps to perform the separation. The proportion was modified from a starting 50% eluent to 25% in 14 min, followed by a gradual rise to 50% in 20 min. The chromatograms were detected at 355 ± 4 nm using UV–VIS diode array detector after setting the eluent flow rate at 1 ml/min. For the assessment of the resulted data, the ChemStation B.04.03 Software (Agilent Technologies, Santa Clara, CA, USA) was used. The retention time of MEL 14.34 min, the linear regression of the calibration line was 0.999, and the determined limit of detection (LOD) was 16 ppm, while the limit of quantification (LOQ) was 49 ppm.

In case of Ins-NPs the encapsulation efficacy (EE) and drug loading (DL) of NPs was determined directly by dissolving 50 mg of freeze-dried particles in 10 mL of 1 M hydrochloric acid. After complete dissolution of the particles, the insulin was separated from the lipid and polymeric components by ultrafiltration using a cellulose dialysis membrane with 10 kDa cut-off (Spectra/Por® Dialysis Membrane, Spectrum Laboratories Inc., Rancho Dominguez, CA, USA). The insulin concentration in the filtrate was measured using the following HPLC method. The insulin quantification was carried out using HPLC (Agilent 1260, agent technologies, Santa Clara, CA, USA). As stationary phase was a Gemini-NX® C18 150 mm × 4.6 mm, 5 µm (Phenomenex, Torrance, CA, USA) column was applied. As mobile phase purified water adjusted pH = 2.8, phosphoric acid and acetonitrile in 68:32 ratio were used. 20 µL of samples were injected with 15 min isocratic elution with 1 mL/min eluent flow at 30 °C temperature for the separation. A UV-Vis diode array detector was applied for the detection of chromatograms at 280 nm. ChemStation B.04.03 Software (Santa Clara, CA, USA) was used for the evaluation of data. The linear regression of the calibration curve was 0.997. The limit of quantification (LOQ) and detection (LOD) of insulin was 87 ppm and 26 ppm, respectively. The EE and DL were calculated by applying the following equations:

$$EE\ (\%) = \frac{\text{The calculated amount of MEL encapsulated in the freeze dried SLNs}}{\text{total amount of MEL used in the preparation}} \times 100$$

$$DL\ (\%) = \frac{\text{The amount of encapsulated insulin in the freeze} - \text{dried nanoparticles}}{\text{The weight of the freeze} - \text{dried nanoparticles}} \times 100$$

4.4.3. Scanning Electron Microscopy (SEM)

The surface morphology of the NPs was tested using Scanning Electron Microscopy (SEM) (Hitachi S4700, Hitachi Scientific Ltd., Tokyo, Japan) at 10 kV. The samples were coated with gold–palladium under an argon atmosphere. The air pressure was 1.3–13 mPa. (Bio-Rad SC 502, VG Microtech, Uckfield, UK).

4.4.4. Fourier-Transform Infrared Spectroscopy (FT-IR)

The compatibility was investigated between the drug and the used excipients by a Thermo Nicolet AVATAR FT-IR spectrometer (Thermo-Fisher, Waltham, USA). FTIR spectra of pure drug, phosphatidylcholine, PLGA, poloxamer 188, chitosan, PLGA NPs, and SLNs were measured as follows: each component was placed along with 150 mg KBr powder, the wavenumber range set on 4000-400 cm^{-1} at a resolution of 4 cm^{-1} before running the measurement.

4.4.5. Raman Spectroscopy

The structural stability of insulin after preparation was investigated using an XRD Dispersive Raman spectroscopy (Thermo Fisher Scientific Inc., Waltham, MA, USA). The instrument was equipped with a 780 nm wavelength diode laser and a CCD camera. A laser power of 12 mW at 50 µm slit aperture size was set. Raman spectra were collected with 2 s exposure and 6 s of acquisition time, for a total of 32 scans per spectrum in the spectral range 3500–200 cm^{-1} with fluorescence and cosmic ray corrections. The Raman spectra of NPs were compared to native insulin to examine structural changes.

4.4.6. X-ray Powder Diffraction (XRPD)

The physical nature and interactions were inspected between the drug and the used excipients by a BRUKER D8 Advance X-ray powder diffractometer (Bruker AXS GmbH, Karlsruhe, Germany). The X-ray powder diffractograms of the pure MEL, excipients, uncoated, and coated NPs were obtained in the angular range of 3–40° 2θ at a step time of 0.1 s and a step size of 0.007° at ambient temperature.

4.5. *In vitro* evaluation of the prepared nanosystems

4.5.1. *In vitro* drug release test

A dialysis bag diffusion technique was employed to investigate the drug release behavior of both MEL-NPs and Ins-NPs at nasal conditions, the modified paddle method (Hanson SR8 Plus, Teledyne Hanson Research, Chatsworth, CA, USA). In case of MEL-NPs 10 mg of MEL and precise aliquots of MEL-NPs equivalent to 10 mg were placed into dialysis bags with a 12–14 kDa

cut-off (Spectra/Por® Dialysis Membrane, Spectrum Laboratories Inc., Rancho Dominguez, CA, USA) and hermetically sealed. The sealed bags were then immersed in dissolution vessel containing volume of 100 ml phosphate buffer (pH 7.4) and left to agitate at 50 rpm at 35° C [169]. The sampling process was executed by withdrawing aliquots from the release medium at pre-established periods up to 6 h and replacing them with an equivalent volume of the fresh medium to maintain the 'sink' condition [170, 171]. Both Ins and MEL content was analyzed using HPLC for. The results were reported as means ± SD.[172]

In case of Ins-NPs the freeze-dried formulation, containing equivalently 0.5 mg of insulin and 0.5 mg of initial insulin, were placed into dialysis bags. Then, the dialysis bags were immersed in dissolution vessels containing 100 mL volumes of 0.08 M potassium dihydrogen phosphate buffer adjusted to pH 7.4 with 0.1 M sodium hydroxide (corresponding to the systemic circulation and CSF pH) and stirred at 50 rpm at 37° C [78]. The aliquots (2 mL) were withdrawn from the release medium at predetermined time intervals up to 6 h and then replaced with an equivalent volume of the fresh release medium to maintain a sink condition [170, 171]. Insulin concentration in the samples was determined with HPLC. The results were reported as means ± SD.

4.5.2. Mucoadhesion test

Mucoadhesion was determined using two coordinated methods: the direct method (turbidimetric method) and the indirect method (Measuring the ZP changes). The direct method was carried out as follows: briefly, equal volumes of NPs suspensions in SNES and porcine mucin solution 0.05% were mixed and incubated at 37° C, and continuously stirred for 4 h with a pre-determined sampling interval for of 1 h. The centrifugation was then performed at 17,000 rpm at 4° C. The supernatant content of the free mucin was determined at 255 nm using a UV spectrophotometer. The mucin binding efficacy (MBE) can be calculated based on the following equation [173, 174]:

$$MBE = \frac{\text{Total mucin} - \text{Free mucin}}{\text{Total mucin}} \times 100$$

The mucoadhesive properties were also evaluated by measuring the ze-ta potential using the Malvern Nano ZS instrument (Malvern Instruments, Worcestershire, UK) through the interaction of negatively charged mucins with SLNs, PLGA NPs, and C-SLNs [175].

4.5.3. Permeability test

The *in vitro* permeation test was completed utilizing a modified Side-bi-Side® type apparatus (Grown Glass, New York, NY, USA), which was designed to similar nasal cavity conditions. This method has been evaluated, validated and previously reported by Bartos et al. [176]. Briefly, the intranasal suspension of the NPs was placed in the first chamber and considered to be the donor phase; this phase was prepared by suspending MEL (1 mg) or MEL-NPs (equivalent to 1 mg) in 9 ml of simulated nasal electrolyte solution (SNES). A semi-permeable cellulose membrane (Synthetic membrane PALL Metricel membrane®), previously impregnated in isopropyl myristate for 1 h, was placed between the two chambers as a membrane to imitate the nasal mucosa. The acceptor phase was represented by 9 ml of pH 7.4 phosphate buffer, and this pH represents the pH of the blood. The donor and the acceptor phase volumes were the same (9 ml) and had a 0.69 cm^2 diffusion area. The temperature of the phases was -set to 35 °C (Thermo Haake C10-P5, Sigma, Aldrich Co.) to simulate the nasal condition, and the agitation using magnetic stirrers that were set to 50 rpm to mimic the movements of the cilia and the blood circulation. The diffused amount of MEL, Ins and NPs was determined with HPLC, and measurements were implemented in triplicate, data was presented as mean±SD.

4.6. *In vitro - in vivo* correlation (IVIVC) for meloxicam nanoparticles

As reported in the FDA guidance [177-179], the IVIVC process represents a predictive mathematical model demonstrating the expected in vivo behavior of a drug product based on its in vitro dissolution and permeation features. In the early-stage development, IVIVC is justified as a regulatory guideline aiming to minimize further animal studies [180]. Level C correlations can be useful in the early stages of formulation development when pilot formulations are being selected, therefore it seems to be a suitable choice for selecting the most suitable NPs for the therapeutic purposes [181]. Therefore, conducting IVIVC for the prepared NPs could be an efficient tool to estimate the *in vivo* behavior of the NPs based on the dissolution and permeation data and to provide assistance in optimizing the in vitro behavior of the NPs [179]. A level-C correlation of IVIVC was investigated between the in vitro drug dissolution and permeation characteristics and the corresponding *in vivo* such as AUC API (Area Under the Curve of the Active Pharmaceutical Ingredient) brain level. Since IVIVC is characterized by a linear relationship between the results obtained from the in vitro measurements and the in vivo tests data, Pearson correlation was applied to disclose the former relationship. To statistically estimate the in vivo brain distribution of MEL

containing PLGA NPs and SLNs, IVIVC was operated using the attained in vitro results and previous in vivo data of similar experiments, i.e., MEL suspension, MEL-human serum albumin NPs (with a surfactant (MEL-HSA-Tween), and without (MEL-HSA)) [182], and a MEL-nanosuspension (nanoMEL) [176]. The mentioned formulations contained the same concentration of MEL. Data were expressed as means ± SD, and the comparison between the groups was established by Student's t-test set with TIBCO Statistica 13.4 software® (StatSoft Hungary, Budapest, Hungary). The differences between the outcomes were considered statistically significant when $p < 0.05$.

4.7. *In Vitro* Cell Line Studies

4.7.1. Human RPMI 2650 Nasal Epithelial Cell Culture

Human RPMI 2650 nasal epithelial cells were purchased from ATCC (cat. no. CCL 30) and used until passage 50 for the experiments. For the cell culturing, Dulbecco's Modified Eagle's Medium (DMEM; Gibco, Life Technologies, Carlsbad, CA, USA) supplemented with 10% fetal bovine serum (FBS; Pan-Biotech GmbH, Aidenbach, Germany) and 50 g/mL gentamicin were used. In addition, the cells were kept in a humidified 37 °C incubator with 5% CO_2. All the plastic surfaces were coated with 0.05% collagen in sterile distilled water before cell seeding in culture dishes, and the medium was changed every 2 days. The cells were trypsinized with 0.05% trypsin 0.02% EDTA solution when they reached about 80–90% confluency in the dishes. To induce tighter epithelial barrier properties, retinoic acid (10 µM) and hydrocortisone (500 nM) were added to the cells 1 day before the experiment [183]. For the permeability measurements, RPMI 2650 epithelial cells were co-cultured with human vascular endothelial cells [184] to create a more physiological barrier [185]. The endothelial cells (≤ P8) were grown in an endothelial culture medium (ECM-NG, Sciencell, Carlsbad, CA, USA) supplemented with 5% FBS, 1% endothelial growth supplement (ECGS, Sciencell, Carlsbad, CA, USA), and 0.5% gentamicin on 0.2% gelatin-coated culture dishes.

4.7.2. Human hCMEC/D3 Brain Endothelial Cell Line

Cultures of hCMEC/D3 cells (≤ P35) were grown in MCDB 131 medium (Pan-Biotech, Aidenbach, Germany) supplemented with 5% FBS, GlutaMAX (100×, Life Technologies, Carlsbad, CA, USA), lipid supplement (100×, Life Technologies, Carlsbad, CA, USA), 10 ng/mL ascorbic acid, 550 nM hydrocortisone, 100 ng/mL heparin, 1 ng/mL basic fibroblast growth factor (bFGF, Roche, San Francisco, CA, USA), 2.5 µg/mL insulin, 2.5 µg/mL transferrin, 2.5 ng/mL

sodium selenite (ITS), and 50 μg/mL gentamicin [186]. All the plastic surfaces were coated with 0.05% collagen in sterile distilled water before cell seeding and the medium was changed every 2 days. Before each experiment, the medium of hCMEC/D3 cells was supplemented with 10 mM LiCl for 24 h to improve the barrier properties [187].

4.7.3. Preparation of Insulin and Insulin-Loaded Nanoparticle Dilutions for Cellular Assays

The concentration of insulin was 0.7 mg/mL (20 IU) in the different NPs after diluting the samples in 1.5 mL culture medium or Ringer HEPES (5 mM Hepes, 136 mM NaCl, 0.9 mM CaCl2, 0.5 mM MgCl2, 2.7 mM KCl, 1.5 mM KH2PO4, 10 mM NaH2PO4, pH 7.4) depending on the experiments. To prepare the insulin stock solution, the powder was first dissolved in 1 M HCl and then in medium or Ringer HEPES to reach a solution of 0.7 mg/mL and the pH was adjusted to 7.4. For cell viability measurements, the different NPs and the insulin working solutions were prepared as 10× (0.07 mg/mL), 30× (0.02 mg/mL), and 100× (0.007 mg/mL) diluted in cell culture medium. The 10, 30, and 100× dilution of HCl and free insulin were prepared in the medium as control treatments. For permeability measurements, the NPs and insulin were applied as 10 times dilution at 0.07 mg/mL concentration diluted in a Ringer-HEPES buffer.

4.7.4. Cell Viability Measurement

The kinetics of the epithelial and endothelial cell reaction to the different treatments were monitored by impedance measurement at 10 kHz (RTCA-SP instrument, Agilent, Santa Clara, CA, USA). The impedance measurement is label-free, non-invasive, and correlates linearly with the adherence, growth, number, and viability of cells in realtime [188, 189]. For background measurements, the 50 μL cell culture medium was added to the wells. Then, the cells were seeded at a density of 2×10^4 RPMI 2650 cells/well and 6×10^3 hCMEC/D3 cells/well in 96-well plates coated with integrated gold electrodes (E-plate 96, Agilent, Santa Clara, CA, USA). The cells were cultured for 5–7 days in a CO_2 incubator at 37° C and monitored every 10 min until the end of experiments. In addition, the cells were treated at the beginning of the plateau phase of growth. The insulin, insulin NPs, and HCl solution were diluted in a cell culture medium and the effects were followed for 20 h. Triton X-100 detergent (1 mg/mL) was used as a reference compound to induce cell toxicity. The cell index was defined as R_n-R_b at each time point of measurement, where R_n is the cell-electrode impedance of the well when it contains cells and R_b is the background impedance of the well with the medium alone.

4.7.5. Permeability Studies

Transepithelial or transendothelial electrical resistance (TEER) reflects the tightness of the intercellular junctions closing the paracellular cleft, resulting in the overall tightness of cell layers of biological barriers. TEER was measured to check the barrier integrity by an EVOM volt-ohmmeter combined with STX-2 electrodes (World Precision Instruments, USA), and was expressed relative to the surface area of the cell layers as Ω cm^2. Resistance of cell-free inserts was subtracted from the measured values, and the cells were treated when the cell layers had reached steady TEER values. To model, the nasal barrier RPMI 2650 epithelial and vascular endothelial cells were co-cultured on inserts (Transwell, polycarbonate membrane, 3 μm pore size, 1.12 cm^2, Corning Costar Co., Cambridge, MA, USA) and placed in 12-well plates for 5 days. Vascular endothelial cells were passaged (1 × 105 cells/cm^2) to the bottom side of tissue culture inserts coated with a low growth factor containing Matrigel (BD Biosciences, East Rutherford, NJ, USA), and nasal epithelial cells were seeded (2 × 105 cells/cm^2) to the upper side of the membranes which were coated with collagen. As a simplified blood-brain barrier model, hCMEC/D3 cells were cultured on collagen-coated Transwell inserts (Transwell, polycarbonate membrane, 3 μm pore size, 1.12 cm^2, Corning Costar Co., Acton, MA, USA) for 5 days in monolayer. The cells were treated when the cell layers had reached steady TEER values. For the permeability experiments, the inserts were transferred to 12-well plates containing 1.5 mL Ringer-HEPES buffer in the acceptor (lower/basal) compartments. In the donor (upper/apical) compartments, 0.5 mL buffer was pipetted containing insulin alone or encapsulated formulations. To avoid the unstirred water layer effect, the plates were kept on a horizontal shaker (120 rpm) during the assay. The assays lasted for 60 min. Samples from both compartments were collected and the insulin concentration was measured by HPLC. The apparent permeability coefficients (P_{app}) were calculated as described previously [88]. Briefly, the cleared volume was calculated from the concentration difference of the tracer in the acceptor compartment (Δ[C]A) after 60 min and in donor compartments at 0h ([C]D), the volume of the acceptor compartment (VA; 1.5 mL), and the surface area available for permeability (A; 1.12 cm^2) using this equation:

$$P_{app}\left(\frac{cm}{s}\right) = \frac{\Delta[C]_A \times V_A}{A \times [C]_D \times \Delta t}$$

Recovery (mass balance) was calculated according to the equation:

$$Recovery\ (\%) = \frac{C_f^D V^D + C_f^A V^A}{C_0^D V^D} \times 100$$

where C_0^D and C_{0f}^D are the initial and final concentrations of the compound in the donor compartment, respectively; C_0^A is the final concentration in the acceptor compartment; V_D and V_A are the volumes of the solutions in the donor and acceptor compartments [190].

5. RESULTS AND DISCUSSION

5.1. Initial Risk Assessment (RA) as a part of QbD

Risk assessment was conducted to rank and prioritize the factors that highly impact the final product quality. The QbD-based risk assessment started by setting the QTPPs encompassing the desired quality attributes in MEL-loaded NPs, as summarized in **Figure 5.**

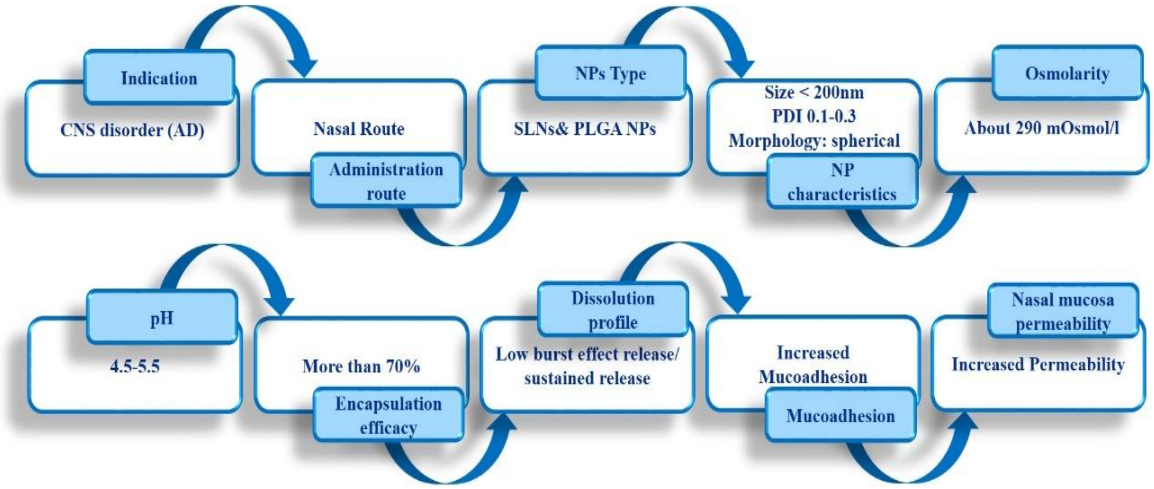

Figure 5. Defining the QTPP for MEL/ INS-loaded NPs. The Figure shows that the indication of the therapy was AD. The application route was the nasal route by encapsulating the drug into SLNs, PLGA NPs, C-PLGA NPs, or C-SLNs. It also demonstrates the desired NPs characters regarding size, PDI, optimal EE, dissolution, mucoadhesion, and permeation behavior.

The following step was to create an Ishikawa fishbone diagram that summarizes the risk analysis process. It clarifies the cause-effect relationship between the significant variables and the CMAs, CQAs, and CPPs of the nanoformulations (**Figure 6**) [191]. This diagram is considered to be an efficient quality management tool aids in exploring the cause-effect relationship [192].

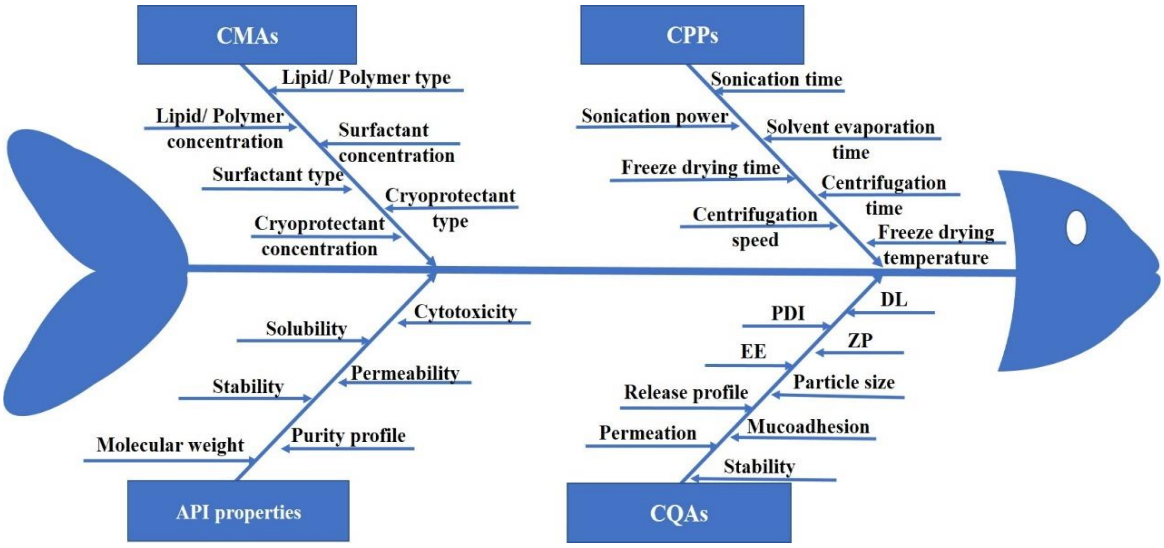

Figure 6. Ishikawa diagram illustrating the risk factors for the nose-to-brain delivery of MEL/ INS-loaded NPs. CQAs: critical quality attributes, CMAs: critical materials attributes, CPPs: critical process parameters, API: active pharmaceutical ingredient, DL: drug load, PDI: polydispersity index, ZP: zeta potential, EE: encapsulation efficacy

This was followed by an initial RA of the CQAs, which were namely: average hydrodynamic diameter (Z-average), zeta potential, PDI, EE, dissolution rate, mucoadhesion, and permeability using Lean QbD software. After that, the evaluation of the selected CMAs and CPPs took place that was based on the thoroughly analyzed relevant literature and the results of experimental research work in addition to the proper prior knowledge. The risk assessment of the highest risky CPPs and CMAs affecting the quality of both SLNs and PLGA NPs for the IN application with the aim of the direct nose to brain delivery demonstrated that the vastly influential CPP was sonication time. In contrast, the immensely influential CMAs were lipid/ polymer type, lipid/ polymer concentration, surfactant type, and surfactant concentration. The calculated and ranked severity scores for the CQAs, CMAs, and CPPs are presented in Pareto charts (**Figure 7**)

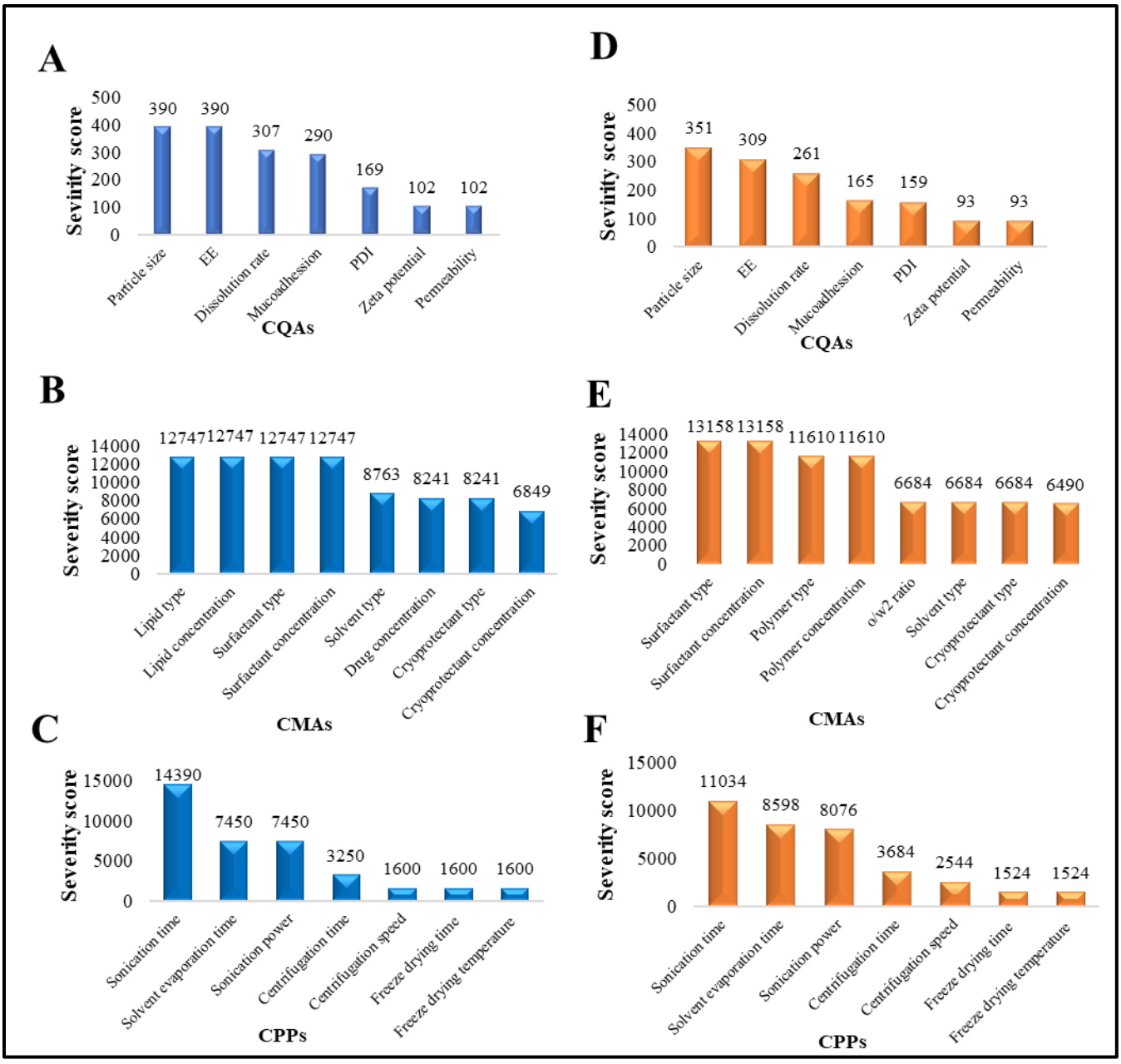

Figure 7. Pareto charts show the calculated and ranked severity scores for the CQAs, CMAs, and CPPs where A, B, C represent the SLNs, while D, E, F represent the PLGA NPs situation

These results are supported by the previously reported literature, which presents particle size [126, 193] and EE [19, 194] as the highly severe CQAs; Lipid type and concentration [195-197], polymer type and concentration [193, 197, 198] and surfactant type[199-201] and concentration [202, 203] as the highly risky CMAs. The sonication time [197, 204-206] was the most critical CPP.

5.2. Characterization of NPs

5.2.1. Mean particle diameter, size distribution, and zeta potential

The mean hydrodynamic diameter, PDI, zeta-potential, EE of the developed formulations in this study are listed in **Table 5**.

Table 5. The Z-average, PDI, ZP of the prepared nanoformulations. Measurements were done in triple (n=3 independent formulations), and data are represented as means ± SD

Sample	Z-average (nm)	PDI	ZP (mV)
MEL - PLGA NPs	142 ± 12.8	0.276 ± 0.02	-16.2 ± 1.8
MEL – SLNs	94.8 ± 7.4	0.148 ± 0.002	-43.7 ± 1.5
MEL C-SLNs	171.2 ± 6.2	0.187 ± 0.01	60.7 ± 0.5
Ins PLGA NPs	135 ± 12.8	0.127 ± 0.02	-28.2 ± 1.8
Ins C-PLGA NPs	174.6 ± 10.7	0.179 ± 0.01	58.4 ± 0.7
Ins SLNs	99.1 ± 5.3	0.195 ± 0.03	-42.3 ± 1.5
Ins C-SLNs	145.2 ± 6.2	0.214 ± 0.007	61.3 ± 0.5

The Z-average of PLGA NPs and SLNs was 142 ± 12.8 nm and 94.8 ± 7.4 nm, respectively; in contrast, C-SLNs demonstrated an increase in the Z-average due to the deposition of chitosan particles on the surface of the SLNs. Both types of NPs, in addition to the coated one, comply with the size requirement of nasal administration for the brain targeting, which preferred to be up to 200 nm [134, 207]

PDI values were lower than 0.3 for all formulations indicating monodisperse size distributions [208]. That is in accordance with the SEM images (Fig. 4), which demonstrate the NPs homogenized dispersion.

The zeta potential values of PLGA NPs and SLNs were negative, which is logical due to the negative charge of phosphatidylcholine approximated in a range of -10 and -30 mV at the neutral pH [209] owing to the presence of phosphate and carboxyl groups, in contrast with the negatively charged carboxyl groups on PLGA that are the only cause behind the negative charge. As expected, the chitosan coating leads to a charge shifting to become positive due to the electrostatic interactions, which suggest appropriate adsorption of the positively charged polymer (chitosan) onto the surface of the NPs. The pronounced surface charge variation from negative to positive charge is an indicator of the successful coating of the NPs surface with chitosan [174]. The

optimized positively charged C-NPs would probably have better adhesion to the negatively charged nasal mucosa, which in turn improves permeability through the nasal mucosa.

5.2.2. Encapsulation efficiency and drug loading results

As **Figure 8** shows, the encapsulation efficacy (EE) and drug loading (DL) were not significantly higher ($p > 0.05$) in the case of SLNs than PLGA NPs, which could be explained by the ability of phosphatidylcholine particles to entrap meloxicam and insulin molecules into the Ins SLNs by forming hydrogen bonds employing the three available electron pairs in each unit, whilst in the case of Ins PLGA NPs these electron pairs are used to attach the lactic-co-glycolic units with each other as described in our previous research work [127]. Another possible explanation could be the special affinity of insulin for the lipophilic surfaces resulting in adsorption of meloxicam/ insulin to the hydrophobic surfaces inducing self-aggregation because of its insolubility in organic solvents [210]. Furthermore, coating the NPs with chitosan seems to be a beneficial tool in getting higher EE and DL due to the formation of an impermeable coating that offers protection against the leakage of insulin molecules from the prepared NPs [211].

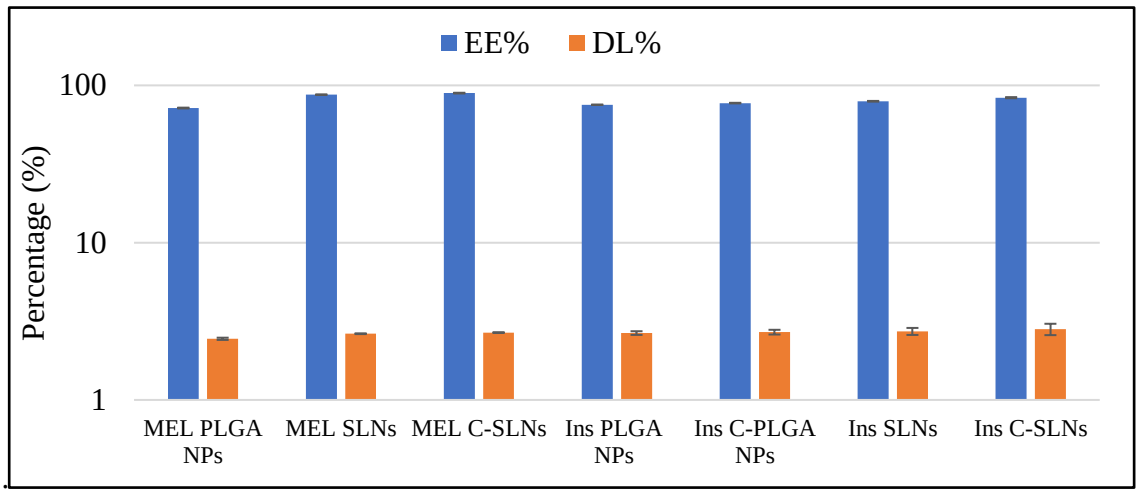

Figure 8. Encapsulation efficacy (EE) and Drug load (DL) of the optimized SLNs and PLGA NPs formulations. ANOVA test was performed to check the significance of the differences between the results of the EE and DL. Measurements were done in triple (n=3 independent formulations), and data are represented as means ± SD.

5.2.3. Scanning Electron Microscopy (SEM)

SEM images of the obtained NPs showed spherical shape with a smooth surface, which provides better dissolution, mucoadhesion, and permeation than the needle- or disk-like shape NPs.

Moreover, the spherical shape of the NPs will result in a minimal membrane bending energy, therefore higher stability and lower chance of entrapped drug leakage compared with the non-spherical counterparts that involve a strong membrane deformation, higher friction and consume energy [35]. **Figure 9** shows the SEM images of the resulted NPs.

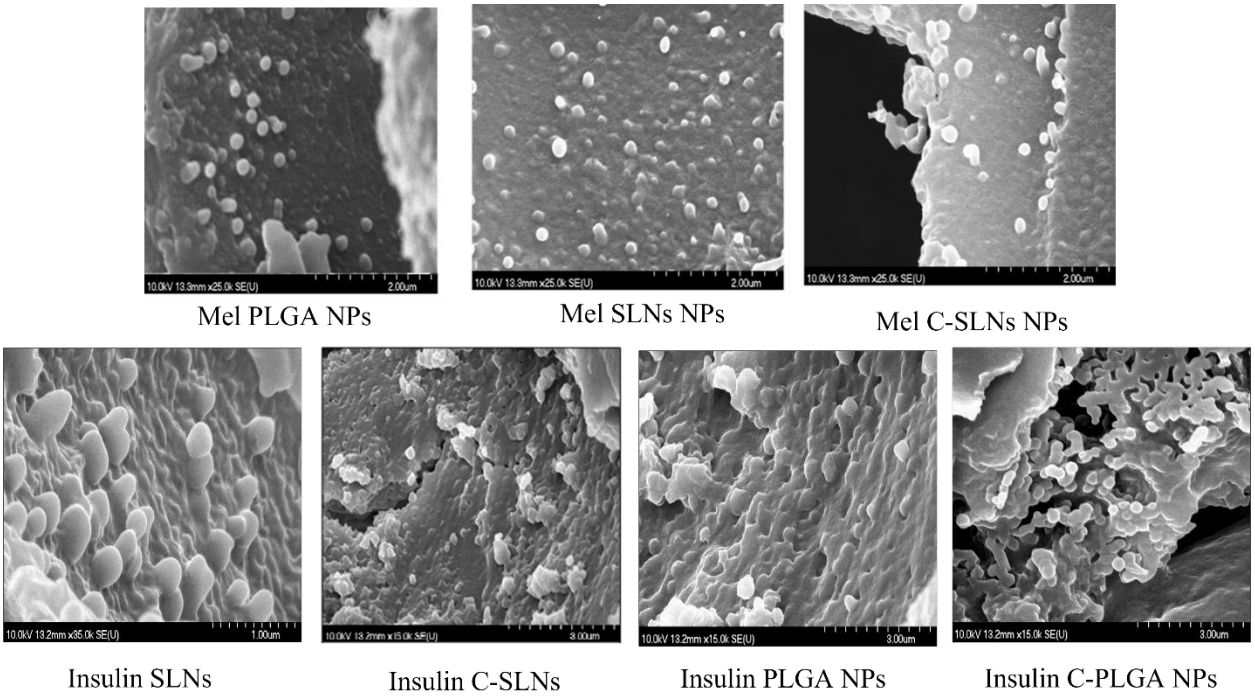

Figure 9. SEM images representing the resulted NPs. The images show the spherical shape and well dispersed NPs with preferable nano-size

5.2.4. Fourier-Transform Infrared Spectroscopy (FT-IR)

The FT-IR spectra of MEL, both loaded NPs formulations, and the used excipients are presented in **Figure 10**.

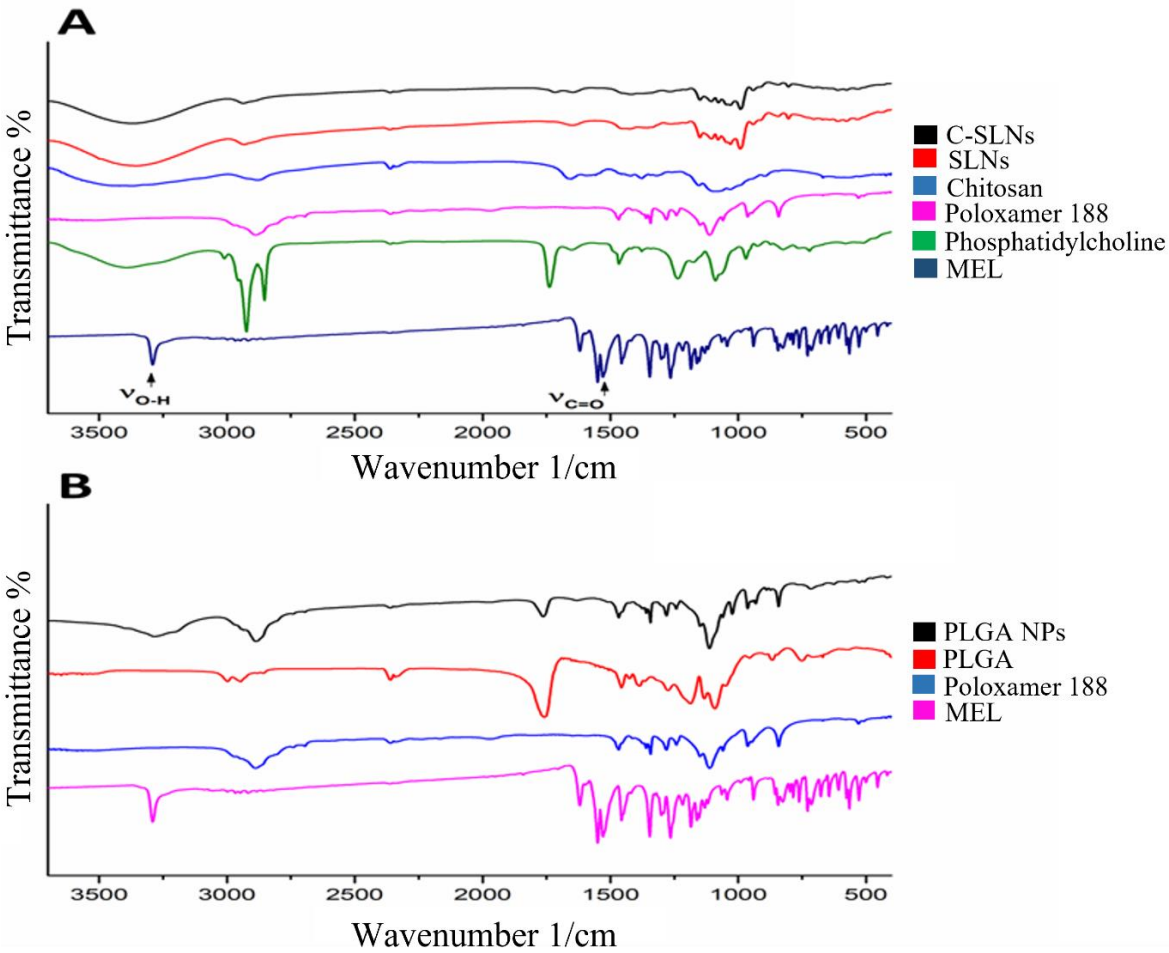

Figure 10. FTIR spectra of MEL, MEL SLNs, MEL C-SLNs, Mel PLGA NPs, and the used excipients

The FT-IR spectra of the NPs showed no changes in the MEL chemical structure and presented no significant difference in the main functional groups of MEL. The absorption band at 3290 cm−1 related to the hydroxyl group attached to an aromatic ring of MEL; furthermore, the carbonyl group vibration at 1550 cm−1 is not visible in the spectrum of C-SLNs. These characteristic peaks fading points out H-bonding formation between SLN and chitosan, which proves that the coating process was achieved.

Hence, there is no interaction between MEL and the other SLNs excipients, and they are compatible with each other. Similarly, absorption peaks of the materials used for PLGA NPs preparation (PLGA, Poloxamer) exhibited compatibility with MEL since the previously mentioned two chemical groups of MEL were maintained the same after PLGA NPs formulations [212].

5.2.5. X-ray Powder Diffraction (XRPD)

An overlay of powder XRPD patterns of MEL, SLNs, C-SLNs, PLGA NPs, and the used excipients is depicted in **Figure 11**.

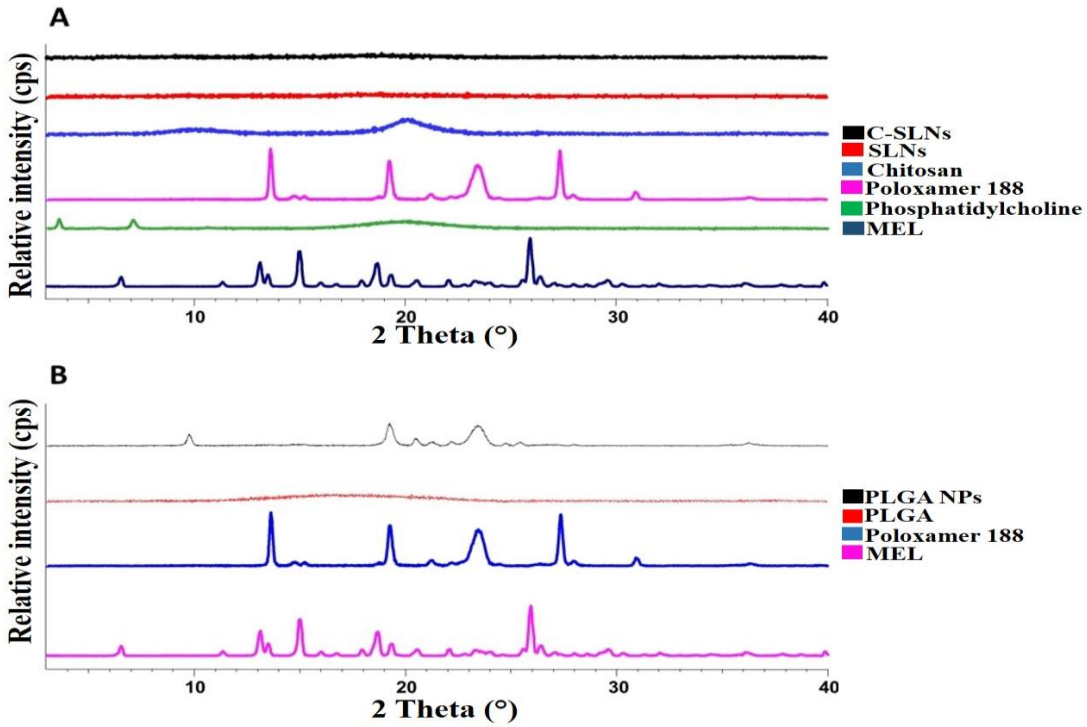

Figure 11. XRPD spectra of SLNs and C-SLNs (A), PLGA NPs (B), and the excipients used in the formulation process emphasizing the compatibility between the used materials and the absence of any changes in MEL structure after the NPs formulation, in addition to confirming the successful coating of the SLNs.

The XRPD of the MEL shows characteristic peaks to its crystalline structure. However, SLNs, C-SLNs, and PLGA NPs did not show the MEL characteristic peaks in their XRPD pattern. This confirms the successful encapsulation of the API into the NPs [213]. The previous results are conforming to the results of FTIR, encapsulation efficacy, and drug loading.

5.2.6. Raman spectroscopy

The structural changes of insulin after preparation of NPs were investigated using Raman spectroscopy. The Raman spectra of insulin-containing NPs were compared to native insulin's spectrum (**Figure 12**).

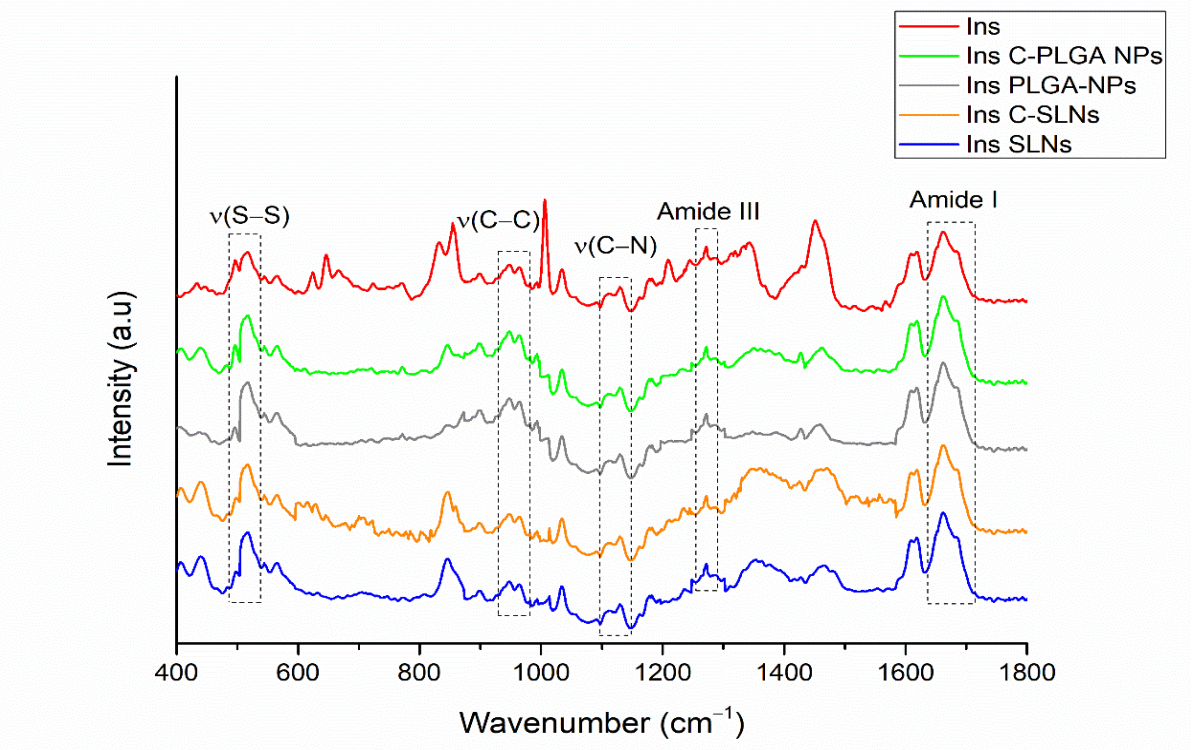

Figure 12. Raman spectra of insulin-containing NPs in comparison to native insulin showing the major spectral regions characteristic for protein structure.

From a stability point of view, one of the most relevant spectral features belongs to the tertiary structure of insulin ascribing disulfide bridges (S–S around 510 cm^{-1}) and S—C around 665 cm^{-1}, whereas the internal polypeptide chain orientation in the wavenumber regions of the C—C and C—N stretching modes (890—990 cm^{-1} and 1110—1160 cm^{-1} respectively) amide III bands (1200—1300 cm^{-1} and amide I band (1600—1700 cm^{-1}) provides information about the secondary structure [214]. Comparing these spectral markers of the protein structure of NPs to native insulin, no Raman shift was observed, which indicates no change or unfolding in the protein structure, encapsulated insulin preserved its native nature.

5.3 In vitro evaluation of the prepared nanosystems

5.3.1. Mucoadhesion test

The mucoadhesion test was performed to understand the behavior of the NPs towards the mucin, which forms the main component of the nasal mucosa, and the higher the mucoadhesion, the better the retaining of the NPs adsorbed to the nasal mucosa [215]. Based on **Figure 13**, it can be noticed that the highest mucoadhesion could be achieved when formulating the C-NPs followed by the uncoated SLNs then the PLGA NPs.

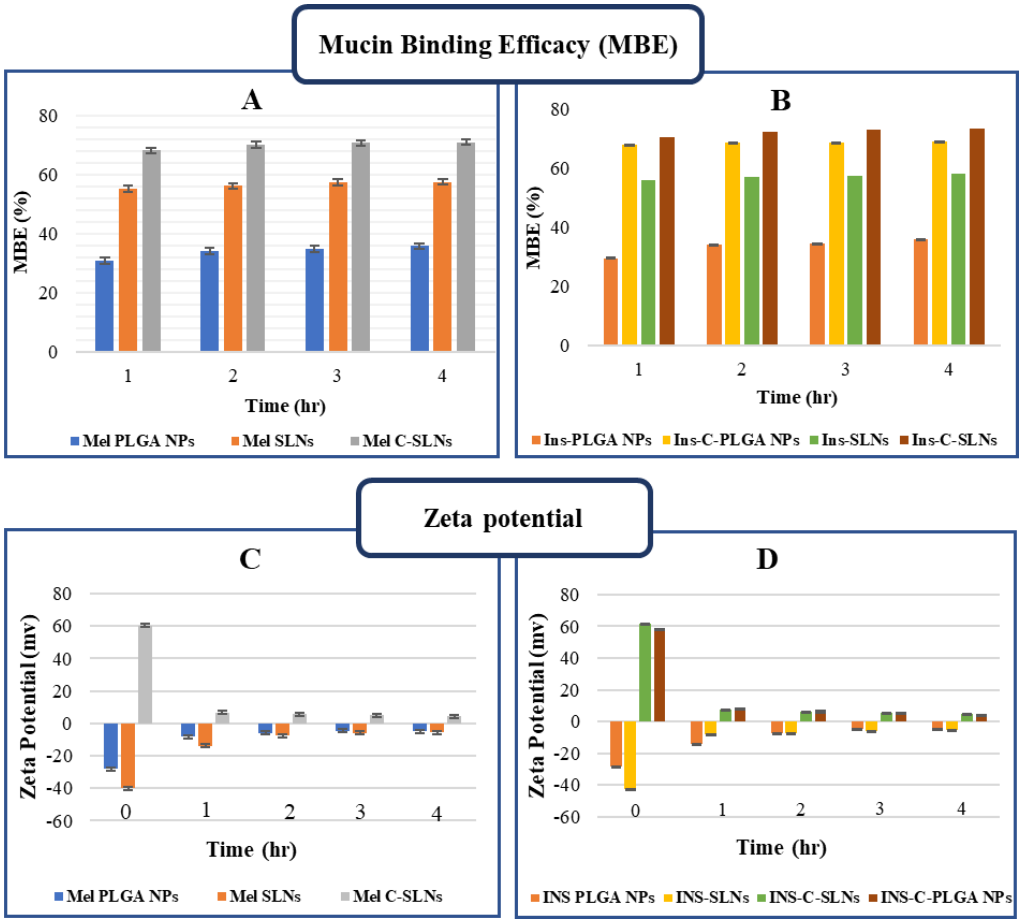

Figure 13 Mucoadhesion assay of MEL and Ins NPs, where A represents ZP analysis method for MEL NPs, B represents ZP analysis method for Ins NPs, C represents Turbidity analysis method for MEL NPs, and D represents Turbidity analysis method for Ins NPs. Measurements were done in triple (n=3 independent formulations), and data are represented as means ± SD.

In the turbidimetric method, the mucoadhesive strength was estimated by calculating mucin binding efficacies to the obtained NPs. The mucin binding efficacy MBE of MEL-PLGA NPs, MEL-SLNs, and MEL-C-SLNs were 36.55%, 57.59%, and 71.09%, respectively, while the MBE for Ins SLNs and Ins PLGA NPs were 35.99% and 58.2%, respectively, which were increased by the chitosan coating to 69.14% and 73.45% by the end of the experiment, as **Figures 13A, 13B** represent. Since the mucin possesses a negative charge along with its glycosylated structure, the positively charged C-NPs will have significantly higher interaction with it than the negatively charged SLNs and PLGA NPs. The first leads to formulating ionic bonds, while the latter occurs by forming electrostatic interactions ($p<0.05$). Since the SLNs are higher in their negative charge,

their electrostatic interactions with the mucin will be significantly higher than the PLGA NPs (p<0.05). This observation goes in line with previous studies results [155, 215].

The mucoadhesion was assessed in the zeta potential method by measuring zeta potential variation values up to 4 hours (**Figure 13C** and **13D**). The high positive charge of the C-NPs led to a significant neutralization in the negative charge of mucin (p<0.05), which may happen by the formation of the ionic bonds [216]. On the other hand, uncoated SLNs and PLGA NPs remained negative; thus, the interaction with mucin happens weakly with insignificant charge changes. (p>0.05). The ZP method results are consistent with those achieved by the turbidity method, as the total changes in ZP values match the MBE of each type of NPs. Both methods demonstrated higher mucoadhesion of the APIs C-SLNs followed by the APIs SLNs, which were superior to the PLGA NPs.

5.3.2. *In vitro* drug release studies

The *in vitro* dissolution profiles of pure MEL and MEL-loaded NPs were investigated in intranasal-simulated conditions, using simulated nasal electrolytic solution (SNES) medium (pH of 5.6) **Figure14A**, while the dissolution behavior of the Ins and Ins NPs was investigated under CSF and systemic circulation conditions to simulate the drug release after nasal absorption, where native insulin was used as a reference, and PBS (pH = 7.4) was employed as the dissolution medium. **Figure 14B**.

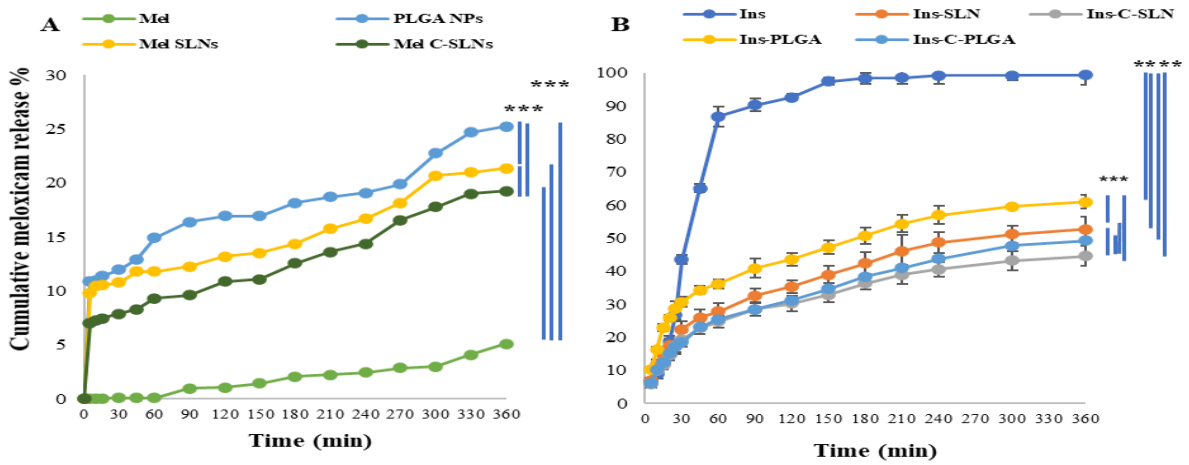

Figure 14. In vitro dissolution behavior of the native APIs and the prepared NPs, where A represents MEL case and B represents Ins case. Measurements were done in triple (n=3 independent formulations), and data are represented as means ± SD.

It is evident that pure MEL demonstrates a modest solubility (5.10 ± 0. 9 µg/mL, over 360 min, at35°C) due to its chemical structure and because of the weak acidic character resulted in this medium (pKa= 3.43) [217]; fabrication of MEL in nanoformulations indicated a significant increase ($p<0.001$) in the dissolution rate compared to pure MEL (approximately 4-5 times higher). This aligns with the results previously reported by Katona *et al.* and might be due to the nano-size and improved specific surface area of the NPs [182]. The release behavior from the NPs demonstrated a sustained release pattern. This begins with a moderate early rapid release over the first hour, where 12.94 ± 0.86%, 11.79± 0.74 of MEL were released from the PLGA NPs and SLNs, respectively. The previous has been frequently reported for PLGA NPs [218, 219] and SLNs [169, 205]. This moderate initial burst effect may be due to the surface-adsorbed drug particles on the NPs in addition to the drug molecules that are placed near the surface having poor links to the NPs system. A slow-release profile followed this until 6 h, where only 25.26 ± 2.39%, 21.37 ± 1.47 of cumulative MEL release was observed for PLGA NPs and SLNs, respectively ($p < 0.05$) since the encapsulated drug was slowly diffused out of the NPs core [169]. The previous results point out that a significant part of the drug was kept encapsulated into the NPs after being surrounded by nasal mimetic conditions. Thus, it can be released into the targeted position.

Turning to insulin case, the native insulin demonstrated the highest dissolution rate among the tested formulations in PBS, which can be related to the isoelectric point of bovine insulin. The applied insulin has an isoelectric point of 5.3-5.4, therefore the application of a medium with a pH value below 4 or above 7 will lead to an enhanced solubility [220]. Moreover, encapsulation of insulin in Ins SLNs and Ins PLGA NPs was significantly accompanied ($p < 0.001$) by 2-folds and 1.67-fold decreasing in the dissolution rate of insulin respectively, which can be explained by the controlled release properties of the lipid and polymeric NPs [221-223]. Ins PLGA NPs showed significantly higher ($p < 0.05$) drug release in comparison to Ins SLNs, which can be explained by the higher lipophilicity, therefore higher drug retention in case of SLNs [210]. Further coating the NPs with chitosan resulted in a significant slower release compared to the uncoated ones ($p<0.05$), which might be explained by the additional controlling release properties presented by the additional polymer layer of chitosan, classified as a water-insoluble polymer at the physiological pH [224-226].

The dissolution test results provide a guarantee that the drug leakage during *in vivo* delivery would be minimal. By preventing premature release, MEL will remain encapsulated in the NPs, avoiding

the systemic effects until reaching the olfactory bulb in a sufficient concentration. Moreover, the enhanced solubility achieved by the formulated nanosystems compared to the pure drug will result in better pharmacokinetics as the dissolution behavior is the determining step of the absorption, the ADME (absorption, distribution, metabolism, and excretion) first process.

5.3.3. *In vitro* Permeability test

Figure 15 shows the permeation behavior of the prepared NPs:

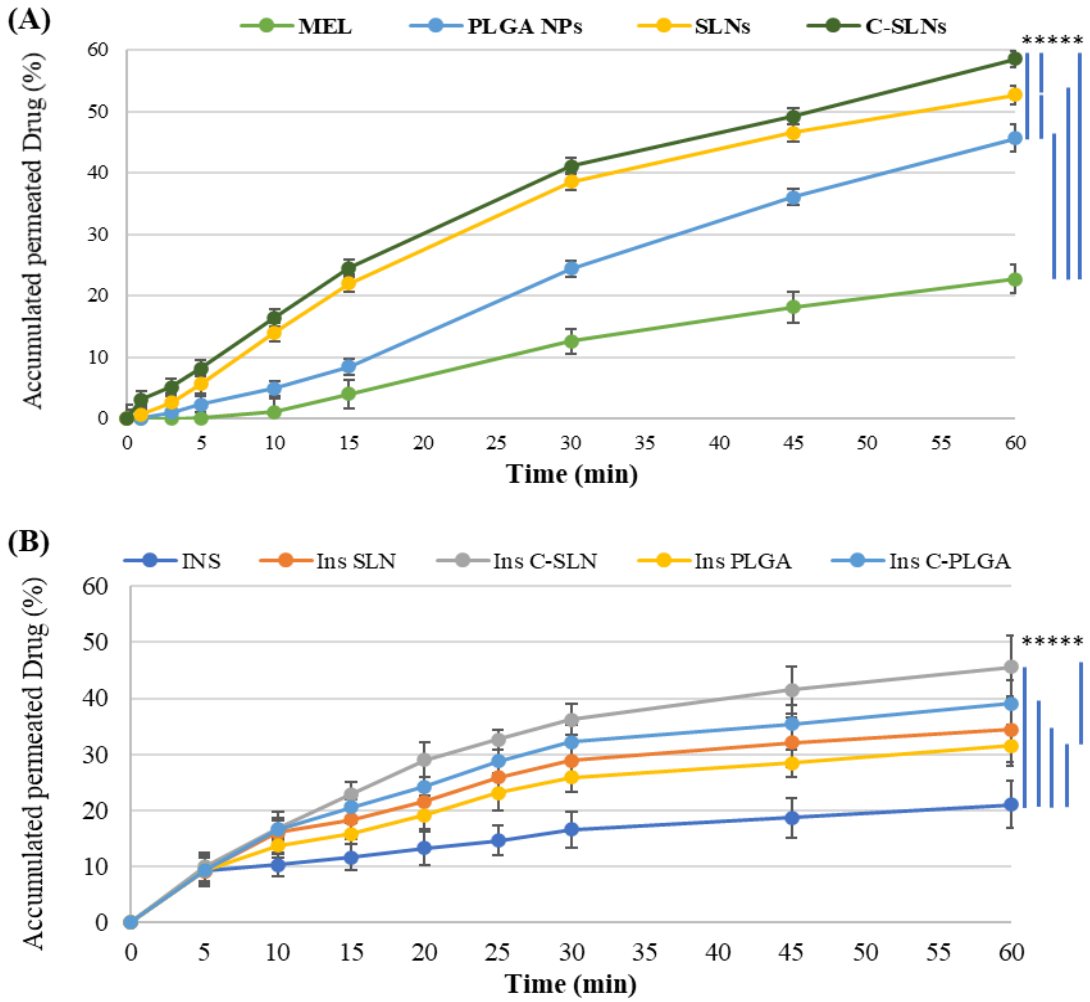

Figure 15. In vitro diffusion of native APIs and their NPS from which A represents MEL case and B represents INS cas. ANOVA test was performed to check the significance of the differences between the diffusion of the native insulin and the prepared NPs, * $p < 0.05$; ** $p < 0.01$; *** $p < 0.001$. Measurements were carried out in triplicate (n = 3 independent formulations), and data are represented as means ± SD.

A significant enhancement of native MEL and Ins permeability through the semi-permeable membrane was achieved when they were formulated in NPs compared to the pure APIs solution ($p<0.001$). This could be due to the nanoscale size of the prepared nanosystems and the increased specific surface area with the best nasal permeation properties, as previously reported by Gänger and Schindowski [134]. Moreover, the spherical and smooth surface of both NPs, as confirmed by SEM images, leads to the least friction with the membrane surface compared to the needle-shape particles. Stabilizing these NPs using poloxamer, a permeation enhancer, further improved their permeation properties [227] by inhibiting the efflux pumps and lowering the membrane fluidity when it is used *in vivo* [228].

Interestingly, SLNs showed significant superior permeability over PLGA NPs ($p<0.001$). This might be explained by the lipid-based nanosystem lipophilicity [229], which exceeds PLGA NPs lipophilicity [127]. Furthermore, surface modification of the NPs by chitosan resulted in better permeation than the uncoated SLNs ($p<0.001$), and this could be due to this polymer permeation enhancement properties [230]. The permeation test results are in correlation with the mucoadhesion results. The higher mucoadhesion properties will increase the contact time of the NPs with the nasal mucosa, leading to a higher residence time inside the nose and a decrease in the mucociliary clearance; thus, giving the NPs enough time and better chances to permeate. This could be translated *in vivo* by increasing the paracellular transport by opening the tight junctions and enhancing mucoadhesion properties [231].

The *in vitro* tests provide a proof on the possible direct N2B transport of the NPs after the nasal application. This starts by protecting the API and sustaining its *in vitro* release. Besides, PLGA NPs, SLNs, and CSLNs enhanced the mucoadhesion properties, which can prolong their contact with the olfactory region, and thus, with the olfactory nerve endings for a longer time. Accordingly, this would improve NPs direct transport to the brain via the olfactory pathway.

Both SLNs and PLGA NPs have already been employed to deliver the intranasally applied drug molecules to the brain directly. The development of drug-SLNs has already been reported with the *in vitro* and *in vivo* evaluation of several APIs, including galantamine [232], donepezil [233], haloperidol [195], paeonol [234], astaxanthin [235] and pueraria flavones [236]. On the other hand, formulating PLGA NPs was an efficient tool employed successfully to enhance brain delivery of

the drugs such as olanzapine [237], Diazepam [238], Midazolam [239], lamotrigine [240], temozolomide [241], and Huperzine [242].

5.4. *In vitro - in vivo* correlation (IVIVC) for Mel NPs

As shown in **Figure 16**, Pearson correlation coefficients confirm good agreement both in vitro dissolution (0.9694) and permeation (0.9957) [213]. According to $AUC_{0\text{-}60}$min values of in vitro dissolution (**Table 6**), in vitro permeation, and in vivo brain distribution, the comparative studies emphasized a significant difference between the measured in vitro and estimated in vivo results of the prepared NPs compared to the pure MEL.

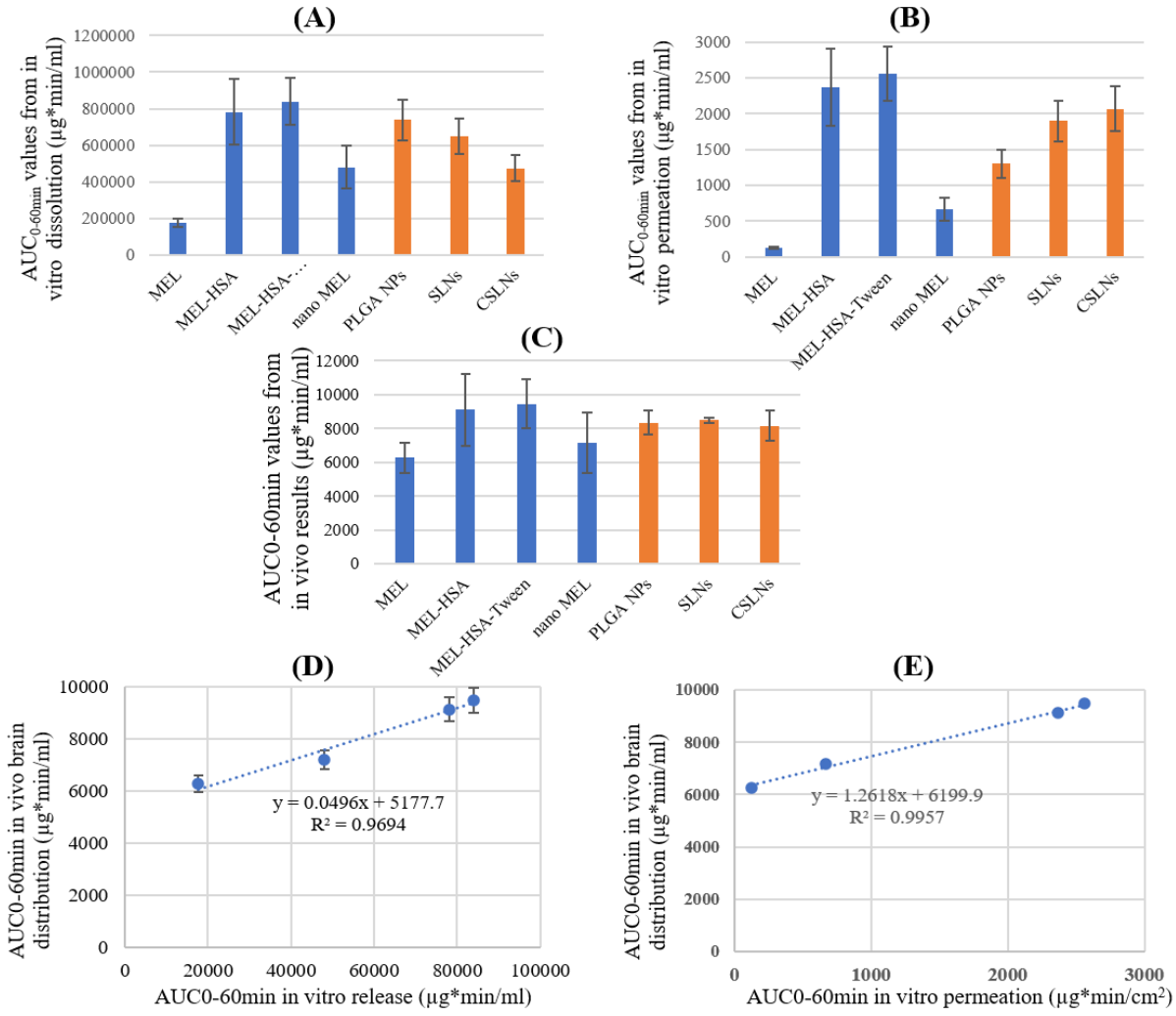

Figure 16. IVIVC diagrams from which: (A) $AUC_{0-60\ min}$ values of the in vitro dissolution test results; (B) $AUC_{0-60\ min}$ values of the in vitro permeation test; (C) $AUC_{0-60\ min}$ values of preliminary in vivo results and estimated $AUC_{0-60\ min}$ values of the prepared formulations (D) Pearson correlation based on dissolution; (E) Pearson correlation based on permeation

Table 6 Input parameter and estimated outcomes of IVIVC. Data are presented as means ± SD, n = 6.

	$AUC_{0\text{-}60min}$ *in vitro* dissolution	$AUC_{0\text{-}60min}$ *in vitro* diffusion	$AUC_{0\text{-}60min}$ *in vivo* brain distribution	Estimated $AUC_{0\text{-}60min}$ *in vivo* brain distribution
	*ug*min/ml*	*ug/cm^2*min*	*ug*min/ml*	*ug*min/ml*
MEL	176.7 ± 24.74	123.5 ±17.3	6.3 ±0.9	
MEL-HSA	780.8 ± 179.6	2370.8 ± 545.3	9.1 ± 2.1	
MEL-HSA-Tween	839.9 ± 126	2560.2 ±384	9.5 ± 1.5	
nano MEL	480.5 ± 115.3	667.5 ±160.2	7.2 ± 1.8	
PLGA NPs	738.5 ± 110.8	1304.6 ±195.7		8.3 ± 0.7
SLNs	649.1 ±97.4	1900.3 ±285		8.4 ± 0.1
CSLNs	473.5 ±71	2071.2 ±310.7		8.1 ± 0.9

As the regression curves show, a possible *in vivo* brain distribution profiles of MEL-PLGA NPs, MEL-SLNs and C-MEL-SLNs were estimated to 8.3 ± 0.7, 8.4 ± 0.1, and 8.1 ± 0.9 μg.min/ml, respectively. Since IVIVC results of the prepared nanoformulations showed consistent results with the previous *in vivo* studies and estimated the excellent potential for *in vivo* brain distribution of MEL; they may hold a great promise to deliver MEL to the brain after the nasal application [127, 176, 182].

5.5. In Vitro Cell Line Studies for Ins NPs

5.5.1. Permeability Studies on Human RPMI 2650 Nasal Epithelial Cell Culture

The permeability of insulin was tested on the nasal epithelial and brain endothelial cell barrier models (**Figure 17**).

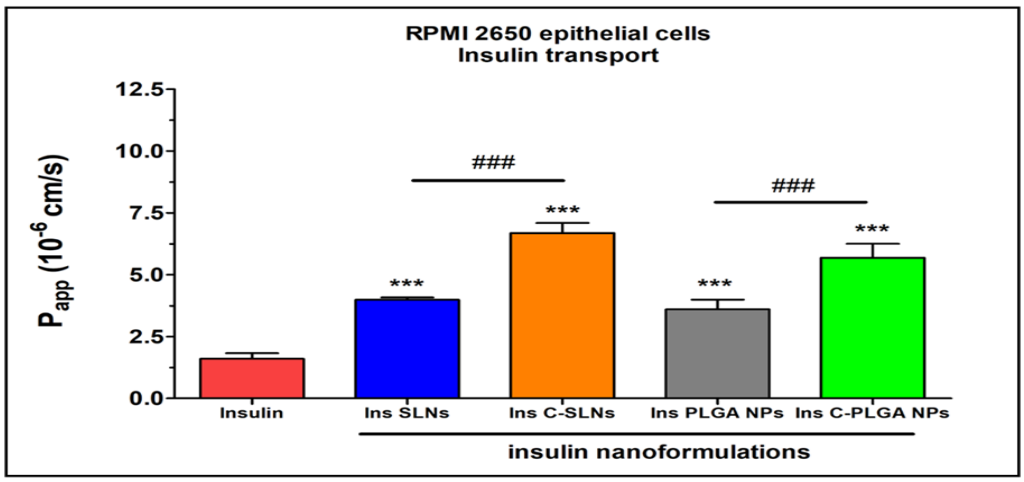

Figure 17. Apparent permeability coefficients (P_{app}) for insulin (0.07 mg/ml in all samples) when applied alone or in different formulations measured across RPMI 2650 epithelial cell layers after 1 hour incubation. Values are presented as means ± SD, n = 4. Statistical analysis: ANOVA followed by Bonferroni test. *** $p < 0.001$ compared to the insulin group, $^{###}$ $p < 0.01$ compared between the indicated groups.

The results of the *in vitro* cell lines nasal permeability test confirmed the previously performed *in vitro* tests that the transport of insulin was lower in the case of the SLNs, and the PLGA-NP (P_{app}: $\leq 5 \times 10^{-6}$ cm/s) compared to the chitosan-coated NPs (Ins C-SLN and Ins C-PLGA NP; Figures 3 and 4). The permeability coefficients of the chitosan-coated NPs were $\geq 6 \times 10^{-6}$ cm/s on both models (**Figure 17** and **18**). The reason for this effect is due to the unique biological properties of chitosan. Chitosan is a linear cationic polysaccharide that is among others non-toxic, biodegradable, and has antibacterial and antimicrobial activity, furthermore, it can enhance the paracellular permeability of biological barriers by modulating tight junction proteins [243]. In the case of the nasal epithelial barrier model, the NPs showed significantly higher permeability (1 to 4-fold) than insulin alone, therefore the NPs increased the flux of insulin through the nasal barrier [244].

5.5.2. Permeability Studies on Human hCMEC/D3 Brain Endothelial Cell Line

The brain endothelial barrier model showed high permeability for free insulin compared to the NPs (**Figure 18**).

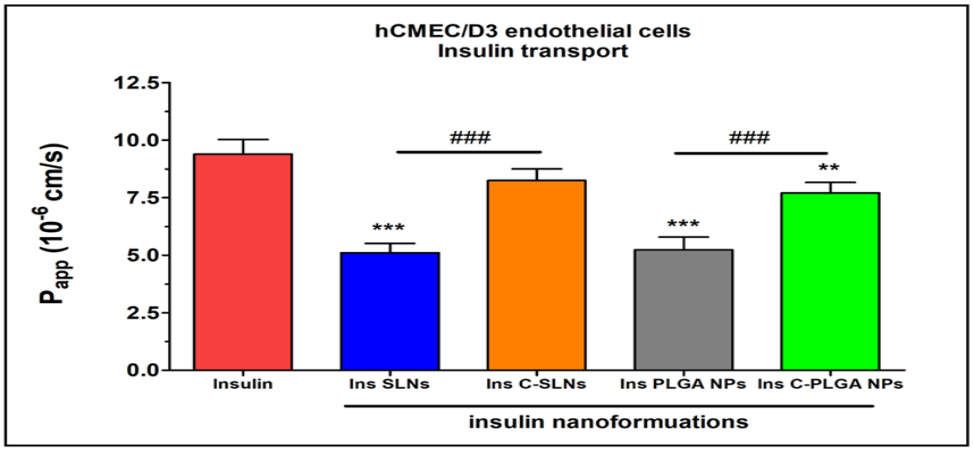

Figure 18. Apparent permeability coefficients (P_{app}) for insulin (0.07 mg/ml in all samples) when applied alone or in different formulations measured across hCMEC/D3 endothelial cell layers after 1 hour incubation. Values are presented as means ± SD, n = 4. Statistical analysis: ANOVA followed by Bonferroni test. *** $p < 0.001$ compared to the insulin group. ### $p < 0.01$ compared between the indicated groups. C-: chitosan coated nanoparticle; NPs: nanoparticles; PLGA: poly (lactic-co-glycolic acid; SLN: solid lipid nanoparticle.

The difference in the insulin permeability between the two types of barrier models was almost one order to magnitude. The permeability coefficient was 1.6×10^{-6} for insulin in the case of the nasal barrier model and 9.4×10^{-6} for the blood-brain barrier model. The reason for this difference could be the physiological function of these barriers. Insulin, as a hormone, has an important role in

blood glucose level regulations in the brain; therefore, the brain endothelial cells contain the highest level of insulin receptors in the human body [245]. The high insulin receptor expression in hCMEC/D3 cells was verified in a quantitative proteomic study [246].

There were no significant differences between the recovery values of the different investigated insulin groups (**Table 7**). In general, permeability assays are considered reliable if the recovery of the molecule after permeability assay is ~ 70%. Furthermore, the tight barrier integrity of brain endothelial cell layers was confirmed by the low P_{app} values of BBB marker molecules.

Table 7 Recovery (mass balance) calculation after insulin permeability on the nasal epithelial and on the brain endothelial barrier model.

Recovery (%) mean±SD		
Formulation	**RPMI 2650**	**hCMEC/D3**
Insulin	77.9 ± 3.9	87.9 ± 2.9
Ins SLNs	71.8 ± 2.9	72.5 ± 2.05
Ins C-SLNs	95.6 ± 22.8	73.5 ± 3.2
Ins PLGA NPs	61.3 ± 4.4	62.01 ± 3.9
Ins C-PLGA NPs	66.4 ± 3.9	72.8 ± 3.1

5.5.3. Cell Viability Measurement

The impedance measurement is a sensitive method for detecting the cellular effects in real-time. Neither RPMI 2650 epithelial cells nor D3 endothelial cells showed notable cell damage after treatments with insulin and insulin-containing NPs (**Figure 19** and **20**).

As a comparison, the reference compound Triton X-100 detergent caused cell death, as reflected by the decrease in impedance in both cell types. **Figure 19A** and **20A** show the kinetics of the cellular effects of treatment solutions, while the columns on **Figure 19B** and **20B** show the effect of insulin and encapsulated NPs at the 1-hour time point.

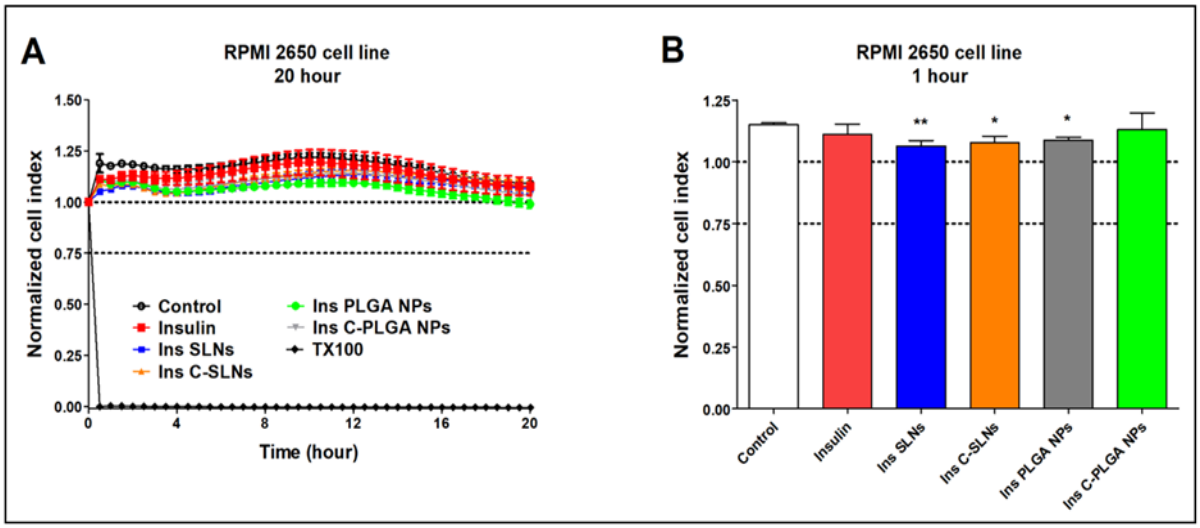

Figure 19. Cell viability of RPMI 2650 nasal epithelial cells after treatment with insulin, insulin NPs, and HCl measured by impedance. The kinetic curve of cell viability during the 20-hour treatment (A) and at the 1-hour time point of the treatment (B). Values are presented as means ± SD, n = 6-12. Statistical analysis: ANOVA followed by Dunett's test. TX-100: Triton X-100. * $p < 0.05$, ** $p < 0.01$ compared to the control group.

The kinetic curves of the NPs ran similarly to the untreated control group during the treatment in both epithelial and endothelial models (**Figure 19A** and **20A**). In the case of the hCMEC/D3 cells a slight decrease in cell index values could be observed in two NPs groups (Ins PLGA-NPs and Ins C-PLGA-NPs), however, the cell index values remained above 0.75, which refers to a non-toxic range. The significant differences observed at both cell types (**Figure 19B** and **20B**) at the 1-hour time point are due to the extremely low standard deviation and not because of the toxic effect of treatments. The non-toxic effects of the NPs were verified by a permeability assay after the insulin transport study: the permeability for paracellular marker molecules was unchanged or even lower indicating tight barrier integrity of the model (**Figure 21**).

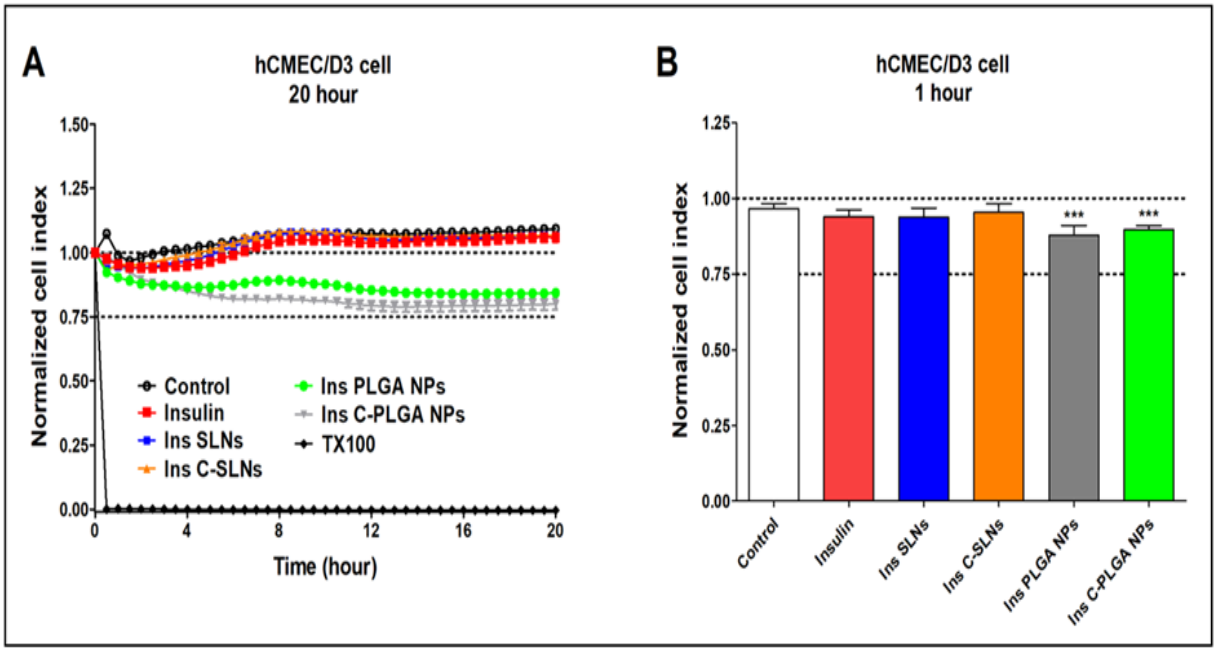

Figure 20. Cell viability of hCMEC/D3 endothelial cells after treatment with insulin, Ins NPs, and HCl measured by impedance. The kinetic curve of cell viability during the 20-hour treatment (A) and at the 1-hour time point of the treatment (B). Values are presented as means ± SD, n = 6-12. Statistical analysis: ANOVA followed by Dunett's test. TX-100: Triton X-100. *** $p < 0.001$ compared to the control group.

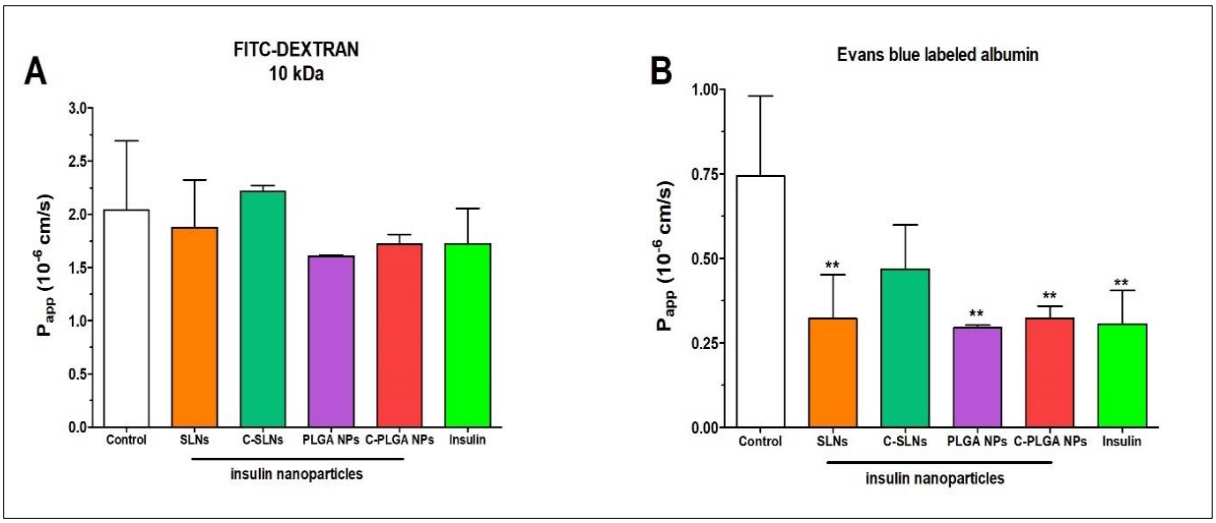

Figure 21. Apparent permeability coefficients (P_{app}) of passive paracellular permeability markers FITC-Dextran (10 kDa) (A) and Evan's blue labelled albumin (EBA, 67.5 kDa) (B) across RPMI 2650 epithelial cell layers after the 1-hour transport study of insulin. Permeability assay lasted for 30 minutes. Values are presented as means ± SD, n = 3. Statistical analysis: ANOVA followed by Dunett's test. **P<0.01, compared to the control group

In the case of brain endothelial cells paracellular permeability for marker molecules was performed parallelly with insulin transport study for 1 hour (**Figure 22**). The concentrations of the marker molecules in the samples from the compartments were determined by a fluorescence multiwall plate reader (Fluostar Optima, BMG Lab technologies, Germany; FITC: excitation wavelength: 485 nm, emission wavelength: 520 nm; Evan's-blue labeled albumin: excitation wavelength: 584 nm, emission wavelength: 680 nm).

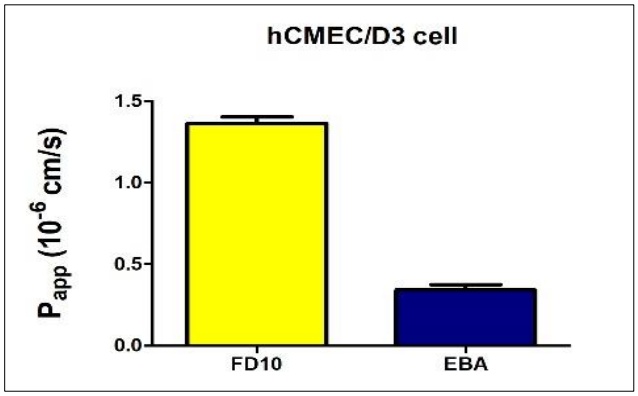

Figure 22. Apparent permeability coefficients (P_{app}) of passive paracellular permeability markers FITC-Dextran (10 kDa) (A) and Evan's blue labelled albumin (EBA, 67.5 kDa) (B) across D3 endothelial cell layers after the 1-hour transport study of insulin. Permeability assay lasted for 30 minutes. Values are presented as means ± SD, n = 3.

6. CONCLUSIONS

Since MEL is a well-reported and widely available anti-neuroinflammation agent, using it in AD management holds great promise. However, its brain concentration following the conventional administration routes is too low. On the other hand, insulin has a multifactorial role in the brain and takes part in the clearance of the amyloid β peptide and phosphorylation of tau through the proteostasis, it can be employed in ameliorating AD by restoring the cerebral insulin function. None the less, the delicate structure and the complex pathway following the conventional administration routes may lower its brain bioavailability. No previously reported studies for formulating meloxicam as coated or uncoated nanoparticles for the IN application aiming to deliver it directly to the brain, while it is limited to find nanoformulated insulin for the IN application with the aim of brain targeting, even though the IN administration of insulin NPs might overcome the drawback presented by the high molecular weight of insulin that can affect the proper delivery to the brain.

In this study, the QbD concept was successfully employed to thoroughly understand and optimize the process parameters affecting the CQAs when developing nanoformulations for N2B delivery after the IN application.

Compared to MEL PLGA NPs, MEL SLNs showed smaller particle size, higher EE and DL while showing a better-sustained release profile. Moreover, the coating with chitosan showed a superior sustaining release behavior over the uncoated NPs. The mucoadhesion properties of C-MEL-SLNs demonstrated 1.25 and 2-fold enhancement over the MEL-SLNs and MEL-PLGA NPs, respectively. The results of *in vivo-in vitro* correlation of MEL NPs confirmed that the "measured" in vitro and "estimated" in vivo characteristics and behavior of PLGA NPs and SLNs are expected to be better than the native MEL. Our findings provide the first reported evidence for the potentiality of encapsulating MEL in both polymeric and lipid NPs for IN application with the superiority of SLNs, which properties were further enhanced by coating with cationic polymer chitosan.

On the other hand, four types of NPs were formulated successfully (Ins SLNs, Ins PLGA NPs, C-Ins-SLNs, and C-PLGA-NPs) with optimal Z-average and ZP characteristics for the brain-delivery of IN insulin. The findings of the present research work shed the light on the potentiality of the encapsulated insulin in both Ins SLNs and Ins PLGA NPs for the IN application with the superiority of SLN and the positive enhancing effect of the chitosan-coating. The *in vitro* tests showed that compared to Ins-PLGA NPs, Ins-SLNs showed lower Z-average, higher EE and DL while ensuring the better insulin sustaining release profile. Moreover, the Ins C-SLNs and Ins C-PLGA NPs showed a promoted sustaining-release behavior and better mucoadhesion properties over the native insulin and the uncoated NPs. Finally, the permeation of the Ins-SLNs and Ins-PLGA NPs was better than the native insulin and was improved by chitosan-coating.

The *in vitro* cell line experiments proved the safety of prepared NPs for the IN application. Furthermore, the permeation of insulin through the nasal mucosa was the highest in the case of C-Ins-SLNs outperforming the C-Ins-PLGA NPs and the uncoated NPs, which were better than the native insulin. On the other hand, the permeability test showed the superiority of the native insulin in brain endothelial barrier model over the prepared NPs, from which the Ins C-SLNs excelled the Ins C-PLGA NPs followed by Ins SLNs, then Ins-PLGA-NPs. Thus, an optimal nose-to-brain

formulation can be obtained using a mixture of the native insulin and Ins C-SLNs. The former ensures the rapid effect, and the latter keeps it for a longer time.

7. Novelty and practical aspects

The delivery of hydrophilic drug moieties especially with the high molecular weight and macro-structure to the brain requires the need of high bioavailability to achieve the targeted therapeutic outcomes. Industrially, selecting the preparation method and delivery strategy does not only depend on the desired therapeutic targets, but also on the technical features, namely: simplicity, scalability, and productivity including the time and costs needed.

- The novelty and strength of this research work come from the ability to optimize and harmonize different aspects starting by analyzing the literature, moving to selecting the administration route, then producing meloxicam and insulin in new dosage forms that has not been studied and developed before.
- Implementing QbD aspects justified the selection of the methodologies and significantly promote the recognizability of seizing optimized formulations based on predefined quality and safety aspects.
- Optimization of critical parameters to produce meloxicam and insulin nanoparticles is considered a significant step toward extending the application of double emulsion solvent evaporation method to formulate different APIs as SLNs and PLGA NPs forms. By these findings, this method can compete with the top-down one in the development of potential products for the market.
- This work provides the first reported evidence for the potential of meloxicam and insulin encapsulation in both polymeric and lipid NPs in the IN delivery with significant SLNs superiority, and their properties were further enhanced by coating with the cationic polymer chitosan. Accordingly, a thorough comparison was performed in vitro, followed by selecting the optimized NPs to be a potential carrier for the IN application of insulin, a potential anti AD drug, with the aim of brain-targeting.
- The cell viability tests proofed the safety of the nanoparticles, and the non-toxic effects of the NPs were verified by a permeability assay, which allows the safe application of these nanoparticles especially after demonstrating good permeation properties through the nasal mucosa and the BBB.

- The obtained SLNs and PLGA NPs can be applied intranasally as a lyophilized powder, which proof their budget friendly usage. The application of lyophilized powdered SLNs and PLGA NPs intranasally with the aim of brain targeting is a new approach in pharmaceutical technology.

8. ACKNOWLEDGEMENTS

Firstly, I would like to express my sincere gratitude to my supervisor and head of department Prof. Ildikó Csóka for giving me the opportunity to pursue my Ph.D. under her supervision. Thank you for the constant support, motivation, and immense knowledge.

I would like to thank Dr. Gábor Katona for hir kindness and great support during my work. His guidance helped me in all every step of the research and writing of this thesis. I could not have imagined having a better advisor and mentor for my Ph.D. study.

I would also thank the laboratory technicians, particularly, Piroska Lakatosné for her care and help that made the hard things easier.

Then, I would like to thank all my colleagues and friends for their moral and scientific support.

I would acknowledge the financial support of the stipendium Hungaricum Program, Ministry of Human Capacities, Hungary (Grant TKP-2020), and the National Research, Development and Innovation Office, Hungary (GINOP 2.3.2-15-2016-00060).

My last words are dedicated to my family. Thanks for your support and encouragement during these years. I know how hard it was to be away, but you have been with me during all the moments of sadness or joy.

9. FINANCIAL SUPPORT

The authors want to express their acknowledgment to the supporters. This study was supported by the Ministry of Human Capacities, Hungary (Grant TKP-2020), and by the National Research, Development and Innovation Office, Hungary (GINOP 2.3.2-15-2016-00060), projects.

10. REFERENCES

1. Akel, H., R. Ismail, and I. Csóka, *Progress and perspectives of brain-targeting lipid-based nanosystems via the nasal route in Alzheimer's disease.* European Journal of Pharmaceutics and Biopharmaceutics, 2020. **148**: p. 38-53.
2. Nowacek, A., L.M. Kosloski, and H.E. Gendelman, *Neurodegenerative disorders and nanoformulated drug development.* Nanomedicine (London, England), 2009. **4**(5): p. 541-555.
3. Weimer, D.L. and M.A. Sager, *Early identification and treatment of Alzheimer's disease: social and fiscal outcomes.* Alzheimers Dement, 2009. **5**(3): p. 215-26.
4. Querbes, O., et al., *Early diagnosis of Alzheimer's disease using cortical thickness: impact of cognitive reserve.* Brain, 2009. **132**(Pt 8): p. 2036-47.
5. Listerud, J., et al., *Neuropsychological patterns in magnetic resonance imaging-defined subgroups of patients with degenerative dementia.* J Int Neuropsychol Soc, 2009. **15**(3): p. 459-70.
6. Pihlajamäki, M., A.M. Jauhiainen, and H. Soininen, *Structural and functional MRI in mild cognitive impairment.* Curr Alzheimer Res, 2009. **6**(2): p. 179-85.
7. Chauvire, V., et al., *[Frontotemporal dementia: a review].* Encephale, 2007. **33**(6): p. 933-40.
8. Galariotis, V., et al., *Frontotemporal dementia--Part II. Differential diagnosis, genetics, molecular pathomechanism and pathology.* Ideggyogy Sz, 2005. **58**(7-8): p. 220-4.
9. Nerelius, C., J. Johansson, and A. Sandegren, *Amyloid beta-peptide aggregation. What does it result in and how can it be prevented?* Front Biosci (Landmark Ed), 2009. **14**(5): p. 1716-29.
10. Watson, D., et al., *Physicochemical characteristics of soluble oligomeric Abeta and their pathologic role in Alzheimer's disease.* Neurol Res, 2005. **27**(8): p. 869-81.
11. Salloway, S., et al., *Disease-modifying therapies in Alzheimer's disease.* Alzheimers Dement, 2008. **4**(2): p. 65-79.
12. Rafii, M.S. and P.S. Aisen, *Recent developments in Alzheimer's disease therapeutics.* BMC Med, 2009. **7**: p. 7.
13. Golde, T.E., *Disease modifying therapy for AD?* J Neurochem, 2006. **99**(3): p. 689-707.
14. Sigurdsson, E.M., *Immunotherapy targeting pathological tau protein in Alzheimer's disease and related tauopathies.* J Alzheimers Dis, 2008. **15**(2): p. 157-68.
15. Gardiner, J., et al., *Neurotrophic support and oxidative stress: converging effects in the normal and diseased nervous system.* Neuroscientist, 2009. **15**(1): p. 47-61.
16. Block, M.L., *NADPH oxidase as a therapeutic target in Alzheimer's disease.* BMC Neurosci, 2008. **9 Suppl 2**(Suppl 2): p. S8.
17. Rojo, L.E., et al., *Neuroinflammation: implications for the pathogenesis and molecular diagnosis of Alzheimer's disease.* Arch Med Res, 2008. **39**(1): p. 1-16.
18. Nazem, A. and G.A. Mansoori, *Nanotechnology solutions for Alzheimer's disease: advances in research tools, diagnostic methods and therapeutic agents.* J Alzheimers Dis, 2008. **13**(2): p. 199-223.
19. Agrawal, M., et al., *Nose-to-brain drug delivery: An update on clinical challenges and progress towards approval of anti-Alzheimer drugs.* Journal of controlled release, 2018. **281**: p. 139-177.
20. Cummings, J., et al., *Role of donepezil in the management of neuropsychiatric symptoms in Alzheimer's disease and dementia with Lewy bodies.* CNS neuroscience & therapeutics, 2016. **22**(3): p. 159-166.
21. Holmes, C., et al., *The efficacy of donepezil in the treatment of neuropsychiatric symptoms in Alzheimer disease.* Neurology, 2004. **63**(2): p. 214-219.
22. Bryan, J., *Donepezil—a major breakthrough in the treatment of Alzheimer's disease.* Suicide, 2019. **14**: p. 20.

23. Black, S., et al., *Donepezil preserves cognition and global function in patients with severe Alzheimer disease.* Neurology, 2007. **69**(5): p. 459-469.
24. Kumar, V., *Potential medicinal plants for CNS disorders: an overview.* Phytotherapy Research: An International Journal Devoted to Pharmacological and Toxicological Evaluation of Natural Product Derivatives, 2006. **20**(12): p. 1023-1035.
25. Nieto, R.A., W.J. Deardorff, and G.T. Grossberg, *Efficacy of rivastigmine tartrate, transdermal system, in Alzheimer's disease.* Expert opinion on pharmacotherapy, 2016. **17**(6): p. 861-870.
26. Foster, P., et al., *Donepezil Versus Rivastigmine in Patients with Alzheimer's Disease: Attention and Working Memory.* Journal of Alzheimer's Neurodegenerative Disease, 2016. **2**(002).
27. Mucke, H.A., *The case of galantamine: repurposing and late blooming of a cholinergic drug.* Future science OA, 2015. **1**(4).
28. Prvulovic, D., H. Hampel, and J. Pantel, *Galantamine for Alzheimer's disease.* Expert opinion on drug metabolism & toxicology, 2010. **6**(3): p. 345-354.
29. Farlow, M.R., S.M. Graham, and G. Alva, *Memantine for the Treatment of Alzheimer's Disease.* Drug safety, 2008. **31**(7): p. 577-585.
30. Ishikawa, I., et al., *The effect of memantine on sleep architecture and psychiatric symptoms in patients with Alzheimer's disease.* Acta neuropsychiatrica, 2016. **28**(3): p. 157-164.
31. Hughes, L.D., *Memantine for fibromyalgia and Alzheimer's disease: An observational case comparison.* British Journal of Mental Health Nursing, 2017. **6**(1): p. 29-34.
32. Nafar, F., J. Clarke, and K. Mearow, *Coconut oil protects cortical neurons from amyloid beta toxicity by enhancing signaling of cell survival pathways.* Neurochemistry international, 2017. **105**: p. 64-79.
33. Olanrewaju, J., et al., *Effects of Virgin Coconut Oil on Aluminium Chloride-Induced Alzheimer-Like Dementia in the Prefrontal Cortex.* Journal of Advances in Medical and Pharmaceutical Sciences, 2018: p. 1-12.
34. Bansal, A., et al., *Coconut oil decreases expression of amyloid precursor protein (APP) and secretion of amyloid peptides through inhibition of ADP-ribosylation factor 1 (ARF1).* Brain research, 2019. **1704**: p. 78-84.
35. Omidi, G., et al., *Effect of coenzyme Q10 supplementation on diabetes induced memory deficits in rats.* Metabolic brain disease, 2019: p. 1-8.
36. Monsef, A., S. Shahidi, and A. Komaki, *Influence of Chronic Coenzyme Q10 Supplementation on Cognitive Function, Learning, and Memory in Healthy and Diabetic Middle-Aged Rats.* Neuropsychobiology, 2019. **77**(2): p. 92-100.
37. Zeng, K., et al., *Ginkgo biloba extract EGb761 attenuates Hyperhomocysteinemia-induced AD like tau hyperphosphorylation and cognitive impairment in rats.* Current Alzheimer Research, 2018. **15**(1): p. 89-99.
38. Liu, X., et al., *Long-term treatment with Ginkgo biloba extract EGb 761 improves symptoms and pathology in a transgenic mouse model of Alzheimer's disease.* Brain, behavior, and immunity, 2015. **46**: p. 121-131.
39. Stein, C., et al., *Effects of Ginkgo biloba extract EGb 761, donepezil and their combination on central cholinergic function in aged rats.* Journal of Pharmacy & Pharmaceutical Sciences, 2015. **18**(4): p. 634-646.
40. Meng, Q., et al., *Intranasal delivery of Huperzine A to the brain using lactoferrin-conjugated N-trimethylated chitosan surface-modified PLGA nanoparticles for treatment of Alzheimer's disease.* International journal of nanomedicine, 2018. **13**: p. 705.
41. Gul, A., J. Bakht, and F. Mehmood, *Huperzine-A response to cognitive impairment and task switching deficits in patients with Alzheimer's disease.* Journal of the Chinese Medical Association, 2018.

42. Tabira, T. and N. Kawamura, *A study of a supplement containing huperzine a and curcumin in dementia patients and individuals with mild cognitive impairment.* Journal of Alzheimer's Disease, 2018(Preprint): p. 1-4.
43. Wang, L., et al., *Protective effects of omega-3 fatty acids against Alzheimer's disease in rat brain endothelial cells.* Brain and behavior, 2018. **8**(11): p. e01037.
44. Fang, G., et al., *The protective role of endogenous n-3 polyunsaturated fatty acids in Tau Alzheimer's disease mouse model.* International Journal of Neuroscience, 2019. **129**(4): p. 325-336.
45. Nolan, J.M., et al., *Nutritional intervention to prevent alzheimer's disease: potential benefits of xanthophyll carotenoids and omega-3 fatty acids combined.* Journal of Alzheimer's Disease, 2018. **64**(2): p. 367-378.
46. Sharman, M.J., et al., *Assessment of diets containing curcumin, epigallocatechin-3-gallate, docosahexaenoic acid and α-lipoic acid on amyloid load and inflammation in a male transgenic mouse model of Alzheimer's disease: Are combinations more effective?* Neurobiology of disease, 2019. **124**: p. 505-519.
47. Liu, Z., et al., *Curcumin improves learning and memory ability via inhibiting activated microglia-mediated inflammation in mouse models of Alzheimer's disease.* INTERNATIONAL JOURNAL OF CLINICAL AND EXPERIMENTAL MEDICINE, 2018. **11**(11): p. 12204-12210.
48. Lu, W.T., et al., *Curcumin Ameliorates Memory Deficits by Enhancing Lactate Content and MCT2 Expression in APP/PS1 Transgenic Mouse Model of Alzheimer's Disease.* The Anatomical Record, 2019. **302**(2): p. 332-338.
49. Abushakra, S., et al., *Clinical benefits of tramiprosate in Alzheimer's disease are associated with higher number of APOE4 alleles: the ''APOE4 gene-dose effect''.* J Prev Alz Dis, 2016. **3**(4): p. 219-228.
50. Abushakra, S., *CLINICALLY MEANINGFUL COGNITIVE AND FUNCTIONAL IMPROVEMENTS WITH TRAMIPROSATE IN ALZHEIMER'S DISEASE (AD) PATIENTS WITH APOE4/4 GENOTYPE: SUBGROUP ANALYSES FROM TWO PHASE 3 STUDIES.* Alzheimer's & Dementia: The Journal of the Alzheimer's Association, 2016. **12**(7): p. P1185.
51. Nishioka, H., et al., *BMS-708163 and Nilotinib restore synaptic dysfunction in human embryonic stem cell-derived Alzheimer's disease models.* Scientific reports, 2016. **6**: p. 33427.
52. Lonskaya, I., et al., *Nilotinib and bosutinib modulate pre-plaque alterations of blood immune markers and neuro-inflammation in Alzheimer's disease models.* Neuroscience, 2015. **304**: p. 316-327.
53. Lonskaya, I., et al., *Nilotinib-induced autophagic changes increase endogenous parkin level and ubiquitination, leading to amyloid clearance.* Journal of Molecular Medicine, 2014. **92**(4): p. 373-386.
54. Kullmann, S., et al., *Brain insulin resistance at the crossroads of metabolic and cognitive disorders in humans.* Physiological reviews, 2016. **96**(4): p. 1169-1209.
55. Suzanne, M., *Type 3 diabetes is sporadic Alzheimer' s disease: mini-review.* European Neuropsychopharmacology, 2014. **24**(12): p. 1954-1960.
56. Willette, A.A., et al., *Association of insulin resistance with cerebral glucose uptake in late middle–aged adults at risk for Alzheimer disease.* JAMA neurology, 2015. **72**(9): p. 1013-1020.
57. Morris, J.K., et al., *Cognitively impaired elderly exhibit insulin resistance and no memory improvement with infused insulin.* Neurobiology of aging, 2016. **39**: p. 19-24.
58. Grillo, C.A., et al., *Hippocampal insulin resistance impairs spatial learning and synaptic plasticity.* Diabetes, 2015. **64**(11): p. 3927-3936.
59. Ma, L., et al., *Insulin resistance is an important risk factor for cognitive impairment in elderly patients with primary hypertension.* Yonsei medical journal, 2015. **56**(1): p. 89-94.

60. Ekblad, L.L., et al., *Insulin resistance is associated with poorer verbal fluency performance in women.* Diabetologia, 2015. **58**(11): p. 2545-2553.
61. Willette, A.A., et al., *Insulin resistance predicts brain amyloid deposition in late middle-aged adults.* Alzheimer's & dementia, 2015. **11**(5): p. 504-510. e1.
62. Craft, S., et al., *Intranasal insulin therapy for Alzheimer disease and amnestic mild cognitive impairment: a pilot clinical trial.* Archives of neurology, 2012. **69**(1): p. 29-38.
63. Claxton, A., et al., *Long-acting intranasal insulin detemir improves cognition for adults with mild cognitive impairment or early-stage Alzheimer's disease dementia.* Journal of Alzheimer's Disease, 2015. **44**(3): p. 897-906.
64. Kamei, N. and M. Takeda-Morishita, *Brain delivery of insulin boosted by intranasal coadministration with cell-penetrating peptides.* Journal of controlled release, 2015. **197**: p. 105-110.
65. Yang, Y., et al., *Subcutaneous administration of liraglutide ameliorates Alzheimer-associated tau hyperphosphorylation in rats with type 2 diabetes.* Journal of Alzheimer's Disease, 2013. **37**(3): p. 637-648.
66. Liu, X.-Y., et al., *Liraglutide prevents beta-amyloid-induced neurotoxicity in SH-SY5Y cells via a PI3K-dependent signaling pathway.* Neurological research, 2016. **38**(4): p. 313-319.
67. Hunter, K. and C. Hölscher, *Drugs developed to treat diabetes, liraglutide and lixisenatide, cross the blood brain barrier and enhance neurogenesis.* BMC neuroscience, 2012. **13**(1): p. 33.
68. McClean, P.L., et al., *The diabetes drug liraglutide prevents degenerative processes in a mouse model of Alzheimer's disease.* Journal of Neuroscience, 2011. **31**(17): p. 6587-6594.
69. Gejl, M., et al., *In Alzheimer's disease, 6-month treatment with GLP-1 analog prevents decline of brain glucose metabolism: randomized, placebo-controlled, double-blind clinical trial.* Frontiers in aging neuroscience, 2016. **8**: p. 108.
70. Batista, A.F., et al., *The diabetes drug liraglutide reverses cognitive impairment in mice and attenuates insulin receptor and synaptic pathology in a non-human primate model of Alzheimer's disease.* The Journal of pathology, 2018. **245**(1): p. 85-100.
71. Sevigny, J., et al., *The antibody aducanumab reduces Aβ plaques in Alzheimer's disease.* Nature, 2016. **537**(7618): p. 50.
72. Budd, S.H., et al., *Clinical Development of Aducanumab, an Anti-Aβ Human Monoclonal Antibody Being Investigated for the Treatment of Early Alzheimer's Disease.* The journal of prevention of Alzheimer's disease, 2017. **4**(4): p. 255-263.
73. Haeberlein, S.B., et al., *Aducanumab 36-month data from PRIME: a randomized, double-blind, placebo-controlled Phase 1b study in patients with prodromal or mild Alzheimer's disease (S2. 004)*. 2018, AAN Enterprises.
74. von Rosenstiel, P., et al., *Aducanumab titration dosing regimen: 24-month analysis from PRIME, a randomized, double-blind, placebo-controlled Phase 1b study in patients with prodromal or mild Alzheimer's disease (S2. 003)*. 2018, AAN Enterprises.
75. Andjelkovic, M., et al., *UPDATE ON THE SAFETY AND TOLERABILITY OF GANTENERUMAB IN THE ONGOING OPEN-LABEL EXTENSION OF THE SCARLET ROAD STUDY IN PATIENTS WITH PRODROMAL ALZHEIMER'S DISEASE AFTER APPROXIMATELY 2 YEARS OF STUDY DURATION.* Alzheimer's & Dementia: The Journal of the Alzheimer's Association, 2018. **14**(7): p. P241-P242.
76. Ostrowitzki, S., et al., *Correction to: A phase III randomized trial of gantenerumab in prodromal Alzheimer's disease.* Alzheimer's research & therapy, 2018. **10**(1): p. 99.
77. Lombardo, I., et al., *Intepirdine (RVT-101), a 5-HT6 Receptor Antagonist, as an Adjunct to Donepezil in Mild-to-Moderate Alzheimer's Disease: Efficacy on Activities of Daily Living Domains.* The American Journal of Geriatric Psychiatry, 2017. **25**(3): p. S120-S121.

78. Molinuevo, J.L., et al., *RESPONDER ANALYSIS OF THE COGNITIVE EFFECT OF COMBINATION THERAPY WITH DONEPEZIL AND INTEPIRDINE (RVT-101) VERSUS DONEPEZIL MONOTHERAPY: RESULTS FROM A 48-WEEK MULTINATIONAL PLACEBO-CONTROLLED STUDY IN MILD TO MODERATE ALZHEIMER'S DISEASE.* Alzheimer's & Dementia: The Journal of the Alzheimer's Association, 2017. **13**(7): p. P259.
79. Sabbagh, M.N., et al., *DIFFERENCE IN COGNITIVE DECLINE BETWEEN COMBINATION THERAPY WITH DONEPEZIL AND INTEPIRDINE (RVT-101) AND DONEPEZIL MONOTHERAPY: RESULTS FROM A 48 WEEK MULTINATIONAL PLACEBO-CONTROLLED STUDY IN MILD TO MODERATE ALZHEIMER'S DISEASE.* Alzheimer's & Dementia: The Journal of the Alzheimer's Association, 2017. **13**(7): p. P263-P264.
80. Eketjäll, S., et al., *AZD3293: a novel, orally active BACE1 inhibitor with high potency and permeability and markedly slow off-rate kinetics.* Journal of Alzheimer's Disease, 2016. **50**(4): p. 1109-1123.
81. Cebers, G., et al., *AZD3293: Pharmacokinetic and pharmacodynamic effects in healthy subjects and patients with Alzheimer's disease.* Journal of Alzheimer's Disease, 2017. **55**(3): p. 1039-1053.
82. Egan, M.F., et al., *Randomized trial of verubecestat for prodromal alzheimer's disease.* New England Journal of Medicine, 2019. **380**(15): p. 1408-1420.
83. Egan, M.F., et al., *Randomized trial of verubecestat for mild-to-moderate Alzheimer's disease.* New England Journal of Medicine, 2018. **378**(18): p. 1691-1703.
84. Timmers, M., et al., *Pharmacodynamics of atabecestat (JNJ-54861911), an oral BACE1 inhibitor in patients with early Alzheimer's disease: randomized, double-blind, placebo-controlled study.* Alzheimer's research & therapy, 2018. **10**(1): p. 85.
85. Timmers, M., et al., *Evaluating Potential QT Effects of JNJ-54861911, a BACE Inhibitor in Single- and Multiple-Ascending Dose Studies, and a Thorough QT Trial With Additional Retrospective Confirmation, Using Concentration-QTc Analysis.* The Journal of Clinical Pharmacology, 2018. **58**(7): p. 952-964.
86. Parsons, C.G. and G. Rammes, *Preclinical to phase II amyloid beta (Aβ) peptide modulators under investigation for Alzheimer's disease.* Expert opinion on investigational drugs, 2017. **26**(5): p. 579-592.
87. Soares, H.D., et al., *The γ-secretase modulator, BMS-932481, modulates Aβ peptides in the plasma and cerebrospinal fluid of healthy volunteers.* Journal of Pharmacology and Experimental Therapeutics, 2016. **358**(1): p. 138-150.
88. Teich, A.F., et al., *Translational inhibition of APP by Posiphen: Efficacy, pharmacodynamics, and pharmacokinetics in the APP/PS1 mouse.* Alzheimer's & Dementia: Translational Research & Clinical Interventions, 2018. **4**: p. 37-45.
89. Hey, J.A., et al., *Clinical pharmacokinetics and safety of ALZ-801, a novel prodrug of tramiprosate in development for the treatment of Alzheimer's disease.* Clinical pharmacokinetics, 2018. **57**(3): p. 315-333.
90. Hey, J., et al., *Phase 1 development of ALZ-801, a novel beta amyloid anti-aggregation prodrug of tramiprosate with improved drug properties, supporting bridging to the phase 3 program.* Alzheimer's & Dementia: The Journal of the Alzheimer's Association, 2016. **12**(7): p. P613.
91. Mitchell, D., et al., *A phase 1 trial of TPI 287 as a single agent and in combination with temozolomide in patients with refractory or recurrent neuroblastoma or medulloblastoma.* Pediatric blood & cancer, 2016. **63**(1): p. 39-46.
92. Keefe, R.S., et al., *Randomized, double-blind, placebo-controlled study of encenicline, an α7 nicotinic acetylcholine receptor agonist, as a treatment for cognitive impairment in schizophrenia.* Neuropsychopharmacology, 2015. **40**(13): p. 3053.

93. Barbier, A.J., et al., *Pharmacodynamics, pharmacokinetics, safety, and tolerability of encenicline, a selective α7 nicotinic receptor partial agonist, in single ascending-dose and bioavailability studies.* Clinical therapeutics, 2015. **37**(2): p. 311-324.
94. Czerkowicz, J., et al., *ANTI-TAU ANTIBODY BIIB092 BINDS SECRETED TAU IN PRECLINICAL MODELS AND ALZHEIMER'S DISEASE CEREBROSPINAL FLUID.* Alzheimer's & Dementia: The Journal of the Alzheimer's Association, 2018. **14**(7): p. P1441.
95. Van Kampen, D., A. Maelicke, and J.M. Van Kampen, *MEMOGAIN REGULATES TAU PHOSPHORYLATION IN AN IMMUNOTOXIN MODEL OF CHOLINERGIC CELL LOSS.* Alzheimer's & Dementia: The Journal of the Alzheimer's Association, 2018. **14**(7): p. P1441-P1442.
96. Bhattacharya, S., A. Maelicke, and D. Montag, *Nasal application of the galantamine pro-drug memogain slows down plaque deposition and ameliorates behavior in 5X familial Alzheimer's disease mice.* Journal of Alzheimer's Disease, 2015. **46**(1): p. 123-136.
97. Maelicke, A., et al., *Memogain is a galantamine pro-drug having dramatically reduced adverse effects and enhanced efficacy.* Journal of molecular neuroscience, 2010. **40**(1-2): p. 135-137.
98. Zandi, P.P., et al., *Reduced risk of Alzheimer disease in users of antioxidant vitamin supplements: the Cache County Study.* Arch Neurol, 2004. **61**(1): p. 82-8.
99. Goverdhan, P., A. Sravanthi, and T. Mamatha, *Neuroprotective effects of meloxicam and selegiline in scopolamine-induced cognitive impairment and oxidative stress.* International journal of Alzheimer's disease, 2012. **2012**: p. 974013-974013.
100. Smith, W.L., D.L. DeWitt, and R.M. Garavito, *Cyclooxygenases: structural, cellular, and molecular biology.* Annual review of biochemistry, 2000. **69**(1): p. 145-182.
101. Ah, Y.C., et al., *A novel transdermal patch incorporating meloxicam: In vitro and in vivo characterization.* International Journal of Pharmaceutics, 2010. **385**(1-2): p. 12-19.
102. Ianiski, F.R., et al., *Meloxicam-loaded nanocapsules as an alternative to improve memory decline in an Alzheimer's disease model in mice: involvement of Na+, K+-ATPase.* Metabolic brain disease, 2016. **31**(4): p. 793-802.
103. Ianiski, F.R., et al., *Protective effect of meloxicam-loaded nanocapsules against amyloid-β peptide-induced damage in mice.* Behavioural Brain Research, 2012. **230**(1): p. 100-107.
104. Goverdhan, P., A. Sravanthi, and T. Mamatha, *Neuroprotective effects of meloxicam and selegiline in scopolamine-induced cognitive impairment and oxidative stress.* International Journal of Alzheimer's Disease, 2012. **2012**.
105. Nivsarkar, M., et al., *Reduction in aluminum induced oxidative stress by meloxicam in rat brain.* 2006.
106. Seedher, N. and S. Bhatia, *Mechanism of interaction of the non-steroidal antiinflammatory drugs meloxicam and nimesulide with serum albumin.* Journal of pharmaceutical and biomedical analysis, 2005. **39**(1-2): p. 257-262.
107. Badran, M.M., et al., *Ultra-fine self nanoemulsifying drug delivery system for transdermal delivery of meloxicam: dependency on the type of surfactants.* Journal of Molecular Liquids, 2014. **190**: p. 16-22.
108. Hanson, L.R. and W.H. Frey, *Intranasal delivery bypasses the blood-brain barrier to target therapeutic agents to the central nervous system and treat neurodegenerative disease.* BMC neuroscience, 2008. **9**(3): p. 1-4.
109. Freiherr, J., et al., *Intranasal Insulin as a Treatment for Alzheimer's Disease: A Review of Basic Research and Clinical Evidence.* CNS Drugs, 2013. **27**(7): p. 505-514.
110. Lochhead, J.J., et al., *Distribution of insulin in trigeminal nerve and brain after intranasal administration.* Scientific Reports, 2019. **9**(1): p. 2621.
111. Yang, Y., et al., *Intranasal Insulin Ameliorates Tau Hyperphosphorylation in a Rat Model of Type 2 Diabetes.* Journal of Alzheimer's Disease, 2013. **33**: p. 329-338.

112. Benedict, C., et al., *Intranasal insulin improves memory in humans.* Psychoneuroendocrinology, 2004. **29**(10): p. 1326-1334.
113. Craft, S., et al., *Intranasal Insulin Therapy for Alzheimer Disease and Amnestic Mild Cognitive Impairment: A Pilot Clinical Trial.* Archives of Neurology, 2012. **69**(1): p. 29-38.
114. Craft, S., et al., *Effects of Regular and Long-Acting Insulin on Cognition and Alzheimer's Disease Biomarkers: A Pilot Clinical Trial.* Journal of Alzheimer's Disease, 2017. **57**: p. 1325-1334.
115. Craft, S., et al., *Safety, Efficacy, and Feasibility of Intranasal Insulin for the Treatment of Mild Cognitive Impairment and Alzheimer Disease Dementia: A Randomized Clinical Trial.* JAMA Neurol, 2020. **77**(9): p. 1099-1109.
116. Giunchedi, P., E. Gavini, and M.C. Bonferoni, *Nose-to-Brain Delivery.* Pharmaceutics, 2020. **12**(2): p. 138.
117. Trevino, J.T., et al., *Non-Invasive Strategies for Nose-to-Brain Drug Delivery.* Journal of clinical trials, 2020. **10**(7): p. 439.
118. Mistry, A., S. Stolnik, and L. Illum, *Nanoparticles for direct nose-to-brain delivery of drugs.* International Journal of Pharmaceutics, 2009. **379**(1): p. 146-157.
119. Haque, S., et al., *Venlafaxine loaded chitosan NPs for brain targeting: Pharmacokinetic and pharmacodynamic evaluation.* Carbohydrate Polymers, 2012. **89**(1): p. 72-79.
120. Haffejee, N., et al., *Intranasal toxicity of selected absorption enhancers.* Pharmazie, 2001. **56**(11): p. 882-8.
121. Nabi-Meibodi, M., et al., *The effective encapsulation of a hydrophobic lipid-insoluble drug in solid lipid nanoparticles using a modified double emulsion solvent evaporation method.* Colloids Surf B Biointerfaces, 2013. **112**: p. 408-14.
122. Cunha, S., et al., *Lipid nanoparticles for nasal/intranasal drug delivery.* Critical Reviews™ in Therapeutic Drug Carrier Systems, 2017. **34**(3).
123. Li, J. and C. Sabliov, *PLA/PLGA nanoparticles for delivery of drugs across the blood-brain barrier.* Nanotechnology Reviews, 2013. **2**(3): p. 241-257.
124. Sharma, D., et al., *Nose-to-brain delivery of PLGA-diazepam nanoparticles.* AAPS pharmscitech, 2015. **16**(5): p. 1108-1121.
125. Shakeri, S., et al., *Multifunctional polymeric nanoplatforms for brain diseases diagnosis, therapy and theranostics.* Biomedicines, 2020. **8**(1): p. 13.
126. Sonvico, F., et al., *Surface-modified nanocarriers for nose-to-brain delivery: from bioadhesion to targeting.* Pharmaceutics, 2018. **10**(1): p. 34.
127. Akel, H., et al., *A comparison study of lipid and polymeric nanoparticles in the nasal delivery of meloxicam: Formulation, characterization, and in vitro evaluation.* International Journal of Pharmaceutics, 2021. **604**: p. 120724.
128. Kulkarni, A.D., et al., *Nanotechnology-mediated nose to brain drug delivery for Parkinson's disease: a mini review.* Journal of drug targeting, 2015. **23**(9): p. 775-788.
129. Gao, H., *Perspectives on Dual Targeting Delivery Systems for Brain Tumors.* J Neuroimmune Pharmacol, 2017. **12**(1): p. 6-16.
130. Selvaraj, K., K. Gowthamarajan, and V. Karri, *Nose to brain transport pathways an overview: potential of nanostructured lipid carriers in nose to brain targeting.* Artif Cells Nanomed Biotechnol, 2018. **46**(8): p. 2088-2095.
131. Kulkarni, A.D., et al., *Nanotechnology-mediated nose to brain drug delivery for Parkinson's disease: a mini review.* J Drug Target, 2015. **23**(9): p. 775-88.
132. Gao, H., *Progress and perspectives on targeting nanoparticles for brain drug delivery.* Acta Pharm Sin B, 2016. **6**(4): p. 268-86.
133. Musumeci, T., et al., *Nose-to-brain delivery: evaluation of polymeric nanoparticles on olfactory ensheathing cells uptake.* J Pharm Sci, 2014. **103**(2): p. 628-35.

134. Gänger, S. and K. Schindowski, *Tailoring Formulations for Intranasal Nose-to-Brain Delivery: A Review on Architecture, Physico-Chemical Characteristics and Mucociliary Clearance of the Nasal Olfactory Mucosa.* Pharmaceutics, 2018. **10**(3): p. 116.
135. Alpar, H.O., et al., *Biodegradable mucoadhesive particulates for nasal and pulmonary antigen and DNA delivery.* Adv Drug Deliv Rev, 2005. **57**(3): p. 411-30.
136. Zhang, Y., H.F. Chan, and K.W. Leong, *Advanced materials and processing for drug delivery: the past and the future.* Adv Drug Deliv Rev, 2013. **65**(1): p. 104-20.
137. Allemann, E., R. Gurny, and E. Doelker, *Drug-loaded nanoparticles: preparation methods and drug targeting issues.* European journal of pharmaceutics and biopharmaceutics, 1993. **39**(5): p. 173-191.
138. Anton, N., J.-P. Benoit, and P. Saulnier, *Design and production of nanoparticles formulated from nano-emulsion templates—a review.* Journal of controlled release, 2008. **128**(3): p. 185-199.
139. Astete, C.E. and C.M. Sabliov, *Synthesis and characterization of PLGA nanoparticles.* Journal of biomaterials science, polymer edition, 2006. **17**(3): p. 247-289.
140. Moinard-Checot, D., et al., *Nanoparticles for drug delivery: review of the formulation and process difficulties illustrated by the emulsion-diffusion process.* Journal of nanoscience and nanotechnology, 2006. **6**(9-10): p. 2664-2681.
141. Bala, I., S. Hariharan, and M.R. Kumar, *PLGA nanoparticles in drug delivery: the state of the art.* Critical Reviews™ in Therapeutic Drug Carrier Systems, 2004. **21**(5).
142. Murakami, H., et al., *Preparation of poly (DL-lactide-co-glycolide) nanoparticles by modified spontaneous emulsification solvent diffusion method.* International journal of pharmaceutics, 1999. **187**(2): p. 143-152.
143. Kwon, H.-Y., et al., *Preparation of PLGA nanoparticles containing estrogen by emulsification–diffusion method.* Colloids and Surfaces A: Physicochemical and Engineering Aspects, 2001. **182**(1-3): p. 123-130.
144. Yoo, H.S., et al., *In vitro and in vivo anti-tumor activities of nanoparticles based on doxorubicin–PLGA conjugates.* Journal of controlled Release, 2000. **68**(3): p. 419-431.
145. Konan, Y.N., et al., *Preparation and characterization of sterile sub-200 nm meso-tetra (4-hydroxylphenyl) porphyrin-loaded nanoparticles for photodynamic therapy.* European journal of pharmaceutics and biopharmaceutics, 2003. **55**(1): p. 115-124.
146. Vauthier, C. and K. Bouchemal, *Methods for the preparation and manufacture of polymeric nanoparticles.* Pharmaceutical research, 2009. **26**(5): p. 1025-1058.
147. Ibrahim, H., et al., *Aqueous nanodispersions prepared by a salting-out process.* International journal of pharmaceutics, 1992. **87**(1-3): p. 239-246.
148. Konan, Y.N., R. Gurny, and E. Allémann, *Preparation and characterization of sterile and freeze-dried sub-200 nm nanoparticles.* International journal of pharmaceutics, 2002. **233**(1-2): p. 239-252.
149. Fessi, H., et al., *Nanocapsule formation by interfacial polymer deposition following solvent displacement.* International journal of pharmaceutics, 1989. **55**(1): p. R1-R4.
150. Govender, T., et al., *PLGA nanoparticles prepared by nanoprecipitation: drug loading and release studies of a water soluble drug.* Journal of controlled release, 1999. **57**(2): p. 171-185.
151. Betancourt, T., B. Brown, and L. Brannon-Peppas, *Doxorubicin-loaded PLGA nanoparticles by nanoprecipitation: preparation, characterization and in vitro evaluation.* 2007.
152. Thioune, O., et al., *Preparation of pseudolatex by nanoprecipitation: influence of the solvent nature on intrinsic viscosity and interaction constant.* International journal of pharmaceutics, 1997. **146**(2): p. 233-238.
153. Jain, R.A., *The manufacturing techniques of various drug loaded biodegradable poly (lactide-co-glycolide)(PLGA) devices.* Biomaterials, 2000. **21**(23): p. 2475-2490.

154. Popescu, R., et al., *New Opportunity to Formulate Intranasal Vaccines and Drug Delivery Systems Based on Chitosan.* International Journal of Molecular Sciences, 2020. **21**(14): p. 5016.
155. Aderibigbe, B.A. and T. Naki, *Chitosan-Based Nanocarriers for Nose to Brain Delivery.* Applied Sciences, 2019. **9**(11): p. 2219.
156. Das, S., et al., *Formulation design, preparation and physicochemical characterizations of solid lipid nanoparticles containing a hydrophobic drug: effects of process variables.* Colloids and surfaces b: biointerfaces, 2011. **88**(1): p. 483-489.
157. Yassin, A.E.B., et al., *Optimization of 5-flurouracil solid-lipid nanoparticles: a preliminary study to treat colon cancer.* International journal of medical sciences, 2010. **7**(6): p. 398.
158. Zielińska, A., et al., *Polymeric Nanoparticles: Production, Characterization, Toxicology and Ecotoxicology.* Molecules (Basel, Switzerland), 2020. **25**(16): p. 3731.
159. Liu, Y., J. Pan, and S.-S. Feng, *Nanoparticles of lipid monolayer shell and biodegradable polymer core for controlled release of paclitaxel: effects of surfactants on particles size, characteristics and in vitro performance.* International journal of pharmaceutics, 2010. **395**(1-2): p. 243-250.
160. Shkodra-Pula, B., et al., *Effect of surfactant on the size and stability of PLGA nanoparticles encapsulating a protein kinase C inhibitor.* International Journal of Pharmaceutics, 2019. **566**: p. 756-764.
161. Keum, C.-G., et al., *Practical preparation procedures for docetaxel-loaded nanoparticles using polylactic acid-co-glycolic acid.* International journal of nanomedicine, 2011. **6**: p. 2225.
162. Pallagi, E., et al., *Initial risk assessment as part of the quality by design in peptide drug containing formulation development.* European Journal of Pharmaceutical Sciences, 2018. **122**: p. 160-169.
163. Ianiski, F.R., et al., *Protective effect of meloxicam-loaded nanocapsules against amyloid-β peptide-induced damage in mice.* Behavioural Brain Research, 2012. **230**(1): p. 100-107.
164. Gordillo-Galeano, A. and C.E. Mora-Huertas, *Solid lipid nanoparticles and nanostructured lipid carriers: A review emphasizing on particle structure and drug release.* European Journal of Pharmaceutics and Biopharmaceutics, 2018. **133**: p. 285-308.
165. Ismail, R., et al., *Synthesis and Statistical Optimization of Poly (Lactic-Co-Glycolic Acid) Nanoparticles Encapsulating GLP1 Analog Designed for Oral Delivery.* Pharm Res, 2019. **36**(7): p. 99.
166. Fonte, P., et al., *Chapter fifteen - Chitosan-Coated Solid Lipid Nanoparticles for Insulin Delivery*, in *Methods in Enzymology*, N. Düzgüneş, Editor. 2012, Academic Press. p. 295-314.
167. Gartziandia, O., et al., *Nanoparticle transport across in vitro olfactory cell monolayers.* International Journal of Pharmaceutics, 2016. **499**(1): p. 81-89.
168. Gartziandia, O., et al., *Chitosan coated nanostructured lipid carriers for brain delivery of proteins by intranasal administration.* Colloids and Surfaces B: Biointerfaces, 2015. **134**: p. 304-313.
169. Yasir, M., et al., *Solid lipid nanoparticles for nose to brain delivery of donepezil: formulation, optimization by Box–Behnken design, in vitro and in vivo evaluation.* Artificial Cells, Nanomedicine, and Biotechnology, 2018. **46**(8): p. 1838-1851.
170. Joshi, A.S., et al., *Solid lipid nanoparticles of ondansetron HCl for intranasal delivery: development, optimization and evaluation.* Journal of Materials Science: Materials in Medicine, 2012. **23**(9): p. 2163-2175.
171. Dalpiaz, A., et al., *Brain Uptake of a Zidovudine Prodrug after Nasal Administration of Solid Lipid Microparticles.* Molecular Pharmaceutics, 2014. **11**(5): p. 1550-1561.
172. Bartos, C., et al., *Transformation of meloxicam containing nanosuspension into surfactant-free solid compositions to increase the product stability and drug bioavailability for rapid analgesia.* Drug design, development and therapy, 2019. **13**: p. 4007.

173. Devkar, T.B., A.R. Tekade, and K.R. Khandelwal, *Surface engineered nanostructured lipid carriers for efficient nose to brain delivery of ondansetron HCl using Delonix regia gum as a natural mucoadhesive polymer.* Colloids and surfaces B: Biointerfaces, 2014. **122**: p. 143-150.
174. Vieira, A.C., et al., *Mucoadhesive chitosan-coated solid lipid nanoparticles for better management of tuberculosis.* International journal of pharmaceutics, 2018. **536**(1): p. 478-485.
175. Rencber, S., et al., *Development, characterization, and in vivo assessment of mucoadhesive nanoparticles containing fluconazole for the local treatment of oral candidiasis.* International journal of nanomedicine, 2016. **11**: p. 2641.
176. Bartos, C., et al., *Investigation of absorption routes of meloxicam and its salt form from intranasal delivery systems.* Molecules, 2018. **23**(4): p. 784.
177. Emami, J., *In vitro-in vivo correlation: from theory to applications.* J Pharm Pharm Sci, 2006. **9**(2): p. 169-189.
178. Shen, J. and D.J. Burgess, *In vitro–in vivo correlation for complex non-oral drug products: where do we stand?* Journal of controlled release, 2015. **219**: p. 644-651.
179. Kim, T.H., et al., *Physiologically relevant in vitro-in vivo correlation (ivivc) approach for sildenafil with site-dependent dissolution.* Pharmaceutics, 2019. **11**(6): p. 251.
180. Uppoor, V.R.S., *Regulatory perspectives on in vitro (dissolution)/in vivo (bioavailability) correlations.* Journal of Controlled Release, 2001. **72**(1): p. 127-132.
181. FDA, U., *Guidance for industry: extended release oral dosage forms: development, evaluation, and application of in vitro/in vivo correlations.* Silver Spring, MD: FDA CDER, 1997.
182. Katona, G., et al., *Development of meloxicam-human serum albumin nanoparticles for nose-to-brain delivery via application of a quality by design approach.* Pharmaceutics, 2020. **12**(2): p. 97.
183. Kürti, L., et al., *Retinoic acid and hydrocortisone strengthen the barrier function of human RPMI 2650 cells, a model for nasal epithelial permeability.* Cytotechnology, 2013. **65**(3): p. 395-406.
184. Gróf, I., et al., *The Effect of Sodium Bicarbonate, a Beneficial Adjuvant Molecule in Cystic Fibrosis, on Bronchial Epithelial Cells Expressing a Wild-Type or Mutant CFTR Channel.* International Journal of Molecular Sciences, 2020. **21**(11): p. 4024.
185. Katona, G., et al., *Development of In Situ Gelling Meloxicam-Human Serum Albumin Nanoparticle Formulation for Nose-to-Brain Application.* Pharmaceutics, 2021. **13**(5).
186. Weksler, B.B., et al., *Blood-brain barrier-specific properties of a human adult brain endothelial cell line.* The FASEB Journal, 2005. **19**(13): p. 1872-1874.
187. Veszelka, S., et al., *Comparison of a Rat Primary Cell-Based Blood-Brain Barrier Model With Epithelial and Brain Endothelial Cell Lines: Gene Expression and Drug Transport.* Front Mol Neurosci, 2018. **11**: p. 166.
188. Kürti, L., et al., *The effect of sucrose esters on a culture model of the nasal barrier.* Toxicology in Vitro, 2012. **26**(3): p. 445-454.
189. Bocsik, A., et al., *Reversible opening of intercellular junctions of intestinal epithelial and brain endothelial cells with tight junction modulator peptides.* Journal of Pharmaceutical Sciences, 2016. **105**(2): p. 754-765.
190. Hellinger, E., et al., *Comparison of brain capillary endothelial cell-based and epithelial (MDCK-MDR1, Caco-2, and VB-Caco-2) cell-based surrogate blood-brain barrier penetration models.* Eur J Pharm Biopharm, 2012. **82**(2): p. 340-51.
191. Ismail, R., *Quality by design driven development of polymeric and lipid-based nanocarriers as potential systems for oral delivery of GLP-1 analogues*. 2020, szte.
192. Rathore, A.S., *Roadmap for implementation of quality by design (QbD) for biotechnology products.* Trends in Biotechnology, 2009. **27**(9): p. 546-553.

193. Kumarasamy, M. and A. Sosnik, *The Nose-To-Brain Transport of Polymeric Nanoparticles Is Mediated by Immune Sentinels and Not by Olfactory Sensory Neurons.* Advanced Biosystems, 2019. **3**(12): p. 1900123.
194. Md, S., et al., *Nanoneurotherapeutics approach intended for direct nose to brain delivery.* Drug Development and Industrial Pharmacy, 2015. **41**(12): p. 1922-1934.
195. Yasir, M. and U.V.S. Sara, *Solid lipid nanoparticles for nose to brain delivery of haloperidol: in vitro drug release and pharmacokinetics evaluation.* Acta Pharmaceutica Sinica B, 2014. **4**(6): p. 454-463.
196. Aboud, H.M., et al., *Development, Optimization, and Evaluation of Carvedilol-Loaded Solid Lipid Nanoparticles for Intranasal Drug Delivery.* AAPS PharmSciTech, 2016. **17**(6): p. 1353-1365.
197. Ismail, R., et al., *Synthesis and Statistical Optimization of Poly (Lactic-Co-Glycolic Acid) Nanoparticles Encapsulating GLP1 Analog Designed for Oral Delivery.* Pharmaceutical Research, 2019. **36**(7): p. 99.
198. Musumeci, T., et al., *Nose-to-Brain Delivery: Evaluation of Polymeric Nanoparticles on Olfactory Ensheathing Cells Uptake.* Journal of Pharmaceutical Sciences, 2014. **103**(2): p. 628-635.
199. Mittal, D., et al., *Insights into direct nose to brain delivery: current status and future perspective.* Drug delivery, 2014. **21**(2): p. 75-86.
200. Shamarekh, K.S., et al., *Development and evaluation of protamine-coated PLGA nanoparticles for nose-to-brain delivery of tacrine: In-vitro and in-vivo assessment.* Journal of Drug Delivery Science and Technology, 2020. **57**: p. 101724.
201. Salem, L.H., et al., *Coated Lipidic Nanoparticles as a New Strategy for Enhancing Nose-to-Brain Delivery of a Hydrophilic Drug Molecule.* Journal of Pharmaceutical Sciences, 2020. **109**(7): p. 2237-2251.
202. Bahadur, S., et al., *Intranasal Nanoemulsions for Direct Nose-to-Brain Delivery of Actives for CNS Disorders.* Pharmaceutics, 2020. **12**(12).
203. Froelich, A., et al., *Microemulsion-Based Media in Nose-to-Brain Drug Delivery.* Pharmaceutics, 2021. **13**(2): p. 201.
204. Vaka, S.R.K., *Nose to Brain Delivery of Therapeutic Agents.* 2011.
205. Singh, A.P., S.K. Saraf, and S.A. Saraf, *SLN approach for nose-to-brain delivery of alprazolam.* Drug Delivery and Translational Research, 2012. **2**(6): p. 498-507.
206. Gupta, S., et al., *Systematic Approach for the Formulation and Optimization of Solid Lipid Nanoparticles of Efavirenz by High Pressure Homogenization Using Design of Experiments for Brain Targeting and Enhanced Bioavailability.* BioMed Research International, 2017. **2017**: p. 5984014.
207. Masserini, M., *Nanoparticles for brain drug delivery.* ISRN biochemistry, 2013. **2013**.
208. Pires, P.C. and A.O. Santos, *Nanosystems in nose-to-brain drug delivery: A review of non-clinical brain targeting studies.* Journal of Controlled Release, 2018. **270**: p. 89-100.
209. Zhou, Y. and R.M. Raphael, *Solution pH alters mechanical and electrical properties of phosphatidylcholine membranes: relation between interfacial electrostatics, intramembrane potential, and bending elasticity.* Biophysical journal, 2007. **92**(7): p. 2451-2462.
210. Barichello, J.M., et al., *Encapsulation of Hydrophilic and Lipophilic Drugs in PLGA Nanoparticles by the Nanoprecipitation Method.* Drug Development and Industrial Pharmacy, 1999. **25**(4): p. 471-476.
211. Masserini, M., *Nanoparticles for Brain Drug Delivery.* ISRN Biochemistry, 2013. **2013**: p. 238428.
212. Alsulays, B.B., et al., *Impact Of Penetratin Stereochemistry On The Oral Bioavailability Of Insulin-Loaded Solid Lipid Nanoparticles.* International journal of nanomedicine, 2019. **14**: p. 9127-9138.
213. Sipos, B., et al., *Quality by Design Based Formulation Study of Meloxicam-Loaded Polymeric Micelles for Intranasal Administration.* Pharmaceutics, 2020. **12**(8): p. 697.

214. Mangialardo, S., et al., *Raman analysis of insulin denaturation induced by high-pressure and thermal treatments.* Journal of Raman Spectroscopy, 2012. **43**(6): p. 692-700.
215. Luo, Y., et al., *Solid lipid nanoparticles for oral drug delivery: chitosan coating improves stability, controlled delivery, mucoadhesion and cellular uptake.* Carbohydr Polym, 2015. **122**: p. 221-9.
216. Grenha, A., et al., *Chitosan nanoparticles are compatible with respiratory epithelial cells in vitro.* European Journal of Pharmaceutical Sciences, 2007. **31**(2): p. 73-84.
217. Avdeef, A., *Permeability—PAMPA In Absorption and Drug Development*. 2012, John Wiley & Sons, Inc.: Hoboken, NJ.
218. Araújo, F., et al., *The impact of nanoparticles on the mucosal translocation and transport of GLP-1 across the intestinal epithelium.* Biomaterials, 2014. **35**(33): p. 9199-9207.
219. Dinarvand, R., et al., *Polylactide-co-glycolide nanoparticles for controlled delivery of anticancer agents.* International journal of nanomedicine, 2011. **6**: p. 877.
220. Brange, J., *Skelbaek-Pedersen.* B., Langkjaer, L. Damgaard. U., Ege, H., Havelund. S.. Heding, LG, Jorgensen. KH, Lykkeberg, J.. Markussen, J., Pingel, M. and Rasmussen. E, 1987: p. 36-38.
221. Liu, J., et al., *Controlled release of insulin from PLGA nanoparticles embedded within PVA hydrogels.* Journal of Materials Science: Materials in Medicine, 2007. **18**(11): p. 2205-2210.
222. Patel, S., et al., *Brain targeting of risperidone-loaded solid lipid nanoparticles by intranasal route.* Journal of drug targeting, 2011. **19**(6): p. 468-474.
223. Son, G.-H., B.-J. Lee, and C.-W. Cho, *Mechanisms of drug release from advanced drug formulations such as polymeric-based drug-delivery systems and lipid nanoparticles.* Journal of Pharmaceutical Investigation, 2017. **47**(4): p. 287-296.
224. Dyawanapelly, S., et al., *Improved mucoadhesion and cell uptake of chitosan and chitosan oligosaccharide surface-modified polymer nanoparticles for mucosal delivery of proteins.* Drug Delivery and Translational Research, 2016. **6**(4): p. 365-379.
225. Piazzini, V., et al., *Chitosan coated human serum albumin nanoparticles: A promising strategy for nose-to-brain drug delivery.* International journal of biological macromolecules, 2019. **129**: p. 267-280.
226. Elnaggar, Y.S., et al., *Intranasal piperine-loaded chitosan nanoparticles as brain-targeted therapy in Alzheimer's disease: optimization, biological efficacy, and potential toxicity.* Journal of pharmaceutical sciences, 2015. **104**(10): p. 3544-3556.
227. Bahadur, S. and K. Pathak, *Physicochemical and physiological considerations for efficient nose-to-brain targeting.* Expert Opinion on Drug Delivery, 2012. **9**(1): p. 19-31.
228. Fischer, S.M., M. Brandl, and G. Fricker, *Effect of the non-ionic surfactant Poloxamer 188 on passive permeability of poorly soluble drugs across Caco-2 cell monolayers.* European journal of pharmaceutics and biopharmaceutics, 2011. **79**(2): p. 416-422.
229. Esim, O., et al., *Nose to brain delivery of eletriptan hydrobromide nanoparticles: Preparation, in vitro/in vivo evaluation and effect on trigeminal activation.* Journal of Drug Delivery Science and Technology, 2020. **59**: p. 101919.
230. Trotta, V., et al., *Brain targeting of resveratrol by nasal administration of chitosan-coated lipid microparticles.* Eur J Pharm Biopharm, 2018. **127**: p. 250-259.
231. Rassu, G., et al., *Nose-to-brain delivery of BACE1 siRNA loaded in solid lipid nanoparticles for Alzheimer's therapy.* Colloids and Surfaces B: Biointerfaces, 2017. **152**: p. 296-301.
232. Misra, S., et al., *Galantamine-loaded solid–lipid nanoparticles for enhanced brain delivery: preparation, characterization, in vitro and in vivo evaluations.* Drug Delivery, 2016. **23**(4): p. 1434-1443.
233. Al Asmari, A.K., et al., *Preparation, characterization, and in vivo evaluation of intranasally administered liposomal formulation of donepezil.* Drug design, development and therapy, 2016. **10**: p. 205-215.

234. Sun, Y., et al., *Primary Studies on Construction and Evaluation of Ion-Sensitive in situ Gel Loaded with Paeonol-Solid Lipid Nanoparticles for Intranasal Drug Delivery.* Int J Nanomedicine, 2020. **15**: p. 3137-3160.
235. Chandra Bhatt, P., et al., *Nose to brain delivery of astaxanthin-loaded solid lipid nanoparticles: fabrication, radio labeling, optimization and biological studies.* RSC Advances, 2016. **6**(12): p. 10001-10010.
236. Wang, L., et al., *Improved brain delivery of pueraria flavones via intranasal administration of borneol-modified solid lipid nanoparticles.* Nanomedicine (Lond), 2019. **14**(16): p. 2105-2119.
237. Seju, U., A. Kumar, and K.K. Sawant, *Development and evaluation of olanzapine-loaded PLGA nanoparticles for nose-to-brain delivery: In vitro and in vivo studies.* Acta Biomaterialia, 2011. **7**(12): p. 4169-4176.
238. Sharma, D., et al., *Nose-To-Brain Delivery of PLGA-Diazepam Nanoparticles.* AAPS PharmSciTech, 2015. **16**(5): p. 1108-21.
239. Sharma, D., et al., *Nose to Brain Delivery of Midazolam Loaded PLGA Nanoparticles: In Vitro and In Vivo Investigations.* Curr Drug Deliv, 2016. **13**(4): p. 557-64.
240. Nigam, K., et al., *Nose-to-brain delivery of lamotrigine-loaded PLGA nanoparticles.* Drug Delivery and Translational Research, 2019. **9**(5): p. 879-890.
241. Chu, L., et al., *Nose-to-brain delivery of temozolomide-loaded PLGA nanoparticles functionalized with anti-EPHA3 for glioblastoma targeting.* Drug Delivery, 2018. **25**(1): p. 1634-1641.
242. Meng, Q., et al., *Intranasal delivery of Huperzine A to the brain using lactoferrin-conjugated N-trimethylated chitosan surface-modified PLGA nanoparticles for treatment of Alzheimer's disease.* Int J Nanomedicine, 2018. **13**: p. 705-718.
243. Kravanja, G., et al., *Chitosan-Based (Nano)Materials for Novel Biomedical Applications.* Molecules, 2019. **24**(10): p. 1960.
244. Akel, H., et al., *In Vitro Comparative Study of Solid Lipid and PLGA Nanoparticles Designed to Facilitate Nose-to-Brain Delivery of Insulin.* International Journal of Molecular Sciences, 2021. **22**(24): p. 13258.
245. Rhea, E.M. and W.A. Banks, *A historical perspective on the interactions of insulin at the blood-brain barrier.* J Neuroendocrinol, 2021. **33**(4): p. e12929.
246. Ohtsuki, S., et al., *Quantitative targeted absolute proteomic analysis of transporters, receptors and junction proteins for validation of human cerebral microvascular endothelial cell line hCMEC/D3 as a human blood-brain barrier model.* Mol Pharm, 2013. **10**(1): p. 289-96.

ANNEX-I

European Journal of Pharmaceutics and Biopharmaceutics 148 (2020) 38–53

Contents lists available at ScienceDirect

European Journal of Pharmaceutics and Biopharmaceutics

journal homepage: www.elsevier.com/locate/ejpb

Review article

Progress and perspectives of brain-targeting lipid-based nanosystems via the nasal route in Alzheimer's disease

Hussein Akel[a], Ruba Ismail[a,b], Ildikó Csóka[a,b,*]

[a] Institute of Pharmaceutical Technology and Regulatory Affairs, Faculty of Pharmacy, University of Szeged, Eötvös utca 6, H-6720 Szeged, Hungary
[b] Institute of Pharmaceutical Technology and Regulatory Affairs, Interdisciplinary Centre of Excellence, University of Szeged, Eötvös u. 6, H-6720 Szeged, Hungary

ARTICLE INFO

Keywords:
Alzheimer's disease (AD)
Nose-to-brain
Liposomes
SLNs
NLCs
QbD

ABSTRACT

Since health care systems dedicate substantial resources to Alzheimer's disease (AD), it poses an increasing challenge to scientists and health care providers worldwide, especially that many decades of research in the medical field revealed no optimal effective treatment for this disease. The intranasal administration route seems to be a preferable route of anti-AD drug delivery over the oral one as it demonstrates an ability to overcome the related obstacles reflected in low bioavailability, limited brain exposure and undesired pharmacokinetics or side effects. This delivery route can bypass the systemic circulation through the intraneuronal and extraneuronal pathways, providing truly needleless and direct brain drug delivery of the therapeutics due to its large surface area, porous endothelial membrane, the avoidance of the first-pass metabolism, and ready accessibility. Among the different nano-carrier systems developed, lipid-based nanosystems have become increasingly popular and have proven to be effective in managing the common symptoms of AD when administered via the nose-to-brain delivery route, which provides an answer to circumventing the BBB. The design of such lipid-based nanocarriers could be challenging since many factors can contribute to the quality of the final product. Hence, according to the authors, it is recommended to follow the quality by design methodology from the early stage of development to ensure high product quality while saving efforts and costs. This review article aims to draw attention to the up-to-date findings in the field of lipid-based nanosystems and the potential role of developing such forms in the management of AD by means of the nose-to-brain delivery route, in addition to highlighting the significant role of applying QbD methodology in this development.

1. Introduction

Neurodegenerative disease (ND) is an umbrella term for debilitating, incurable diseases which are characterized by the gradual and progressive degeneration of the structure and function of the central nervous system or the peripheral nervous system [1], affecting especially neurons as the building blocks. These neurons are non-reproducible and nonrenewable, so when the body loses them, they cannot be replaced anymore [2]. These diseases are one of the most important medical and socio-economic problems of our time, affecting a wide range of aged people, resulting in a major impact at professional, social and family levels of patients and can lead to a complete inability to carry out any type of everyday activity [3]. These diseases can be listed as follows: Alzheimer's disease (AD), Parkinson's disease(PD), Huntington's disease (HD), Amyotrophic lateral sclerosis (ALS) and Prion diseases [4].

The importance of focusing on these diseases comes from the high percentage of people suffering from them, for example, Europe has a rapidly aging population from which more than 18% are over 65. As shown in Fig. 1, this percentage is expected to reach 25% and 35% by 2030 and 2060 respectively [5].

In 2015 the total dementia costs per patient in Europe amounted to approximately €32,500, whilein the case of United States this value reached almost €43,000, which imposes a great burden with high expenses [6]; Fig. 2 shows this in detail.

2. Why is it crucial to focus on Alzheimer's disease?

AD is one of the brain disorders in which irreversible and progressive neurodegeneration takes place. It was first described by Dr. Alois Alzheimer after noticing changes in the brain tissues of a patient who had died of an unusual mental illness [7]. The post-mortem brain

* Corresponding author at: Institute of Pharmaceutical Technology and Regulatory Affairs, Faculty of Pharmacy, University of Szeged, Eötvös utca 6, H-6720 Szeged, Hungary.
E-mail address: csoka@pharm.u-szeged.hu (I. Csóka).

https://doi.org/10.1016/j.ejpb.2019.12.014
Received 7 June 2019; Received in revised form 28 October 2019; Accepted 31 December 2019
Available online 08 January 2020
0939-6411/

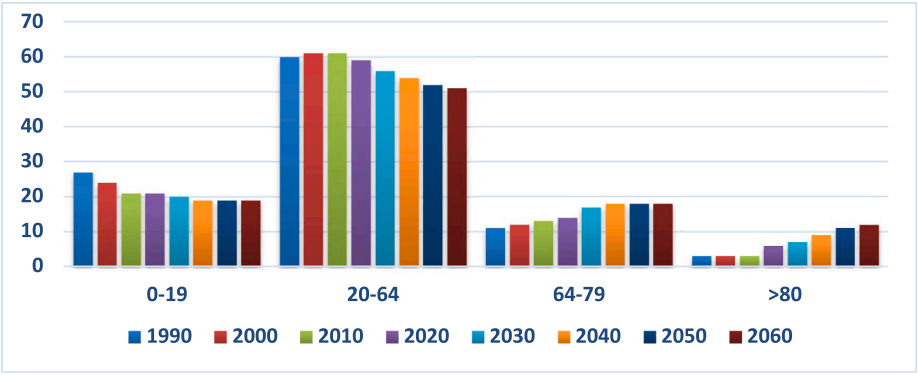

Fig. 1. Age structure of the population in the EU between 1990 and 2060 showing an increase in the number of elderly people in the next few decades.

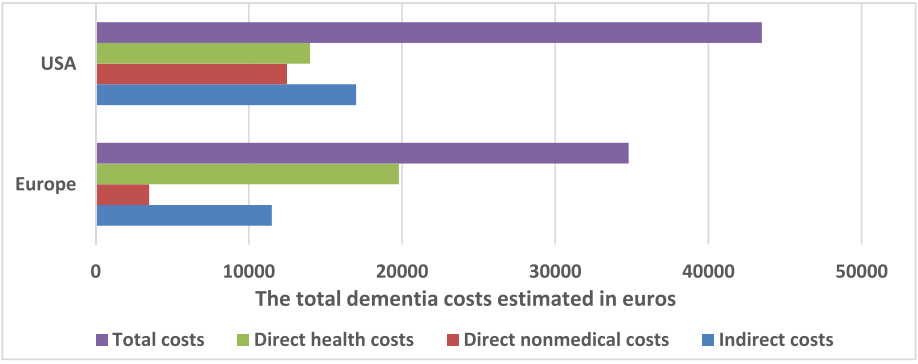

Fig. 2. Comparison of the costs of dementia between Europe and the USA.

examination demonstrated many abnormal clumps called amyloid β-peptides (Aβ), deposited as plaques in the brain tissues and causing the neurodegeneration [8].

Alzheimer's disease comes in priority of neuroscientists because of the following reasons:

- Firstly, more than two-thirds of AD patients suffer from disabilities in cognitive functioning, thinking, remembering and behavioral abilities, which leads them to stay at home in need of health care, which has a significant impact on their families. With the progression of the disease, symptoms will grow worse to include confusion, irritability, aggression, mood swings, language breakdown and long-term memory loss. The disease progress is often accompanied by social withdrawal and changes in behavioral and psychotic symptoms [9], and in developed stages, bodily functions could be lost [10]
- Secondly, it is considered the most dangerous and prevalent neurodegenerative disease, forming the most common cause of dementia worldwide and making up 60–80% of all dementia cases affecting an estimated 24 million people globally [11–13]. It has been ranked as the 6th leading cause of death in the United States, following these five diseases: heart diseases, malignant neoplasms, chronic lower respiratory diseases, accidents (unintentional injuries) and cerebrovascular diseases, and preceding diabetes mellitus, influenza and pneumonia, nephritis, and intentional self-harm (suicide) [14]. In Europe few studies were conducted to evaluate AD riskiness and expansion. The results of the latest research which was done by H. Niu et al demonstrated that the prevalence of AD in Europe was estimated at 5.05%, the prevalence in men was 3.31% while in women 7.13% and increased with age [15].
- Finally, all the available treatments which target AD nowadays are of limited benefits and help just in managing the symptoms demonstrating no noticeable effect on reversing the associated decline in cognition [16,17].

3. Medicinal management of Alzheimer's disease

As the prevalence of AD shows a progressive increase, great efforts were made to deal with this issue, especially in pharmaceutical fields. Many investigations, research efforts, and clinical trials were conducted focusing on discovery and development of many medications which could indeed enhance the quality of patients' life. However they cannot heal the disease 100% and they are still in a continuously developing situation on the way to obtaining the optimal solution. Unfortunately, the available medicines face many problems, including short-time efficacy, severe side effects and high costs, which provide mainly symptomatic short-term benefits without counteracting the progression of the disease [18]. The clinical development and drug discovery in AD have attempted in the last decade to develop disease modifying drugs with the help of preclinical models, but none of these drugs has succeeded in phase 3. The factors that might explain this failure include suboptimal study design (lacking and/or inadequate biomarkers and outcome measurements) and, most importantly, time course of treatment in relation to the development of the disease [19]. Recently, the nasal application of brain-targeting therapeutics has been of high interest due to its potential to overcome limitations facing the currently available anti-AD drugs. However, there are several barriers that may limit the nose-to-brain delivery route, namely, poor drug permeability from nasal mucosa, mucociliary clearance, enzymatic degradation of the drug, low drug retention time and naso-mucosal toxicity [20]. Table 1 presents the available choices of AD medications:

4. Nose-to-brain delivery of therapeutics

In humans and other animal species, the major functions of the nasal cavity are breathing and olfaction; it also provides an important protective activity of filtering, warming up and humidifying the inhaled air before reaching the lowest airways with the help of the mucus layer and hairs, which cover the internal side of the nasal cavity trapping

Table 1
Variety of potential AD therapies.

FDA approved medicines	Donepezil [21–24] Rivastigmine [25–27] Galantamine [28,29] Memantine [30–32]
FDA non-approved available supplements	Coconut oil [33–35] Coenzyme Q10 [36,37] Ginkgo biloba [38–40] Huperzine A [41–43] Poly unsaturated fatty acids [44–46] Curcumin [47–49] Tramiprosate [50,51]
Under-development medicines	Nilotinib [52–54] Insulin [55–65] GLP1 analogues [66–71] Monoclonal antibodies: Aducanumab [72–75], Gantenerumab [76,77] Serotonin Receptors Ligands: Intepirdine [78–80] BACE1 inhibitors: AZD3293 [81,82], Verubecestat [83,84], Atabecestat [85,86], EVP-0962 [87], BMS-932481 [88] Antiaggregation of beta-amyloid: Posiphen [89], ALZ-801 [90,91] Tau aggregation modulators: TPI-287 [92] Acetylcholine receptors ligands: Encenicline hydrochloride [93,94]
Under-development marketed medicines for direct nose-to-brain application	Galantamine prodrug (Memogain®) [95–98]

inhaled particles and pathogens. Inside the nasal cavity, two halves can be differentiated and are separated with the nasal septum, which extends posteriorly to the nasopharynx [99].

The nasal cavity is divided by a septum into two symmetrical halves, each one opening at the face through nostrils and extending posteriorly to the nasopharynx. Both symmetrical halves consist of the four following areas (Fig. 3):

- **Nasal vestibule**: the region that is just inside the nostrils with an area of about 0.6 cm^2.
- **Atrium**: it is the intermediate area between the nasal vestibule and the respiratory region. Its anterior section is constituted by a stratified squamous epithelium and the posterior area by pseudostratified columnar cells presenting microvilli.
- **Olfactory region**: the olfactory region is located in the roof of the nasal cavity and covers only about 10% of the total nasal area and extends a short way down the septum and lateral wall. It is the part of the nasal cavity which is responsible for the delivery of drugs from the nose to the CNS through its neuroepithelium.
- **Respiratory region**: it forms the largest part of the nasal cavity, and it is divided into superior, middle and inferior turbinates. The mucosa of this region is considered the most important section for delivering drugs systemically, it is constituted by the epithelium [100].

Traditionally, the nasal route has been exploited for the delivery of drugs for the treatment of local diseases like nasal allergy, sinusitis, nasal infections and nasal congestion. Lately, the nasal route has attracted wide attention as a reliable, safe, non-invasive and convenient route to accomplish faster and higher levels of drug absorption to the systemic circulation due to many advantageous points including: (i) the highly vascularized epithelium of nasal mucosa, (ii) porous endothelial

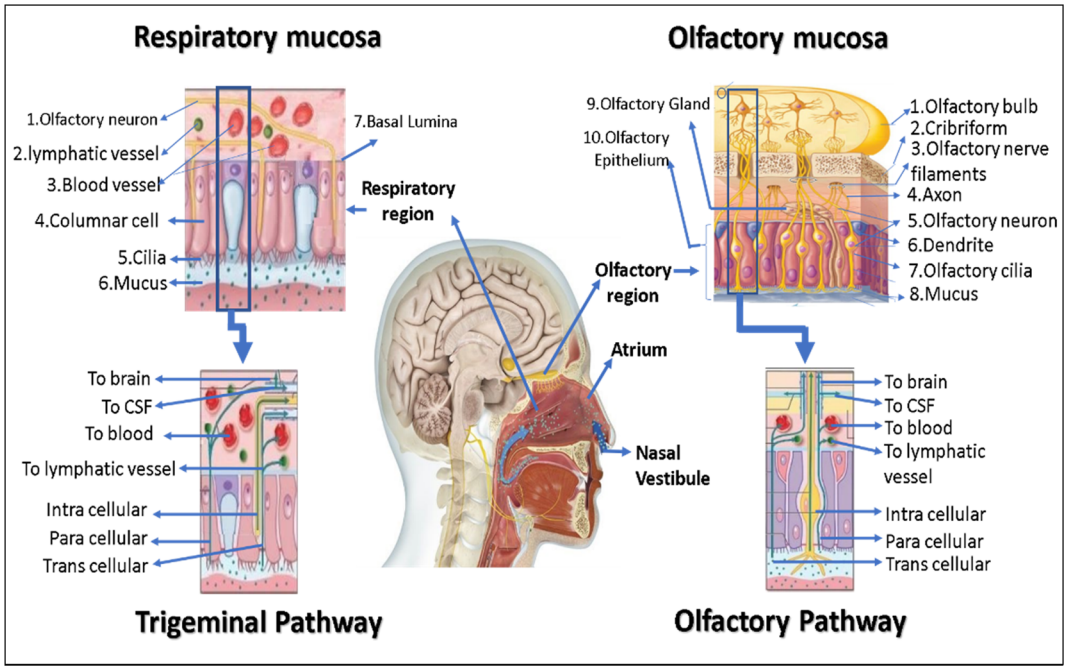

Fig. 3. Nasal cavity parts and the possible pathways of direct drug transportation through the nasal mucosa.

membrane (iii) its ready accessibility (iv) its large surface area for rapid drug absorption (v) rapid onset of action (vi) lower enzyme levels compared with the gastrointestinal tract and the liver (vii) high total blood flow per cm^3 (viii) direct drug transport to systemic circulation and thereby avoiding first-pass hepatic metabolism and enhancing bioavailability.

The nose-to-brain delivery of drug moieties has been tried by several researchers to explore the merits of this route, such as circumvention of the BBB, avoidance of hepatic first-pass metabolism, practicality, safety and convenience of administration and non-invasive (painless) nature [18,101]. The effectiveness of a CNS-targeting drug molecule is closely related to its bioavailability in the site of action (CSF or brain tissues). This constitutes the main challenge for currently development in neurodegenerative therapeutics, which aims to provide the best penetration of the drug's active molecule into the brain efficiently, while minimizing its peripheral availability and the related adverse effects [102]. The following table shows the main advantages and accompanying disadvantages of the nose-to-brain pathway [103]:

4.1. Nose-to-brain as a direct delivery route in CNS disorders

Not only neurodegenerative disorders such as AD and PD, but also others like obesity, behavior disorders, and sexual dysfunction were found to have associations with the troubles in one or more sites in the brain. Because of their growing severity affecting more and more people worldwide, it becomes necessary to develop a drug delivery system which is sufficiently effective in providing the active form of the drug into the desired site of action, leading to better results with minimal side effects [104].

The brain is considered the noblest organ in the body because of the crucial role it plays in managing and regulating the functions of the various body systems and organs in addition to its high sensitivity to any foreign material. Therefore, the presence of a supportive system is essential to protect the brain, and to keep it performing its functions to the fullest. This supportive system consists of the outer liquid cover called cerebrospinal fluid (CSF), and the inner microvascular layer called the blood-brain barrier (BBB). The BBB forms the interface between blood capillaries and brain tissues. It provides the selective access of necessary nutrients and hormones while restricting the entry of other external materials including, therapeutic agents or drugs. Any drug that needs to reach the central nervous system (CNS) requires crossing the BBB, and almost all large drug molecules and most of the small ones cannot enter the brain or the CNS after oral or systemic administration. Active transport and passive diffusion through endothelial cells are the two principal mechanisms by which molecules can enter the brain. However, the problem is that the endothelial cells of capillaries present in the BBB are effectively precluded by very narrow and tight junctions; therefore, only the modified forms of drug delivery systems designed for the CNS can provide the drug at the site of action, while the normal oral or parenteral route of drug administration is not capable enough of doing so. This problem is much more serious in the case of water-soluble drugs [105].

The olfactory region, which is located at the upper region in the nasal cavity, is kept in direct contact with the brain (frontal cortex, especially the olfactory bulb) via the olfactory nerves, while the respiratory region is supplied by the trigeminal sensory neurons and blood vessels. When administering a drug into the nasal cavity, first it must pass the mucociliary clearance in the vestibular region, then the drug molecule reaches the internal portion of the nasal cavity where it meets the blood vessels in the respiratory epithelium and the neuronal network represented by olfactory and respiratory epithelium [106]. After that, the drug enters the systemic circulation from the blood vessels and then it is distributed throughout the body. This systemic bioavailability remains a minor route of drug transport to the brain through the BBB, as the "direct neuronal pathway" forms the primary one [107].

4.2. Pathways of nose-to-brain transport

Intranasally administered therapeutic agents are delivered to the CNS by the olfactory, trigeminal or systemic circulation to CNS pathways as follows:

4.2.1. Olfactory pathway

Once the brain targeting formulations are administered nasally and reach the olfactory mucosa, they will be in a direct contact with olfactory receptors on the cilia located at the end of the olfactory receptor neurons [108]. The drug passes through the axon and the nerve bundle across the cribriform plate to enter the olfactory bulb and the cerebrospinal fluid (CSF) [109]. The drug distribution from the CSF to the brain can occurred by mixing with the interstitial fluid in the brain. The intraneuronal and the extra-neuronal pathways are the two different pathways of the olfactory neuronal pathway into the brain. The intraneuronal pathway involves axonal transport, while in the case of extraneuronal pathway transport through perineural channels occurs [110,111].

4.2.2. Trigeminal pathway

The trigeminal nerve route constitutes a substitutional, less explored pathway to the brain and takes place among the branches of the trigeminal nerves, which innervate both the respiratory and olfactory mucosa, transferring drug molecules/formulation directly to the brainstem and other connected structures [112,113].

Even though the trigeminal nerve fiber endings are not available to reach directly in the nasal cavity, it is supposed that the first step of this pathway takes place along the branches of the trigeminal nerve, which innervate the dorsal nasal mucosa, the anterior part of the nasal cavity and the lateral walls of the nasal mucosa [114,115]. The branches of the trigeminal pathway enter the brainstem at the pons level, before subsequently being directed to the rest of the hindbrain and forebrain [116,117]. Transport via the trigeminal pathway may occur either intracellularly or extracellularly [102,118]. Several studies have been published regarding the axonal transport of various agents through the trigeminal nerves following intranasal administration such as lidocaine [113], insulin-like growth factor 1 (IGF-1) [119], interferon-β- 1b [120], etc.

4.2.3. Systemic pathway

The uptake of an active substance into the brain from nasal cavity may also take place through blood circulation. Since the respiratory epithelium is rich in blood vessels more than the olfactory mucosa, a fraction of the drug will be absorbed into the systemic circulation [112]. Small lipophilic molecules are absorbed to the blood and penetrate the BBB much easier than the high molecular weight and hydrophilic molecules. After the active molecule is distributed throughout the systemic circulation, it enters into the nasal blood vessels and then rapidly transferred to the carotid arterial blood supply to the brain and spinal cord, this process is called counter current exchange [108]. This pathway in not preferable in the case of nose to brain delivery as the drug will reach the systemic circulation causing a peripheral effects, which is responsible for the side effects of the most available medications and is not desired and may be dangerous in some cases (e.g. insulin).

Fig. 3, demonstrates the possible pathways of direct drug transportation through the nasal mucosa.to the brain including olfactory and trigeminal pathways:

Despite the potential of this patient-friendly drug delivery route, there are significant challenges associated with this modality of administration. Nose-to-brain transport is significantly affected by the surface and structural properties of the administered biomolecules as they greatly affect the permeability throughout the nasal membranes (especially size, lipophilicity and the degree of ionization). Proteins, because of their larger size (> 1000 Da) and hydrophilicity, are

transported to a far less extent than smaller lipophilic molecules. Another important factor is the presence of metabolic enzymes (cytochrome P450, esterases and transferases) in the mammalian olfactory mucosa. On the other hand, from an anatomical point of view, the localization of the olfactory epithelium in the roof of the nasal cavity makes it difficult for drugs to gain access to the targeted region. To address these pitfalls and enhance the bioavailability of the protein molecules, different approaches have been suggested, such as the use of permeation enhancers, cell penetrating molecules, mucoadhesives or nano-based drug delivery systems [104].

The contribution of nano-based drug delivery systems to this field is crucial since not only they allow the protection of the delicate therapeutic agent from degradation, but most importantly they also improve the uptake by the olfactory mucosa and the access to the CNS, based either on passive or active targeting, as they can protect the encapsulated peptides and poteins from chemical and/or enzymatic degradation as well as extracellular transport by efflux transporters [121]. The surface modification of the NPs (e.g., Polysorbate 80 coating) could achieve the targeted CNS delivery of a number of different drugs including peptides [122,123]. In addition, the small particle size of nanocarriers potentially allows them to be transported transcellularly through neurons to the CNS via various endocytic pathways after intranasal administration [121].

As a result, the use of drug delivery nanocarriers has led to enhanced drug concentrations and extended half-life times with the subsequent improved therapeutic effect of the delivered molecules [124].

5. Lipid-based nanoparticles as carriers for nose-to-brain delivery

Nanoparticles have been classified as preferable nose-to-brain carriers due to their notable improvement of drug delivery, since they are able to protect the encapsulated drug from biological as well as chemical degradation, and from extracellular transport by P-gp efflux proteins [117,125]. One of the key considerations for their development as nasal dosage forms is the safety and toxicological assessment of the matrix [126]. Among colloidal carriers, lipid-based nanoparticles (LNs) are considered the most promising for nasal drug delivery, especially regarding their biocompatibility. They vary in diameter between 50 and 1000 nm. So far, when compared to other colloidal systems, LNs have been described as superior carriers [127]. Table 3 below, summarizes the main types of LNs, which will be discussed in the following in detail, with their structures:

5.1. Liposomes

Since their early discovery, liposomes have seemed to be ideal drug-carrier systems due to their morphology, which has many similarities to the biological cellular membranes, and because of their ability to incorporate various substances. Primary liposomes were formulated using only natural lipids, however, there is a wide range of natural and synthetic lipids from which the one suitable for and compatible with the encapsulated material and the way of preparation can be selected [128] (Table4).

The capability of entrapping includes both lipophilic and hydrophilic agents, in the lipid membrane in the aqueous core, respectively as shown in Table2.

Liposomes applied for medical use range in their size between 50 and 450 nm [129]. Only certain sizes will allow passage across the BBB for neurotherapy (such as in AD). The consideration of size should be made according to some factors such as their therapeutic application, encapsulation efficiency, and stability [130].

The action of liposomes on nasal mucosa is related to the incorporation of phospholipids in the membrane opening “new pores” in the paracellular tight junctions. Therefore, administering drug-containing liposomes trans-nasally would attain more effective and systemic absorption [131].

Liposomes are promising systems for drug delivery via the nasal route because of the following:

- The components used for liposomal formulation and their characteristics play an important role in the pharmacokinetics of the drug and its bioavailability: (1) lipids: phosphatidylcholine, cholesterol, etc. which have many similarities to the nature of the lipids in the biological membranes [132]; (2) some other components like PEG, which minimize interactions with mucin, increase mucus diffusivity and favor a close contact with the underlying epithelium [133].
- The smaller size of the vesicles has the potential to increase the absorption of the drug [134].
- The high encapsulation efficacy that is achieved through the suitable selection of the lipid phase that fits the encapsulated molecules, which results in a better bioavailability of the drug [135,136].
- The high zeta potential is associated with better physical stability and reduces the chances of coalescence [137]

Unfortunately, liposomal formulations face some disadvantages such as: poor storage stability, difficulties in sterilization and rapid leakage of water-soluble drugs [138,139].

5.1.1. Liposomes as carriers for nose-to-brain delivery in some AD treatments

Abdulrahman et al. explored the efficacy of brain delivery of

Table 2
Advantages and disadvantages of nose-to-brain drug delivery systems.

Advantages	Disadvantages
It is a safe, painless and convenient method of drug delivery	Rapid elimination of drug substances from the nasal cavity due to mucocilliary clearance
It avoids drug degradation in the gastrointestinal tract, particularly peptide drugs	The small size of the olfactory region in humans compared to that in rats 3–8% and 50% respectively
It avoids hepatic first-pass metabolism and gut-wall metabolism of drugs, allowing enhanced brain bioavailability	Absorption enhancers used in these formulations may cause mucosal toxicity
It bypasses the BBB, thereby providing CNS targeted drug delivery, thus reducing systemic exposure of drugs and associated systemic side effects	There is a great deal of variability in the concentrations attainable in different regions of the brain and the spinal cord
Better patient compliance, because self-medication is also possible with this route of drug administration	High-molecular-weight drugs may result in decreased permeability across the nasal mucosa
It serves as an alternative route for parenteral administration, especially for protein and peptide drugs	Some therapeutic agents may cause irritation to the nasal mucosa or may be susceptible to enzymatic degradation and metabolism in the nasal milieu at mucosal surface
It shows excellent bioavailability for low molecular weight drugs	Nasal congestion due to a cold or an allergic condition may interfere with this technique of drug delivery
	Frequent use of this route may cause mucosal damage like infection or anosmia
	Mechanical loss of the dosage form could occur due to improper technique of administration
	Mechanisms of drug transport are still unclear

Table 3
The main types of lipid nanoparticles with their structures.

Liposomes	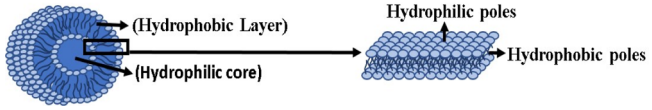
Solid lipid nanoparticles	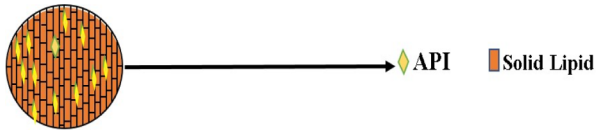
Nanostructured lipid carriers	
Nanoemulsions	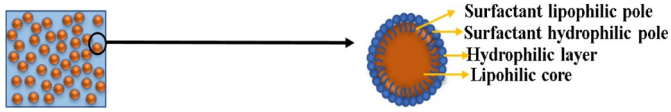
Niosomes	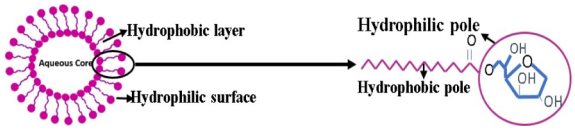
Cubosomes	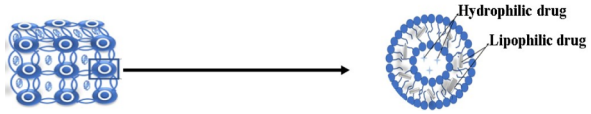

Table4
Classical and new large scale teqniques for liposomes preparation.

Classical Technique	Hydration of a Thin Lipid Film Reverse-Phase Evaporation (REV) Technique Solvent (Ether or Ethanol) Injection Technique Detergent Dialysis	
New Large-Scale Techniques	Heating Method Spray-Drying Freeze Drying Super Critical Reverse Phase Evaporation (SCRPE) Modified Ethanol Injection	Crossflow Injection Technique Microfluidization. Membrane Contactor

donepezil as a form of liposomes, and the results revealed that donepezil liposome formulation was stable and had noticeably increased concentrations in the plasma and the brain after intranasal administration with no toxicity, which could be explained by the following possible reasons: (i) the ideal characteristics of the liposomal formulation including uniform particle size (102 ± 3.3) and low PI (0.28 ± 0.03), the smaller size of the vesicles having the potential to facilitate the absorption of the drug; (ii) the higher EE of the system (84.91 ± 3.31)%, which may result in a better bioavailability of the drug; (iii) the results of the in vitro drug release studies demonstrated a good distribution of the drug particles, which enhances the absorption of DNP from the nasal cavity; (iv) the pharmacokinetics study demonstrated a significantly improved brain bioavailability of liposomal formulations following the nasal route of administration as they may enhance the cellular uptake and transport of drugs across the capillary endothelium via receptor-mediated endocytosis and passage through the BBB [132]. The effects of intranasal administration of galantamine-loaded flexible liposomes have been investigated regarding the inhibition efficiency of acetylcholinesterase as well as the pharmacokinetic behavior of galantamine (GH). It has been revealed that the efficiency of acetylcholinesterase inhibition of GH was greatly enhanced by intranasal administration compared with the oral one, with special regards to GH loaded in flexible liposomes, in addition to providing enhanced pharmacokinetics without any cytotoxicity, which could be due to the good properties of the prepared liposomes (diameter of 112 ± 8 nm, PDI of −49.2 ± 0.7 mv and high entrapment efficiency (83.6 ± 1.8%)). Besides that, the fluid membrane of the prepared flexible liposomes gives them high elasticity, which eases their passage through the mucosal membranes. Flexible liposomes consist of phospholipids, an edge activator and water. The edge activator (e.g. ethanol and propylene glycol) helps in increasing the fluidity and flexibility of the phospholipid bilayers [140]. Curcumin was formulated in a liposomal form in a way to develop mucoadhesive properties of the drug delivery system via the nasal route. The in vivo study for the assessment of drug bioavailability in the brain after intranasal administration suggested that the xanthan gum coated curcumin liposomes are a promising drug delivery system to deliver the drug to the brain through the nasal route. The resulting liposomes showed higher drug distribution in the brain compared to the drug solution, which could be due to the small particle size of 100.2–150 nm with good stability in addition to the absence of any deleterious effect on the nasal mucosa [141].

The efficacy of formulating rivastigmine as liposomes was studied in comparison with the free form of the drug after either intranasal or oral administration. Firstly, a significantly higher level of the drug was found in the brain with the intranasal liposomes of rivastigmine than with the intranasal free drug or through the oral route, which could be due to the relatively high EE (80%). Secondly, the intranasally applied liposomes showed a longer brain half-life compared to intranasally or orally administered free drug This phenomenon could be explained by the fact that the free drug reached the systemic circulation rapidly via the nasal route, whereas the liposomal drug might have been accumulated in the nasal mucosa, giving the opportunity for direct transportation to the brain to take place [142]. Results from another study demonstrated that liposomes, especially CPP-liposomes, can enhance the permeability of rivastigmine across the BBB. The intranasal administration of rivastigmine liposomes demonstrated a higher capacity to improve both rivastigmine distribution and retention in CNS regions

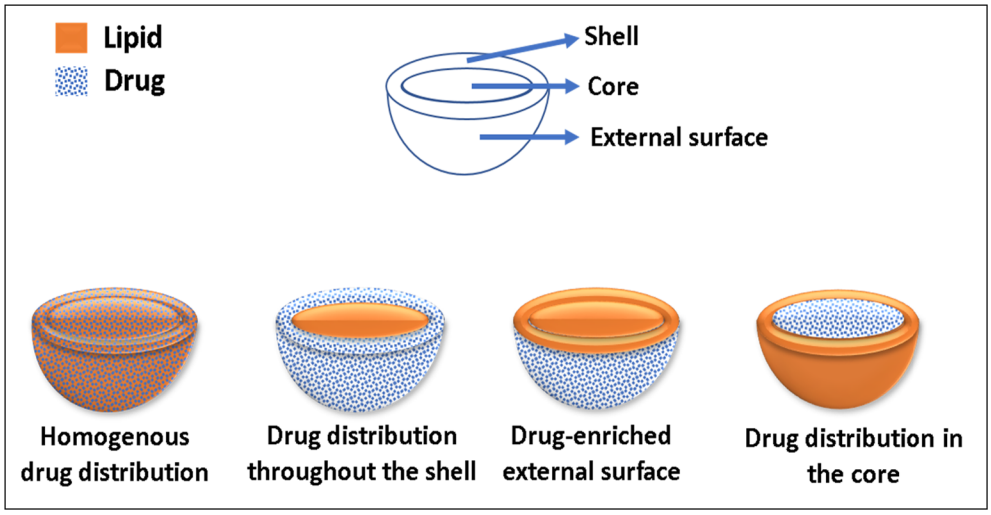

Fig. 4. Structure of a solid lipid nanoparticle and types of the drug distribution in it.

(especially in the hippocampus and the cortex) than in the case of IV administration. This could be explained as follows: attaching a cell penetrating peptide to the liposomes can improve drug transmembrane effect due to a receptor-mediated uptake and enhancing penetration, in addition to improving targeting efficacy and brain uptake through endocytosis [143].

5.2. Solid lipid nanoparticles (SLNs)

SLNs represent a class of colloidal particles composed of lipids being solid at both room and body temperatures, with unique size-dependent properties, in a range of 50–80 to 1000 nm combining the advantages of lipid-based nanocarriers and polymeric nanoparticles while avoiding their limitations [144]. The active substance may be located in the particle core, shell, or can be dispersed within the whole lipid matrix as Fig. 4 demonstrates. Many ligands like proteins, oligosaccharides, and antibodies could be attached to the outer shell of SLNs, providing them a specific activity when administered to the body [145].

Many different methods are available to prepare SLNs to suit the properties of the chosen active pharmaceutical ingredients and the available equipment [146], as shown by the following table (Table 5).

SLNs exhibit a great potential as suitable drug delivery systems due to the following possible reasons:

1- They are tiny biodegradable particles with easy surface functionalization regarding both hydrophobic and hydrophilic drugs [147]
2- They help increase the solubility of the drug, thus offering targeted release and stability to the solid lipid matrix [148]. The formulation of the active substances as solid-lipid nanoparticles holds a strong promise in providing them directly to the brain, as their lipid nature and submicron size give them a natural tendency to cross the BBB with a very low cytotoxicity [149]
3- A variety of components could be used to prepare these SLNs, as shown below (Table 6) [145]. Additionally, the suitable surface modification of SLNs can significantly modify the release of the drug substance and minimize the “burst effect” [150]
4- They demonstrate simple and economical large-scale production as they do not need very sophisticated equipment or high-energy input, and the use of organic solvents is avoided (microemulsion method).
5- The enhanced absolute bioavailability with intranasal SLNs can create a higher driving force for diffusion across the BBB due to the increased concentration gradient from the systemic circulation to the brain [151]
6- Drug-loaded SLNs are known to have preferential BBB permeation compared with the free drug form. The enhanced BBB permeation of the SLNs can be due to their lipid content, which can enhance transcellular diffusion across the BBB. Also, the surfactants associated with SLNs can act as absorption enhancers, decrease nanoparticle clearance by the reticuloendothelial system and inhibit the efflux system, especially P-glycoprotein enhancing the transport across the BBB [152]. The associated surfactants can also increase brain uptake via the transient opening of the brain endothelial tight junctions [153]. SLNs can also be endocytosed by the BBB endothelial cells [154], from where they can be transcytosed into the brain [155] or release AGM within the endothelial cells, which diffuses into the brain.

The favored brain drug delivery can be related to the route of administration, where the formula applied by the intranasal route has the ability to be directly transported to the brain using the direct pathways of the olfactory and trigeminal nerves without having to cross the BBB, whereas the intravenously administrated AGM does not have any direct pathway to the brain and must cross the BBB to reach it [151].

Nonetheless, these nanoparticles also present some disadvantages

Table 5
General methods of preparation of solid lipid nanoparticles.

Hot homogenization	A dispersion of the aqueous phase into the lipid phase is prepared, high-pressure homogenization is applied using a homogenizer, then solidification takes place by cooling down
High-pressure homogenization	Preliminary homogenization of melted lipids with water, then high-pressure homogenization takes place, and finally a rapid cooling down with cold water is applied
Solvent evaporation	Preparation of an emulsion from lipids, surfactants and water immiscible solvent followed by homogenization, then solvent evaporation
Solvent emulsification diffusion	Preparation of an emulsion from lipids, surfactants and water immiscible solvent follows by stirring, then solvent diffusion
Microemulsion	Mixing lipids and aqueous phases to form a transparent or translucent mixture, then dispersing it in a cold aqueous phase with mild stirring till the formation of fine particles
Double emulsion solvent evaporation	Mixing lipid with water immiscible solvent then homogenization with water and surfactant followed by solvent evaporation

Table 6
A variety of components could be used to formulate SLNs.

Lipids	**Glycerol esters**			
	Glyceryl trimyristate	Glyceryl trioleate	Hydrogenated palm kernel glycerides,	
	Glyceryl tristearate	Glyceryl tripalmitate	Hydrogenated castor oil	
	Glyceryl mono stearate	Glyceryl di stearate	Soybean oil	
	Glyceryl behenate	Glyceryl palmitostearate	Peanut oil	
	Waxes		**Fatty acids**	
	Cetyl palmitate	Carnauba wax	Myristic acid	Stearic acid
	Beeswax		Palmitic acid	
Emulsifiers	**Phospholipids**	**Steroids**		
	Egg lecithin	Cholesteryl oleate		
	Soya lecithin, Hydrogenated soya lecithin	Cholesterol		
	Non-ionic surfactants			
	Poloxamer188,	Poloxamer 407	Polysorbate 20,80	
	POE-20-cetyl ether	POE-20-oleyl ether	POE-20-isohexadecyl ether	
	PEG (15)-hydroxy stearate,	PEG monostearate	Sorbitan monooleate	
	Polyvinyl alcohol	Macrogol (25)-cetostearyl ether		
	Anionic surfactants			
	Sodium lauryl sulphate			
Co-surfactants	**Alcohols**	**Bile salts**		
	1-Butanol	Cholate	Taurocholate	
		Taurodeoxycholate		

related to the recrystallization process, such as a low drug loading capacity and the possibility of drug expulsion during their storage, together with the high polydispersity shown by some SLN preparations [156].

5.2.1. SLNPs as carriers for nose-to-brain delivery in some AD treatments

Donepezil was formulated as a form of SLNs to evaluate the efficacy of delivering donepezil directly to the brain through the intranasal route. When the in-vitro and in vivo release studies took place, donepezil SLNs showed a greater release rate compared to IV and IN donepezil solution, which could be attributed to the ability of the formulated SLNs to protect the encapsulated drug from biological and/or chemical degradation and extracellular transport by P-gp efflux proteins; in addition, the contact time between DPL-SLNs and the nasal mucosa increases, which results in a higher nasal retention time due to the occlusive nature of lipids in the SLNs. Moreover, the improved delivery by SLNs may be related to the use of Tween 80 in the preparation of SLNs, which is reported to improve the brain delivery of nanoparticles by one of the following mechanisms: (i) solubilization of endothelial cell membrane lipids and membrane fluidization; (ii) the temporary opening of inulin spaces; (iii) endocytosis of nanoparticles and (iv) inhibition of the efflux system, especially P-gp present on the intranasal membrane [157,158].

With the help of the quality by design approach, an optimal formulation of rivastigmine SLNs was prepared, then it was compared to rivastigmine solution, rivastigmine SLNs showed higher in vitro and ex vivo diffusion outcomes. The higher diffusion of SLN could be a result of their lipid surface which had imperfect crystal lattices through which the drug diffused out easily because it requires less energy than in the case of perfect crystal substance. The higher value of diffusion and diffusion coefficient for RHT-SLN in ex vivo studies could be attributed to the lipidic nature of the SLN system, which diffused across the nasal mucosa in a superior way compared to the drug solution. Another reason for the higher diffusion of RHT-SLN could be either the formation of amorphous dispersion or the solubilization of RHT in the Compritol matrix [159].

The poor brain penetration of tarenflurbil (TFB) was one of the major reasons for its failure in phase III clinical trials asa potential AD medication. Eameema Muntimadugu et al designed a study aimed at improving TFB delivery to the brain intranasally. The in vitro release studies proved a sustained release of TFB from TFB-SLNs in comparison with the pure drug, indicating prolonged residence time of the drug at the targeted site. Pharmacokinetics suggested improved circulation behavior of SLNs, the absolute bioavailability of which was higher than that of either the intranasal solution or the oral suspension of TFB [160].

5.3. Nanostructured lipid carriers (NLCs)

NLCs are a new generation of solid lipid nanoparticles, which were developed mainly to overcome their related limitations. NLCs exist also as solid matrices of lipids at room and body temperature, but the main difference from SLNs is the replacement of a part of solid lipids with oil, resulting in a less ordered lipid matrix [161], which may be the reason behind their high drug payload, reducing drug expulsion and burst release phenomena compared to SLNs [162]. Based on the variation in the composition of lipid and oil mixtures, in addition to the various fabrication methods like those followed to prepare SLNs, NLCs can be categorized into three types [163,164] as shown in the Fig. 5 below:

The methods of NLCs preparation are the same as the ones followed to prepare SLNs with a newly developed method called “Hot-melt extrusion technology” [165]. NLCs are considered potential drug carriers due to their biocompatibility and superior formulation properties over SLNs as they are more flexible in their ingredients and contain lipids in both liquid and solid states [166]. NLCs have shown the inhibition of p-gp efflux pump and thereby achieved higher drug concentrations in the brain, with the potential of circulating for a longer period of time [165]. They are made of surfactants and lipids that are approved by the FDA and/or EMA, they can be prepared in the absence of an organic solvent and the process is easily scalable into large batch sizes by high pressure homogenization [167]. Finally, NLCs were found to be more permeable through nose-to-brain as compared to the drug solution [168]In addition to the advantages that SLNs present, NLCs have improved drug encapsulation efficiency and release properties but unfortunately, they still have the drawback of rapid mucociliary clearance [169].

The carrier-mediated efflux transport process is known to play a role in the drug transportation of nasally applied NLCs to the brain [170], Transcellular transportation through the olfactory neurons is another mechanism to deliver NLCs to the brain via the various endocytic pathways of neuronal cells in the olfactory membrane [117,171]. It is also suggested that the transport of NLCs could be done by slow intraaxonal transport or by a faster transfer through the perineural space surrounding the nerve cells [172].

5.3.1. NLCs as carriers for nose-to-brain delivery in some AD treatments

An exploration of the potential role of NLCs to enhance brain

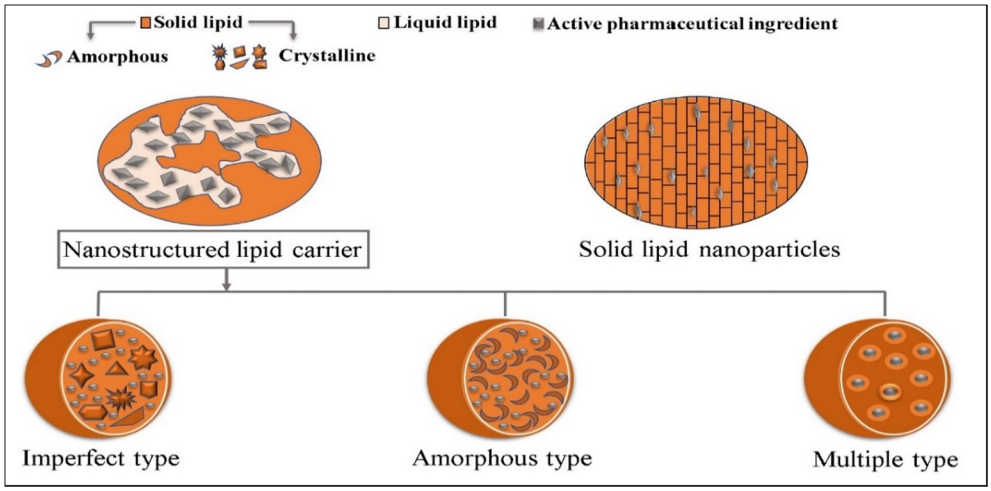

Fig. 5. The main difference between SLNs and NLCs, with the three types of NLCs.

delivery of rivastigmine (RV) via the intranasal route was done by Preeti Wavikar et al. Rivastigmine-loaded in situ gelling nanostructured lipid carriers (NLCs) were formulated as a nose-to-brain delivery system. RV in situ gel showed an increase in nasal permeation and enzyme inhibition efficacy of the drug over the plain RV solution which could be due to the fact that RV in situ gel showed excellent elasticity, rheology, mucoadhesion and adhesiveness to facilitate its adhesion to the upper nasal mucosa. NLC-based in situ gel showed a 2-fold increase in the nasal permeation of the drug over the plain RV solution, which could be related to its content of surfactants, which opens the tight junctions in the nasal epithelial and as a result increases nasal permeation of the drug. In situ gelling NLCs showed a 3-fold increase in enzyme inhibition efficacy which could be related to NLC content of lecithin, which is known to inhibit acetylcholine esterase enzyme and is also a precursor for choline, which is deficient in the brain in AD, resulting in enhanced enzyme inhibition efficacy [173]. Later, an in situ gelling system was developed in which, RV-NLCs containing 6.25% w/w RV were formulated with some formulation process modifications. Results showed a sustained release of IN and IV NLCs when comparing with RV solutions by the same routes with significantly higher AUC and $T_{1/2}$. Biodistribution investigations demonstrated an enhancement of brain drug concentration, which means a potential penetration of the BBB when applying NLCs compared to the solutions The lipophilic nature of the NLCs combined with their nano size (123 ± 2.3 nm) make them more permeable across the nasal mucosa in addition to improving the rheological properties through the NLCs formulation. Besides, enhance the mucoadhesiveness of this system and thus increase the residence and adherence of the formulation to the upper nasal mucosa for a longer period. Also, using stearylamine as a positively charged lipid enables the adherent to the negatively charged nasal epithelium. Similar results were obtained in pharmacodynamics when faster recovery of memory loss in amnesic mice was obtained when applying NLCs compared to plain RV solution by both IV and IN routes with the absence of inflammation or cytotoxicity signs. This could be due to the decrease in escape latency of intranasal in situ gelling NLCs compared with IV NLCs suggesting brain targeting potential via the nose-to-brain pathway [174]. Curcumin-donepezil loaded NLCs were prepared by Sumeet Sood et al for the delivery to the brain via the nasal route, the resulting NLCs had a particle size less than 50 nm suitable for intranasal delivery. In vivo pharmacokinetic studies revealed that a higher drug concentration was achieved in the brain via the IN route compared to the intravenous one with slower clearance. Along with the above, behavioral tasks showed an improvement in memory and learning skills in the group treated with NLCs compared to those treated with pure drugs. Acetylcholine levels were significantly improved in the brains of NLCs treated group, and oxidative stress was much lower in animals treated with combination therapy [175]. A suitable chitosan-coated nanostructured lipid carrier (CS-NLC) formulation has been designed by O. Gartziandia et al with the aim of detecting the effectiveness of brain delivery following intranasal administration. The biodistribution study of CS-NLCs loaded with near-infrared dye demonstrated an efficient brain delivery of the particles after intranasal administration, this was probably due to the mucoadhesive property of chitosan diminishing mucociliary clearance and thereby enabling the drug to target the olfactory region. Furthermore, chitosan enhances drug delivery across the epithelial mucosa, opening the tight junctions between cells. The above makes CS-NLC a safe and effective potential nanocarrier for nose-to-brain drug delivery in neurodegenerative diseases [172]. Amarjitsing Rajput et al conducted research work aimed to develop resveratrol nanostructured in-situ gel for the treatment of AD. The optimized in situ gel showed higher nasal mucosa permeation compared to the suspension-based in situ gel for the following reasons: (i) the higher residence time of the optimized formulation in the nasal cavity compared to the suspension; (ii) the lipophilic nature of the nanostructured lipid carrier may increase uptake of the drug; (iii) the aqueous fluid present in the formulation causes an increase in the interlamellar volume of the tissue and causes leakages in the membrane structure, which results in higher drug uptake through the tissue. Additionally, a significant improvement in memory function was achieved when using optimized nasal in-situ gel-based treatment compared to orally administered resveratrol suspension and that could be due to the enhanced brain function [176].

5.4. Nanoemulsions

Nanoemulsions are fine emulsions, either water in oil or oil in water, prepared by using two immiscible phases, with the help of one or more suitable surfactants (Table 3) [177]. The range of the droplet size of these forms varies approximately between a few to 200 nm, which makes them appear in a transparent-to-milky-white appearance to the naked eye [178].

The preparation of nanoemulsions can be categorized into two basic methods, the first one is the high energy method that includes preparing a primary o/w macroemulsion, then either by ultrasonication or by high-pressure homogenization the final nanoemulsion will be produced. The second method uses low energy, in which a primary w/o emulsion is prepared, then either by heating or dilution with water in the presence of continuous high-speed stirring, the primary emulsion will be converted into an o/w final nanoemulsion [179]. The advantages of NE include a higher surface area; they can be formulated in

a variety of formulations such as liquids, sprays, foams, creams, ointments and gels from which an ideal nasal formulation can be chosen to provide the best mucoadhesive properties [180,181]. Lipidic nanoemulsions require a lesser amount of surfactants and cosurfactants for their formation which means an increase in surfactant-related cytotoxicity [182]. they can save money since they are considered as an energy-saving procedure [183].

Nose-to-brain transport pathways of nanoemulsions involve one or more of the following: neuronal pathway, vascular pathways, CSF, or lymphatic system distribution [180].

5.4.1. Nanoemulsions as carriers for nose-to-brain delivery of some AD treatments

Sumeet Sood et al tried in a research project to enhance the brain targeting of curcumin–donepezil nanoemulsion via the nasal route of administration. The study revealed an increased brain concentration of the drug when it was applied intranasally more than IV, which could be the result of the very small size of the particles < 50 nm in addition to their enhanced mucoadhesiveness and mucus permeation properties. The other result was improvement in memory function, and learning abilities in the group that received nanoemulsions more than pure drugs [184]. Maha Nasr found in a research project that lipid-based hyaluronic acid nanoemulsion could be a special candidate as a carrier system for the brain delivery of therapeutics since the result from this work presented special nanoemulsion properties regarding the drug concentration in the brain due to the lipidic matrix of the nanoemulsion which is expected to have favored the partitioning of the nanoemulsion into the lipid bilayer of the nasal epithelial cells. In addition, the surfactant content enhanced the cell membrane fluidity and the surface modification with hyaluronic acid delayed the mucociliary clearance as it enhanced the mucoadhesive nature of the particles [182]. Finally, since neuroinflammation is one of the characteristic signs of neurodegenerative disorders, Sunita Yadav et al detected the efficacy of the intranasal route in delivering TNFα siRNA nanoemulsion. The results demonstrated a remarkable decrease in TNFα levels in LPS-stimulated cells, and an almost 5-fold increase in the rat brain uptake compared to non-encapsulated siRNA. this could be due to the multifunctional potential of the nanoemulsion to serve as a mucoadhesive and to enhance endocytosis due to its smaller particle size [185].

5.5. Niosomes

Niosomes have a multi-thin-layer vesicular structure and contain basically nonionic surfactants, a hydration medium, and lipids such as cholesterol(Table 3) [186]. Niosomes, which are prepared by following the same procedures and under the same variety of conditions, are similar to liposomes [187].

Recently, niosomes have gained interesting attention in the field of neurodegeneration treatments for the following reasons: (i) their potential possibility to increase nose-to-brain drug delivery as well as enhance drug chemical and biological stability; (ii) their unique structures make them capable of encapsulating both hydrophilic and lipophilic substances [188]; (iii) the possibility of controlling their properties like surface charge; (iv) the absence of special conditions required for handling and storage [189]. Niosomes have been shown to provide stable encapsulation for various drugs and offer distinct advantages over unencapsulated agents [190].

Compared with liposomes, niosomes have advantages such as good stability, low cost, ease of formulation and scaling-up. They are much more stable because their forming materials, non-ionic surfactants, are more stable than those of lipids both in terms of physical and chemical stability. Also, the PEG on the surface of liposomes which could prolong the half-life after being administrated was limited because the lipid bilayer can maximally tolerate about 5–6% mol% of PEG and may cause some stability problems such as the lysis of liposomes at high concentrations. Lastly, the formulation process was much easier due to the good stability of niosomes, which are much cheaper than liposomes [191]. However, the stability issue is not clear yet and is a serious drawback that faces niosomes [192].

5.5.1. Niosomes as carriers for nose-to-brain delivery in some AD treatments

Federica Rinaldi et al formulated and characterized drug-free and pentamidine loaded chitosan glutamate coated niosomes in aa attempt to provide them to the brain through the intranasal route. Pentamidine entrapment and mucin interaction were the two evaluated properties of the prepared systems. Entrapment efficiency was 10.96% which is relatively high and is considered useful to achieve therapeutic efficacy. In addition, the presence of PEG units in Tween 20 molecules, and consequently, on niosomal surface enhances mucoadhesive properties. Moreover, the addition of CG and its presence on niosomal surface is considered fundamental because of its penetration enhancer properties [193]. Based on the hypothesis that the low blood level of folates is the primary cause of depression in AD, and since folic acid is a water-soluble vitamin showing difficulty in crossing the BBB, Ravouru Nagaraju et al. prepared niosomes of folic acid using different formulations. The niosomes prepared with Span 60 and cholesterol in the ratio of 1:1(50 mg: 50 mg) showed higher entrapment efficiency of 69.42% and better in vitro drug release of 64.2% at the end of 12 h [194].

5.6. Cubosomes

Cubosomes are highly stable nanoparticles formed from the lipid cubic phase and stabilized by a polymer-based outer layer. The bicontinuous lipid cubic phases consist of a single lipid bilayer that forms a continuous periodic membrane lattice structure with pores formed by two interwoven water channels (Table 3). The composition of the cubosome can be modified to control the pore sizes or to include specific types of lipids. Their outer polymer layer can be used to enhance targeting. They are highly stable forms under physiological conditions [195].

The two main components of the cubosomes are the amphiphilic lipids, which are limited nowadays to glyceryl monooleate (GMO) and surfactants (stabilizers). The following figure demonstrates the two ways of preparing cubosomes (Fig. 6) [196]:

In comparison with liposomes, the structure of cubosomes provides a significantly higher drug entrapment due to their high internal surface area and cubic crystalline structures. Moreover, they are considered as easy to prepare. They are biodegradable formulations that have the capability of encapsulating hydrophilic, hydrophobic, amphiphilic substances and acheaving a targeted or controlled release of bioactive agents. The only major drawback facing these forms is that large-scale production is sometimes difficult to apply because of their high viscosity [197].

The suggested mechanisms of the direct transportation of

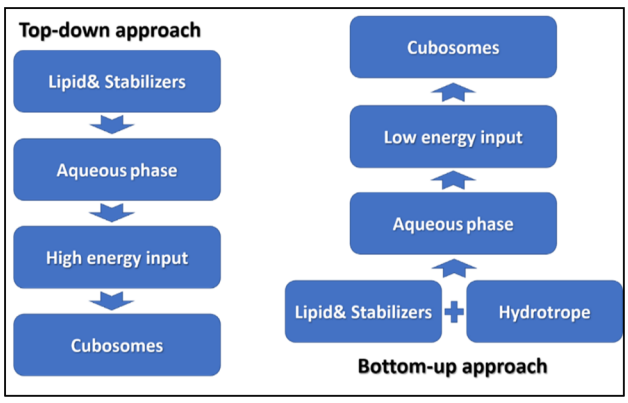

Fig. 6. Top-down vs Bottom up approaches in preparing cubosomes.

Table 7
A comparison between the advantages and disadvantages of lipid-based NPs and polymeric-based NPs with their varieties.

Advantages	
Lipid Based NPs	Polymeric Based NPs
Production on a large industrial scale	Incorporation of hydrophilic and hydrophobic drugs
Low toxicity due to their biocompatible and biodegradable components and absence of organic solvent(s) in their process	Tunable chemical and physical properties
Incorporation of lipophilic and hydrophilic drugs	Use of biodegradable materials when desired
Protecting drug from environmental conditions	Representing special properties when choosing the proper polymer
Relatively low cost	Reproducible data when using synthetic polymers
low toxicity	Higher stability than lipid based ones
Good biocompatibility and biodegradability	Variety of the methods of preparation
Relative high encapsulation efficiency and stability	Drug release in a controlled manner
Simple and inexpensive manufacturing process	Protecting drug from environmental conditions
Enhanced penetration and permeation properties	Increasing solubility of highly lipophilic drugs
Disadvantages	
Lipid Based NPs	**Polymeric Based NPs**
Low drug-loading for SLNs	Insufficient toxicological assessment in the literature
Poor stability& the risk of gelation for SLNs	Difficulty in their scale-up
Drug expulsion during storage cause by lipid polymorphism for SLNs	Low drug-loading capacity
Special requirements of storage	Not a good candidate carrier for hydrophilic drugs

cubosomes are: (i) active transport of cubosomes through the nasal mucosa, especially the olfactory mucosa; (ii) direct transport to the brain tissues through the trigeminal nerves at the respiratory epithelium [198].

5.6.1. Cubosomes as carriers for nose-to-brain delivery in some AD treatments

Rahul P. Patil et al conducted a research study aimed to develop cubosomal mucoadhesive in situ nasal gel of donepezil HCl for direct brain delivery. The optimal cubosomal dispersion and cubosomal mucoadhesive in situ nasal gel showed significantly higher trans nasal permeation and better distribution in the brain when compared to the drug solution. This could be a result of the ability of the cubosomes to retain the drug in the nasal cavity for prolonged period resulting into increased permeation which may be attributed to increasing contact time with nasal mucosa. Thus, the formulated cubosomal mucoadhesive in situ gel could be considered as a promising carrier for brain targeting of CNS acting drugs through the trans-nasal route [199].

Table 7 below, demonstrates clearly the main differences between lipid –based and polymeric-based nanosystems regarding their advantages and disadvantages.

6. Fate of nasally applied brain-targeting lipid nanosystems

Mucociliary clearance is a major physiological factor that significantly affects nasal drug delivery and nose-to-brain transport. It works as a protection mechanism of the respiratory apparatus by efficiently and rapidly eliminating harmful substances, microorganisms, particulate matter, and enclosing them in the mucus layer. However, this system greatly limits the residence time of the nanoparticles administered inside the nasal cavity. Therefore, as far as the nanoparticles have good mucoadhesive properties, they will stick properly to the olfactory mucosa leading to a higher mucosal permeability. Thus, traditional nasal formulations contain excipients able to increase viscosity and/or provide bioadhesion to limit mucociliary clearance, prolong formulation residence time, improve brain bioavailability, and reduce nasal absorption variability [133]. For instance, Chitosan and low molecular-weight pectins were shown to prolong the residence time of nasal formulations in the olfactory region in humans [200], and sodium hyaluronate showed an improvement in the brain delivery of a high-molecular-weight hydrophilic model compound after nasal administration to rats [201].

Although there are many studies regarding drug incorporation into lipid-based nanosystems as we mentioned before very few data on release mechanisms are available nowadays. The major problem in early work with lipid nanoparticles was the generally observed burst release of encapsulated drugs. The amount of drug in the outer layer and on the particle surface is generally released in the form of a burst, while the drug incorporated in the particle core is released in a prolonged manner. Therefore, the extent of burst release can be controlled by controlling drug solubility in the lipid phase during production, which, in turn, can be controlled via the temperature employed and the surfactant type and concentration used. To avoid or minimize burst release, lipid based nanoparticles can be produced surfactant-free or with surfactants unable to solubilize the drug [202]. After the drug is released from the lipid-based nanosystem, it will be transported via either the olfactory or the trigeminal nerves in order to reach the brain and particularly the olfactory bulb.

Once the drug particles are available in the human olfactory bulb, the ensuing distribution of the drug in the CNS appears to be mediated via bulk flow of the CSF, while in rodents, the distribution may be mediated via the rostral migratory stream [106,107,203].

However, for charged, hydrophilic and large particles it is more difficult to cross. Subsequent to a drugs passage through the mucus, there are several mechanisms for permeation through the nasal mucosa. It can happen either by paracellular transport via movement between cells and transcytosis by vesicle carrier's pathway or both passively and actively via transcellular or simple diffusion. Several mechanisms such as carrier-mediated transport, transcytosis and transports through intercellular tight junctions have been proposed [204].

7. Toxicological concerns

Since the nasal mucosa demonstrates a variety of tolerability reactions to the drugs and additives used in the nasally administered formulations, the careful selection of the used excipients must be considered because it could influence pharmacokinetics and toxicity. For example, some surfactants have toxic effects when they are used over a specific limit [205], and the same applies to absorption enhancers since they could create mucosal toxicity [103].

In general, lipid-based nanosystems can be classified as safe forms to apply due to the absence of any previously reported mutagenic effects. However, the magnitude of evaluating the potential negative impact on mucociliary clearance, and epithelial and cilia toxicity should be taken into consideration [206]. In order to determine the possible toxicological effects of the intranasal application of rivastigmine-loaded

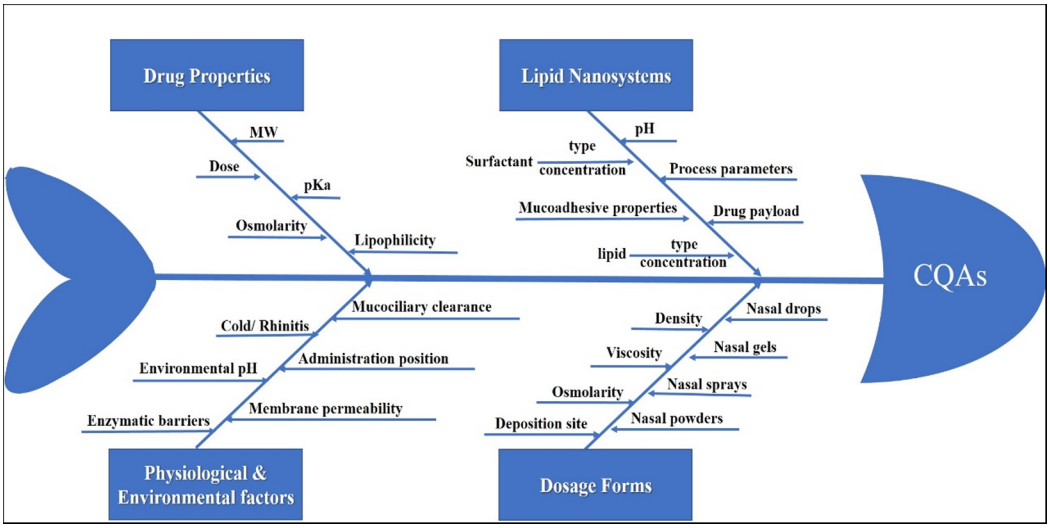

Fig. 7. Ishikawa fish bone diagram defining factors affecting nose-to-brain delivery of lipid based nanosystems.

liposomes, Zhen-Zhen Yang et al conducted a number of experiments that aimed to evaluate the changes in the morphology of the nasal mucosa in rats after the intranasal application of the prepared forms. Results demonstrated no significant disruption or harmful effects in either the nasal epithelium or the cilia, in addition to noticing reduced accomplished hemolysis in sheep erythrocytes [143]. Gartziandia et al investigated the safety and efficacy of chitosan-coated nanostructured lipid carriers as suitable drug carriers for nose-to-brain delivery formulations. The findings demonstrated the biocompatibility of the nanocarrier system and its cellular uptake by 16HBE14o- cells. Also, it was found to be nasal mucosa friendly with no harmful effect [172]. Finally, when examining lamotrigine-loaded liposomes for the nasal toxicity in goat nasal mucosa, Praveen et al noticed the absence of any damage or toxicity caused to the nasal epithelial layer accomplished with the nose-to-brain delivery of lamotrigine [207]. Shweta Gupta et al reported no cell necrosis or cilia removal after applying the Efavirenz brain targeting SLNs intranasally, and the microscopic structure of the nasal mucosa showed no harmful changes caused by these nanoparticles [208]. Nehal L Patil et al found no noticeable changes in the sheep nasal mucosa or epithelium cilia or any remarkable inflammation following the nasal application of brain targeting quercetin-loaded NLCs [169].

8. General comments and opinion

8.1. Importance of applying quality by design (QbD) concept in the development of LNs

Since lipid-based nanosystems are complex forms in their nature, their characteristics are expected to be influenced by many formulation parameters such as drug physiochemical properties, drug payload, pH, surface charge, lipid type and concentration, surfactant type and concentration, coating with mucoadhesive polymers in addition to process parameters that differ according the selected preparation technique (Fig. 7) [151,209–211].The application of the quality by design (QbD) approach presents a logic strategy that saves time, money and efforts, especially when dealing with complex drugs like proteins, peptides, and sophisticated nanosystems such as lipid-based nanoparticles [212]. The first step of this methodology starts by defining the quality target product profile (QTPP), followed by defining the critical process parameters (CPPs) and critical material attributes (CMAs) that can highly affect the critical quality attributes (CQAs) of the product. In case of lipid nanosystem designed for nose-to-brain delivery, the CQAs are particle size, surface charge, pdI, encapsulation efficacy, stability, mucoadhesiveness, cytotoxicity, nasal mucosa permeability.

Risk assessment (RA) is conducted then to show the factors with the highest impact on product quality, which are usually the key elements of the systemically designed experiments in practice.

The quality by design (QbD) approach aims to design a high-quality product, starting by optimizing the manufacturing process seeking to reach the targeted performance of the desired product. Depending on the information and knowledge obtained from the previous development studies and manufacturing experiences in the pharmaceutical field, a good scientific understanding to support the establishment of the design space, specifications, and manufacturing controls can be gained [213].

When the application of this methodology takes place in the early research phases (R&D activities), it offers many advantages like i) achieving meaningful product quality properties; ii) increasing process capability and iii) reducing product variability and defects by enhancing product and process design [214].

9. Conclusion

The development of lipid-based nanosized drug delivery systems with substantial pharmaceutical and biomedical significance has brought new opportunities and challenges for nose-to-brain delivery, which has emerged as an alternative route to the systemic ones. It provides a promise of overcoming the shortfall of absorption and reaching the brain in the presence of the BBB, which have been the two obstacles during many decades of research work in this field. However, targeting the olfactory mucosa and retaining these forms there as long as possible are considered the key factors of providing the applied active pharmaceutical agents to the CNS. Furthermore, long-term safety and effectiveness trials of these forms through the nasal route are needed before being recommended as the therapies of choice since they might be instable in vivo or have a poor brain bioavailability, taking into consideration that the high-cost manufacturing process of these systems is a real major obstacle to their development.

References

[1] M.-T. Heemels, Neurodegenerative diseases, Nature 539 (7628) (2016) 179–180.
[2] A.D. Gitler, P. Dhillon, J. Shorter, Neurodegenerative disease: models, mechanisms, and a new hope, The Company of Biologists Ltd., 2017.
[3] P. Batista, A. Pereira, Quality of life in patients with neurodegenerative diseases, Dimensions 1 (2016) 3.
[4] R. Gowthaman, et al., Database of neurodegenerative disorders, Bioinformation 2 (4) (2007) 153.
[5] A.C. Serban, Aging population and effects on labour market, Procedia Econ.

Finance 1 (2012) 356–364.
[6] D. Cantarero-Prieto, et al., The economic cost of dementia: A systematic review, Dementia (2019) p. 1471301219837776.
[7] H. Hippius, G. Neundörfer, The discovery of Alzheimer's disease, Dialogues Clin. Neurosci. 5 (1) (2003) 101.
[8] J. Hardy, D.J. Selkoe, The amyloid hypothesis of Alzheimer's disease: progress and problems on the road to therapeutics, Science 297 (5580) (2002) 353–356.
[9] C. Wattmo, L. Minthon, Å.K. Wallin, Mild versus moderate stages of Alzheimer's disease: three-year outcomes in a routine clinical setting of cholinesterase inhibitor therapy, Alzheimer's Res. Therapy 8 (1) (2016) 7.
[10] J.A. Opara, Activities of daily living and quality of life in Alzheimer disease, J. Med. Life 5 (2) (2012) 162.
[11] C. Reitz, C. Brayne, R. Mayeux, Epidemiology of Alzheimer disease, Nat. Rev. Neurol. 7 (3) (2011) 137.
[12] R. Mayeux, Y. Stern, Epidemiology of Alzheimer disease, Cold Spring Harbor Perspect. Med. 2 (8) (2012) a006239.
[13] A.L. Sosa-Ortiz, I. Acosta-Castillo, M.J. Prince, Epidemiology of dementias and Alzheimer's disease, Arch. Med. Res. 43 (8) (2012) 600–608.
[14] M.P. Heron, Deaths: leading causes for 2013. 2016.
[15] H. Niu, et al., Prevalence and incidence of Alzheimer's disease in Europe: A meta-analysis, Neurología (English Edition) 32 (8) (2017) 523–532.
[16] D.A. Casey, D. Antimisiaris, J. O'Brien, Drugs for Alzheimer's disease: are they effective? Pharm. Therapeut. 35 (4) (2010) 208.
[17] K. Mullane, M. Williams, Alzheimer's disease (AD) therapeutics-1: Repeated clinical failures continue to question the amyloid hypothesis of AD and the current understanding of AD causality, Biochem. Pharmacol. (2018).
[18] J. Rohrer, N. Lupo, A. Bernkop-Schnürch, Advanced formulations for intranasal delivery of biologics, Int. J. Pharm. (2018).
[19] S. Salomone, et al., New pharmacological strategies for treatment of Alzheimer's disease: focus on disease modifying drugs, Br. J. Clin. Pharmacol. 73 (4) (2012) 504–517.
[20] M. Agrawal, et al., Nose-to-brain drug delivery: An update on clinical challenges and progress towards approval of anti-Alzheimer drugs, J. Control. Release 281 (2018) 139–177.
[21] J. Cummings, et al., Role of donepezil in the management of neuropsychiatric symptoms in Alzheimer's disease and dementia with Lewy bodies, CNS Neurosci. Ther. 22 (3) (2016) 159–166.
[22] C. Holmes, et al., The efficacy of donepezil in the treatment of neuropsychiatric symptoms in Alzheimer disease, Neurology 63 (2) (2004) 214–219.
[23] J. Bryan, Donepezil—a major breakthrough in the treatment of Alzheimer's disease, Suicide 14 (2019) 20.
[24] S. Black, et al., Donepezil preserves cognition and global function in patients with severe Alzheimer disease, Neurology 69 (5) (2007) 459–469.
[25] V. Kumar, Potential medicinal plants for CNS disorders: an overview, Phytotherapy Res.: Int. J. Devoted Pharmacol. Toxicol. Evaluat. Natural Product Derivatives 20 (12) (2006) 1023–1035.
[26] R.A. Nieto, W.J. Deardorff, G.T. Grossberg, Efficacy of rivastigmine tartrate, transdermal system, in Alzheimer's disease, Expert Opin. Pharmacother. 17 (6) (2016) 861–870.
[27] P. Foster, et al., Donepezil Versus Rivastigmine in Patients with Alzheimer's Disease: Attention and Working Memory, J. Alzheimer's Neurodegenerative Dis. 2 (002) (2016).
[28] H.A. Mucke, The case of galantamine: repurposing and late blooming of a cholinergic drug, Future Sci. OA 1 (4) (2015).
[29] D. Prvulovic, H. Hampel, J. Pantel, Galantamine for Alzheimer's disease, Expert Opin. Drug Metab. Toxicol. 6 (3) (2010) 345–354.
[30] M.R. Farlow, S.M. Graham, G. Alva, Memantine for the Treatment of Alzheimer's Disease, Drug Saf. 31 (7) (2008) 577–585.
[31] I. Ishikawa, et al., The effect of memantine on sleep architecture and psychiatric symptoms in patients with Alzheimer's disease, Acta Neuropsychiatrica 28 (3) (2016) 157–164.
[32] L.D. Hughes, Memantine for fibromyalgia and Alzheimer's disease: An observational case comparison, British J. Mental Health Nursing 6 (1) (2017) 29–34.
[33] F. Nafar, J. Clarke, K. Mearow, Coconut oil protects cortical neurons from amyloid beta toxicity by enhancing signaling of cell survival pathways, Neurochem. Int. 105 (2017) 64–79.
[34] J. Olanrewaju, et al., Effects of virgin coconut oil on aluminium chloride-induced alzheimer-like dementia in the prefrontal cortex, J. Adv. Med. Pharmaceut. Sci. (2018) 1–12.
[35] A. Bansal, et al., Coconut oil decreases expression of amyloid precursor protein (APP) and secretion of amyloid peptides through inhibition of ADP-ribosylation factor 1 (ARF1), Brain Res. 1704 (2019) 78–84.
[36] G. Omidi, et al., Effect of coenzyme Q10 supplementation on diabetes induced memory deficits in rats, Metab. Brain Dis. (2019) 1–8.
[37] A. Monsef, S. Shahidi, A. Komaki, Influence of chronic coenzyme Q10 supplementation on cognitive function, learning, and memory in healthy and diabetic middle-aged rats, Neuropsychobiology 77 (2) (2019) 92–100.
[38] K. Zeng, et al., Ginkgo biloba extract EGb761 attenuates Hyperhomocysteinemia-induced AD like tau hyperphosphorylation and cognitive impairment in rats, Curr. Alzheimer Res. 15 (1) (2018) 89–99.
[39] X. Liu, et al., Long-term treatment with Ginkgo biloba extract EGb 761 improves symptoms and pathology in a transgenic mouse model of Alzheimer's disease, Brain Behav. Immun. 46 (2015) 121–131.
[40] C. Stein, et al., Effects of Ginkgo biloba extract EGb 761, donepezil and their combination on central cholinergic function in aged rats, J. Pharm. Pharmaceut. Sci. 18 (4) (2015) 634–646.
[41] Q. Meng, et al., Intranasal delivery of Huperzine A to the brain using lactoferrin-conjugated N-trimethylated chitosan surface-modified PLGA nanoparticles for treatment of Alzheimer's disease, Int. J. Nanomed. 13 (2018) 705.
[42] A. Gul, J. Bakht, F. Mehmood, Huperzine-A response to cognitive impairment and task switching deficits in patients with Alzheimer's disease, J. Chinese Med. Assoc. (2018).
[43] T. Tabira, N. Kawamura, A study of a supplement containing huperzine a and curcumin in dementia patients and individuals with mild cognitive impairment, J. Alzheimer's Dis. (2018) 1–4 (Preprint).
[44] L. Wang, et al., Protective effects of omega-3 fatty acids against Alzheimer's disease in rat brain endothelial cells, Brain Behavior 8 (11) (2018) e01037.
[45] G. Fang, et al., The protective role of endogenous n-3 polyunsaturated fatty acids in Tau Alzheimer's disease mouse model, Int. J. Neurosci. 129 (4) (2019) 325–336.
[46] J.M. Nolan, et al., Nutritional intervention to prevent alzheimer's disease: potential benefits of xanthophyll carotenoids and omega-3 fatty acids combined, J. Alzheimers Dis. 64 (2) (2018) 367–378.
[47] M.J. Sharman, et al., Assessment of diets containing curcumin, epigallocatechin-3-gallate, docosahexaenoic acid and α-lipoic acid on amyloid load and inflammation in a male transgenic mouse model of Alzheimer's disease: Are combinations more effective? Neurobiol. Disease 124 (2019) 505–519.
[48] Z. Liu, et al., Curcumin improves learning and memory ability via inhibiting activated microglia-mediated inflammation in mouse models of Alzheimer's disease, Int. J. Clin. Exp. Med. 11 (11) (2018) 12204–12210.
[49] W.T. Lu, et al., Curcumin ameliorates memory deficits by enhancing lactate content and MCT2 expression in APP/PS1 transgenic mouse model of Alzheimer's disease, Anatom. Rec. 302 (2) (2019) 332–338.
[50] S. Abushakra, et al., Clinical benefits of tramiprosate in Alzheimer's disease are associated with higher number of APOE4 alleles: the "APOE4 gene-dose effect", J. Prev. Alz. Dis. 3 (4) (2016) 219–228.
[51] S. Abushakra, Clinically meaningful cognitive and functional improvements with tramiprosate in alzheimer's disease (ad) patients with APOE4/4 genotype: subgroup analyses from two phase 3 studies, Alzheimer's Dementia: J. Alzheimer's Assoc. 12 (7) (2016) P1185.
[52] H. Nishioka, et al., BMS-708163 and Nilotinib restore synaptic dysfunction in human embryonic stem cell-derived Alzheimer's disease models, Sci. Rep. 6 (2016) 33427.
[53] I. Lonskaya, et al., Nilotinib and bosutinib modulate pre-plaque alterations of blood immune markers and neuro-inflammation in Alzheimer's disease models, Neuroscience 304 (2015) 316–327.
[54] I. Lonskaya, et al., Nilotinib-induced autophagic changes increase endogenous parkin level and ubiquitination, leading to amyloid clearance, J. Mol. Med. 92 (4) (2014) 373–386.
[55] S. Kullmann, et al., Brain insulin resistance at the crossroads of metabolic and cognitive disorders in humans, Physiol. Rev. 96 (4) (2016) 1169–1209.
[56] M. Suzanne, Type 3 diabetes is sporadic Alzheimer′ s disease: mini-review, Eur. Neuropsychopharmacol. 24 (12) (2014) 1954–1960.
[57] A.A. Willette, et al., Association of insulin resistance with cerebral glucose uptake in late middle–aged adults at risk for Alzheimer disease, JAMA Neurol. 72 (9) (2015) 1013–1020.
[58] J.K. Morris, et al., Cognitively impaired elderly exhibit insulin resistance and no memory improvement with infused insulin, Neurobiol. Aging 39 (2016) 19–24.
[59] C.A. Grillo, et al., Hippocampal insulin resistance impairs spatial learning and synaptic plasticity, Diabetes 64 (11) (2015) 3927–3936.
[60] L. Ma, et al., Insulin resistance is an important risk factor for cognitive impairment in elderly patients with primary hypertension, Yonsei Med. J. 56 (1) (2015) 89–94.
[61] L.L. Ekblad, et al., Insulin resistance is associated with poorer verbal fluency performance in women, Diabetologia 58 (11) (2015) 2545–2553.
[62] A.A. Willette, et al., Insulin resistance predicts brain amyloid deposition in late middle-aged adults, Alzheimer's Dementia 11 (5) (2015) 504–510 e501.
[63] S. Craft, et al., Intranasal insulin therapy for Alzheimer disease and amnestic mild cognitive impairment: a pilot clinical trial, Arch. Neurol. 69 (1) (2012) 29–38.
[64] A. Claxton, et al., Long-acting intranasal insulin detemir improves cognition for adults with mild cognitive impairment or early-stage Alzheimer's disease dementia, J. Alzheimers Dis. 44 (3) (2015) 897–906.
[65] N. Kamei, M. Takeda-Morishita, Brain delivery of insulin boosted by intranasal coadministration with cell-penetrating peptides, J. Control. Release 197 (2015) 105–110.
[66] Y. Yang, et al., Subcutaneous administration of liraglutide ameliorates Alzheimer-associated tau hyperphosphorylation in rats with type 2 diabetes, J. Alzheimers Dis. 37 (3) (2013) 637–648.
[67] X.-Y. Liu, et al., Liraglutide prevents beta-amyloid-induced neurotoxicity in SH-SY5Y cells via a PI3K-dependent signaling pathway, Neurol. Res. 38 (4) (2016) 313–319.
[68] K. Hunter, C. Hölscher, Drugs developed to treat diabetes, liraglutide and lixisenatide, cross the blood brain barrier and enhance neurogenesis, BMC Neurosci. 13 (1) (2012) 33.
[69] P.L. McClean, et al., The diabetes drug liraglutide prevents degenerative processes in a mouse model of Alzheimer's disease, J. Neurosci. 31 (17) (2011) 6587–6594.
[70] M. Gejl, et al., In Alzheimer's disease, 6-month treatment with GLP-1 analog prevents decline of brain glucose metabolism: randomized, placebo-controlled, double-blind clinical trial, Front. Aging Neurosci. 8 (2016) 108.
[71] A.F. Batista, et al., The diabetes drug liraglutide reverses cognitive impairment in mice and attenuates insulin receptor and synaptic pathology in a non-human primate model of Alzheimer's disease, J. Pathol. 245 (1) (2018) 85–100.
[72] J. Sevigny, et al., The antibody aducanumab reduces Aβ plaques in Alzheimer's disease, Nature 537 (7618) (2016) 50.

[73] S.H. Budd, et al., Clinical development of aducanumab, an Anti-Aβ human monoclonal antibody being investigated for the treatment of early alzheimer's disease, J. Prevent. Alzheimer's Dis. 4 (4) (2017) 255–263.
[74] S.B. Haeberlein, et al., Aducanumab 36-month data from PRIME: a randomized, double-blind, placebo-controlled Phase 1b study in patients with prodromal or mild Alzheimer's disease (S2. 004), AAN Enterprises, 2018.
[75] P. von Rosenstiel, et al., Aducanumab titration dosing regimen: 24-month analysis from PRIME, a randomized, double-blind, placebo-controlled Phase 1b study in patients with prodromal or mild Alzheimer's disease (S2. 003), AAN Enterprises, 2018.
[76] M. Andjelkovic, et al., Update on the safety and tolerability of gantenerumab in the ongoing open-label extension of the scarlet road study in patients with prodromal alzheimer's disease after approximately 2 years of study duration, Alzheimer's Dementia: J. Alzheimer's Assoc. 14 (7) (2018) P241–P242.
[77] S. Ostrowitzki, et al., Correction to: A phase III randomized trial of gantenerumab in prodromal Alzheimer's disease, Alzheimer's Res. Therapy 10 (1) (2018) 99.
[78] I. Lombardo, et al., Intepirdine (RVT-101), a 5-HT6 receptor antagonist, as an adjunct to donepezil in mild-to-moderate Alzheimer's disease: efficacy on activities of daily living domains, Am. J. Geriatric Psychiatry 25 (3) (2017) S120–S121.
[79] J.L. Molinuevo, et al., Responder analysis of the cognitive effect of combination therapy with donepezil and intepirdine (RVT-101) versus donepezil monotherapy: results from a 48-week multinational placebo-controlled study in mild to moderate alzheimer's disease, Alzheimer's Dementia: J. Alzheimer's Assoc. 13 (7) (2017) P259.
[80] M.N. Sabbagh, et al., Difference in cognitive decline between combination therapy with donepezil and intepirdine (RVT-101) and donepezil monotherapy: results from a 48 week multinational placebo-controlled study in mild to moderate alzheimer's disease, Alzheimer's Dementia: J. Alzheimer's Assoc. 13 (7) (2017) P263–P264.
[81] S. Eketjäll, et al., AZD3293: a novel, orally active BACE1 inhibitor with high potency and permeability and markedly slow off-rate kinetics, J. Alzheimer's Dis. 50 (4) (2016) 1109–1123.
[82] G. Cebers, et al., AZD3293: Pharmacokinetic and pharmacodynamic effects in healthy subjects and patients with Alzheimer's disease, J. Alzheimer's Dis. 55 (3) (2017) 1039–1053.
[83] M.F. Egan, et al., Randomized trial of verubecestat for prodromal alzheimer's disease, N. Engl. J. Med. 380 (15) (2019) 1408–1420.
[84] M.F. Egan, et al., Randomized trial of verubecestat for mild-to-moderate Alzheimer's disease, N. Engl. J. Med. 378 (18) (2018) 1691–1703.
[85] M. Timmers, et al., Pharmacodynamics of atabecestat (JNJ-54861911), an oral BACE1 inhibitor in patients with early Alzheimer's disease: randomized, double-blind, placebo-controlled study, Alzheimer's Res. Therapy 10 (1) (2018) 85.
[86] M. Timmers, et al., Evaluating potential QT effects of JNJ-54861911, a BACE inhibitor in single-and multiple-ascending dose studies, and a thorough QT trial with additional retrospective confirmation, using concentration-QTc analysis, J. Clin. Pharmacol. 58 (7) (2018) 952–964.
[87] C.G. Parsons, G. Rammes, Preclinical to phase II amyloid beta (Aβ) peptide modulators under investigation for Alzheimer's disease, Expert Opin. Invest. Drugs 26 (5) (2017) 579–592.
[88] H.D. Soares, et al., The γ-secretase modulator, BMS-932481, modulates Aβ peptides in the plasma and cerebrospinal fluid of healthy volunteers, J. Pharmacol. Exp. Ther. 358 (1) (2016) 138–150.
[89] A.F. Teich, et al., Translational inhibition of APP by Posiphen: Efficacy, pharmacodynamics, and pharmacokinetics in the APP/PS1 mouse, Alzheimer's Dementia: Transl. Res. Clin. Interv. 4 (2018) 37–45.
[90] J.A. Hey, et al., Clinical pharmacokinetics and safety of ALZ-801, a novel prodrug of tramiprosate in development for the treatment of Alzheimer's disease, Clin. Pharmacokinet. 57 (3) (2018) 315–333.
[91] J. Hey, et al., Phase 1 development of ALZ-801, a novel beta amyloid anti-aggregation prodrug of tramiprosate with improved drug properties, supporting bridging to the phase 3 program, Alzheimer's Dementia: J. Alzheimer's Assoc. 12 (7) (2016) P613.
[92] D. Mitchell, et al., A phase 1 trial of TPI 287 as a single agent and in combination with temozolomide in patients with refractory or recurrent neuroblastoma or medulloblastoma, Pediatr. Blood Cancer 63 (1) (2016) 39–46.
[93] R.S. Keefe, et al., Randomized, double-blind, placebo-controlled study of encenicline, an α7 nicotinic acetylcholine receptor agonist, as a treatment for cognitive impairment in schizophrenia, Neuropsychopharmacology 40 (13) (2015) 3053.
[94] A.J. Barbier, et al., Pharmacodynamics, pharmacokinetics, safety, and tolerability of encenicline, a selective α7 nicotinic receptor partial agonist, in single ascending-dose and bioavailability studies, Clin. Ther. 37 (2) (2015) 311–324.
[95] J. Czerkowicz, et al., Anti-tau antibody BIIB092 binds secreted tau in preclinical models and Alzheimer's disease cerebrospinal fluid, Alzheimer's Dementia: J. Alzheimer's Assoc. 14 (7) (2018) P1441.
[96] D. Van Kampen, A. Maelicke, J.M. Van Kampen, Memogain regulates tau phosphorylation in an immunotoxin model of cholinergic cell loss, Alzheimer's Dementia: J. Alzheimer's Assoc. 14 (7) (2018) P1441–P1442.
[97] S. Bhattacharya, A. Maelicke, D. Montag, Nasal application of the galantamine pro-drug memogain slows down plaque deposition and ameliorates behavior in 5X familial Alzheimer's disease mice, J. Alzheimers Dis. 46 (1) (2015) 123–136.
[98] A. Maelicke, et al., Memogain is a galantamine pro-drug having dramatically reduced adverse effects and enhanced efficacy, J. Mol. Neurosci. 40 (1–2) (2010) 135–137.
[99] L. Illum, Nasal drug delivery—possibilities, problems and solutions, J. Control. Release 87 (1–3) (2003) 187–198.
[100] A. Serralheiro, et al., Nose as a route for drug delivery, Nasal Physiology and Pathophysiology of Nasal Disorders, Springer, 2013, pp. 191–215.
[101] L.C. Espinoza, et al., Formulation strategies to improve nose-to-brain delivery of donepezil, Pharmaceutics 11 (2) (2019) 64.
[102] L.R. Hanson, W.H. Frey 2nd, Intranasal delivery bypasses the blood-brain barrier to target therapeutic agents to the central nervous system and treat neurodegenerative disease, BMC Neurosci. 9 (Suppl 3) (2008) S5.
[103] C.V. Pardeshi, V.S. Belgamwar, Direct nose to brain drug delivery via integrated nerve pathways bypassing the blood–brain barrier: an excellent platform for brain targeting, Expert Opinion Drug Deliv. 10 (7) (2013) 957–972.
[104] E. Samaridou, M.J. Alonso, Nose-to-brain peptide delivery–The potential of nanotechnology, Bioorg. Med. Chem. 26 (10) (2018) 2888–2905.
[105] B. Chatterjee, Nose to brain drug delivery: a recent update, J. Formul. Sci. Bioavailab 1 (2) (2017).
[106] T.P. Crowe, et al., Mechanism of intranasal drug delivery directly to the brain, Life Sci. 195 (2018) 44–52.
[107] J.J. Lochhead, R.G. Thorne, Intranasal delivery of biologics to the central nervous system, Adv. Drug Deliv. Rev. 64 (7) (2012) 614–628.
[108] K. Selvaraj, et al., Nose to brain transport pathways an overview: Potential of nanostructured lipid carriers in nose to brain targeting, Artif. Cells Nanomed. Biotechnol. 46 (8) (2018) 2088–2095.
[109] S.V. Dhuria, et al., Novel vasoconstrictor formulation to enhance intranasal targeting of neuropeptide therapeutics to the central nervous system, J. Pharmacol. Exp. Therapeutics 328 (1) (2009) 312–320.
[110] X.-Q. Chen, et al., Delivery of nerve growth factor to the brain via the olfactory pathway, J. Alzheimer's Dis. 1 (1) (1998) 35–44.
[111] W.H. Frey, et al., Delivery of 125I-NGF to the brain via the olfactory route, Drug Deliv. 4 (2) (1997) 87–92.
[112] M.L. Schaefer, et al., Trigeminal collaterals in the nasal epithelium and olfactory bulb: a potential route for direct modulation of olfactory information by trigeminal stimuli, J. Comparative Neurol. 444 (3) (2002) 221–226.
[113] N.J. Johnson, L.R. Hanson, W.H. Frey, Trigeminal pathways deliver a low molecular weight drug from the nose to the brain and orofacial structures, Mol. Pharm. 7 (3) (2010) 884–893.
[114] S. Gizurarson, Anatomical and histological factors affecting intranasal drug and vaccine delivery, Curr. Drug. Deliv. 9 (6) (2012) 566–582.
[115] S.V. Dhuria, L.R. Hanson, W.H. Frey 2nd, Intranasal delivery to the central nervous system: mechanisms and experimental considerations, J. Pharm. Sci. 99 (4) (2010) 1654–1673.
[116] L. Kozlovskaya, M. Abou-Kaoud, D. Stepensky, Quantitative analysis of drug delivery to the brain via nasal route, J. Control Release 189 (2014) 133–140.
[117] A. Mistry, S. Stolnik, L. Illum, Nanoparticles for direct nose-to-brain delivery of drugs, Int. J. Pharm. 379 (1) (2009) 146–157.
[118] M.J. Ruigrok, E.C. de Lange, Emerging insights for translational pharmacokinetic and pharmacokinetic-pharmacodynamic studies: towards prediction of nose-to-brain transport in humans, AAPS J. 17 (3) (2015) 493–505.
[119] R.G. Thorne, et al., Delivery of insulin-like growth factor-I to the rat brain and spinal cord along olfactory and trigeminal pathways following intranasal administration, Neuroscience 127 (2) (2004) 481–496.
[120] T.M. Ross, et al., Intranasal administration of interferon beta bypasses the blood-brain barrier to target the central nervous system and cervical lymph nodes: a non-invasive treatment strategy for multiple sclerosis, J. Neuroimmunol. 151 (1–2) (2004) 66–77.
[121] S. Qian, Q. Wang, Z. Zuo, Improved brain uptake of peptide-based CNS drugs via alternative routes of administrations of its nanocarrier delivery systems: a promising strategy for CNS targeting delivery of peptides, Expert Opin. Drug Metab. Toxicol. 10 (11) (2014) 1491–1508.
[122] Y. Ruan, et al., Nanoparticle-mediated delivery of neurotoxin-II to the brain with intranasal administration: an effective strategy to improve antinociceptive activity of neurotoxin, Drug Dev. Ind. Pharm. 38 (1) (2012) 123–128.
[123] J. Kreuter, et al., Direct evidence that polysorbate-80-coated poly (butylcyanoacrylate) nanoparticles deliver drugs to the CNS via specific mechanisms requiring prior binding of drug to the nanoparticles, Pharm. Res. 20 (3) (2003) 409–416.
[124] X. Gao, et al., Brain delivery of vasoactive intestinal peptide enhanced with the nanoparticles conjugated with wheat germ agglutinin following intranasal administration, J. Control. Release 121 (3) (2007) 156–167.
[125] S. Haque, et al., Venlafaxine loaded chitosan NPs for brain targeting: pharmacokinetic and pharmacodynamic evaluation, Carbohydr. Polym. 89 (1) (2012) 72–79.
[126] N. Haffejee, et al., Intranasal toxicity of selected absorption enhancers, Pharmazie 56 (11) (2001) 882–888.
[127] L. Battaglia, et al., Lipid nanoparticles for intranasal administration: application to nose-to-brain delivery, Expert Opinion Drug Deliv. 15 (4) (2018) 369–378.
[128] G. Bozzuto, A. Molinari, Liposomes as nanomedical devices, Int. J. Nanomed. 10 (2015) 975.
[129] M.L. Etheridge, et al., The big picture on nanomedicine: the state of investigational and approved nanomedicine products, Nanomed. Nanotechnol. Biol. Med. 9 (1) (2013) 1–14.
[130] C. Ross, et al., Liposome delivery systems for the treatment of Alzheimer's disease, Int. J. Nanomed. 13 (2018) 8507.
[131] R. Mara Mainardes, et al., Liposomes and micro/nanoparticles as colloidal carriers for nasal drug delivery, Curr. Drug Deliv. 3 (3) (2006) 275–285.
[132] A.K. Al Asmari, et al., Preparation, characterization, and in vivo evaluation of intranasally administered liposomal formulation of donepezil, Drug Des., Develop. Therapy 10 (2016) 205.
[133] F. Sonvico, et al., Surface-modified nanocarriers for nose-to-brain delivery: from

bioadhesion to targeting, Pharmaceutics 10 (1) (2018) 34.
[134] X. Wang, et al., Novel nanoliposomal delivery system for polydatin: preparation, characterization, and in vivo evaluation, Drug Des., Develop. Therapy 9 (2015) 1805.
[135] S.V. Bhujbal, P. de Vos, S.P. Niclou, Drug and cell encapsulation: alternative delivery options for the treatment of malignant brain tumors, Adv. Drug Deliv. Rev. 67 (2014) 142–153.
[136] F. Ungaro, et al., Dry powders based on PLGA nanoparticles for pulmonary delivery of antibiotics: modulation of encapsulation efficiency, release rate and lung deposition pattern by hydrophilic polymers, J. Contr. Release 157 (1) (2012) 149–159.
[137] B. Heurtault, et al., Physico-chemical stability of colloidal lipid particles, Biomaterials 24 (23) (2003) 4283–4300.
[138] K.S. Soppimath, et al., Biodegradable polymeric nanoparticles as drug delivery devices, J. Control. Release 70 (1–2) (2001) 1–20.
[139] R.M. Mainardes, L.P. Silva, Drug delivery systems: past, present, and future, Curr. Drug Targets 5 (5) (2004) 449–455.
[140] W. Li, et al., Pharmacokinetic behavior and efficiency of acetylcholinesterase inhibition in rat brain after intranasal administration of galanthamine hydrobromide loaded flexible liposomes, Environ. Toxicol. Pharmacol. 34 (2) (2012) 272–279.
[141] S. Samudre, et al., Xanthan gum coated mucoadhesive liposomes for efficient nose to brain delivery of curcumin, Drug Deliv. Lett. 5 (3) (2015) 201–207.
[142] K. Arumugam, et al., A study of rivastigmine liposomes for delivery into the brain through intranasal route, Acta Pharmaceutica 58 (3) (2008) 287–297.
[143] Z.-Z. Yang, et al., Enhanced brain distribution and pharmacodynamics of rivastigmine by liposomes following intranasal administration, Int. J. Pharm. 452 (1–2) (2013) 344–354.
[144] I. Cacciatore, et al., Solid lipid nanoparticles as a drug delivery system for the treatment of neurodegenerative diseases, Expert Opinion Drug Deliv. 13 (8) (2016) 1121–1131.
[145] M. Geszke-Moritz, M. Moritz, Solid lipid nanoparticles as attractive drug vehicles: Composition, properties and therapeutic strategies, Mater. Sci. Eng., C 68 (2016) 982–994.
[146] C.-H. Lin, et al., Recent advances in oral delivery of drugs and bioactive natural products using solid lipid nanoparticles as the carriers, J. Food Drug Anal. 25 (2) (2017) 219–234.
[147] C. Tapeinos, M. Battaglini, G. Ciofani, Advances in the design of solid lipid nanoparticles and nanostructured lipid carriers for targeting brain diseases, J. Control. Release 264 (2017) 306–332.
[148] S. Bhatt, J. Sharma, M. Singh, V. Saini, Solid lipid nanoparticles: a promising technology for delivery of poorly water-soluble drugs, ACTA Pharmaceutica Sciencia 56 (3) (2018).
[149] A.R. Neves, et al., Solid lipid nanoparticles as a vehicle for brain-targeted drug delivery: two new strategies of functionalization with apolipoprotein E, Nanotechnology 26 (49) (2015) 495103.
[150] X.-Y. Ying, et al., Solid lipid nanoparticles modified with chitosan oligosaccharides for the controlled release of doxorubicin, Carbohydr. Polym. 84 (4) (2011) 1357–1364.
[151] A.M. Fatouh, et al., Intranasal agomelatine solid lipid nanoparticles to enhance brain delivery: formulation, optimization and in vivo pharmacokinetics, Drug Des., Develop. Therapy 11 (2017) 1815.
[152] E. Esposito, et al., Solid lipid nanoparticles as delivery systems for bromocriptine, Pharmaceut. Res. 25 (7) (2008) 1521–1530.
[153] M.I. Alam, et al., Strategy for effective brain drug delivery, Euro. J. Pharmaceut. Sci. 40 (5) (2010) 385–403.
[154] Jörg Kreuter, Application of nanoparticles for the delivery of drugs to the brain, International Congress Series, Elsevier, 2005.
[155] B. Dehouck, et al., A new function for the LDL receptor: transcytosis of LDL across the blood–brain barrier, J. Cell Biol. 138 (4) (1997) 877–889.
[156] L. Bayón-Cordero, I. Alkorta, L. Arana, Application of solid lipid nanoparticles to improve the efficiency of anticancer drugs, Nanomaterials 9 (3) (2019) 474.
[157] M. Yasir, et al., Solid lipid nanoparticles for nose to brain delivery of donepezil: formulation, optimization by Box-Behnken design, in vitro and in vivo evaluation, Artif. Cells Nanomed. Biotechnol. 46 (8) (2018) 1838–1851.
[158] M. Yasir, et al., Formulation and evaluation of glyceryl behenate based solid lipid nanoparticles for the delivery of donepezil to brain through nasal route, Res. J. Pharm. Technol. 11 (7) (2018) 2836–2844.
[159] B. Shah, et al., Application of quality by design approach for intranasal delivery of rivastigmine loaded solid lipid nanoparticles: effect on formulation and characterization parameters, Eur. J. Pharm. Sci. 78 (2015) 54–66.
[160] E. Muntimadugu, et al., Intranasal delivery of nanoparticle encapsulated tarenflurbil: a potential brain targeting strategy for Alzheimer's disease, Eur. J. Pharm. Sci. 92 (2016) 224–234.
[161] S. Weber, A. Zimmer, J. Pardeike, Solid lipid nanoparticles (SLN) and nanostructured lipid carriers (NLC) for pulmonary application: a review of the state of the art, Eur. J. Pharm. Biopharm. 86 (1) (2014) 7–22.
[162] S. Gänger, K.J.P. Schindowski, Tailoring formulations for intranasal nose-to-brain delivery: A review on architecture, physico-chemical characteristics and mucociliary clearance of the nasal olfactory mucosa, Pharmaceutics 10 (3) (2018) 116.
[163] N. Naseri, H. Valizadeh, P. Zakeri-Milani, Solid lipid nanoparticles and nanostructured lipid carriers: structure, preparation and application, Adv. Pharmaceut. Bull. 5 (3) (2015) 305.
[164] A. Khosa, S. Reddi, R.N. Saha, Nanostructured lipid carriers for site-specific drug delivery, Biomed. Pharmacother. 103 (2018) 598–613.
[165] V.R. Salvi, P. Pawar, Nanostructured lipid carriers (NLC) system: a novel drug targeting carrier, J. Drug Delivery Sci. Technol. (2019).
[166] C.-L. Fang, S.A. Al-Suwayeh, J.-Y. Fang, Nanostructured lipid carriers (NLCs) for drug delivery and targeting, Recent Pat. Nanotechnol. 7 (1) (2013) 41–55.
[167] A. Beloqui, et al., Nanostructured lipid carriers: Promising drug delivery systems for future clinics, Nanomed. Nanotechnol. Biol. Med. 12 (1) (2016) 143–161.
[168] M.I. Alam, et al., Intranasal infusion of nanostructured lipid carriers (NLC) containing CNS acting drug and estimation in brain and, Blood 20 (6) (2013) 247–251.
[169] O. Gartziandia López de Goikoetxea, Nanostructured lipid carriers for nose-to-brain delivery in neurodegenerative diseases therapy, 2016.
[170] A. Kakee, et al., In vivo evidence for brain-to-blood efflux transport of valproic acid across the blood–brain barrier, Microvascular Res. 63 (2) (2002) 233–238.
[171] R.G. Madane, H.S. Mahajan, Curcumin-loaded nanostructured lipid carriers (NLCs) for nasal administration: design, characterization, and in vivo study, Drug Deliv. 23 (4) (2016) 1326–1334.
[172] O. Gartziandia, et al., Chitosan coated nanostructured lipid carriers for brain delivery of proteins by intranasal administration, Colloids Surf., B 134 (2015) 304–313.
[173] P.R. Wavikar, P.R. Vavia, Rivastigmine-loaded in situ gelling nanostructured lipid carriers for nose to brain delivery, J. Liposome Res. 25 (2) (2015) 141–149.
[174] P. Wavikar, R. Pai, P. Vavia, Nose to brain delivery of rivastigmine by in situ gelling cationic nanostructured lipid carriers: enhanced brain distribution and pharmacodynamics, J. Pharm. Sci. 106 (12) (2017) 3613–3622.
[175] S. Sood, K. Jain, K. Gowthamarajan, Curcumin-donepezil–loaded nanostructured lipid carriers for intranasal delivery in an Alzheimer's disease model, Alzheimer's Dementia: J. Alzheimer's Assoc. 9 (4) (2013) P299.
[176] A. Rajput, et al., In situ nanostructured hydrogel of resveratrol for brain targeting: in vitro-in vivo characterization, Drug Deliv. Transl. Res. 8 (5) (2018) 1460–1470.
[177] M.C. Bonferoni, et al., Nanoemulsions for “Nose-to-Brain” drug delivery, Pharmaceutics 11 (2) (2019) 84.
[178] P. Thiagarajan, Nanoemulsions for drug delivery through different routes, Res. Biotechnol. 2 (3) (2011).
[179] A. Gupta, et al., Nanoemulsions: formation, properties and applications, Soft Matter 12 (11) (2016) 2826–2841.
[180] S. Yadav, et al., Comparative biodistribution and pharmacokinetic analysis of cyclosporine-A in the brain upon intranasal or intravenous administration in an oil-in-water nanoemulsion formulation, Mol. Pharm. 12 (5) (2015) 1523–1533.
[181] M. Kumar, et al., Mucoadhesive nanoemulsion-based intranasal drug delivery system of olanzapine for brain targeting, J. Drug Target. 16 (10) (2008) 806–814.
[182] M. Nasr, Development of an optimized hyaluronic acid-based lipidic nanoemulsion co-encapsulating two polyphenols for nose to brain delivery, Drug Deliv. 23 (4) (2016) 1444–1452.
[183] M. Jaiswal, R. Dudhe, P. Sharma, Nanoemulsion: an advanced mode of drug delivery system, 3 Biotech. 5 (2) (2015) 123–127.
[184] S. Sood, K. Jain, K. Gowthamarajan, Intranasal delivery of curcumin–/INS; donepezil nanoemulsion for brain targeting in Alzheimer's disease, J. Neurol. Sci. 333 (2013) e316–e317.
[185] S. Yadav, et al., Intranasal brain delivery of cationic nanoemulsion-encapsulated TNFα siRNA in prevention of experimental neuroinflammation, Nanomed. Nanotechnol. Biol. Med. 12 (4) (2016) 987–1002.
[186] D. Ag Seleci, et al., Niosomes as nanoparticular drug carriers: fundamentals and recent applications, J. Nanomater. 2016 (2016).
[187] C. Marianecci, et al., Niosomes from 80s to present: the state of the art, Adv. Colloid Interface Sci. 205 (2014) 187–206.
[188] A. Pardakhty, E. Moazeni, Nano-niosomes in drug, vaccine and gene delivery: a rapid overview, Nanomed. J. 1 (1) (2013) 1–12.
[189] D. Kaur, S. Kumar, Niosomes: present scenario and future aspects, J. Drug Deliv. Therapeutics 8 (5) (2018) 35–43.
[190] D.G. Kautkar, A. Pawar, R. Bhamber, Intranasal niosomes: an approach for drug delivery to brain, 2015.
[191] X. Ge, et al., Advances of non-ionic surfactant vesicles (niosomes) and their application in drug delivery, Pharmaceutics 11 (2) (2019) 55.
[192] Z. Ceren Ertekin, Z. Sezgin Bayindir, N. Yuksel, Stability studies on piroxicam encapsulated niosomes, Curr. Drug Deliv. 12 (2) (2015) 192–199.
[193] F. Rinaldi, et al., Chitosan glutamate-coated niosomes: A proposal for nose-to-brain delivery, Pharmaceutics 10 (2) (2018) 38.
[194] N. Ravouru, P. Kondreddy, D. Korakanchi, Formulation and evaluation of niosomal nasal drug delivery system of folic acid for brain targeting, Curr. Drug Discov. Technol. 10 (4) (2013) 270–282.
[195] H.M. Barriga, M.N. Holme, M.M. Stevens, Cubosomes: the next generation of smart lipid nanoparticles? Angew. Chem. Int. Ed. 58 (10) (2019) 2958–2978.
[196] Z. Karami, M. Hamidi, Cubosomes: remarkable drug delivery potential, Drug Discov. Today 21 (5) (2016) 789–801.
[197] R.R. Bhosale, et al., Cubosomes: the inimitable nanoparticulate drug carriers, Scholars Acad. J. Pharm. 2 (6) (2013) 481–486.
[198] H. Wu, et al., A novel small Odorranalectin-bearing cubosomes: Preparation, brain delivery and pharmacodynamic study on amyloid-β25–35-treated rats following intranasal administration, Eur. J. Pharm. Biopharm. 80 (2) (2012) 368–378.
[199] R.P. Patil, et al., Nanostructured cubosomes in an in situ nasal gel system: an alternative approach for the controlled delivery of donepezil HCl to brain, J. Liposome Res. (2019) 1–10.
[200] S. Charlton, et al., Distribution and clearance of bioadhesive formulations from the olfactory region in man: effect of polymer type and nasal delivery device, Eur. J. Pharm. Sci. 30 (3–4) (2007) 295–302.
[201] S. Horvát, et al., Sodium hyaluronate as a mucoadhesive component in nasal formulation enhances delivery of molecules to brain tissue, Eur. J. Pharm. Biopharm. 72 (1) (2009) 252–259.

[202] C. Pardeshi, et al., Solid lipid based nanocarriers: an overview/Nanonosači na bazi čvrstih lipida: Pregled, Acta Pharmaceutica 62 (4) (2012) 433–472.
[203] J.J. Lochhead, et al., Rapid transport within cerebral perivascular spaces underlies widespread tracer distribution in the brain after intranasal administration, J. Cereb. Blood Flow Metab. 35 (3) (2015) 371–381.
[204] S. Bahadur, K. Pathak, Physicochemical and physiological considerations for efficient nose-to-brain targeting, Expert Opinion Drug Deliv. 9 (1) (2012) 19–31.
[205] Y. Singh, et al., Nanoemulsion: Concepts, development and applications in drug delivery, J. Control. Release 252 (2017) 28–49.
[206] V. Bourganis, et al., Recent advances in carrier mediated nose-to-brain delivery of pharmaceutics, Eur. J. Pharm. Biopharm. 128 (2018) 337–362.
[207] A. Praveen, et al., Lamotrigine encapsulated intra-nasal nanoliposome formulation for epilepsy treatment: Formulation design, characterization and nasal toxicity study, Colloids Surf., B 174 (2019) 553–562.
[208] S. Gupta, et al., Systematic approach for the formulation and optimization of solid lipid nanoparticles of efavirenz by high pressure homogenization using design of experiments for brain targeting and enhanced bioavailability, Biomed Res. Int. (2017. 2017.).
[209] M. Yasir, et al., Solid lipid nanoparticles for nose to brain delivery of donepezil: formulation, optimization by Box-Behnken design, in vitro and in vivo evaluation, Artif. Cells Nanomed. Biotechnol. 46 (8) (2018) 1838–1851.
[210] H. Wu, K. Hu, X. Jiang, From nose to brain: understanding transport capacity and transport rate of drugs, Expert Opinion Drug Deliv. 5 (10) (2008) 1159–1168.
[211] A. Alexander, et al., Recent expansions of novel strategies towards the drug targeting into the brain, Int. J. Nanomed. 14 (2019) 5895.
[212] E. Pallagi, et al., Initial Risk Assessment as part of the Quality by Design in peptide drug containing formulation development, Eur. J. Pharm. Sci. 122 (2018) 160–169.
[213] I.H.T. Guideline, Pharmaceutical development, Q8 (2R). As revised in August, 2009.
[214] X.Y. Lawrence, et al., Understanding pharmaceutical quality by design, AAPS J. 16 (4) (2014) 771–783.

ANNEX-II

International Journal of Pharmaceutics 604 (2021) 120724

Contents lists available at ScienceDirect

International Journal of Pharmaceutics

journal homepage: www.elsevier.com/locate/ijpharm

A comparison study of lipid and polymeric nanoparticles in the nasal delivery of meloxicam: Formulation, characterization, and *in vitro* evaluation

Hussein Akel [a], Ruba Ismail [a,b], Gábor Katona [a], Fakhara Sabir [a], Rita Ambrus [a], Ildikó Csóka [a,*]

[a] Institute of Pharmaceutical Technology and Regulatory Affairs, Faculty of Pharmacy, University of Szeged, H-6720 Szeged, Hungary
[b] Institute of Chemistry, Faculty of Science and Informatics, University of Szeged, H-6720 Szeged, Hungary

ARTICLE INFO

Keywords:
Nose-to-brain delivery
PLGA nanoparticles
Solid lipid nanoparticles
Permeability
Mucoadhesion
Quality by Design

ABSTRACT

With the increasingly widespread of central nervous system (CNS) disorders and the lack of sufficiently effective medication, meloxicam (MEL) has been reported as a possible medication for Alzheimer's disease (AD) management. Unfortunately, following the conventional application routes, the low brain bioavailability of MEL forms a significant limitation. The intranasal (IN) administration route is considered revolutionary for CNS medications delivery. The objective of the present study was to develop two types of nanocarriers, poly (lactic-co-glycolic acid) nanoparticles (PLGA NPs) and solid lipid nanoparticles (SLNs), for the IN delivery of MEL adapting the Quality by Design approach (QbD). Turning then to further enhance the optimized nanoformulation behavior by chitosan-coating. SLNs showed higher encapsulation efficacy (EE) and drug loading (DL) than PLGA NPs 87.26% (EE) and 2.67% (DL); 72.23% (EE) and 2.55% (DL), respectively. MEL encapsulated into the nanoformulations improved *in vitro* release, mucoadhesion, and permeation behavior compared to the native drug with greater superiority of chitosan-coated SLNs (C-SLNs). *In vitro-in vivo* correlation (IVIVC) results estimated a significant *in vivo* brain distribution of the nanoformulations compared to native MEL with estimated greater potential in the C-SLNs. Hence, MEL encapsulation into C-SLNs towards IN route can be promising in enhancing its brain bioavailability.

1. Introduction

Delivering drugs to the brain is a fascinating research field that has gained researchers' interest in the field of neurological disorders for the past few decades (Zhu et al., 2019). However, the drug delivery to the site of action in brains is blocked by the blood–brain barrier (BBB), which forms an endothelial membrane separating the systemic circulation from the CNS (Mistry et al., 2009). Additionally, the efflux of drugs, from the brain to the blood, decreases the drug permeation and bioavailability (Patel et al., 2013).

IN drug delivery has been introduced as an alternative way to deliver drugs to the brain over the traditional systemic drug delivery routes. It demonstrates various advantages such as direct delivery of the drug into the brain via the olfactory route, the presence of the drug in the olfactory bulb, which in turn, enhances the drug brain bioavailability and lowers the drug degradation via the systemic clearance (Agrawal et al., 2018, Pardeshi and Belgamwar, 2013, Alexander and Saraf, 2018). Moreover, targeting the olfactory region in the nasal cavity can lower the peripheral drug levels and ultimately minimize the drug-related adverse effects (Erdő et al., 2018).

Previous clinical studies have revealed the effect of the long-term usage of some non-steroidal anti-inflammatory (NSAIDs) drugs in reducing the prevalence of AD (Moore and O'Banion, 2002). Amongst the NSAIDs, MEL labors its pharmacological efficacy by inhibiting the enzymatic activity of cyclooxygenase-2 (COX-2) (Ah et al., 2010), which is linked with a neuroprotective action in Alzheimer's disease (Ianiski et al., 2016, Ianiski et al., 2012, Goverdhan et al., 2012, Nikvsarkar et al., 2006). However, the high rate of plasma protein binding and low apparent distribution volumes of MEL decrease its pharmacological effect (Seedher and Bhatia, 2005). Furthermore, MEL lipophilicity and its low water solubility (Badran et al., 2014) lower its bioavailability following the conventional administration routes.

Nanoparticles (NPs) have presented themselves as preferable carriers for IN delivery of therapeutics due to their distinguishing characteristics.

* Corresponding author.
E-mail address: csoka.ildiko@szte.hu (I. Csóka).

https://doi.org/10.1016/j.ijpharm.2021.120724
Received 11 February 2021; Received in revised form 17 May 2021; Accepted 18 May 2021
Available online 21 May 2021

NPs have a relatively high survival in the nasal cavity due to their mucoadhesion properties, and thanks to their tiny diameter, their transportation through the neurons to the brain is enhanced throughout the olfactory and respiratory pathways after being in proper contact with the olfactory and respiratory nerves endings (Mistry et al., 2009). NPs have been accomplished with an increase in nasal permeability and control drug release (Sharma et al., 2014). Besides, NPs with high entrapment efficiency can increase apparent drug solubility and prevent the active molecule degradation in the nasal mucosa (Kumari et al., 2010).

Based on the nature of the materials used to prepare the NPs, two main types could be distinguished: lipid NPs and polymeric NPs. Among these NPs, SLNs which are made up of a solid lipid core matrix, and PLGA NPs, which consist of PLGA, a biocompatible and biodegradable polymer. These two NPs hold great promise for the nasal drug delivery directly to the brain due to their: (i) biocompatibility, (ii) biodegradability, (iii) enhancing penetration and permeation properties, (iv) modified drug release properties and (v) reduced drug toxicity (Nabi-Meibodi et al., 2013, Cunha et al., 2017, Akel et al., 2020, Li and Sabliov, 2013, Sharma et al., 2015a, Shakeri et al., 2020). Moreover, their nanoscale size (up to 100 nm for lipid NPs and 220 nm for PLGA nanoparticles) is preferable for direct transport to the brain (Sonvico et al., 2018).

The two chosen types of NPs are different in their nature and composition, thus many preparation methods have been designed or modified to fit each of them and obtain the desired characteristics. The double-emulsion solvent-evaporation technique is a standard and widely used method for preparing SLNs and PLGA NPs. Therefore, adopting this process for the development of NPs will unify the preparation conditions of the two types of NPs and minimize the differences belonging to the preparation method (Nabi-Meibodi et al., 2013, He et al., 2015, Yassin et al., 2010, Cao et al., 2011, Soppimath et al., 2001, Zambaux et al., 1998).

Due to the complex composition of these nanosystems, their characteristics could be impacted by many formulation parameters such as: lipid type and concentration (Das et al., 2011, Yassin et al., 2010), the surfactant type (Liu et al., 2010, Shkodra-Pula et al., 2019), and concentration (Keum et al., 2011). Therefore, following the QbD approach as the first step of the research is considered logical to save time, costs, and efforts (Akel et al., 2020). This methodology starts by identifying the quality target product profile (QTPP), then moving to define the critical process parameters (CPPs) and critical material attributes (CMAs), which remarkably influence the critical quality attributes (CQAs) of the final output (Pallagi et al., 2018).

In the present study, two types of NPs containing MEL were prepared following the QbD approach. Physical, chemical, and morphological characterizations were conducted. This was followed by the *in vitro* assessment of drug release profile, mucoadhesion, permeation properties and the *in vitro-in vivo* correlation (IVIVC) using earlier results to evaluate the acceptability of prepared NPs. Accordingly, a thorough comparison was performed, then followed by selecting the optimized NPs to be a potential candidate for nasally applied brain-targeting anti AD drug formulation. This work provides the first reported evidence for the potential of MEL encapsulation in both polymeric and lipid NPs in the IN delivery with significant SLNs superiority, and their properties were further enhanced by coating with the cationic polymer chitosan.

2. Materials and methods

2.1. Materials

MEL was obtained from Egis Pharmaceuticals Ltd. (Budapest, Hungary). Cholesterol was purchased from Molar Chemicals (Budapest, Hungary), while phosphatidylcholine, PLGA 75/25 Mw 4,000–15,000 Da, polycaprolactone (PCL) Mw 45,000 Da, and Mucin from porcine stomach (Type II) Mw 640 kDa were supplied by Sigma Aldrich (Steinheim-Germany), Poloxamer 188 Mw 102 Da was purchased from Alfa Aesar Ltd. (Kandel, Germany). Chitosan, trehalose dihydrate, and all the organic solvents (analytical grade) were purchased from Merck (Darmstadt, Germany).

2.2. Initial Risk Assessment (RA) as a part of QbD

The QTPP of MEL-loaded NPs was defined as the first step of QbD. According to literature evaluation and preliminary experiments, after selecting double emulsion solvent evaporation as the method of preparation, CQAs, CPPs and CMAs were identified. RA tools were then used to rank CPPs and CMAs that significantly impact the quality (CQAs) of the final MEL loaded NPs.

The initial RA was carried out using Lean QbD Software (Lean QbD® Software, QbD Works LLC. USA, CA, Fremont). The RA process results are presented in Pareto charts, which were obtained by the used software. These charts prioritize and rank the CQAs, CMAs, and CPPs based on their severity scores.

2.3. Preparation of MEL-NPs

First, it is worth mentioning that the used amount of MEL for the preparations (15 mg/ml) was chosen depending on the literature evaluation and our previous experience. In this concentration, MEL exhibited a protective effect against the oxidative stress in a mouse model of AD induced by Aβ peptide (Ianiski et al., 2012, 2016).

MEL-SLNs were prepared following a modified double-emulsion solvent-evaporation technique (Gordillo-Galeano and Mora-Huertas, 2018). The water-in-oil-in-water (W1/O/W2) emulsion was prepared as follows: 0.2 ml of meloxicam aqueous solution (15 mg/ml) was added dropwise to the oily phase, which was prepared by dissolving either 9 mg of phosphatidylcholine in 1 ml of cyclohexane or 9 mg of cholesterol in 1 ml ethanol, using a homogenizing mixer (Hielscher, Germany) (0.5 cycles with 75% amplitude) for 1 min. The resultant nanoemulsion was then added dropwise into 1.6 ml of 2% poloxamer 188 aqueous solution (W2) using the homogenizing mixer (0.5 cycles with 75% amplitude) for another 1 min. The final mixture was left under stirring over the night using a magnetic stirrer to allow the organic solvent evaporation, thus forming the SLNs.

MEL polymeric NPs were produced by following another modified double emulsion solvent evaporation technique (Ismail et al., 2019b). First, the primary water in oil emulsion (W1/O) was prepared by adding MEL aqueous solution (15 mg/ml) to the polymer organic solution (PLGA in ethyl acetate or PCL in chloroform (12 mg/ml)) under sonication (0.5 cycles with 75% amplitude) for 1 min. The primary emulsion was then dispersed in the external aqueous solution of poloxamer 2% under sonication. Finally, the organic solvent was evaporated by leaving the mixtures stirred over the night, thus forming the PLGA NPs.

Chitosan-coated SLNs (C-SLNs) were obtained utilizing the physical attraction (ionic interaction) between the negatively charged SLNs and the positively charged chitosan. Briefly, chitosan solution was prepared by dissolving chitosan in 0.1% acetic acid solution at a concentration of 0.1 mg/ml, then filtered using a 0.45 μm membrane to get rid of any impurities. After that, equal volumes of SLNs suspension and chitosan solution were mixed and kept under the magnetic stirring for two continuous hours to ensure the successful formulation of C-SLNs, which was checked by measuring the surface charge of the SLNs before and after the coating process (Fonte et al., 2012, Gartziandia et al., 2015, Vieira et al., 2018, Gartziandia et al., 2016). The acquired positive charge of the negatively charged and freshly prepared SLNs confirms the successful coating.

As the last step, NPs were harvested by centrifugation (16,000 rpm for 1 h at 4 °C) (Hermle Z323, Hermle AG, Germany) and washed with deionized water. The NPs were resuspended in 1.5 ml of 5% (w/v) trehalose aqueous solution and then freeze-dried (Scanvac Coolsafe, Labogene, Lynge, Denmark) at −40 °C for 72 h under a pressure of

0.013 mbar.

2.4. Characterization of NPs

2.4.1. Mean particle diameter, size distribution, and zeta potential

The mean particle diameter (Z-average), polydispersity index (PDI), and surface charge (zeta potential) of the NPs were analyzed in folded capillary cells, using Malvern Nano zetasizer instrument (Malvern Instruments, Worcestershire, UK).

The temperature and refractive index of the apparatus were set at 25 °C and 1.755, respectively, with a total number of scans of 17. For the analysis, a sample of the NPs suspensions was withdrawn before and after the incubation with chitosan to compare size and PDI, then dispersed in ultrapure water (1:200 v/v) and placed in a cuvette for the analysis. The measurements were repeated three times, and the average value of each was calculated.

2.4.2. Encapsulation efficacy and drug load

The EE and DL are two essential parameters in developing drug delivery systems, especially nanotechnology-based ones, following the NPs characterization regarding size, PDI, and ZP.

The obtained NPs were withdrawn from the preparation medium by centrifugation at 16,000 rpm for 1 h, washed with deionized water, and centrifuged to obtain NPs pellets. The pellet was then immersed in a precise amount of chloroform, which can dissolve both the MEL and the lipid; then, a calculated volume of 0.1 M NaOH was added to extract only the used drug quantity and separate it from the organic solution.

After vortexing the mixture, it was moved to a separatory funnel, and the aqueous phase was withdrawn to determine its drug content. The encapsulated MEL was analyzed by high-pressure liquid chromatography (HPLC) following the method developed by Sipos et al. (2020),

as follows: an accurately weighed amount of formulation was tested utilizing the Agilent 1260 HPLC system (Agilent Technologies, Santa Clara, CA, USA). A C18 column (Kinetex® (5 µm, 150 mm × 4.6 mm)) was used as the stationary phase (Phenomenex, Torrance, CA, USA). 10 µl aliquots of the samples were then introduced to determine the concentration of MEL with the temperature adjusted to 30 °C. The mobile phases used were 0.065 M KH_2PO_4 solution adjusted to pH 2.8 with phosphoric acid (A) and methanol (B). The gradient elution was employed in two steps to perform the separation. The proportion was modified from a starting 50% eluent to 25% in 14 min, followed by a gradual rise to 50% in 20 min. The chromatograms were detected at 355 ± 4 nm using UV–VIS diode array detector after setting the eluent flow rate at 1 ml/min. For the assessment of the resulted data, the ChemStation B.04.03 Software (Agilent Technologies, Santa Clara, CA, USA) was used. The retention time of MEL 14.34 min, the linear regression of the calibration line was 0.999, and the determined limit of detection (LOD) was 16 ppm, while the limit of quantification (LOQ) was 49 ppm.

The EE and DL were calculated by applying the following equations:

$$EE\ (\%) = \frac{\text{The calculated amount of MEL encapsulated in the freeze} - \text{dried SLNs}}{\text{The total amount of MEL used in the preparation}} \times 100$$

$$DL\ (\%) = \frac{\text{The calculated amount of MEL encapsulated in the freeze} - \text{dried SLNs}}{\text{The weight of the freeze} - \text{dried SLNs}} \times 100$$

2.4.3. Scanning Electron Microscopy (SEM)

The surface morphology of the NPs was tested using Scanning Electron Microscopy (SEM) (Hitachi S4700, Hitachi Scientific Ltd., Tokyo, Japan) at 10 kV. The samples were coated with gold–palladium under an argon atmosphere. The air pressure was 1.3–13 mPa. (Bio-Rad SC 502, VG Microtech, Uckfield, UK).

2.4.4. Fourier-Transform Infrared Spectroscopy (FT-IR)

The compatibility was investigated between the drug and the used excipients by a Thermo Nicolet AVATAR FT-IR spectrometer (ThermoFisher, Waltham, USA). FTIR spectra of pure drug, phosphatidylcholine, PLGA, poloxamer 188, chitosan, PLGA NPs, and SLNs were measured as follows: each component was placed along with 150 mg KBr powder, the wavenumber range set on 4000–400 cm^{-1} at a resolution of 4 cm^{-1} before running the measurement.

2.4.5. X-ray Powder Diffraction (XRPD)

The physical nature and interactions were inspected between the drug and the used excipients by a BRUKER D8 Advance X-ray powder diffractometer (Bruker AXS GmbH, Karlsruhe, Germany). The X-ray powder diffractograms of the pure MEL, excipients, uncoated, and coated NPs were obtained in the angular range of 3–40° 2θ at a step time of 0.1 s and a step size of 0.007° at ambient temperature.

2.4.6. Differential Scanning Calorimetry (DSC)

DSC instrument (METTLER-Toledo 821e DSC, Mettler-Toledo GmbH, Giessen, Germany) provided with an intercooler and associated with the nitrogen gas was employed to acquire the thermograms of the samples, which were: pure MEL, the used excipients, and the optimized uncoated and coated NPs. The investigated samples were perfectly sealed in aluminum pans, and the thermal conductivity was analyzed compared to an empty pan (reference). The DSC records were obtained from the heat range of 20–300 °C with the heating rate of 10 °C/min under dry nitrogen purge. Finally, the measurements were set to the sample size and the evaluation was performed using STAR^e Software.

2.5. Evaluation of the prepared nanosystems:

2.5.1. Dissolution test

A dialysis bag diffusion technique was employed to investigate the dissolution behavior of the prepared NPs using dialysis membranes. 10 mg of MEL and precise aliquots of MEL-NPs equivalent to 10 mg were placed into dialysis bags and hermetically sealed. The sealed bags were then positioned in dissolution vessels containing volumes of 100 ml/each phosphate buffer (pH 7.4) and left to agitate at 50 rpm at 35 °C (Yasir et al., 2018a).

The sampling process was executed by withdrawing aliquots from the release medium at pre-established periods up to 6 h and replacing them with an equivalent volume of the fresh medium to maintain the 'sink' condition (Joshi et al., 2012, Dalpiaz et al., 2014).

The samples were analyzed using a UV–VIS spectrophotometer

(Jasco V730, ABL&E-JASCO Ltd., Budapest, Hungary) at λ max of 346 nm (Bartos et al., 2019).

2.5.2. Mucoadhesion study

Mucoadhesion was determined using two coordinated methods: the direct method (turbidimetric method) and the indirect method (Measuring the ZP changes). The direct method was carried out as follows: briefly, equal volumes of NPs suspensions in SNES and porcine mucin solution 0.05% were mixed and incubated at 37 °C, and continuously stirred for 4 h with a pre-determined sampling interval for of 1 h. The centrifugation was then performed at 17,000 rpm at 4 °C. The supernatant content of the free mucin was determined at 255 nm using a UV spectrophotometer. The mucin binding efficacy (MBE) can be calculated based on the following equation (Devkar et al., 2014, Vieira et al., 2018):

$$Mucin\ \ binding\ \ efficacy\ \ (\%) = \frac{\text{Total mucin} - \text{Free mucin}}{\text{Total mucin}} \times 100$$

The mucoadhesive properties were also evaluated by measuring the zeta potential using the Malvern Nano ZS instrument (Malvern Instruments, Worcestershire, UK) through the interaction of negatively charged mucins with SLNs, PLGA NPs, and C-SLNs (Rençber et al., 2016).

2.5.3. In vitro permeability study

The *in vitro* permeation test was completed utilizing a modified Side-bi-Side® type apparatus (Grown Glass, New York, NY, USA), which was designed to similar nasal cavity conditions. This method has been evaluated, validated and previously reported by Bartos et al. (2018). The intranasal suspension of MEL or MEL-NPs was placed in the first chamber and considered to be the donor phase; this phase was prepared by suspending MEL (1 mg) or MEL-NPs (equivalent to 1 mg) in 9 ml of simulated nasal electrolyte solution (SNES). This solution consists of 8.77 g NaCl, 2.98 g KCl, 0.59 g $CaCl_2$ anhydrous per 1000 ml solution in deionized water at a pH of 5.60, representing the pH of the nasal cavity. A semi-permeable cellulose membrane (Synthetic membrane PALL Metricel membrane®), previously impregnated in isopropyl myristate for 1 h, was placed between the two chambers as a membrane to imitate the lipophilicity of the nasal mucosa. The acceptor phase was represented by 9 ml of pH 7.4 phosphate buffer, and this pH represents the pH of the blood. The donor and the acceptor phase volumes were the same (9 ml) and had a 0.69 cm^2 diffusion area. The temperature of the phases was set to 35 °C (Thermo Haake C10-P5, Sigma, Aldrich Co.) to simulate the nasal condition, and the agitation using magnetic stirrers that were set to 50 rpm to mimic the movements of the cilia and the blood circulation. The diffused amount of MEL and MEL NPs was detected spectrophotometrically (Unicam UV/VIS) at 364 nm, and measurements were implemented in triplicate.

2.5.4. In vitro and in vivo correlation (IVIVC)

As reported in the FDA guidance (Emami, 2006, Shen and Burgess, 2015, Kim et al., 2019), the IVIVC process represents a predictive mathematical model demonstrating the expected *in vivo* behavior of a drug product based on its *in vitro* dissolution and permeation features. In the early-stage development, IVIVC is justified as a regulatory guideline aiming to minimize further animal studies (Uppoor, 2001). Level C correlations can be useful in the early stages of formulation development when pilot formulations are being selected, therefore it seems to be a suitable choice for selecting the most suitable NPs for the therapeutic purposes (FDA, 1997). Therefore, conducting IVIVC for the prepared NPs could be an efficient tool to estimate the *in vivo* behavior of the NPs based on the dissolution and permeation data and to provide assistance in optimizing the *in vitro* behavior of the NPs (Kim et al., 2019). A level-C correlation of IVIVC was investigated between the *in vitro* drug dissolution and permeation characteristics and the corresponding *in vivo* pharmacokinetic parameters such as AUC API (Area Under the Curve of the Active Pharmaceutical Ingredient) brain level. Since IVIVC is characterized by a linear relationship between the results obtained from the *in vitro* measurements and the *in vivo* tests data, Pearson correlation was applied to disclose the former relationship. To statistically estimate the *in vivo* brain distribution of MEL containing PLGA NPs and SLNs, IVIVC was operated using the attained *in vitro* results and previous *in vivo* data of similar experiments, i.e., MEL suspension, MEL-human serum albumin NPs (with a surfactant (MEL-HSA-Tween), and without (MEL-HSA)) (Katona et al., 2020), and a MEL-nanosuspension (nanoMEL) (Bartos et al., 2018). The mentioned formulations contained the same concentration of MEL. Data were expressed as means ± SD, and the comparison between the groups was established by Student's *t*-test set with TIBCO Statistica 13.4 software® (StatSoft Hungary, Budapest, Hungary). The differences between the outcomes were considered statistically significant when $p < 0.05$.

2.5.5. Statistical analysis

All the presented data were expressed as mean ± SD. The differences between the groups were assessed either by the two-way analysis of variance (ANOVA) or by Student's T test analysis using STATISTICA software. The differences were considered statistically significant when $p < 0.05$.

3. Results and discussion

3.1. RA as a part of QbD

Risk assessment was conducted to rank and prioritize the factors that highly impact the final product quality. The QbD-based risk assessment started by setting the QTPPs encompassing the desired quality attributes in MEL-loaded NPs, as summarized in Fig. 1.

The following step was to create an Ishikawa fishbone diagram that summarizes the risk analysis process. It clarifies the cause-effect relationship between the significant variables and the CMAs, CQAs, and CPPs of the nanoformulations (Fig. 2) (Ismail, 2020). This diagram is considered to be an efficient quality management tool aids in exploring the cause-effect relationship (Rathore, 2009).

This was followed by an initial RA of the CQAs, which were namely: average hydrodynamic diameter (Z-average), zeta potential, PDI, EE, dissolution rate, mucoadhesion, and permeability using Lean QbD software. After that, the evaluation of the selected CMAs and CPPs took place that was based on the thoroughly analyzed relevant literature and the results of experimental research work in addition to the proper prior knowledge. The risk assessment of the highest risky CPPs and CMAs affecting the quality of both SLNs and PLGA NPs for the IN application with the aim of the direct nose to brain delivery demonstrated that the vastly influential CPP was sonication time. In contrast, the immensely influential CMAs were lipid/ polymer type, lipid/ polymer concentration, surfactant type, and surfactant concentration. The calculated and ranked severity scores for the CQAs, CMAs, and CPPs are presented in Pareto charts (Fig. 3)

These results are supported by the previously reported literature, which presents particle size (Sonvico et al., 2018, Kumarasamy and Sosnik, 2019) and EE (Md et al., 2015, Agrawal et al., 2018) as the highly severe CQAs; Lipid type and concentration (Yasir and Sara, 2014, Aboud et al., 2016, Ismail et al., 2019b), polymer type and concentration (Musumeci et al., 2014, Kumarasamy and Sosnik, 2019, Ismail et al., 2019b) and surfactant type(Mittal et al., 2014, Shamarekh et al., 2020, Salem et al., 2020) and concentration (Bahadur et al., 2020, Froelich et al., 2021) as the highly risky CMAs. The sonication time (Vaka, 2011, Singh et al., 2012, Gupta et al., 2017, Ismail et al., 2019b) was the most critical CPP.

3.2. Preparation of MEL-loaded NPs

Based on the results of QbD and the preliminary experiments, SLNs

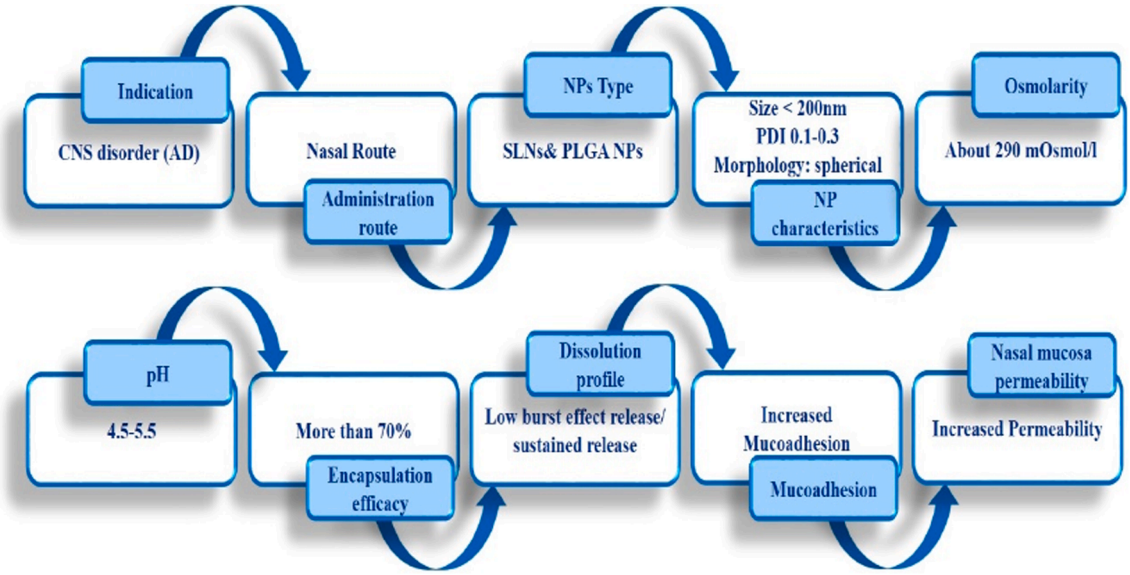

Fig. 1. Defining the QTPP for MEL-loaded NPs. The figure shows that the indication of the therapy was AD. The application route was the nasal route by encapsulating the drug into SLNs, PLGA NPs, or C-SLNs. It also demonstrates the desired NPs characters regarding size, PDI, optimal EE, dissolution, mucoadhesion, and permeation behavior.

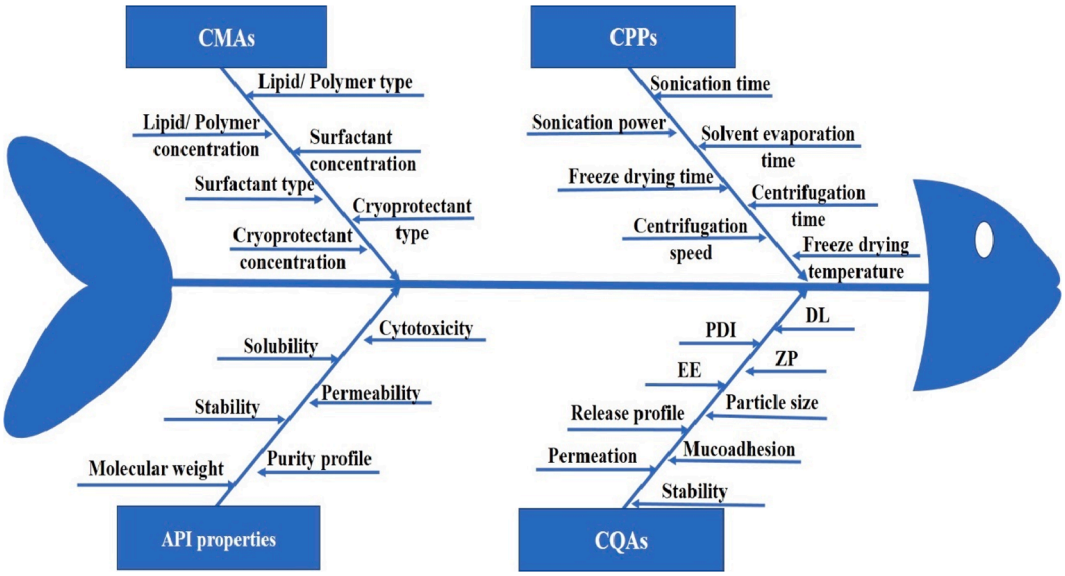

Fig. 2. Ishikawa diagram illustrating the risk factors for the nose-to-brain delivery of MEL-loaded NPs. CQAs: critical quality attributes, CMAs: critical materials attributes, CPPs: critical process parameters, API: active pharmaceutical ingredient, DL: drug load, PDI: polydispersity index, ZP: zeta potential, EE: encapsulation efficacy.

were successfully prepared using phosphatidylcholine as a lipid due to its ability to form SLNs, which were stabilized by poloxamer 188. Finally, an aliquot of NPs was coated by chitosan to modify zeta potential and increase the nanoformulation mucoadhesion. On the other hand, using cholesterol alone or in a mixture with phosphatidylcholine stabilized by PVA or Tween 80 resulted in a high PDI (>0.3), so the results could be neglected. In case of polymeric NPs, PLGA was utilized as a polymer of choice and poloxamer 188 for stabilization. In the contrary, using PCL for the formulation alone or with PLGA led to polymeric NPs with undesirable characteristics. The chitosan coating was later performed successfully on the SLNs after the demonstrated superior properties compared to PLGA NPs. The resulted NPs were smooth and spherical, as shown in Fig. 4.

3.3. Characterization of NPs

3.3.1. Mean diameter, PDI, and ZP

The mean hydrodynamic diameter, PDI, zeta-potential, EE of the developed formulations in this study are listed in Table 1.

The Z-average of PLGA NPs and SLNs was 142 ± 12.8 nm and 94.8 ± 7.4 nm, respectively; in contrast, C-SLNs demonstrated an increase in the Z-average due to the deposition of chitosan particles on the surface of the SLNs. Both types of NPs, in addition to the coated one, comply with the size requirement of nasal administration for the brain targeting, which preferred to be up to 200 nm (Gänger and Schindowski, 2018, Masserini, 2013).

PDI values were lower than 0.3 for all formulations indicating monodisperse size distributions (Pires and Santos, 2018). That is in

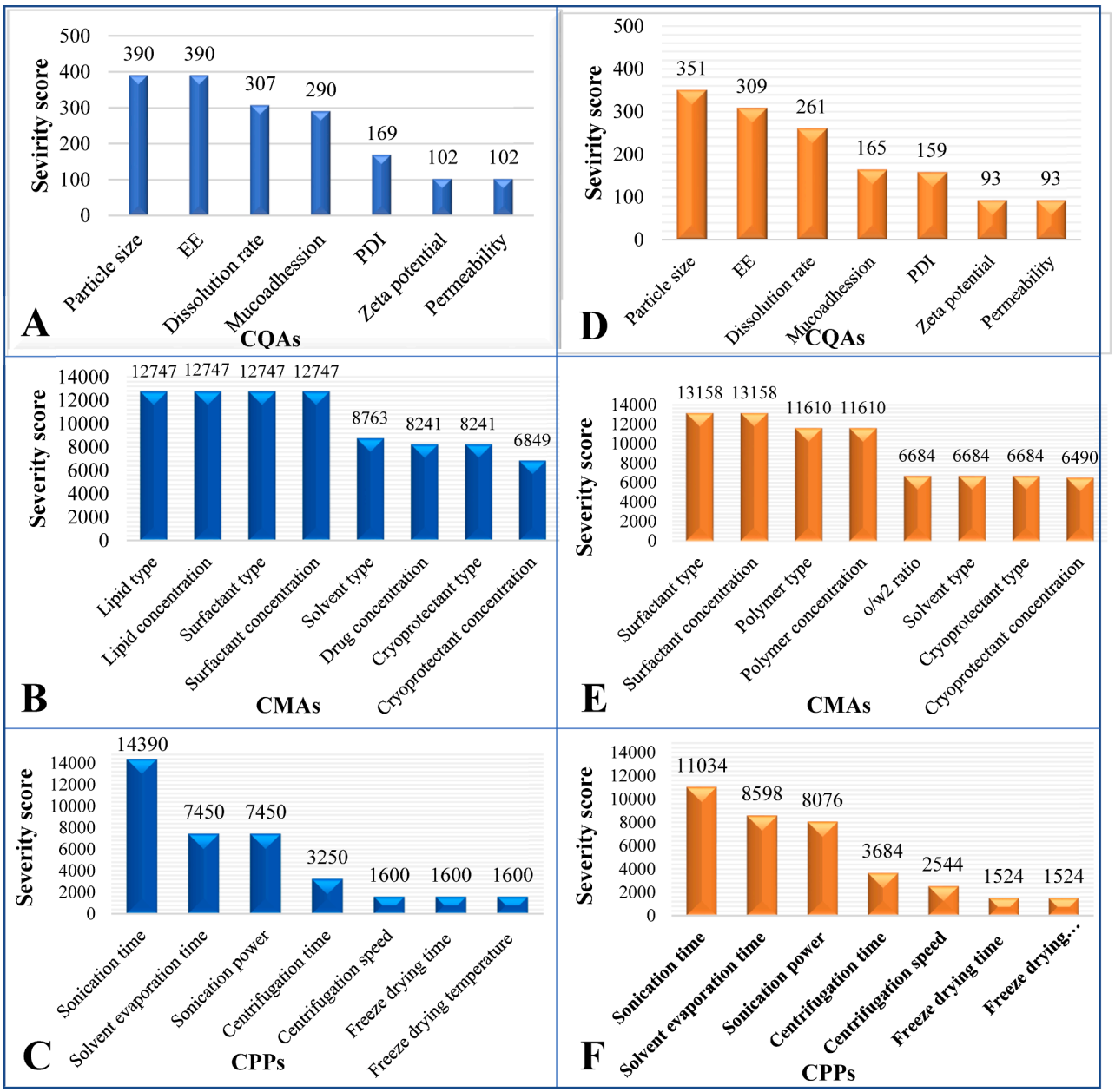

Fig. 3. Pareto charts indicates the highly risky CQAs, CMAs, and CPPs, which were calculated and ranked by the severity scores generated by Lean QbD software. Charts A, B, C are related to the SLNs and charts D, E, F are related to PLGA NPs. Abbreviations: CQAs critical quality attributes, CMAs critical materials attributes, CPPs critical process parameters, QbD quality by design, SLNs solid lipid nanoparticles, PLGA NPs poly lactic co glycolic acid nanoparticles.

accordance with the SEM images (Fig. 4), which demonstrate the NPs homogenized dispersion.

The zeta potential values of PLGA NPs and SLNs were −16.2 ± 1.8 and −43.7 ± 1.5 mV, respectively. This is logical due to the negative charge of phosphatidylcholine approximated in a range of −10 and −30 mV at the neutral pH (Zhou and Raphael, 2007) owing to the presence of phosphate and carboxyl groups, in contrast with the negatively charged carboxyl groups on PLGA that are the only cause behind the negative charge. As expected, the chitosan coating leads to a charge shifting of the SLNs to become positive (+60.7 ± 0.5) due to the electrostatic interactions, which suggest appropriate adsorption of the positively charged polymer (chitosan) onto the surface of the NPs. The pronounced surface charge variation from negative to positive charge is an indicator of the successful coating of the NPs surface with chitosan (Vieira et al., 2018). The optimized positively charged C-SLNs would probably have better adhesion to the negatively charged nasal mucosa, which in turn improves permeability through the nasal mucosa.

3.3.2. *Encapsulation efficacy and drug load*

As shown in Fig. 5, SLNs were superior to PLGA NPs regarding the EE and DL values. The highest EE and DL (87.26%, 2.64%, respectively) were obtained with SLNs when phosphatidylcholine was used alone as a lipid and poloxamer 188 as an emulsifier.

The higher the poloxamer 188 concentration, the lower the EE and DL ($p < 0.05$). A possible explanation could be that the increased concentration of poloxamer 188 leads to the formation of more monomers, which will create more micelles in the outer aqueous phase. Subsequently, more drug will diffuse from the inner aqueous phase to the outer one (Venkateswarlu and Manjunath, 2004, Sharma et al., 2016b, Sanjula et al., 2009).

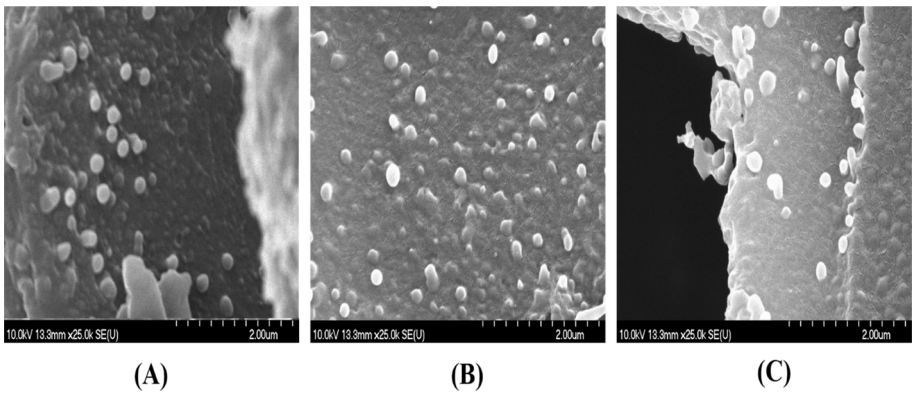

Fig. 4. SEM images representing the resulted NPs, where: (A) PLGA NPs, (B) SLNs, and (C) C-SLNs. The images show the spherical shape and well dispersed NPs with preferable nano-size.

Table 1
The Z-average, PDI, ZP of the prepared nanoformulations. Measurements were done in triple (n = 3 independent formulations), and data are represented as means ± SD.

Sample	Z-average (nm)	PDI	ZP (mV)
PLGA NPs	142 ± 12.8	0.276 ± 0.02	−16.2 ± 1.8
SLNs	94.8 ± 7.4	0.148 ± 0.002	−43.7 ± 1.5
C-SLNs	171.2 ± 6.2	0.187 ± 0.01	60.7 ± 0.5

3.3.3. *Fourier-transform infrared spectroscopy (FT-IR)*

The FT-IR spectra of MEL, both loaded NPs formulations, and the used excipients are presented in Fig. S1 (Supplementary data).

The FT-IR spectra of the NPs showed no changes in the MEL chemical structure and presented no significant difference in the main functional groups of MEL. The absorption band at 3290 cm^{-1} related to the hydroxyl group attached to an aromatic ring of MEL; furthermore, the carbonyl group vibration at 1550 cm^{-1} is not visible in the spectrum of C-SLNs. These characteristic peaks fading points out H-bonding formation between SLN and chitosan, which proves that the coating process was achieved.

Hence, there is no interaction between MEL and the other SLNs excipients, and they are compatible with each other. Similarly, absorption peaks of the materials used for PLGA NPs preparation (PLGA, Poloxamer) exhibited compatibility with MEL since the previously mentioned two chemical groups of MEL were maintained the same after PLGA NPs formulations (Alsulays et al., 2019).

3.3.4. *X-ray powder diffraction XRPD*

An overlay of powder XRPD patterns of MEL, SLNs, C-SLNs, PLGA NPs, and the used excipients is depicted in Fig. 6.

The XRPD of the MEL shows characteristic peaks to its crystalline structure. However, SLNs, C-SLNs, and PLGA NPs did not show the MEL characteristic peaks in their XRPD pattern. This confirms the successful encapsulation of the API into the NPs (Sipos et al., 2020). The previous results are conforming to the results of FT-IR, encapsulation efficacy, and drug loading.

3.3.5. *Differential scanning calorimetry DSC*

The results of the DSC (the thermograms of the prepared NPs and the used materials) are represented in Fig. S2 (Supplementary data).

The pure drug has a crystalline nature with an exact melting peak at 264 °C. When MEL is encapsulated MEL in the NPs, the melting peak disappears. This could be the result of the high dispersing speed used when formulating the SLNs, the continuous stirring when evaporating the solvent in addition to using a surfactant, which let the drug stay in an amorphous phase and suggests that MEL was successfully entrapped in the NPs (Sipos et al., 2020). These findings are in agreement with encapsulation efficacy, drug load, and XRPD results.

3.3.6. *Evaluation of the prepared nanosystems*

3.3.6.1. In vitro dissolution profiles. The *in vitro* dissolution profiles of pure MEL and MEL-loaded NPs were investigated in intranasal-simulated conditions, using simulated nasal electrolytic solution (SNES) medium (pH of 5.6), and the results are presented in Fig. 7.

It is evident that pure MEL demonstrates a modest solubility (5.10 ± 0. 9 μg/ml, over 360 min, at 35 °C) due to its chemical structure and because of the weak acidic character resulted in this medium (pKa = 3.43) (Avdeef, 2012); fabrication of MEL in nanoformulations indicated

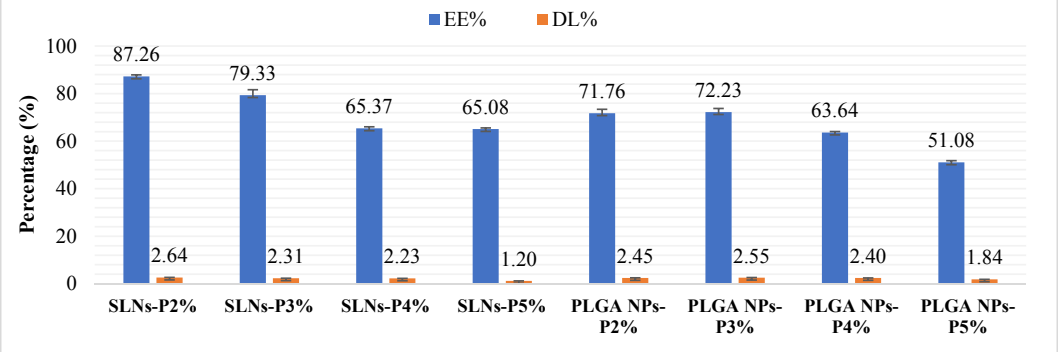

Fig. 5. Encapsulation efficacy (EE) and Drug load (DL) of the optimized SLNs and PLGA NPs formulations showing the negative effect of increasing poloxamer concentration. Anova test was performed to check the significance of the differences between the results of the EE and DL. Measurements were done in triple (n = 3 independent formulations), and data are represented as means ± SD.

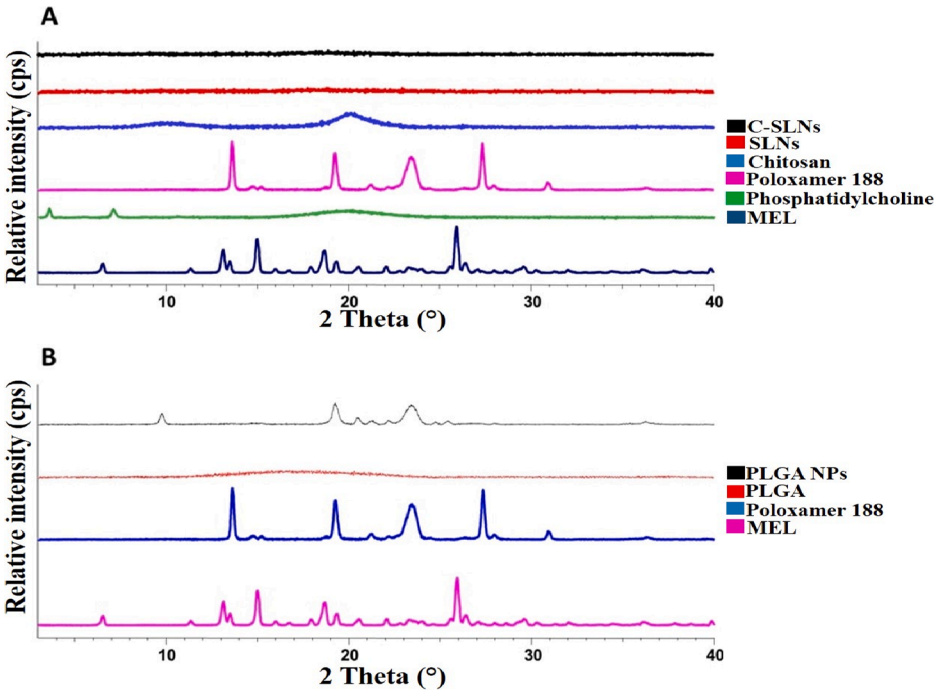

Fig. 6. XRPD spectra of SLNs and C-SLNs (A), PLGA NPs (B), and the excipients used in the formulation process emphasizing the compatibility between the used materials and the absence of any changes in MEL structure after the NPs formulation, in addition to confirming the successful coating of the SLNs.

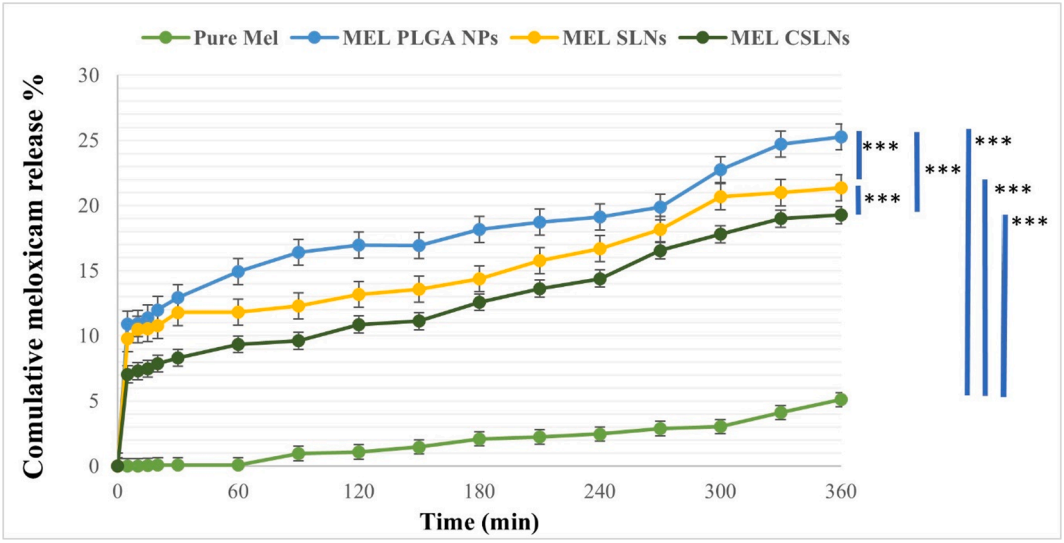

Fig. 7. MEL dissolution behavior as a pure drug and from MEL optimized nanoformulation (MEL-PLGA NPs, MEL-SLNs, and MEL-C-SLN. Anova test was performed to check the significance of the differences between the results of the nanoformulations and the pure MEL while Student T test was employed to assess the significance of the differences between each type of NPs and the pure MEL. Measurements were done in triple (n = 3 independent formulations), and data are represented as means ± SD. ***$p < 0.001$.

a significant increase ($p < 0.001$) in the dissolution rate compared to pure MEL (approximately 4–5 times higher). This aligns with the results previously reported by Katona *et al.* and might be due to the nano-size and improved specific surface area of the NPs (Katona et al., 2020).

The release behavior from the NPs demonstrated a sustained release pattern. This begins with a moderate early rapid release over the first hour, where 12.94 ± 0.86%, 11.79 ± 0.74 of MEL were released from the PLGA NPs and SLNs, respectively. The previous has been frequently reported for PLGA NPs (Araújo et al., 2014, Dinarvand et al., 2011) and SLNs (Yasir et al., 2018b, Singh et al., 2012). This moderate initial burst effect may be due to the surface-adsorbed drug particles on the NPs in addition to the drug molecules that are placed near the surface having poor links to the NPs system. A slow-release profile followed this until 6 h, where only 25.26 ± 2.39%, 21.37 ± 1.47% of cumulative MEL release was observed for PLGA NPs and SLNs, respectively ($p < 0.05$) since the encapsulated drug was slowly diffused out of the NPs core (Yasir et al., 2018b). The previous results point out that a significant part of the drug was kept encapsulated into the NPs after being surrounded by nasal mimetic conditions. Thus, it can be released into the targeted position.

Furthermore, chitosan-coated SLNs lead to a significantly slower release compared to the uncoated ones ($p < 0.05$). This could be explained by the additional controlling release properties presented by

the additional polymer layer of chitosan, classified as a water-insoluble polymer at the physiological pH (Dyawanapelly et al., 2016, Piazzini et al., 2019, Elnaggar et al., 2015).

These dissolution test results provide a guarantee that the drug leakage during *in vivo* delivery would be minimal. By preventing premature release, MEL will remain encapsulated in the NPs, avoiding the systemic effects until reaching the olfactory bulb in a sufficient concentration. Moreover, the enhanced solubility achieved by the formulated nanosystems compared to the pure drug will result in better pharmacokinetics as the dissolution behavior is the determining step of the absorption, the ADME (absorption, distribution, metabolism, and excretion) first process.

3.3.6.2. In vitro mucoadhesion. The mucoadhesion test was performed to understand the behavior of the NPs towards the mucin, which forms the main component of the nasal mucosa, and the higher the mucoadhesion, the better the retaining of the NPs adsorbed to the nasal mucosa (Luo et al., 2015).

Based on Fig. 8, it can be noticed that the highest mucoadhesion could be achieved when formulating the C-SLNs followed by uncoated SLNs then the MEL-PLGA NPs.

In the turbidimetric method, the mucoadhesive strength was estimated by calculating mucin binding efficacies to the obtained NPs. The mucin binding efficacy of PLGA NPs, SLNs, and C-SLNs were 36.55%, 57.59%, and 71.09%, respectively, by the end of the experiment, as Fig. 8A represents.

Based on the fact that the mucin possesses a negative charge along with its glycosylated structure, the positively charged C-SLNs will have significantly higher interaction with it than the negatively charged SLNs. The first leads to formulating ionic bonds, while the latter occurs by forming electrostatic interactions ($p < 0.05$). Since SLNs are higher in their negative charge, their electrostatic interactions with the mucin will be significantly higher than the PLGA NPs ($p < 0.05$). This observation goes in line with previous studies results (Luo et al., 2015, Aderibigbe and Naki, 2019).

The mucoadhesion was assessed in the zeta potential method by measuring zeta potential variation values up to 4 h (Fig. 8B). The high positive charge of the C-SLNs led to a significant neutralization in the negative charge of mucin ($p < 0.05$), which may happen by the formation of the ionic bonds (Grenha et al., 2007). On the other hand, uncoated SLNs and PLGA NPs remained negative; thus, the interaction with mucin happens weakly with insignificant charge changes. ($p > 0.05$). The ZP method results are consistent with those achieved by the turbidity method, as the total changes in ZP values match the MBE of each type of NPs. Both methods demonstrated higher mucoadhesion of the C-SLNs followed by the SLNs, which were superior to the PLGA NPs.

3.3.6.3. In vitro permeation test. Permeation test has been performed *in vitro* for pure MEL solution, MEL loaded NPs, and C-SLNs following similar conditions for the potential nose-to-brain delivery after the IN administration (Fig. 9).

A significant enhancement of MEL permeability through the semi-permeable membrane was achieved when MEL was formulated in NPs compared to the pure MEL solution ($p < 0.001$). This could be due to the nanoscale size of the prepared nanosystems and the increased specific surface area with the best nasal permeation properties, as previously reported by Gänger and Schindowski (Gänger and Schindowski, 2018). Moreover, the spherical and smooth surface of both NPs, as confirmed by SEM images, leads to the least friction with the membrane surface compared to the needle-shape particles (Ismail et al., 2019a). Stabilizing these NPs using poloxamer, a permeation enhancer, further improved their permeation properties (Bahadur and Pathak, 2012) by inhibiting the efflux pumps and lowering the membrane fluidity when it is used *in vivo* (Fischer et al., 2011).

Interestingly, SLNs showed significant superior permeability over PLGA NPs ($p < 0.001$). This might be explained by the lipid-based nanosystem lipophilicity (Esim et al., 2020), which exceeds PLGA NPs lipophilicity (Ismail et al., 2019a).

Furthermore, surface modification of SLNs by chitosan resulted in better permeation than the uncoated SLNs ($p < 0.001$), and this could be due to this polymer permeation enhancement properties (Trotta et al., 2018).

The permeation test results are in correlation with the mucoadhesion results. The higher mucoadhesion formulation will increase NPs contact time with the nasal mucosa, leading to a higher residence time inside the nose and a decrease in the mucociliary clearance; thus, giving the NPs enough time and better chances to permeate.

This could be translated *in vivo* by increasing the paracellular transport by opening the tight junctions and enhancing mucoadhesion properties (Rassu et al., 2017).

The *in vitro* tests provide a proof on the possible direct nose-to-brain transport of the NPs after the nasal application. This starts by protecting MEL and sustaining its *in vitro* release. Besides, PLGA NPs, SLNs, and C-SLNs enhanced the mucoadhesion properties, which can prolong their contact with the olfactory region, and thus, with the olfactory nerve endings for a longer time. Accordingly, this would improve NPs direct transport to the brain via the olfactory pathway. Moreover, the NPs adhesion to the respiratory mucosae would prolong their contact with the trigeminal nerve endings; therefore, boosting their possibilities to be directly transported to the brain via the trigeminal pathway. Additionally, the permeated NPs will also have the chance to reach the brain after being transported into the bloodstream, but in this case, they will have the challenge of crossing the BBB.

Both SLNs and PLGA NPs have already been employed to deliver the

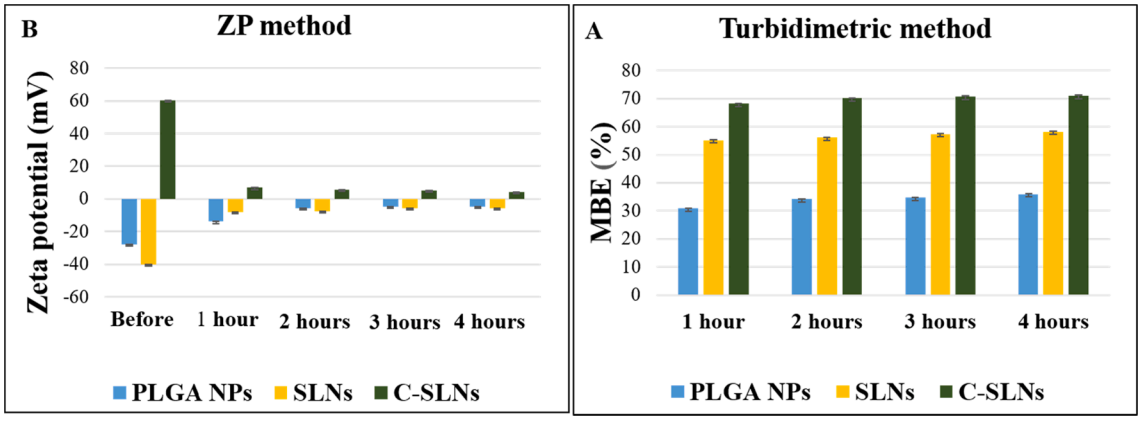

Fig. 8. Mucoadhesion assay of PLGA NPs, SLNs, and C-SLNs, where A represents Turbidity analysis method, and B represents ZP analysis method. Measurements were done in triple (n = 3 independent formulations), and data are represented as means ± SD.

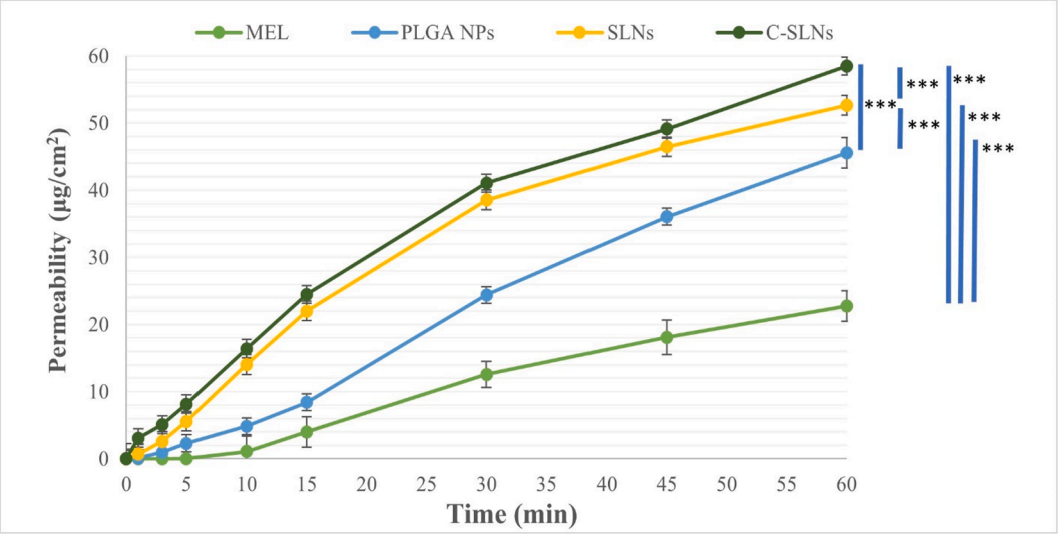

Fig. 9. *In vitro* permeability of pure MEL and MEL optimized nanoformulation (PLGA NPs, SLNs, and C-SLN). Anova test was performed to check the significance of the differences between the permeation of the nanoformulations and the pure MEL, then Student's T test was employed to assess the differences between MEL and each type of NPs, and between each two of the three types of NPs (***$p < 0.001$). Measurements were done in triple (n = 3 independent formulations), and data are represented as means ± SD.

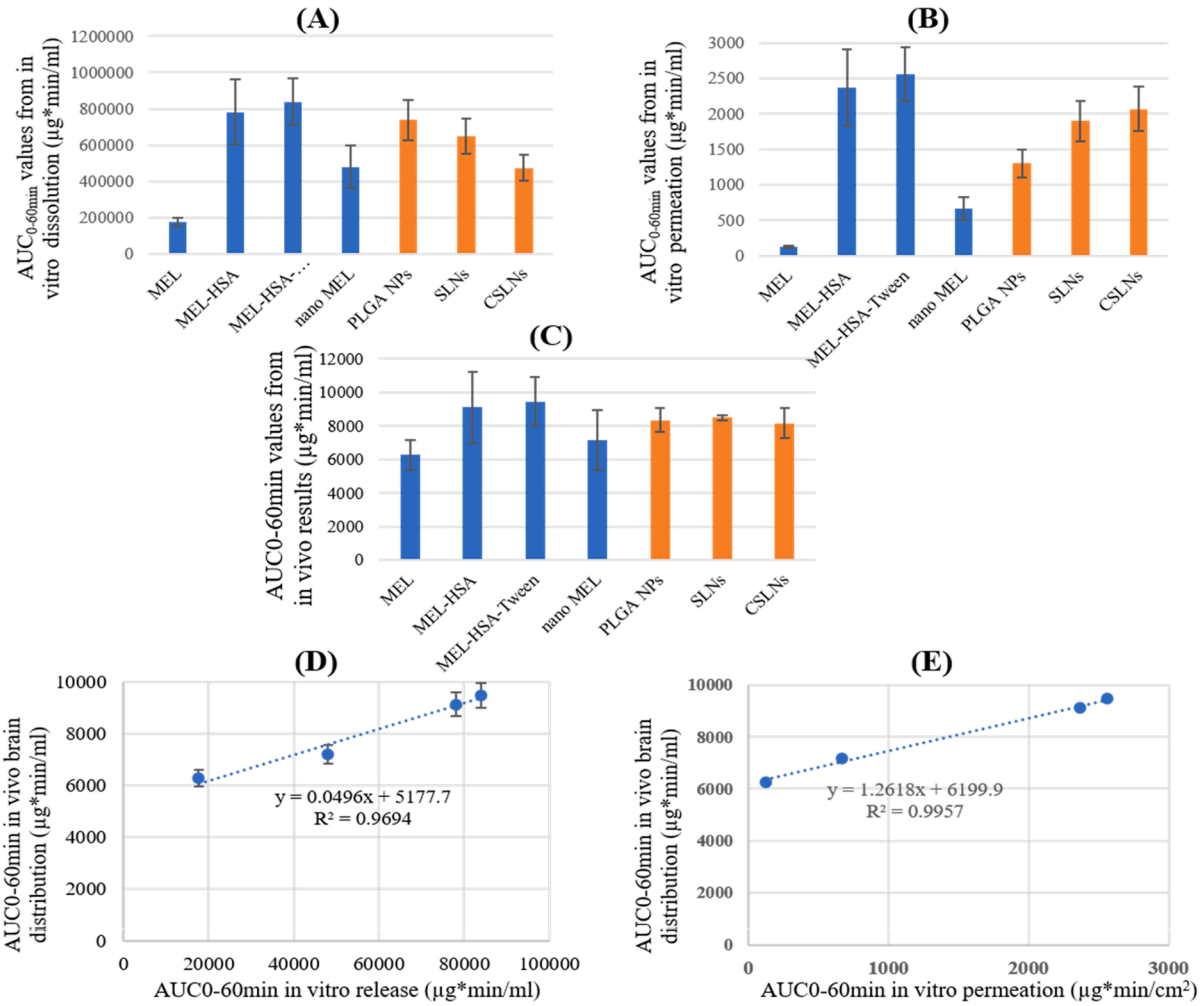

Fig. 10. IVIVC diagrams from which: (A) $AUC_{0–60\ min}$ values of the *in vitro* dissolution test results; (B) $AUC_{0–60\ min}$ values of the *in vitro* permeation test; (C) $AUC_{0–60\ min}$ values of preliminary *in vivo* results and estimated $AUC_{0–60\ min}$ values of the prepared formulations (D) Pearson correlation based on dissolution; (E) Pearson correlation based on permeation.

Table 2
Input parameter and estimated outcomes of IVIVC. Data are presented as means ± SD, n = 6.

	$AUC_{0\text{-}60min}$ *in vitro* dissolution ug*min/ml	$AUC_{0\text{-}60min}$ *in vitro* diffusion ug/cm^2*min	$AUC_{0\text{-}60min}$ *in vivo* brain distribution ug*min/ml	Estimated $AUC_{0\text{-}60min}$ *in vivo* brain distribution ug*min/ml
MEL	176.7 ± 24.74	123.5 ± 17.3	6.3 ± 0.9	
MEL-HSA	780.8 ± 179.6	2370.8 ± 545.3	9.1 ± 2.1	
MEL-HSA-Tween	839.9 ± 126	2560.2 ± 384	9.5 ± 1.5	
Nano MEL	480.5 ± 115.3	667.5 ± 160.2	7.2 ± 1.8	
PLGA NPs	738.5 ± 110.8	1304.6 ± 195.7		8.3 ± 0.7
SLNs	649.1 ± 97.4	1900.3 ± 285		8.4 ± 0.1
C-SLNs	473.5 ± 71	2071.2 ± 310.7		8.1 ± 0.9

intranasally applied drug molecules to the brain directly. The development of drug-SLNs has already been reported with the *in vitro* and *in vivo* evaluation of several APIs, including galantamine (Misra et al., 2016), donepezil (Al Asmari et al., 2016), haloperidol (Yasir and Sara, 2014), paeonol (Sun et al., 2020), astaxanthin (Chandra Bhatt et al., 2016) and pueraria flavones (Wang et al., 2019). On the other hand, formulating PLGA NPs was an efficient tool employed successfully to enhance brain delivery of the drugs such as olanzapine (Seju et al., 2011), Diazepam (Sharma et al., 2015b), Midazolam (Sharma et al., 2016a), lamotrigine (Nigam et al., 2019), temozolomide (Chu et al., 2018), and Huperzine (Meng et al., 2018).

3.3.6.4. In vitro-in vivo correlation (IVIVC). As shown in Fig. 10, Pearson correlation coefficients confirm good agreement both *in vitro* dissolution (0.9694) and permeation (0.9957) (Sipos et al., 2020). According to $AUC_{0\text{-}60min}$ values of *in vitro* dissolution (Table 2), *in vitro* permeation, and *in vivo* brain distribution, the comparative studies emphasized a significant difference between the measured *in vitro* and estimated *in vivo* results of the prepared NPs compared to the pure MEL.

As the regression curves show, a possible *in vivo* brain distribution profiles of PLGA NPs, SLNs and C-SLNs were estimated to 8.3 ± 0.7, 8.4 ± 0.1, and 8.1 ± 0.9 μg*min/ml, respectively. Since IVIVC results of the prepared nanoformulations showed consistent results with the previous *in vivo* studies and estimated the excellent potential for *in vivo* brain distribution of MEL; they may hold a great promise to deliver MEL to the brain after the nasal application (Bartos et al., 2018, Katona et al., 2020).

4. Conclusion

Since MEL is a well-reported and widely available anti-neuroinflammation agent, using it in AD management holds great promise. However, its brain concentration following the conventional administration routes is too low, with no reported studies for formulating MEL as coated or uncoated nanoparticles for the IN application aiming to deliver it directly to the brain.

In this study, the QbD concept was successfully employed to thoroughly understand and optimize the process parameters affecting the CQAs when developing nanoformulations for nose-to-brain delivery after the IN application.

Compared to PLGA NPs, SLNs showed smaller particle size, higher EE and DL while showing a better-sustained release profile. Moreover, coating SLNs with chitosan showed a superior sustaining release behavior over the uncoated MEL-loaded SLNs. The mucoadhesion properties of C-SLNs demonstrated 1.25 and 2-fold enhancement over the SLNs and PLGA NPs, respectively. The results of *in vivo* brain distribution of MEL NPs confirmed that the "measured" *in vitro* and "estimated" *in vivo* characteristics and behavior of PLGA NPs and SLNs are expected to be better than the native MEL. Our findings provide the first reported evidence for the potentiality of encapsulating MEL in both polymeric and lipid NPs for IN application with the superiority of SLNs, which properties were further enhanced by coating with cationic polymer chitosan.

Declaration of Competing Interest

The authors declare that they have no known competing financial interests or personal relationships that could have appeared to influence the work reported in this paper.

Acknowledgment

This research was supported by the Ministry of Human Capacities, Hungary (Grant TKP-2020) and by the National Research, Development, and Innovation Office, Hungary (GINOP 2.3.2-15-2016-00060) projects.

Appendix A. Supplementary material

Supplementary data to this article can be found online at https://doi.org/10.1016/j.ijpharm.2021.120724.

References

Aboud, H.M., El Komy, M.H., Ali, A.A., El Menshawe, S.F., Abd Elbary, A., 2016. Development, optimization, and evaluation of carvedilol-loaded solid lipid nanoparticles for intranasal drug delivery. AAPS PharmSciTech 17, 1353–1365.
Aderibigbe, B.A., Naki, T., 2019. Chitosan-based nanocarriers for nose to brain delivery. Appl. Sci. 9, 2219.
Agrawal, M., Saraf, S., Saraf, S., Antimisiaris, S.G., Chougule, M.B., Shoyele, S.A., Alexander, A., 2018. Nose-to-brain drug delivery: An update on clinical challenges and progress towards approval of anti-Alzheimer drugs. J. Control. Release 281, 139–177.
Ah, Y.-C., Choi, J.-K., Choi, Y.-K., Ki, H.-M., Bae, J.-H., 2010. A novel transdermal patch incorporating meloxicam: In vitro and in vivo characterization. Int. J. Pharm. 385, 12–19.
Akel, H., Ismail, R., Csóka, I., 2020. Progress and perspectives of brain-targeting lipid-based nanosystems via the nasal route in Alzheimer's disease. Eur. J. Pharm. Biopharm. 148, 38–53.
Al Asmari, A.K., Ullah, Z., Tariq, M., Fatani, A., 2016. preparation, characterization, and in vivo evaluation of intranasally administered liposomal formulation of donepezil. Drug Design, Dev. Therapy 10, 205–215.
Alexander, A., Saraf, S., 2018. Nose-to-brain drug delivery approach: A key to easily accessing the brain for the treatment of Alzheimer's disease. Neural Regener. Res. 13, 2102–2104.
Alsulays, B.B., Anwer, M.K., Soliman, G.A., Alshehri, S.M., Khafagy, E.-S., 2019. Impact of penetratin stereochemistry on the oral bioavailability of insulin-loaded solid lipid nanoparticles. Int. J. Nanomed. 14, 9127–9138.
Araújo, F., Shrestha, N., Shahbazi, M.-A., Fonte, P., Mäkilä, E.M., Salonen, J.J., Hirvonen, J.T., Granja, P.L., Santos, H.A., Sarmento, B., 2014. The impact of nanoparticles on the mucosal translocation and transport of GLP-1 across the intestinal epithelium. Biomaterials 35, 9199–9207.
Avdeef, A., 2012. Permeability—PAMPA In Absorption and Drug Development. John Wiley & Sons Inc:, Hoboken, NJ.
Badran, M.M., Taha, E.I., Tayel, M.M., Al-Suwayeh, S.A., 2014. Ultra-fine self nanoemulsifying drug delivery system for transdermal delivery of meloxicam: Dependency on the type of surfactants. J. Mol. Liq. 190, 16–22.
Bahadur, S., Pardhi, D.M., Rautio, J., Rosenholm, J.M., Pathak, K., 2020. Intranasal nanoemulsions for direct nose-to-brain delivery of actives for CNS disorders. Pharmaceutics 12.
Bahadur, S., Pathak, K., 2012. Physicochemical and physiological considerations for efficient nose-to-brain targeting. Expert Opin. Drug Deliv. 9, 19–31.
Bartos, C., Ambrus, R., Katona, G., Sovány, T., Gáspár, R., Márki, Á., Ducza, E., Ivanov, A., Tömösi, F., Janáky, T., Szabó-Révész, P., 2019. Transformation of meloxicam containing nanosuspension into surfactant-free solid compositions to increase the product stability and drug bioavailability for rapid analgesia. Drug Design, Dev. Therapy 13, 4007–4020.
Bartos, C., Ambrus, R., Kovács, A., Gáspár, R., Sztojkov-Ivanov, A., Márki, Á., Janáky, T., Tömösi, F., Kecskeméti, G., Szabó-Révész, P., 2018. Investigation of absorption

routes of meloxicam and its salt form from intranasal delivery systems. Molecules 23, 784.
Cao, Q., Wu, H., Zhu, L., Wu, D., Zhu, Y., Zhu, Z., Cui, J., 2011. Preparation and evaluation of zanamivir-loaded solid lipid nanoparticles. J. Control. Release 152.
Chandra Bhatt, P., Srivastava, P., Pandey, P., Khan, W., Panda, B.P., 2016. Nose to brain delivery of astaxanthin-loaded solid lipid nanoparticles: fabrication, radio labeling, optimization and biological studies. RSC Adv. 6, 10001–10010.
Chu, L., Wang, A., Ni, L., Yan, X., Song, Y., Zhao, M., Sun, K., Mu, H., Liu, S., Wu, Z., Zhang, C., 2018. Nose-to-brain delivery of temozolomide-loaded PLGA nanoparticles functionalized with anti-EPHA3 for glioblastoma targeting. Drug Delivery 25, 1634–1641.
Cunha, S., Amaral, M., Lobo, J.S., Silva, A.C., 2017. Lipid nanoparticles for nasal/intranasal drug delivery. Crit. Reviews™ Therapeut. Drug Carrier Syst. 34.
Dalpiaz, A., Ferraro, L., Perrone, D., Leo, E., Iannuccelli, V., Pavan, B., Paganetto, G., Beggiato, S., Scalia, S., 2014. Brain uptake of a Zidovudine prodrug after nasal administration of solid lipid microparticles. Mol. Pharm. 11, 1550–1561.
Das, S., Ng, W.K., Kanaujia, P., Kim, S., Tan, R.B.H., 2011. Formulation design, preparation and physicochemical characterizations of solid lipid nanoparticles containing a hydrophobic drug: Effects of process variables. Colloids Surf., B 88, 483–489.
Devkar, T.B., Tekade, A.R., Khandelwal, K.R., 2014. Surface engineered nanostructured lipid carriers for efficient nose to brain delivery of ondansetron HCl using Delonix regia gum as a natural mucoadhesive polymer. Colloids Surf., B 122, 143–150.
Dinarvand, R., Sepehri, N., Manoochehri, S., Rouhani, H., Atyabi, F., 2011. Polylactide-co-glycolide nanoparticles for controlled delivery of anticancer agents. Int. J. Nanomed. 6, 877.
Dyawanapelly, S., Koli, U., Dharamdasani, V., Jain, R., Dandekar, P., 2016. Improved mucoadhesion and cell uptake of chitosan and chitosan oligosaccharide surface-modified polymer nanoparticles for mucosal delivery of proteins. Drug Deliv. Translat. Res. 6, 365–379.
Elnaggar, Y.S., Etman, S.M., Abdelmonsif, D.A., Abdallah, O.Y., 2015. Intranasal piperine-loaded chitosan nanoparticles as brain-targeted therapy in Alzheimer's disease: optimization, biological efficacy, and potential toxicity. J. Pharm. Sci. 104, 3544–3556.
Emami, J., 2006. In vitro-in vivo correlation: from theory to applications. J. Pharm. Pharm. Sci. 9, 169–189.
Erdő, F., Bors, L.A., Farkas, D., Bajza, Á., Gizurarson, S., 2018. Evaluation of intranasal delivery route of drug administration for brain targeting. Brain Res. Bull. 143, 155–170.
Esim, O., Savaser, A., Ozkan, C.K., Oztuna, A., Goksel, B.A., Ozler, M., Tas, C., Ozkan, Y., 2020. Nose to brain delivery of eletriptan hydrobromide nanoparticles: Preparation, in vitro/in vivo evaluation and effect on trigeminal activation. J. Drug Delivery Sci. Technol. 59, 101919.
FDA, U., 1997. Guidance for Industry: Extended Release Oral Dosage Forms: Development, Evaluation, and Application of In Vitro. vivo Correlat.
Fischer, S.M., Brandl, M., Fricker, G., 2011. Effect of the non-ionic surfactant Poloxamer 188 on passive permeability of poorly soluble drugs across Caco-2 cell monolayers. Eur. J. Pharm. Biopharm. 79, 416–422.
Fonte, P., Andrade, F., Araújo, F., Andrade, C., Das Neves, J., Sarmento, B., 2012. Chitosan-coated solid lipid nanoparticles for insulin delivery. Methods Enzymol. 508, 295–314.
Froelich, A., Osmałek, T., Jadach, B., Puri, V., Michniak-Kohn, B., 2021. Microemulsion-based media in nose-to-brain drug delivery. Pharmaceutics 13, 201.
Gänger, S., Schindowski, K., 2018. Tailoring Formulations for Intranasal Nose-to-Brain Delivery: A Review on Architecture, Physico-Chemical Characteristics and Mucociliary Clearance of the Nasal Olfactory Mucosa. Pharmaceutics 10, 116.
Gartziandia, O., Egusquiaguirre, S.P., Bianco, J., Pedraz, J.L., Igartua, M., Hernandez, R. M., Préat, V., Beloqui, A., 2016. Nanoparticle transport across in vitro olfactory cell monolayers. Int. J. Pharm. 499, 81–89.
Gartziandia, O., Herran, E., Pedraz, J.L., Carro, E., Igartua, M., Hernandez, R.M., 2015. Chitosan coated nanostructured lipid carriers for brain delivery of proteins by intranasal administration. Colloids Surf., B 134, 304–313.
Gordillo-Galeano, A., Mora-Huertas, C.E., 2018. Solid lipid nanoparticles and nanostructured lipid carriers: A review emphasizing on particle structure and drug release. Eur. J. Pharm. Biopharm. 133, 285–308.
Goverdhan, P., Sravanthi, A., Mamatha, T., 2012. Neuroprotective effects of meloxicam and selegiline in scopolamine-induced cognitive impairment and oxidative stress. Int. J. Alzheimer's Dis. 2012.
Grenha, A., Grainger, C.I., Dailey, L.A., Seijo, B., Martin, G.P., Remuñán-López, C., Forbes, B., 2007. Chitosan nanoparticles are compatible with respiratory epithelial cells in vitro. Eur. J. Pharm. Sci. 31, 73–84.
Gupta, S., Kesarla, R., Chotai, N., Misra, A., Omri, A., 2017. Systematic Approach for the Formulation and Optimization of Solid Lipid Nanoparticles of Efavirenz by High Pressure Homogenization Using Design of Experiments for Brain Targeting and Enhanced Bioavailability. Biomed Res. Int. 2017, 5984014.
He, H., Wang, P., Cai, C., Yang, R., Tang, X., 2015. VB12-coated Gel-Core-SLN containing insulin: Another way to improve oral absorption. Int. J. Pharm. 493, 451–459.
Ianiski, F.R., Alves, C.B., Ferreira, C.F., Rech, V.C., Savegnago, L., Wilhelm, E.A., Luchese, C., 2016. Meloxicam-loaded nanocapsules as an alternative to improve memory decline in an Alzheimer's disease model in mice: involvement of Na+, K+-ATPase. Metab. Brain Dis. 31, 793–802.
Ianiski, F.R., Alves, C.B., Souza, A.C.G., Pinton, S., Roman, S.S., Rhoden, C.R., Alves, M. P., Luchese, C., 2012. Protective effect of meloxicam-loaded nanocapsules against amyloid-β peptide-induced damage in mice. Behav. Brain Res. 230, 100–107.
Ismail, R., 2020. Quality by design driven development of polymeric and lipid-based nanocarriers as potential systems for oral delivery of GLP-1 analogues. Szte.
Ismail, R., Bocsik, A., Gábor, K., Grof, I., Deli, M., Csoka, I., 2019a. Encapsulation in Polymeric Nanoparticles Enhances the Enzymatic Stability and the Permeability of the GLP-1 Analog, Liraglutide, Across a Culture Model of Intestinal Permeability. Pharmaceutics 11, 599.
Ismail, R., Sovány, T., Gácsi, A., Ambrus, R., Katona, G., Imre, N., Csóka, I., 2019b. Synthesis and Statistical Optimization of Poly (Lactic-Co-Glycolic Acid) Nanoparticles Encapsulating GLP1 Analog Designed for Oral Delivery. Pharm. Res. 36, 99.
Joshi, A.S., Patel, H.S., Belgamwar, V.S., Agrawal, A., Tekade, A.R., 2012. Solid lipid nanoparticles of ondansetron HCl for intranasal delivery: development, optimization and evaluation. J. Mater. Sci. - Mater. Med. 23, 2163–2175.
Katona, G., Balogh, G.T., Dargó, G., Gáspár, R., Márki, Á., Ducza, E., Sztojkov-Ivanov, A., Tömösi, F., Kecskeméti, G., Janáky, T., 2020. Development of meloxicam-human serum albumin nanoparticles for nose-to-brain delivery via application of a quality by design approach. Pharmaceutics 12, 97.
Keum, C.-G., Noh, Y.-W., Baek, J.-S., Lim, J.-H., Hwang, C.-J., Na, Y.-G., Shin, S.-C., Cho, C.-W., 2011. Practical preparation procedures for docetaxel-loaded nanoparticles using polylactic acid-co-glycolic acid. Int. J. Nanomed. 6, 2225–2234.
Kim, T.H., Shin, S., Jeong, S.W., Lee, J.B., Shin, B.S., 2019. Physiologically relevant in vitro-in vivo correlation (ivivc) approach for sildenafil with site-dependent dissolution. Pharmaceutics 11, 251.
Kumarasamy, M., Sosnik, A., 2019. The Nose-To-Brain Transport of Polymeric Nanoparticles Is Mediated by Immune Sentinels and Not by Olfactory Sensory Neurons. Adv. Biosyst. 3, 1900123.
Kumari, A., Yadav, S.K., Yadav, S.C., 2010. Biodegradable polymeric nanoparticles based drug delivery systems. Colloids Surf., B 75, 1–18.
Li, J., Sabliov, C., 2013. PLA/PLGA nanoparticles for delivery of drugs across the blood-brain barrier. Nanotechnol. Rev. 2, 241–257.
Liu, Y., Pan, J., Feng, S.-S., 2010. Nanoparticles of lipid monolayer shell and biodegradable polymer core for controlled release of paclitaxel: Effects of surfactants on particles size, characteristics and in vitro performance. Int. J. Pharm. 395, 243–250.
Luo, Y., Teng, Z., Li, Y., Wang, Q., 2015. Solid lipid nanoparticles for oral drug delivery: chitosan coating improves stability, controlled delivery, mucoadhesion and cellular uptake. Carbohydr. Polym. 122, 221–229.
Masserini, M., 2013. Nanoparticles for brain drug delivery. ISRN Biochem. 2013.
Md, S., Mustafa, G., Baboota, S., Ali, J., 2015. Nanoneurotherapeutics approach intended for direct nose to brain delivery. Drug Dev. Ind. Pharm. 41, 1922–1934.
Meng, Q., Wang, A., Hua, H., Jiang, Y., Wang, Y., Mu, H., Wu, Z., Sun, K., 2018. Intranasal delivery of Huperzine A to the brain using lactoferrin-conjugated N-trimethylated chitosan surface-modified PLGA nanoparticles for treatment of Alzheimer's disease. Int. J. Nanomed. 13, 705–718.
Misra, S., Chopra, K., Sinha, V.R., Medhi, B., 2016. Galantamine-loaded solid–lipid nanoparticles for enhanced brain delivery: preparation, characterization, in vitro and in vivo evaluations. Drug Delivery 23, 1434–1443.
Mistry, A., Stolnik, S., Illum, L., 2009. Nanoparticles for direct nose-to-brain delivery of drugs. Int. J. Pharm. 379, 146–157.
Mittal, D., Ali, A., Md, S., Baboota, S., Sahni, J.K., Ali, J., 2014. Insights into direct nose to brain delivery: current status and future perspective. Drug Delivery 21, 75–86.
Moore, A.H., O'Banion, M.K., 2002. Neuroinflammation and anti-inflammatory therapy for Alzheimer's disease. Adv. Drug Deliv. Rev. 54, 1627–1656.
Musumeci, T., Pellitteri, R., Spatuzza, M., Puglisi, G., 2014. Nose-to-Brain Delivery: Evaluation of Polymeric Nanoparticles on Olfactory Ensheathing Cells Uptake. J. Pharm. Sci. 103, 628–635.
Nabi-Meibodi, M., Vatanara, A., Najafabadi, A.R., Rouini, M.R., Ramezani, V., Gilani, K., Etemadzadeh, S.M.H., Azadmanesh, K., 2013. The effective encapsulation of a hydrophobic lipid-insoluble drug in solid lipid nanoparticles using a modified double emulsion solvent evaporation method. Colloids Surf., B 112, 408–414.
Nigam, K., Kaur, A., Tyagi, A., Nematullah, M., Khan, F., Gabrani, R., Dang, S., 2019. Nose-to-brain delivery of lamotrigine-loaded PLGA nanoparticles. Drug Delivery Translat. Res. 9, 879–890.
Nikvsarkar, M., Banerjee, A., Shah, D., Trivedi, J., Patel, M., Cherian, B., Padh, H., 2006. Reduction in aluminum induced oxidative stress by meloxicam in rat brain. Iran. Biomed. J. 10, 151–155.
Pallagi, E., Ismail, R., Paal, T., Csóka, I., 2018. Initial risk assessment as part of the quality by design in peptide drug containing formulation development. Eur. J. Pharm. Sci. 122, 160–169.
Pardeshi, C.V., Belgamwar, V.S., 2013. Direct nose to brain drug delivery via integrated nerve pathways bypassing the blood–brain barrier: an excellent platform for brain targeting. Expert Opin. Drug Delivery 10, 957–972.
Patel, M., Souto, E.B., Singh, K.K., 2013. Advances in brain drug targeting and delivery: limitations and challenges of solid lipid nanoparticles. Expert Opin. Drug Delivery 10, 889–905.
Piazzini, V., Landucci, E., D'Ambrosio, M., Fasiolo, L.T., Cinci, L., Colombo, G., Pellegrini-Giampietro, D.E., Bilia, A.R., Luceri, C., Bergonzi, M.C., 2019. Chitosan coated human serum albumin nanoparticles: A promising strategy for nose-to-brain drug delivery. Int. J. Biol. Macromol. 129, 267–280.
Pires, P.C., Santos, A.O., 2018. Nanosystems in nose-to-brain drug delivery: A review of non-clinical brain targeting studies. J. Control. Release 270, 89–100.
Rassu, G., Soddu, E., Posadino, A.M., Pintus, G., Sarmento, B., Giunchedi, P., Gavini, E., 2017. Nose-to-brain delivery of BACE1 siRNA loaded in solid lipid nanoparticles for Alzheimer's therapy. Colloids Surf., B 152, 296–301.
Rathore, A.S., 2009. Roadmap for implementation of quality by design (QbD) for biotechnology products. Trends Biotechnol. 27, 546–553.
Rençber, S., Karavana, S.Y., Yilmaz, F.F., Eraç, B., Nenni, M., Özbal, S., Pekçetin, Ç., Gurer-Orhan, H., Hoşgör-Limoncu, M., Güneri, P., Ertan, G., 2016. Development,

characterization, and in vivo assessment of mucoadhesive nanoparticles containing fluconazole for the local treatment of oral candidiasis. Int. J. Nanomed. 11, 2641–2653.
Salem, L.H., El-Feky, G.S., Fahmy, R.H., el Gazayerly, O.N., Abdelbary, A., 2020. Coated lipidic nanoparticles as a new strategy for enhancing nose-to-brain delivery of a hydrophilic drug molecule. J. Pharm. Sci. 109, 2237–2251.
Sanjula, B., Shah, F.M., Javed, A., Alka, A., 2009. Effect of poloxamer 188 on lymphatic uptake of carvedilol-loaded solid lipid nanoparticles for bioavailability enhancement. J. Drug Target. 17, 249–256.
Seedher, N., Bhatia, S., 2005. Mechanism of interaction of the non-steroidal antiinflammatory drugs meloxicam and nimesulide with serum albumin. J. Pharm. Biomed. Anal. 39, 257–262.
Seju, U., Kumar, A., Sawant, K.K., 2011. Development and evaluation of olanzapine-loaded PLGA nanoparticles for nose-to-brain delivery: In vitro and in vivo studies. Acta Biomater. 7, 4169–4176.
Shakeri, S., Ashrafizadeh, M., Zarrabi, A., Roghanian, R., Afshar, E.G., Pardakhty, A., Mohammadinejad, R., Kumar, A., Thakur, V.K., 2020. Multifunctional polymeric nanoplatforms for brain diseases diagnosis, therapy and theranostics. Biomedicines 8, 13.
Shamarekh, K.S., Gad, H.A., Soliman, M.E., Sammour, O.A., 2020. Development and evaluation of protamine-coated PLGA nanoparticles for nose-to-brain delivery of tacrine: In-vitro and in-vivo assessment. J. Drug Delivery Sci. Technol. 57, 101724.
Sharma, D., Maheshwari, D., Philip, G., Rana, R., Bhatia, S., Singh, M., Gabrani, R., Sharma, S.K., Ali, J., Sharma, R.K., 2014. Formulation and optimization of polymeric nanoparticles for intranasal delivery of lorazepam using Box-Behnken design: in vitro and in vivo evaluation. BioMed Res. Int. 2014.
Sharma, D., Sharma, R.K., Bhatnagar, A., Nishad, D.K., Singh, T., Gabrani, R., Sharma, S. K., Ali, J., Dang, S., 2016a. Nose to Brain Delivery of Midazolam Loaded PLGA Nanoparticles. In Vitro and In Vivo Investigations. Curr. Drug Deliv. 13, 557–564.
Sharma, D., Sharma, R.K., Sharma, N., Gabrani, R., Sharma, S.K., Ali, J., Dang, S., 2015. Nose-to-brain delivery of PLGA-diazepam nanoparticles. AAPS Pharmscitech 16, 1108–1121.
Sharma, N., Madan, P., Lin, S., 2016b. Effect of process and formulation variables on the preparation of parenteral paclitaxel-loaded biodegradable polymeric nanoparticles: A co-surfactant study. Asian J. Pharm. Sci. 11, 404–416.
Shen, J., Burgess, D.J., 2015. In vitro–in vivo correlation for complex non-oral drug products: where do we stand? J. Control. Release 219, 644–651.
Shkodra-Pula, B., Grune, C., Traeger, A., Vollrath, A., Schubert, S., Fischer, D., Schubert, U.S., 2019. Effect of surfactant on the size and stability of PLGA nanoparticles encapsulating a protein kinase C inhibitor. Int. J. Pharm. 566, 756–764.
Singh, A.P., Saraf, S.K., Saraf, S.A., 2012. SLN approach for nose-to-brain delivery of alprazolam. Drug Delivery Translat. Res. 2, 498–507.
Sipos, B., Szabó-Révész, P., Csóka, I., Pallagi, E., Dobó, D.G., Bélteky, P., Kónya, Z., Deák, Á., Janovák, L., Katona, G., 2020. Quality by Design Based Formulation Study of Meloxicam-Loaded Polymeric Micelles for Intranasal Administration. Pharmaceutics 12, 697.
Sonvico, F., Clementino, A., Buttini, F., Colombo, G., Pescina, S., Stanisçuaski Guterres, S., Raffin Pohlmann, A., Nicoli, S., 2018. Surface-Modified Nanocarriers for Nose-to-Brain Delivery: From Bioadhesion to Targeting. Pharmaceutics 10, 34.
Soppimath, K.S., Aminabhavi, T.M., Kulkarni, A.R., Rudzinski, W.E., 2001. Biodegradable polymeric nanoparticles as drug delivery devices. J. Control. Release 70, 1–20.
Sun, Y., Li, L., Xie, H., Wang, Y., Gao, S., Zhang, L., Bo, F., Yang, S., Feng, A., 2020. Primary Studies on Construction and Evaluation of Ion-Sensitive in situ Gel Loaded with Paeonol-Solid Lipid Nanoparticles for Intranasal Drug Delivery. Int. J. Nanomed. 15, 3137–3160.
Trotta, V., Pavan, B., Ferraro, L., Beggiato, S., Traini, D., Des Reis, L.G., Scalia, S., Dalpiaz, A., 2018. Brain targeting of resveratrol by nasal administration of chitosan-coated lipid microparticles. Eur. J. Pharm. Biopharm. 127, 250–259.
Uppoor, V.R.S., 2001. Regulatory perspectives on in vitro (dissolution)/in vivo (bioavailability) correlations. J. Controll. Release 72, 127–132.
Vaka, S.R.K., 2011. Nose to Brain Delivery of Therapeutic Agents.
Venkateswarlu, V., Manjunath, K., 2004. Preparation, characterization and in vitro release kinetics of clozapine solid lipid nanoparticles. J. Control. Release 95, 627–638.
Vieira, A.C., Chaves, L.L., Pinheiro, S., Pinto, S., Pinheiro, M., Lima, S.C., Ferreira, D., Sarmento, B., Reis, S., 2018. Mucoadhesive chitosan-coated solid lipid nanoparticles for better management of tuberculosis. Int. J. Pharm. 536, 478–485.
Wang, L., Zhao, X., Du, J., Liu, M., Feng, J., Hu, K., 2019. Improved brain delivery of pueraria flavones via intranasal administration of borneol-modified solid lipid nanoparticles. Nanomedicine (London) 14, 2105–2119.
Yasir, M., Sara, U.V.S., 2014. Solid lipid nanoparticles for nose to brain delivery of haloperidol: in vitro drug release and pharmacokinetics evaluation. Acta Pharm. Sin. B 4, 454–463.
Yasir, M., Sara, U.V.S., Chauhan, I., Gaur, P.K., Singh, A.P., Puri, D.A., 2018a. Solid lipid nanoparticles for nose to brain delivery of donepezil: formulation, optimization by Box-Behnken design, in vitro and in vivo evaluation. Artificial Cells. Nanomed. Biotechnol. 46, 1838–1851.
Yasir, M., Sara, U.V.S., Chauhan, I., Gaur, P.K., Singh, A.P., Puri, D., Ameeduzzafar, 2018b. Solid lipid nanoparticles for nose to brain delivery of donepezil: formulation, optimization by Box-Behnken design, in vitro and in vivo evaluation. Artificial Cells Nanomed. Biotechnol. 46, 1838–1851.
Yassin, A.E.B., Anwer, M.K., Mowafy, H.A., El-Bagory, I.M., Bayomi, M.A., Alsarra, I.A., 2010. Optimization of 5-flurouracil solid-lipid nanoparticles: a preliminary study to treat colon cancer. Int. J. Med. Sci. 7, 398–408.
Zambaux, M.F., Bonneaux, F., Gref, R., Maincent, P., Dellacherie, E., Alonso, M.J., Labrude, P., Vigneron, C., 1998. Influence of experimental parameters on the characteristics of poly(lactic acid) nanoparticles prepared by a double emulsion method. J. Control. Release 50, 31–40.
Zhou, Y., Raphael, R.M., 2007. Solution pH alters mechanical and electrical properties of phosphatidylcholine membranes: relation between interfacial electrostatics, intramembrane potential, and bending elasticity. Biophys. J . 92, 2451–2462.
Zhu, Y., Liu, C., Pang, Z., 2019. Dendrimer-based drug delivery systems for brain targeting. Biomolecules 9, 790.

ANNEX-III

International Journal of
Molecular Sciences

MDPI

Article

In Vitro Comparative Study of Solid Lipid and PLGA Nanoparticles Designed to Facilitate Nose-to-Brain Delivery of Insulin

Hussein Akel [1], Ildikó Csóka [1], Rita Ambrus [1], Alexandra Bocsik [2], Ilona Gróf [2], Mária Mészáros [2], Anikó Szecskó [2], Gábor Kozma [3], Szilvia Veszelka [2], Mária A. Deli [2], Zoltán Kónya [3] and Gábor Katona [1,*]

1 Faculty of Pharmacy, Institute of Pharmaceutical Technology and Regulatory Affairs, University of Szeged, Eötvös Str. 6, H-6720 Szeged, Hungary; hussein.akel@szte.hu (H.A.); csoka.ildiko@szte.hu (I.C.); ambrus.rita@szte.hu (R.A.)
2 Biological Research Centre, Institute of Biophysics, Temesvári Blvd. 62, H-6726 Szeged, Hungary; bocsik.alexandra@brc.hu (A.B.); grof.ilona@brc.hu (I.G.); meszaros.maria@brc.hu (M.M.); szecskoaniko@gmail.com (A.S.); veszelka.szilvia@brc.hu (S.V.); deli.maria@brc.hu (M.A.D.)
3 Department of Applied & Environmental Chemistry, Faculty of Science and Informatics, Rerrich Béla Sqr. 1, H-6720 Szeged, Hungary; kozmag@chem.u-szeged.hu (G.K.); konya@chem.u-szeged.hu (Z.K.)
* Correspondence: katona.gabor@szte.hu; Tel.: +36-62-545-575

Abstract: The brain insulin metabolism alteration has been addressed as a pathophysiological factor underlying Alzheimer's disease (AD). Insulin can be beneficial in AD, but its macro-polypeptide nature negatively influences the chances of reaching the brain. The intranasal (IN) administration of therapeutics in AD suggests improved brain-targeting. Solid lipid nanoparticles (SLNs) and poly(lactic-co-glycolic acid) nanoparticles (PLGA NPs) are promising carriers to deliver the IN-administered insulin to the brain due to the enhancement of the drug permeability, which can even be improved by chitosan-coating. In the present study, uncoated and chitosan-coated insulin-loaded SLNs and PLGA NPs were formulated and characterized. The obtained NPs showed desirable physicochemical properties supporting IN applicability. The in vitro investigations revealed increased mucoadhesion, nasal diffusion, and drug release rate of both insulin-loaded nanocarriers over native insulin with the superiority of chitosan-coated SLNs. Cell-line studies on human nasal epithelial and brain endothelial cells proved the safety IN applicability of nanoparticles. Insulin-loaded nanoparticles showed improved insulin permeability through the nasal mucosa, which was promoted by chitosan-coating. However, native insulin exceeded the blood-brain barrier (BBB) permeation compared with nanoparticulate formulations. Encapsulating insulin into chitosan-coated NPs can be beneficial for ensuring structural stability, enhancing nasal absorption, followed by sustained drug release.

Keywords: insulin; nose-to-brain delivery; solid lipid nanoparticles; PLGA nanoparticles; chitosan-coating; mucoadhesion; nasal mucosa permeability; blood-brain barrier permeability

Citation: Akel, H.; Csóka, I.; Ambrus, R.; Bocsik, A.; Gróf, I.; Mészáros, M.; Szecskó, A.; Kozma, G.; Veszelka, S.; Deli, M.A.; et al. In Vitro Comparative Study of Solid Lipid and PLGA Nanoparticles Designed to Facilitate Nose-to-Brain Delivery of Insulin. *Int. J. Mol. Sci.* **2021**, *22*, 13258. https://doi.org/10.3390/ijms222413258

Academic Editor: Manuel Vázquez-Carrera

Received: 4 November 2021
Accepted: 6 December 2021
Published: 9 December 2021

1. Introduction

Alzheimer's disease (AD) has been addressed as the significant cause of dementia nowadays [1–3], with a high worldwide prevalence and a considerable mortality rate [4]. To date, there is no remarkably effective treatment for AD, and most of the currently available therapies are concerned with delivering the anti-AD medication systemically following the traditional oral or intravenous routes of administration [5]. The importance of insulin in the normal brain function has been confirmed by evidence that insulin dysregulation plays a role in the pathophysiology of Alzheimer's disease (AD) [6–8]. Recent studies revealed the evidence that insulin plays a critical role in maintaining the mitochondrial homeostasis and cerebral bioenergetics in the brain. Moreover, it has a major influence on

the clearance of the amyloid β peptide and the phosphorylation of tau protein, which are key factors in the pathomechanism of AD [9]. Intranasal (IN) administration of insulin with the aim of central nervous system (CNS) delivery demonstrated positive effects on AD patients. Additionally, it can help in improving memory recall [10], ameliorating memory levels [11], and reducing the progression of hypometabolism in the brain [12]. Clinical studies have documented substantial, progressive disturbances in brain glucose utilization and responsiveness to insulin and insulin-like growth factor stimulation that co-occur with the progression of AD [13,14]. Disruption in the regulation of the central insulin levels induces pathological features of AD and can be caused by attenuated expression of insulin receptors and insulin-like growth factor, reduced brain insulin receptor sensitivity or increased serine phosphorylation of downstream insulin signaling molecules [6,15,16]. Impaired transport of insulin across the blood-brain barrier may also result in deficient levels of insulin in the CNS. Therefore, enhancing brain insulin may prevent AD-related pathological processes [17]. Additionally, as a result, the potential of the IN delivery of insulin presents significant therapeutic benefits [18].

With the presence of the blood-brain barrier (BBB), conventional administration routes are limited in the effective therapy as it forms a high permeability selective obstacle for the drug transport to the brain [19]. Therefore, nose-to-brain drug delivery is considered a revolutionary way of introducing an effective medication for several CNS related diseases, among them AD [20]. In addition, it is a patient-friendly, noninvasive route of administration. The protection of the drug from the enzymatic degradation and acidic environment contrary to oral administration indicates an additional advantage. The direct nose-to-brain transport depends on the fact that the brain and nose compartments are connected to each other via the olfactory and trigeminal route, and via the peripheral circulation [21,22]. However, recent studies revealed that insulin has been absorbed into the systemic circulation after IN administration, and may also reach the brain indirectly by crossing the BBB or blood-CSF barrier (BCSFB) through a saturable transcellular transport mechanism. Insulin receptors are present both at the BBB and the BCSFB, and have been proposed to mediate the transport of insulin from the blood to the CNS [23]. However, insulin may face some drawbacks that hinder its proper delivery to the site of action, due to its high molecular weight and fragile peptide structure. The high molecular weight negatively influences the permeation through the biological barriers. Furthermore, degradation of IN administered insulin might occur as a result of harsh conditions following nasal administration, due to the environmental pH and enzymatic activity [24]. To minimize these risks, the formulation of insulin in a suitable nano carrier system presents a smart tool.

Nanoparticles (NPs) are considered favorable for the purpose of facilitating the indirect transport of insulin to the brain, which is IN administered [25]. They offer the protection of the delicate peptide structure of insulin from degradation that may cause the nasal environment and enhance its permeability through the nasal mucosa [26,27]. In addition, two different types of carriers, solid lipid NPs (SLNs) and poly(lactic-co-glycolic acid) NPs (PLGA NPs) have been used for the aim of the nose-to-brain delivery of peptides. These NPs preserve the structural stability of insulin in the nasal cavity owing to their mucoadhesive properties. Their nano-scale size improves their absorption to the brain via either the olfactory or respiratory pathways. Furthermore, the insulin liberation at the site of action is supported by the prolonged drug release [28].

The surface modification of SLNs and PLGA NPs ensures better mucoadhesion and permeability properties towards the biological membranes and barriers [29]. Since the nasal mucosa is negatively charged, the application of a positively charged polymer as a coating material, e.g., chitosan ensures higher residence time of NPs on the nasal mucosa. Therefore, this facilitates drug absorption both to the olfactory neuron and systemic blood circulation [30–32].

The aim of the present study was the incorporation of insulin into four different nanocarriers, namely SLNs (Ins SLNs), PLGA NPs (Ins PLGA NPs), chitosan-coated SLNs (Ins C-SLNs), and chitosan-coated PLGA NPs (Ins C-PLGA NPs). Then, the in vitro

characterization of NPs and comparison to native insulin, according to the nose-to-brain applicability. After the physico-chemically and morphologically characterization of the prepared NPs, the in vitro behavior of NPs regarding mucoadhesion, drug release, and penetration across human nasal epithelial and human brain endothelial cells was investigated. This work provides the first reported evidence of the potential of encapsulating insulin into both polymeric and lipid NPs for IN delivery with a remarkable superiority of SLNs. Chitosan-coating was an efficient tool to further improve the NPs properties. Accordingly, a thorough comparison was performed in vitro, followed by selecting the optimized NPs in order to be a potential carrier for the IN application of insulin, a potential anti-AD drug, with the aim of brain-targeting.

2. Results

2.1. Characterization of the Prepared NPs

2.1.1. Average Hydrodynamic Diameter, Polydispersity Index, Zeta Potential

The characteristics of the NPs are presented in Table 1. The average hydrodynamic diameter (Z-average) of Ins PLGA NPs and Ins SLNs was 135 ± 1.17 nm and 99.1 ± 5.3 nm, respectively. On the other hand, Ins C-SLNs and Ins C-PLGA NPs demonstrated a slight increase in particle size (174.6 ± 10.7 nm and 145.2 ± 6.2 nm, respectively) due to the positioning of the chitosan units on the surface of the NPs. The size of all the prepared formulations adheres to the particle size requirement of the IN-applied NPs for brain targeting, which is preferred to be under 200 nm. This directly facilitates both the nose-to-brain transport via the olfactory nerve as well as receptor-mediated endocytosis [33,34]. The lower polydispersity index (PDI) values of NPs, which are lower than 0.3 point out monodisperse size distributions [35] that support the successful formulation of reproducible, stable, and efficient nanocarriers suitable for intranasal delivery [36]. The uncoated SLNs and PLGA NPs showed a negative zeta potential (ZP), which were −28.2 ± 1.8 and −42.3 ± 1.5, respectively. This can be explained by the negative charge of phosphatidylcholine at neutral pH [37] due to the presence of negatively charged oxygen atoms in phosphate and carboxyl groups. On the other hand, PLGA contains only the negatively charged carboxyl groups [28]. Moreover, the coating process using chitosan as a positively charged polymer resulted in a shifting of the NPs surface charge into positive values (+58.4 ± 0.7 and 61.3 ± 0.5 for Ins C-PLGA NPs and Ins C-SLNs, respectively), as a result of the electrostatic interactions that led to the proper adsorption of chitosan units onto the surface of the NPs. The remarkable conversion of the surface charge from negative to positive and Z-average increase indicates the successful coating of the NPs [38]. It is anticipated that chitosan-coated NPs would show better adhesion to the negatively charged nasal mucosa, which can in turn predict improved permeability through the nasal mucosa.

Table 1. The Z-average, PDI, and ZP of the prepared nanoformulations. Measurements were performed in triplicate (n = 3 independent formulations), data are represented as means ± SD.

Formulation	Z-Average (nm)	PDI	ZP (mV)
Ins PLGA NPs	135 ± 12.8	0.127 ± 0.02	−28.2 ± 1.8
Ins C-PLGA NPs	174.6 ± 10.7	0.179 ± 0.01	58.4 ± 0.7
Ins SLNs	99.1 ± 5.3	0.195 ± 0.03	−42.3 ± 1.5
Ins C-SLNs	145.2 ± 6.2	0.214 ± 0.007	61.3 ± 0.5

2.1.2. Encapsulation Efficacy and Drug Loading

As shown in Figure 1, the encapsulation efficacy (EE) and drug loading (DL) were not significantly higher ($p > 0.05$) in the case of Ins SLNs than Ins PLGA NPs. This could be explained by the ability of phosphatidylcholine particles to entrap insulin molecules into the Ins SLNs through the formation of hydrogen bonds employing the three available electron pairs in each unit, whilst in the case of Ins PLGA NPs, these electron pairs are used to attach the lactic-co-glycolic units with each other, as described in our previous

research work [28]. Another possible explanation could be the special affinity of insulin for the lipophilic surfaces, resulting in the adsorption of insulin to the hydrophobic surfaces that induce self-aggregation due to its insolubility in organic solvents [39]. Furthermore, coating the NPs with chitosan seems to be a beneficial tool in getting higher EE and DL due to the formation of an impermeable coating that offers protection against the leakage of insulin molecules from the prepared NPs [40–42].

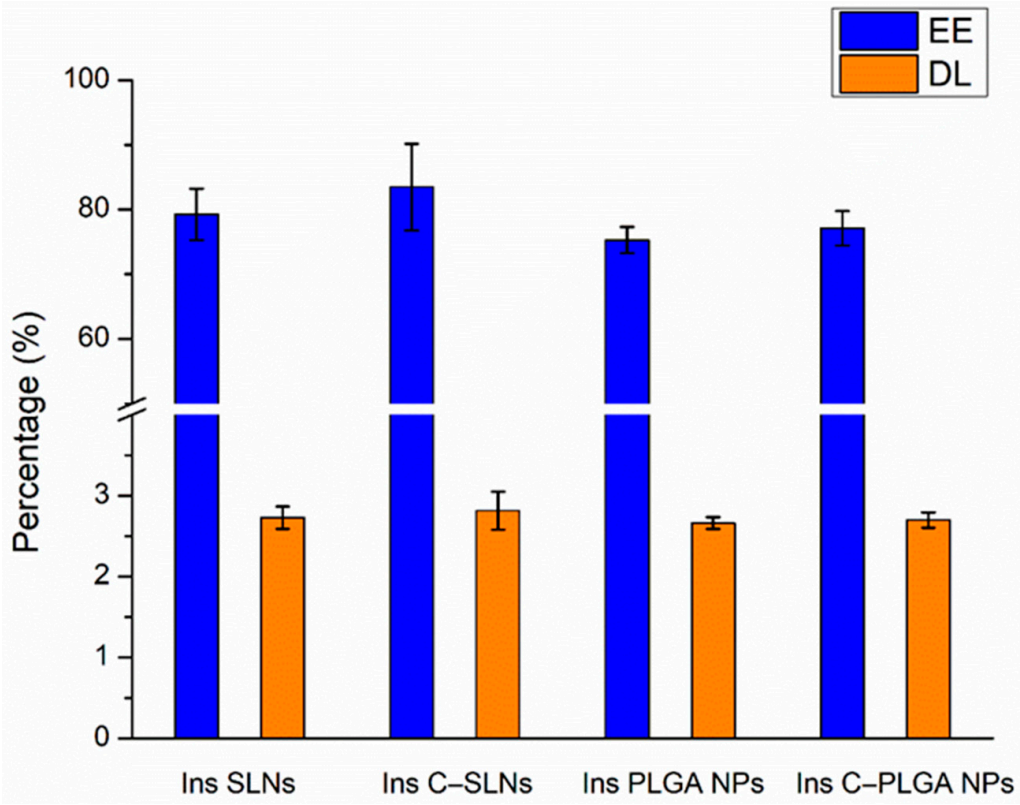

Figure 1. Encapsulation efficacy (EE) and drug loading (DL) of the prepared nanoparticles: Ins PLGA NPs, Ins C-PLGA NPs, Ins SLNs, and Ins C-SLNs. The ANOVA test was performed to check the significance of the differences between the results of the EE and DL. Measurements were performed in triplicate (n = 3 independent formulations), and data are represented as means ± SD.

2.1.3. Morphological Study

Scanning electron microscopy (SEM) images of the obtained NPs showed a spherical shape with a smooth surface, which provides better dissolution, mucoadhesion, and permeation than the needle- or disk-like shape NPs (Figure 2). Moreover, the spherical shape of the NPs will result in a minimal membrane bending energy, resulting in a higher stability and lower chance of entrapped drug leakage compared with the non-spherical counterparts that involve a strong membrane deformation, higher friction, and energy consumption [43].

2.1.4. Raman Spectroscopy

The structural changes of insulin after the preparation of NPs were investigated using Raman spectroscopy. The Raman spectra of insulin-containing NPs were compared with the native insulin's spectrum (Figure 3).

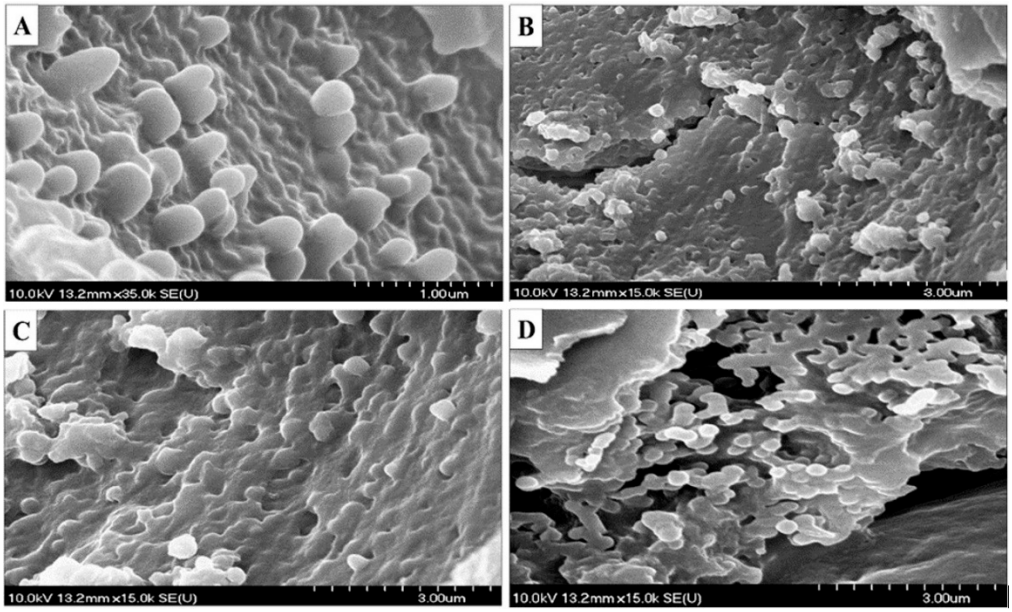

Figure 2. SEM images for the prepared nanoparticles. (**A**) Ins SLNs, (**B**) Ins C-SLNs, (**C**) Ins PLGA NPs, and (**D**) Ins C-PLGA NPs.

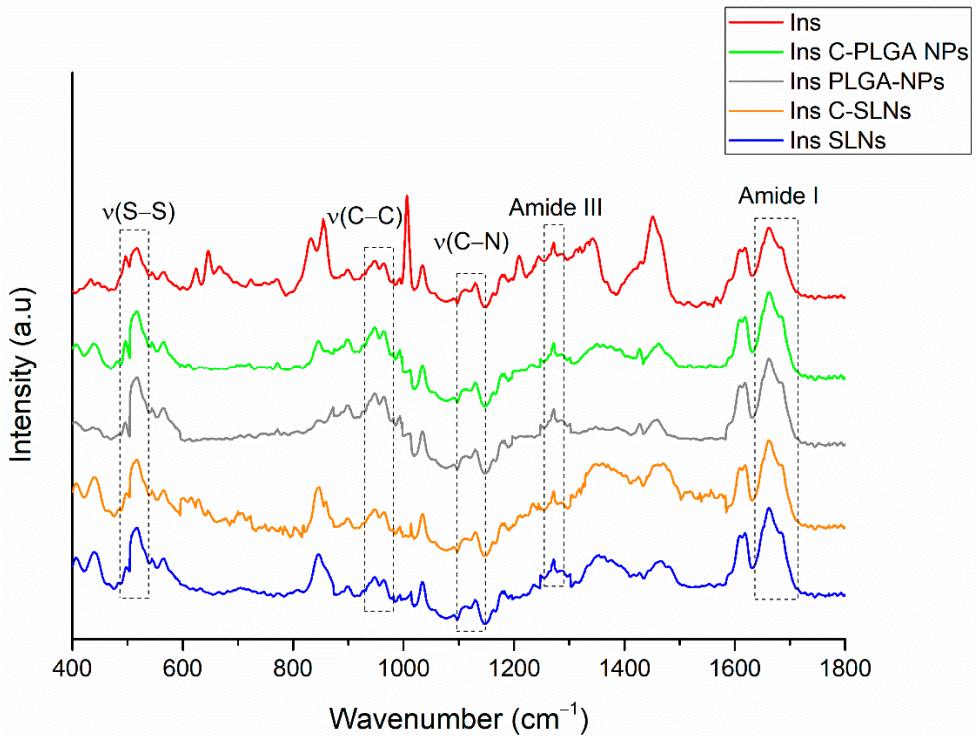

Figure 3. Raman spectra of insulin-containing NPs in comparison with native insulin, showing the major spectral regions that are characteristic for the protein structure.

From a stability point of view, one of the most relevant spectral features belongs to the tertiary structure of insulin ascribing disulfide bridges (S—S around 510 cm^{-1}) and (S—C around 665 cm^{-1}), whereas the internal polypeptide chain orientation in the wavenumber regions of the C—C and C—N stretching modes (890–990 cm^{-1} and 1110–1160 cm^{-1}, respectively) amide III bands (1200–1300 cm^{-1} and amide I band (1600–1700 cm^{-1}) provide information regarding the secondary structure [44]. Comparing these spectral markers of the protein structure of NPs to native insulin, no Raman shift was observed, which

indicates no change or unfolding in the protein structure. Therefore, the encapsulated insulin preserved its native nature.

2.1.5. Analysis of the Residual Solvent Amount by GC-MS

As cyclohexane belongs to the Class 2 solvents, whereas ethyl acetate to Class 3 solvents, their residual concentration is maximized according to the International Council of Harmonization (ICH) Q3C (R5) guideline for residual solvents. In this case, it should be less than 3880 and 5000 ppm in the daily dose of the final product, respectively. The residual cyclohexane and ethyl acetate content were determined in the different NP formulations after freeze-drying using the GC-MS. The concentration of both residuals was under 0.1 ppm, the limit of quantification (LOQ) of GC-MS method, which supports the successful elimination of the residual organic solvents during the freeze-drying process.

2.2. In Vitro Evaluation

2.2.1. Mucoadhesion Test

The mucoadhesive behavior of the prepared NPs was tested by assessing the reaction of the prepared NPs with the mucin, the main component of the nasal mucosa. As shown in Figure 4, the highest mucoadhesion was obtained when formulating the chitosan-coated NPs (Ins C-SLNs and Ins C-PLGA NPs), followed by Ins SLNs, while Ins PLGA NPs was ranked last. To illustrate, there are two explanations based on the performed test, as follows:

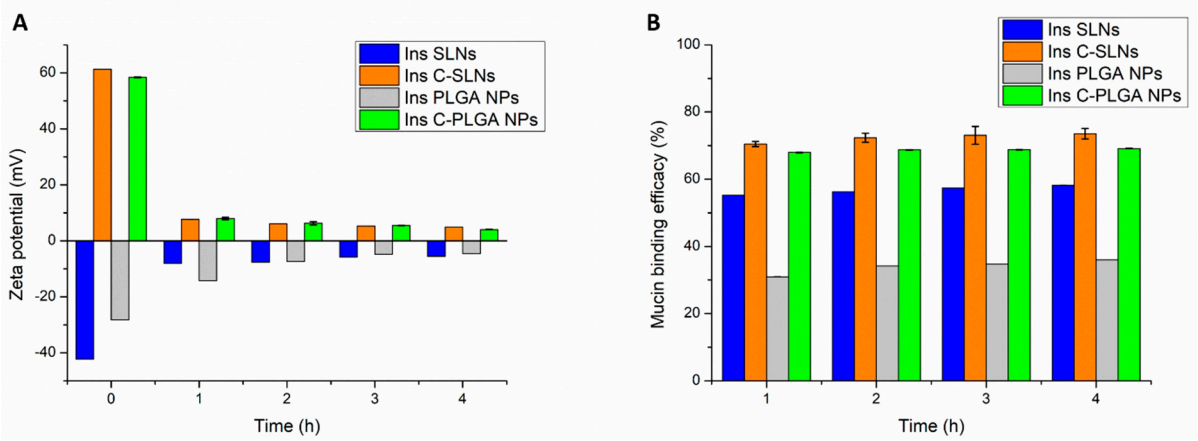

Figure 4. Mucoadhesion assay of Ins PLGA NPs, Ins SLNs, Ins C-PLGA NPs, and Ins C-SLNs. (**A**) The ZP analysis method; (**B**) the Turbidity analysis method. The measurements were performed in triplicate (n = 3 independent formulations), and data are represented as means ± SD.

In the zeta potential method (Figure 4A), both of the chitosan-coated NPs (Ins C-SLNs and Ins C-PLGA NPs) demonstrated a significant decrease in their ZP values after the embedding with the mucin ($p < 0.05$) due to the interaction between the positively charged Ins C-SLNs and Ins C-PLGA NPs and the negatively charged mucin, thus the formation of ionic bonds [45]. On the other hand, Ins SLNs and Ins PLGA NPs have negative surface charges, which result in a weaker interaction with mucin and a formation of intermolecular non-covalent interactions, such as hydrogen bonding, hydrophobic interactions, electrostatic interactions, and Van der Waals forces [46].

In the turbidimetric method, the mucoadhesion was assessed by measuring the mucin binding efficacy (MBE) to each type of the prepared NPs. The mucin binding efficacies of Ins SLNs and Ins PLGA NPs were 35.99% and 58.2%, respectively, and they were increased by the chitosan-coating to 69.14% and 73.45%, as shown in Figure 4B. Since the mucin possesses a negative charge along with its glycosylated structure, the positively charged Ins C-SLNs and Ins C-PLGA NPs will have a significantly higher interaction with the mucin than the negatively charged Ins SLNs and Ins PLGA NPs. The first leads to the

formulation of ionic bonds, while the latter occurs by the formulation of electrostatic interactions ($p < 0.05$). Since the Ins SLNs have a higher negative charge, their electrostatic interactions with the mucin will be significantly higher than the Ins PLGA NPs ($p < 0.05$). Similar results were obtained in previous studies [32,47].

The results of the zeta potential method are in accordance with the outcomes of the turbidimetric method, as the MBE value of each type of the NPs matches the total changes in the ZP values. Both of the methods proved the superior mucoadhesion of the Ins C-SLNs and Ins C-PLGA NPs, followed by the Ins SLNs, which excelled to the Ins PLGA NPs.

2.2.2. In Vitro Diffusion Studies

The nasal diffusion behavior of the native insulin, the insulin-loaded NPs (Ins SLNs and Ins PLGA NPs), and the chitosan-coated insulin-loaded NPs (Ins C-SLNs and Ins C-PLGA NPs) was tested in vitro in comparable conditions with the probable nose-to-brain delivery of insulin, following the IN application. The results are shown in Figure 5.

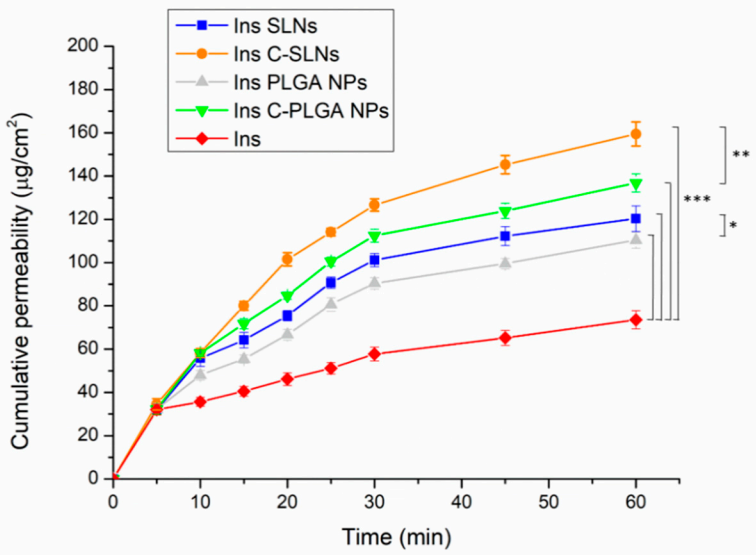

Figure 5. In vitro diffusion of native insulin and insulin-loaded NPs (Ins PLGA NPs, Ins SLNs, Ins C-PLGA NPs, and Ins C-SLNs). The ANOVA test was performed to check the significance of the differences between the diffusion of the native insulin and the prepared NPs, * $p < 0.05$; ** $p < 0.01$; *** $p < 0.001$. Measurements were carried out in triplicate ($n = 3$ independent formulations), and data are represented as means ± SD.

A significant increase in the diffusion of insulin through the used semi-permeable cellulose membrane was attained when formulating insulin into NPs ($p < 0.001$). This can be explained by the special characters that are offered by the prepared NPs, such as the nanoscale size and the augmentation of the specific surface area, which result in better nasal permeation properties [33]. Furthermore, the spherical and smooth surface of the NPs as revealed by the SEM images will ensure the minimum friction with the membrane surface [28,48].

Characteristically, the diffusion of both Ins SLNs and Ins C-SLNs was significantly higher than in the case of Ins PLGA-NPs ($p < 0.05$) and Ins C-PLGA NPs ($p < 0.01$). This could be the result of the higher lipophilicity of Ins SLNs [49] in comparison with Ins PLGA NPs [48]. Moreover, the chitosan-coating of the NPs led to a significantly better ($p < 0.001$) membrane diffusion and this might be a result of the permeation enhancer properties of chitosan [50].

The results of the diffusion test support the outcomes of the mucoadhesion test, which indicate better mucoadhesion properties for NPs with the nasal mucosa. This provides a longer residence time in the nasal cavity, decreasing the elimination by mucociliary clearance, and thus supporting a longer time for the absorption of NPs.

2.2.3. In Vitro Drug Release

The dissolution behavior of the prepared NPs was investigated under CSF and systemic circulation conditions to simulate the drug release after nasal absorption, where native insulin was used as a reference, and PBS (pH = 7.4) was employed as the dissolution medium. Figure 6 represents the results of the dissolution test.

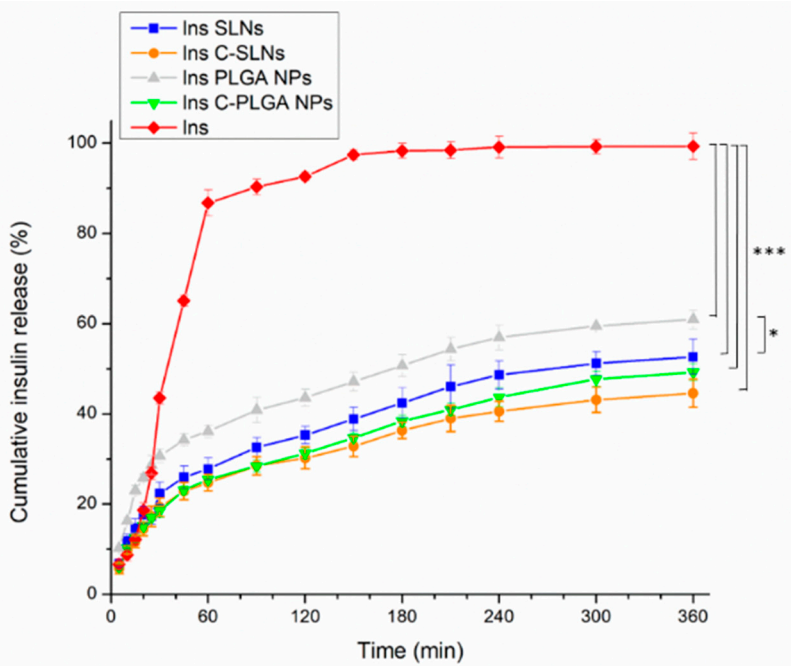

Figure 6. The dissolution behavior of the native insulin and the insulin loaded nanoparticles (Ins PLGA NPs, Ins SLNs, Ins C-PLGA NPs, and Ins C-SLNs). The ANOVA test was performed to check the significance of the differences between the diffusion of the native insulin and the prepared NPs, * $p < 0.05$; *** $p < 0.001$. Measurements were carried out in triplicate ($n = 3$ independent formulations), and data are represented as means ± SD.

The native insulin demonstrated the highest dissolution rate among the tested formulations in PBS, which can be related to the isoelectric point of bovine insulin. The applied insulin has an isoelectric point of 5.3–5.4. Therefore, the application of a medium with a pH value below 4 or above 7 will lead to an enhanced solubility [51]. Moreover, the encapsulation of insulin in Ins SLNs and Ins PLGA NPs was significantly accompanied ($p < 0.001$) by a 2- and 1.67-fold decrease in the dissolution rate of insulin, respectively. This can be explained by the controlled release properties of the lipid and polymeric NPs [52–54]. The Ins PLGA NPs showed a significantly higher ($p < 0.05$) drug release in comparison with the Ins SLNs, which can be explained by the higher lipophilicity, and thus the drug release retention of SLNs [39]. Furthermore, the chitosan-coating was a useful procedure to ensure the extra prolonged release (0.1-fold in the two types of the NPs), which is due to the water-insoluble properties of chitosan at the physiological pH [41,42]. Moreover, the significant difference between the different carriers in the drug release disappeared.

2.3. In Vitro Cell Culture Studies

2.3.1. Cell Viability Assay

The impedance measurement is a sensitive method for detecting the cellular effects in real-time. Additionally, neither RPMI 2650 epithelial cells nor D3 endothelial cells showed notable cell damage after the treatments with insulin and insulin-containing NPs (Figures 7 and 8).

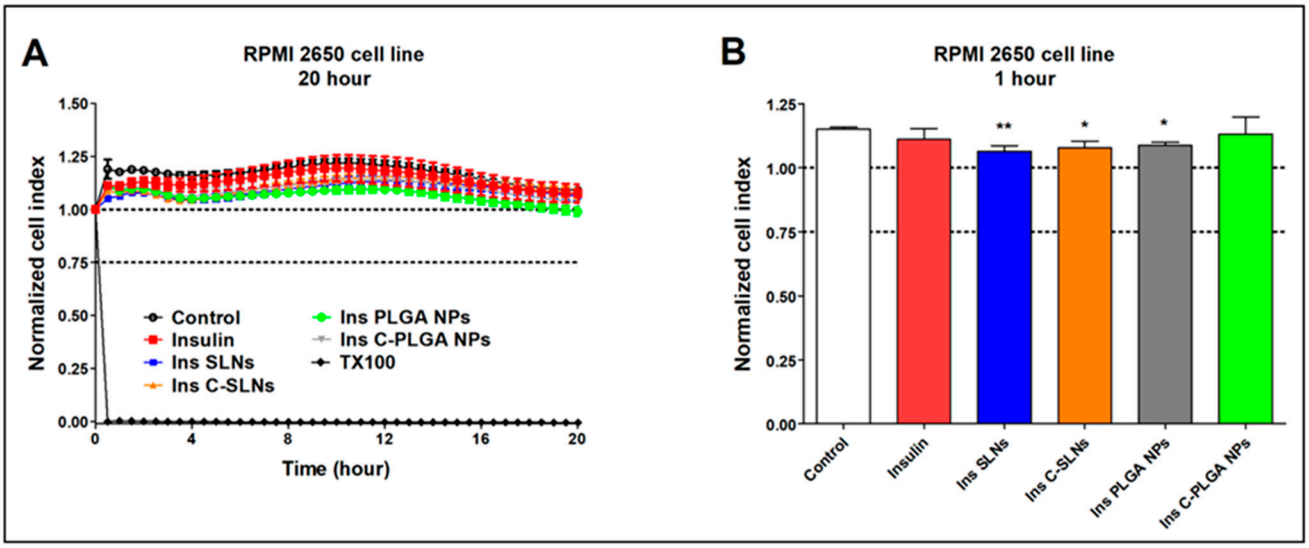

Figure 7. Cell viability of RPMI 2650 nasal epithelial cells after the treatment with insulin, insulin NPs, and HCl measured by impedance. The kinetic curve of cell viability during the 20-h treatment (**A**) and at the 1-h time point of the treatment (**B**). Values are presented as means ± SD, n = 6–12. Statistical analysis: ANOVA followed by Dunett's test. TX-100: Triton X-100. * $p < 0.05$, ** $p < 0.01$ compared with the control group.

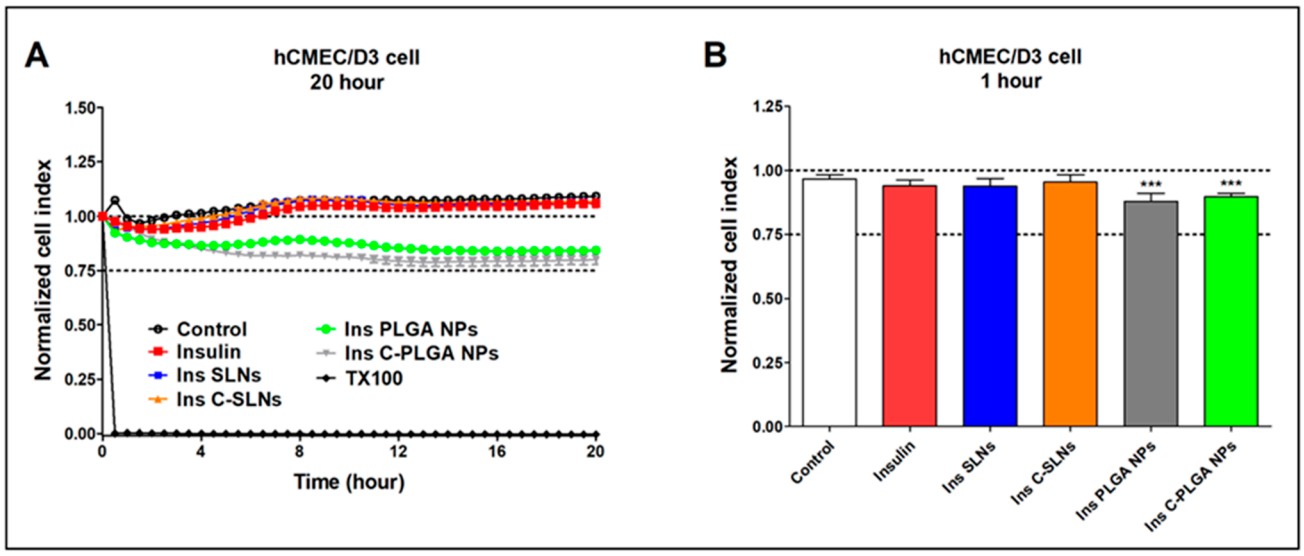

Figure 8. Cell viability of hCMEC/D3 endothelial cells after the treatment with insulin, Ins NPs, and HCl measured by impedance. The kinetic curve of cell viability during the 20-h treatment (**A**) and at the 1-h time point of the treatment (**B**). Values are presented as means ± SD, n = 6–12. Statistical analysis: ANOVA followed by Dunett's test. TX-100: Triton X-100. *** $p < 0.001$ compared with the control group.

For comparison, the reference compound Triton X-100 detergent (Merck LtD., Budapest, Hungary) caused cell death, as reflected by the decrease in impedance in both cell types (Figures 7A and 8A). Figures 7A and 8A show the kinetics of the cellular effects of treatment solutions, while the columns in Figures 7B and 8B show the effect of insulin and encapsulated NPs at the 1-h time point.

The kinetic curves of the NPs ran similarly to the untreated control group during the treatment in both the epithelial and endothelial models (Figures 7A and 8A). In the case of the hCMEC/D3 cells, a slight decrease in cell index values could be observed in two NPs groups (Ins PLGA-NPs and Ins C-PLGA-NPs). However, the cell index values remained above 0.75, which refer to a non-toxic range. The significant differences observed at both cell types (Figures 7B and 8B) at the 1-h time point are due to the extremely low

standard deviation and not the toxic effect of treatments. The non-toxic effects of the NPs were verified by a permeability assay after the insulin transport study: The permeability for paracellular marker molecules was unchanged or even lower, which indicates a tight barrier integrity of the model (Supplementary Figure S1).

2.3.2. Insulin Permeability across the Culture Models of the Nasal Mucosa and Blood-Brain Barrier

The permeability of insulin was tested on the nasal epithelial and brain endothelial cell barrier models (Figures 9 and 10). The insulin NPs showed a similar trend in both models.

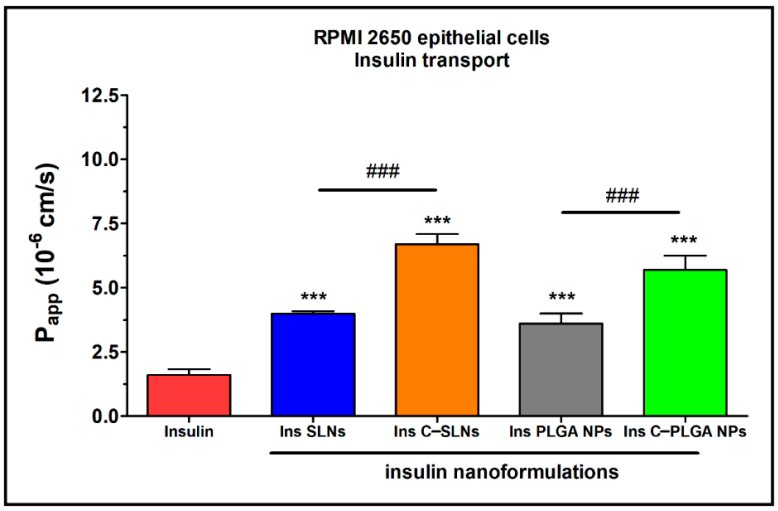

Figure 9. Apparent permeability coefficients (P_{app}) for insulin (0.07 mg/mL in all samples) when applied alone or in different formulations measured across RPMI 2650 epithelial cell layers after 1 h of incubation. Values are presented as means ± SD, $n = 4$. Statistical analysis: ANOVA followed by Bonferroni test. *** $p < 0.001$ compared with the insulin group, ### $p < 0.01$ compared between the indicated groups.

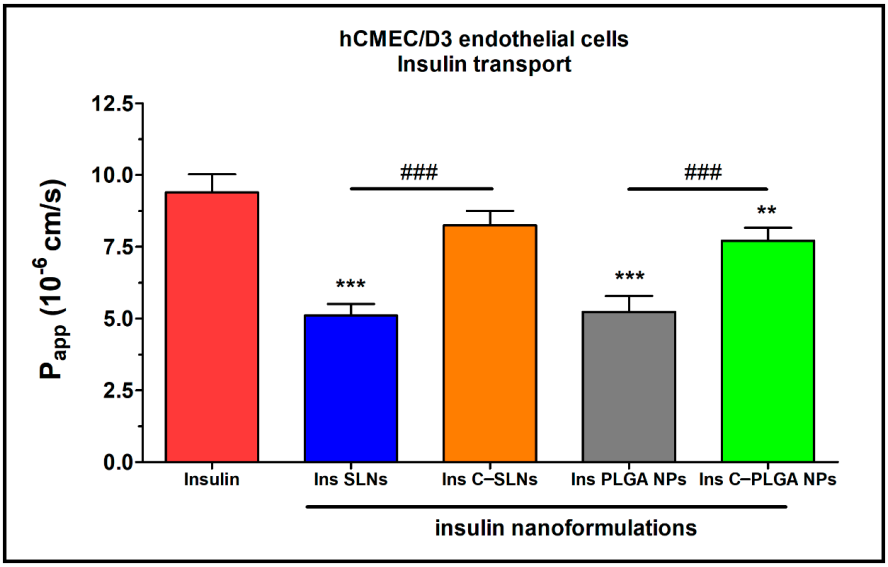

Figure 10. Apparent permeability coefficients (P_{app}) for insulin (0.07 mg/mL in all samples) when applied alone or in different formulations measured across hCMEC/D3 endothelial cell layers after 1 h of incubation. Values are presented as means ± SD, $n = 4$. Statistical analysis: ANOVA followed by the Bonferroni test. ** $p < 0.01$, *** $p < 0.001$ compared with the insulin group. ### $p < 0.01$ compared between the indicated groups. C-: Chitosan coated nanoparticle; NPs: Nanoparticles; PLGA: Poly (lactic-co-glycolic acid; SLN: Solid lipid nanoparticle.

The results of the ex vivo nasal permeability test confirmed the previously performed in vitro tests that the transport of insulin was lower in the case of SLNs, and the PLGA-NP (P_{app}: $\leq 5 \times 10^{-6}$ cm/s) compared with the chitosan-coated NPs (Ins C-SLNs and Ins C-PLGA NPs; Figures 3 and 4). The permeability coefficients of the chitosan-coated NPs were $\geq 6 \times 10^{-6}$ cm/s on both models (Figures 9 and 10). The reason for this effect is due to the unique biological properties of chitosan. Chitosan is a linear cationic polysaccharide, is which is among others non-toxic, biodegradable, and has antibacterial and antimicrobial activity. Furthermore, it can enhance the paracellular permeability of biological barriers by modulating tight junction proteins [55].

In the case of the nasal epithelial barrier model, the NPs showed a significantly higher permeability (1- to 4-fold) than insulin alone. Therefore, the NPs increased the flux of insulin through the nasal barrier (Figure 9).

The brain endothelial barrier model showed high permeability for free insulin compared with the NPs (Figure 10). The difference in the insulin permeability between the two types of barrier models was almost one order of magnitude. The permeability coefficient was 1.6×10^{-6} for insulin in the case of the nasal barrier model and 9.4×10^{-6} for the blood-brain barrier model. The reason for this difference could be the physiological function of these barriers. Insulin, as a hormone, has an important role in blood glucose level regulations in the brain. Therefore, the brain endothelial cells contain the highest level of insulin receptors in the human body [56]. The high insulin receptor expression in hCMEC/D3 cells was verified in a quantitative proteomic study [57].

There were no significant differences between the recovery values of the different investigated insulin groups (Table 2). In general, permeability assays are considered reliable if the recovery of the molecule after the permeability assay is ~70%. Furthermore, the tight barrier integrity of brain endothelial cell layers was confirmed by the low P_{app} values of BBB marker molecules (Supplementary Figure S2).

Table 2. Recovery (mass balance) calculation after insulin permeability on the nasal epithelial and on the brain endothelial barrier model.

Formulation	Recovery (%) Means ± SD	
	RPMI 2650	hCMEC/D3
Insulin	77.9 ± 3.9	87.9 ± 2.9
Ins SLNs	71.8 ± 2.9	72.5 ± 2.05
Ins C-SLNs	95.6 ± 22.8	73.5 ± 3.2
Ins PLGA NPs	61.3 ± 4.4	62.01 ± 3.9
Ins C-PLGA NPs	66.4 ± 3.9	72.8 ± 3.1

3. Discussion

A relation between tauopathies and insulin resistance has been revealed. Therefore, insulin supplied IN, in subjects presenting with amnestic mild cognitive disorder or AD, showed cognitive benefits [58,59]. Insulin has a multifactorial role in the brain and takes part in the clearance of the amyloid β peptide and phosphorylation of tau through proteostasis. In addition, it can be employed in ameliorating AD by restoring the cerebral insulin function. This observation opened the way to a new clinical trial: The Study of Nasal Insulin in the Fight Against Forgetfulness (SNIFF, NCT01767909) [60]. This trial studies the effects of IN insulin on cognition and brain atrophy. It is not actually certain how insulin, administered in this way, affects the tau protein [61].

The hypothesis of "nose-to-brain" transport of bioactive proteins and protein-loaded NPs is well supported by previous animal studies. The intranasally administered insulin-like growth factor-I, a 7.65 kDa protein, can bypass the BBB via olfactory- and trigeminal-associated extracellular pathways to rapidly elicit biological effects at multiple sites within the brain and spinal cord [62]. Chitosan nanoparticles enhanced the nasal absorption of insulin to a greater extent than an aqueous solution of chitosan [63]. Insulin is able to enter the brain tissue through the BBB by receptor-mediated transcytosis. However, its fragile

structure and the complex pathway following the conventional administration routes result in a low brain bioavailability. The IN administration of insulin might overcome these drawbacks, especially when formulating it in a nanoparticulate system. However, only a few studies reported the nasal delivery of insulin-loaded nanoparticles. It has been revealed that chitosan is able to dramatically enhance the nasal absorption of polar molecules, including peptides and proteins that otherwise are only poorly absorbed via the IN route [64]. Therefore, the effect of chitosan-coating on nanoparticle characteristics, mucoadhesion, drug release, cytotoxicity, and permeability was investigated in comparison with the uncoated nanoparticles. PLGA nanoparticles (NPs) have been reported to improve drug penetration across the BBB both in vitro and in vivo. PLGA NPs can cross the BBB passively or through active endocytosis mechanisms. Unmodified PLGA NPs cross the BBB primarily through passive internalization based on size, which was found to result in a low brain uptake. Several strategies have been developed to improve the penetration of NPs into the brain. These strategies modify NPs with components that are designed to take advantage of BBB endocytosis pathways [65]. PLGA NP surfaces can be modified with positive charges, e.g., with chitosan, that electrostatically interact with negatively charged regions of the luminal surfaces, which help PLGA in crossing the BBB by adsorption-mediated transcytosis [66].

Four types of NPs were formulated successfully (Ins SLNs, Ins C-SLNs, Ins PLGA NPs, and C-PLGA-NPs) with optimal nanoparticulate characteristics for the brain delivery of IN insulin. Insulin was loaded into the nanoparticles before the chitosan-coating process to ensure a sufficiently low Z-average, as previously reported by Dyer et al. [67]. Based on the literature data, a good correlation between the structural stability and biological activity of insulin encapsulated in SLNs has been described. SLNs preserved the biological activity of encapsulated insulin both during the preparation and intracellular transport [68]. Furthermore, SLNs prepared by the solvent-in-water diffusion-emulsion technique were tested in animal studies and no reduction in the biological activity of the encapsulated insulin was found [69].

The in vitro studies revealed that Ins SLNs showed a lower Z-average, higher EE, and DL, as well as a lower dissolution rate compared with Ins PLGA NPs. Chitosan-coated formulations (Ins C-SLNs and Ins C-PLGA NPs) showed a promoted sustained-release behavior and improved mucoadhesion properties over the native insulin and the uncoated NPs. The permeation of the Ins SLNs and Ins PLGA NPs was increased compared with native insulin and was further improved by chitosan-coating. The in vitro cell line studies proved the safety of prepared NPs for the IN application. Furthermore, the permeation of insulin through the nasal mucosa was the highest in the case of Ins C-SLNs outperforming the Ins C-PLGA NPs and uncoated NPs, and the lowest in the case of native insulin. On the other hand, the permeability study showed the superiority of the native insulin in the brain endothelial barrier model over the prepared NPs, from which the Ins C-SLNs excelled the Ins C-PLGA NPs followed by Ins SLNs, then Ins PLGA-NPs. Therefore, an optimal nose-to-brain formulation can be obtained using a mixture of native insulin and Ins C-SLNs. The former ensures the rapid effect, and the latter supports sustained drug release. Similarly, the results were achieved by Lu et al. in the case of insulin-loaded PLGA NPs, which can be further improved by the application of cell-penetrating peptides [70].

These findings shed light on the potential of the encapsulated insulin in both Ins SLNs and Ins PLGA NPs for the IN application, with the superiority of SLN and the positive enhancing effect of chitosan-coating.

4. Materials and Methods

4.1. Materials

Insulin from the bovine pancreas, phosphatidylcholine, PLGA (poly(lactic-co-glycolic acid)) 75/25, and poloxamer 188 were purchased from Sigma-Aldrich (Steinheim, Germany). Trehalose dihydrate, chitosan, and all of the organic solvents (cyclohexane and ethyl acetate,

both analytical grade) and reagents were purchased from Merck (Darmstadt, Germany), unless otherwise indicated.

4.2. Preparation of Insulin NPs

4.2.1. Preparation of SLNs

Insulin SLNs were obtained following a previously reported double-emulsion solvent-evaporation technique with some modifications [71]. The double emulsion (W1/O/W2) was prepared according to the following steps. First, the primary W1/O emulsion was prepared by adding 0.35 mL of insulin solution in 0.1 M aqueous HCl solution (2 mg/mL) dropwise to a phosphatidylcholine solution in cyclohexane (9 mg/mL), using an ultrasonic homogenizer (Hielscher, Germany) (0.5 cycles with 75% amplitude) for 1 min. Then, the resultant emulsion was added dropwise into 1.6 mL of 2% w/v poloxamer 188 aqueous solution (W2), using the homogenizing mixer (0.5 cycles with 75% amplitude) for another 1 min. The final mixture was left overnight in a laminar flow hood under stirring using a magnetic stirrer at 500 rpm, in order to allow for the evaporation of the organic solvent, thus forming the SLNs. Finally, freeze-drying was applied in the presence of 5% w/v trehalose as a cryoprotectant to obtain a lyophilized powder. For that purpose, a Scanvac CoolSafe laboratory freeze-dryer (Labogene, Lynge, Denmark) was operated at -40 °C for 12 h under a 0.013 mbar pressure, with an additional 3 h of secondary drying at 25 °C. The lyophilized powder was stored at 5 ± 3 °C until further investigation.

4.2.2. Preparation of PLGA NPs

PLGA NPs were prepared following a modified double-emulsion solvent evaporation method [72]. The previously described insulin-containing primary W1/O emulsion was added dropwise into the PLGA solution in ethyl acetate (12 mg/mL) in the presence of the ultrasonic homogenization (0.5 cycles, with 75% amplitude) for 1 min. Then, the resultant emulsion was added dropwise into the W2 phase (poloxamer 188, 2% w/v) with the presence of the ultrasonic homogenization (0.5 cycles, with 75% amplitude) for another 1 min. Finally, the resultant W1/O/W2 emulsion was left overnight in a laminar flow hood under constant stirring at 500 rpm to allow for the evaporation of the organic solvent, thus allowing the PLGA NPs to freeze dry, as previously described.

4.2.3. Preparation of Chitosan-Coated NPs

The coating of both NPs with chitosan was performed by incubating the resultant SLNs and PLGA NPs colloidal solutions with an equal volume of 0.1% w/v chitosan solution, which is dissolved in 1% v/v acetic acid under constant stirring at 500 rpm for 1 h. After the coating reaction, the mixture was purified through 3-cycle centrifugation using an Hermle Z323K high-performance refrigerated centrifuge (Hermle AG, Gosheim, Germany) for 30 min at 16,000 rpm, in order to separate the NPs pellet and supernatant that contain the residual chitosan solution, which did not take place in the coating process. The zeta potential (ZP) of the NPs was measured using a Malvern Nano ZS instrument (Malvern Instruments, Worcestershire, UK) before and after the coating process, in order to prove the successful coating with the positively charged chitosan.

4.3. Characterization of the NPs

4.3.1. Dynamic Light Scattering and Zeta Potential

The characterization of the NPs started by analyzing the average hydrodynamic diameter (Z-average), polydispersity index (PDI), and the ZP. These parameters were analyzed after redispersing the freeze-dried samples in purified water, then placing the suspensions in folded capillary cells using a Malvern Nano ZS instrument (Malvern Instruments, Worcestershire, UK). The temperature and refractive index of the apparatus were set at 25 °C and 1.755, respectively, and the total number of scans was 17. For the analysis, aliquots of the NPs colloidal solution were sampled before and after the incubation with the chitosan. Then, they were dispersed in ultrapure water (1:200 v/v) and placed in

a cuvette to check the size, PDI, and ZP changes. The measurements were performed in triplicate, and the data were reported as means ± SD.

4.3.2. Encapsulation Efficacy and Drug Loading

Calculating the encapsulation efficacy (EE) and drug loading (DL) of NPs was determined directly by dissolving 50 mg of freeze-dried particles in 10 mL of 1 M hydrochloric acid. After the complete dissolution of the particles, the insulin was separated from the lipid and polymeric components by ultrafiltration using a cellulose dialysis membrane with a 10 kDa cut-off (Spectra/Por® Dialysis Membrane, Spectrum Laboratories Inc., Rancho Dominguez, CA, USA). The insulin concentration in the filtrate was measured using HPLC. The EE and DL were calculated by applying the two following equations [73]:

$$\text{EE } (\%) = \frac{\text{The amount of encapsulated insulin in the freeze} - \text{dried nanoparticles}}{\text{The total amount of insulin used in the preparation}} \times 100 \quad (1)$$

$$\text{DL } (\%) = \frac{\text{The amount of encapsulated insulin in the freeze} - \text{dried nanoparticles}}{\text{The weight of the freeze} - \text{dried nanoparticles}} \times 100 \quad (2)$$

4.3.3. HPLC Method

The insulin quantification was carried out using HPLC (Agilent 1260, agent technologies, Santa Clara, CA, USA). As the stationary phase, a Gemini-NX® C18 150 mm × 4.6 mm, 5 µm (Phenomenex, Torrance, CA, USA) column was applied. As mobile phase purified water and acetonitrile were used in a ratio of 68:32 adjusted to pH = 2.8 with phosphoric acid. Then, for the separation, 20 µL of the samples were injected using a 15-min isocratic elution with 1 mL/min eluent flow at 30 °C temperature. An UV-Vis diode array detector was applied for the detection of chromatograms at 280 nm. The ChemStation B.04.03 Software (Santa Clara, CA, USA) was used for the evaluation of data. The linear regression of the calibration curve was 0.997. The limit of quantification (LOQ) and detection (LOD) values of insulin were 87 and 26 ppm, respectively.

4.3.4. Scanning Electron Microscope (SEM)

SEM was employed to investigate the surface morphology of the NPs (Hitachi S4700, Hitachi Scientific Ltd., Tokyo, Japan) at 10 kV and 10 mA. Approximately 10 nm of coating the samples with gold-palladium was carried out under an argon atmosphere with an air pressure of 1.3–13 mPa (Bio-Rad SC 502, VG Microtech, Uckfield, UK).

4.3.5. Raman Spectroscopy

The structural stability of insulin after the preparation was investigated using an XRD Dispersive Raman spectroscopy (Thermo Fisher Scientific Inc., Waltham, MA, USA). The instrument was equipped with a 780 nm wavelength diode laser and a CCD camera. A laser power of 12 mW at 50 µm slit aperture size was set. Raman spectra were collected with 2 s of exposure and 6 s of acquisition time, for a total of 32 scans per spectrum in the spectral range of 3500–200 cm^{-1} with fluorescence and cosmic ray corrections. The Raman spectra of NPs were compared with the native insulin to examine the structural changes.

4.3.6. Analysis of the Residual Solvent Amount by Gas Chromatography

Gas chromatography (GC) measurements have been carried out to exclude the presence of residual solvents (cyclohexane and ethyl acetate) in the freeze-dried NPs by a Shimadzu GCMS-QP2010 SE instrument (Shimadzu Corporation, Kyoto, Japan) using a 30 m long 0.25 mm diameter ZBWax-Plus column with the carrier gas. The freeze-dried NPs were dissolved in 5.0 mL of toluol, then filtered with a 0.45 µm membrane filter into a headspace vial. The temperature for the injector port was set at 200 °C and a 1 µL sample was injected into the GC/MS system. The oven temperature was programmed from 80 °C (held for 5 min) to 160 °C at 10 °C/min. For the identification of the residual solvents present in the samples, the mass spectrometer was operated to monitor only the

40–100 m/z ratios from 1–1.7 min after injection, which is specific for the investigated organic solvents.

4.3.7. Mucoadhesion Study

The mucoadhesive behavior of the prepared NPs and pure insulin was determined using two complimented methods: The direct turbidimetric method and the indirect ZP change-based method. The direct method was carried out by mixing equal volumes of the nanoparticulate colloidal solution in a simulated nasal electrolyte solution (SNES) (8.77 g/L sodium chloride (NaCl), 2.98 g/L potassium chloride (KCl), 0.59 g/L anhydrous calcium chloride (CaCl2) dissolved in purified water, pH 5.6) with porcine stomach mucin (Type III) solution 0.05% w/v. Then, the mixture was incubated at 37 °C, and continuously stirred for 4 h with a 1-h sampling interval. Thereafter, the samples were centrifuged at 17,000 rpm and 4 °C. The concentration of the free mucin in the supernatant was measured at 255 nm using a Jasco V-730 UV spectrophotometer (ABL&E JASCO Ltd., Budapest, Hungary). Then, following that step, the mucin binding efficacy (MBE) was calculated based on the following equation [74]:

$$\text{Mucin binding efficacy } (\%) = \frac{\text{Total mucin} - \text{Free mucin}}{\text{Total mucin}} \times 100 \quad (3)$$

The indirect method was also employed to further evaluate the mucoadhesive properties. In this method, the ZP values were measured using a Malvern Nano ZS instrument (Malvern Instruments, Worcestershire, UK). This method assessed the ZP variations during the interaction between the negatively charged mucin and the various nanocarriers [75].

4.3.8. In Vitro Diffusion Studies

The in vitro diffusion test was carried out employing a modified side-by-side® type apparatus (Grown Glass, New York, NY, USA), which was designed in a similar way to the nasal cavity conditions. This method has been evaluated, validated, and previously reported by Gieszinger et al. [76,77]. The experiments were performed under thermostated conditions at 35 °C (Thermo Haake C10-P5, Sigma-Aldrich Co. LLC, St. Louis, MO, USA) with constant stirring at 100 rpm. The donor and receptor compartments were isolated with an isopropyl myristate impregnated artificial cellulose membrane (0.45 μm pore size, Pall Metri-cel cellulose membrane) with a 0.69 cm^2 diffusion surface. The donor compartment consisted of 9 mL pH 5.6 SNES, whereas the acceptor compartment consisted of PBS (corresponding to the systemic circulation of pH 7.4). The freeze-dried NPs, containing equivalently 0.5 mg of insulin and 0.5 mg of initial insulin, were placed into the donor phase. In addition, the aliquots (0.5 mL) were withdrawn from the acceptor phase at predetermined time intervals up to 60 min and replaced with the same volume of fresh medium. The amount of the drug diffused through the membrane was quantified using HPLC. Each formulation was analyzed in triplicate. The results were reported as means ± SD.

4.3.9. In Vitro Drug Release of NPs

In order to investigate the drug release profile of insulin-containing NPs in comparison with the initial insulin at nasal conditions, the modified paddle method (Hanson SR8 Plus, Teledyne Hanson Research, Chatsworth, CA, USA) was used. The freeze-dried NPs, containing equivalently 0.5 mg of insulin and 0.5 mg of initial insulin, were placed into dialysis bags with a 12–14 kDa cut-off (Spectra/Por® Dialysis Membrane, Spectrum Laboratories Inc., Rancho Dominguez, CA, USA). Then, the dialysis bags were immersed in dissolution vessels containing 100 mL volumes of 0.08 M potassium dihydrogen phosphate buffer adjusted to pH 7.4 with 0.1 M sodium hydroxide (corresponding to the systemic circulation and CSF pH) and stirred at 50 rpm at 37 °C [78]. The aliquots (2 mL) were withdrawn from the release medium at predetermined time intervals up to 6 h and then replaced with an equivalent volume of the fresh release medium to maintain a sink condition [79,80].

The insulin concentration in the samples was determined with HPLC. The results were reported as means ± SD.

4.4. In Vitro Cell Line Studies

4.4.1. Human RPMI 2650 Nasal Epithelial Cell Culture

Human RPMI 2650 nasal epithelial cells were purchased from ATCC (cat. no. CCL 30) and used until passage 50 for the experiments. For the cell culturing, Dulbecco's Modified Eagle's Medium (DMEM; Gibco, Life Technologies, Carlsbad, CA, USA) supplemented with 10% fetal bovine serum (FBS; Pan-Biotech GmbH, Aidenbach, Germany) and 50 µg/mL gentamicin were used. In addition, the cells were kept in a humidified 37 °C incubator with 5% CO_2. All of the plastic surfaces were coated with 0.05% collagen in sterile distilled water before cell seeding in culture dishes, and the medium was changed every 2 days. The cells were trypsinized with 0.05% trypsin 0.02% EDTA solution when they reached about 80–90% confluency in the dishes. To induce tighter epithelial barrier properties, retinoic acid (10 µM) and hydrocortisone (500 nM) were added to the cells 1 day before the experiment [81].

For the permeability measurements, RPMI 2650 epithelial cells were co-cultured with human vascular endothelial cells [82] to create a more physiological barrier [83]. The endothelial cells (≤P8) were grown in an endothelial culture medium (ECM-NG, Sciencell, Carlsbad, CA, USA) supplemented with 5% FBS, 1% endothelial growth supplement (ECGS, Sciencell, Carlsbad, CA, USA), and 0.5% gentamicin on 0.2% gelatin-coated culture dishes.

4.4.2. Human hCMEC/D3 Brain Endothelial Cell Line

Cultures of hCMEC/D3 cells (≤P35) were grown in MCDB 131 medium (Pan-Biotech, Aidenbach, Germany) supplemented with 5% FBS, GlutaMAX (100×, Life Technologies, Carlsbad, CA, USA), lipid supplement (100×, Life Technologies, Carlsbad, CA, USA), 10 µg/mL ascorbic acid, 550 nM hydrocortisone, 100 µg/mL heparin, 1 ng/mL basic fibroblast growth factor (bFGF, Roche, San Francisco, CA, USA), 2.5 µg/mL insulin, 2.5 µg/mL transferrin, 2.5 ng/mL sodium selenite (ITS), and 50 µg/mL gentamicin [84]. All of the plastic surfaces were coated with 0.05% collagen in sterile distilled water before cell seeding and the medium was changed every 2 days. Before each experiment, the medium of hCMEC/D3 cells was supplemented with 10 mM LiCl for 24 h to improve the barrier properties [85].

4.4.3. Preparation of Insulin and Insulin-Loaded Nanoparticle Dilutions for Cellular Assays

The concentration of insulin was 0.7 mg/mL (20 IU) in the different NPs after diluting the samples in 1.5 mL culture medium or Ringer HEPES (5 mM Hepes, 136 mM NaCl, 0.9 mM $CaCl_2$, 0.5 mM $MgCl_2$, 2.7 mM KCl, 1.5 mM KH_2PO_4, 10 mM NaH_2PO_4, pH 7.4) depending on the experiments. To prepare the insulin stock solution, the powder was first dissolved in 1 M HCl and then in medium or Ringer HEPES to reach a solution of 0.7 mg/mL and the pH was adjusted to 7.4. For cell viability measurements, the different NPs and the insulin working solutions were prepared as 10× (0.07 mg/mL), 30× (0.02 mg/mL), and 100× (0.007 mg/mL) diluted in cell culture medium. The 10, 30, and 100× dilution of HCl and free insulin were prepared in the medium as control treatments. For permeability measurements, the NPs and insulin were applied as 10 times dilution at 0.07 mg/mL concentration diluted in a Ringer-HEPES buffer.

4.4.4. Cell Viability Measurement

The kinetics of the epithelial and endothelial cell reaction to the different treatments were monitored by impedance measurement at 10 kHz (RTCA-SP instrument, Agilent, Santa Clara, CA, USA). The impedance measurement is label-free, non-invasive, and correlates linearly with the adherence, growth, number, and viability of cells in real-time [86,87]. For background measurements, the 50 µL cell culture medium was added to

the wells. Then, the cells were seeded at a density of 2×10^4 RPMI 2650 cells/well and 6×10^3 hCMEC/D3 cells/well in 96-well plates coated with integrated gold electrodes (E-plate 96, Agilent, Santa Clara, CA, USA). The cells were cultured for 5–7 days in a CO_2 incubator at 37 °C and monitored every 10 min until the end of experiments. In addition, the cells were treated at the beginning of the plateau phase of growth. The insulin, insulin NPs, and HCl solution were diluted in a cell culture medium and the effects were followed for 20 h. Triton X-100 detergent (1 mg/mL) was used as a reference compound to induce cell toxicity. The cell index was defined as Rn-Rb at each time point of measurement, where Rn is the cell-electrode impedance of the well when it contains cells and Rb is the background impedance of the well with the medium alone.

4.4.5. Permeability Studies

Transepithelial or transendothelial electrical resistance (TEER) reflects the tightness of the intercellular junctions closing the paracellular cleft, resulting in the overall tightness of cell layers of biological barriers. TEER was measured to check the barrier integrity by an EVOM volt-ohmmeter combined with STX-2 electrodes (World Precision Instruments, USA), and was expressed relative to the surface area of the cell layers as $\Omega \times cm^2$. Resistance of cell-free inserts was subtracted from the measured values, and the cells were treated when the cell layers had reached steady TEER values.

To model, the nasal barrier RPMI 2650 epithelial and vascular endothelial cells were co-cultured on inserts (Transwell, polycarbonate membrane, 3 µm pore size, 1.12 cm^2, Corning Costar Co., Cambridge, MA, USA) and placed in 12-well plates for 5 days. Vascular endothelial cells were passaged (1×10^5 cells/cm^2) to the bottom side of tissue culture inserts coated with a low growth factor containing Matrigel (BD Biosciences, East Rutherford, NJ, USA), and nasal epithelial cells were seeded (2×10^5 cells/cm^2) to the upper side of the membranes which were coated with collagen. As a simplified blood-brain barrier model, hCMEC/D3 cells were cultured on collagen-coated Transwell inserts (Transwell, polycarbonate membrane, 3 µm pore size, 1.12 cm^2, Corning Costar Co., Acton, MA, USA) for 5 days in monolayer. The cells were treated when the cell layers had reached steady TEER values.

For the permeability experiments, the inserts were transferred to 12-well plates containing 1.5 mL Ringer-HEPES buffer in the acceptor (lower/basal) compartments. In the donor (upper/apical) compartments, 0.5 mL buffer was pipetted containing insulin alone or encapsulated formulations. To avoid the unstirred water layer effect, the plates were kept on a horizontal shaker (120 rpm) during the assay. The assays lasted for 60 min. Samples from both compartments were collected and the insulin concentration was measured by HPLC. The apparent permeability coefficients (P_{app}) were calculated as described previously [88]. Briefly, the cleared volume was calculated from the concentration difference of the tracer in the acceptor compartment ($\Delta[C]_A$) after 60 min and in donor compartments at 0 h ($[C]_D$), the volume of the acceptor compartment (V_A; 1.5 mL), and the surface area available for permeability (A; 1.12 cm^2) using this equation:

$$P_{app}\left(\frac{cm}{s}\right) = \frac{\Delta[C]_A \times V_A}{A \times [C]_D \times \Delta t} \quad (4)$$

Recovery (mass balance) was calculated according to the equation:

$$\text{Recovery } (\%) = \frac{C_f^D V^D + C_f^A V^A}{C_0^D V^D} \times 100 \quad (5)$$

where C_0^D and C_{0f}^D are the initial and final concentrations of the compound in the donor compartment, respectively; C_0^A is the final concentration in the acceptor compartment; V^D and V^A are the volumes of the solutions in the donor and acceptor compartments [89].

4.5. Statistical Analysis

Data are presented as means ± SD. The values were compared using the analysis of variance (ANOVA) followed by Dunett's test using the GraphPad Prism 5.0 software (GraphPad Software Inc., San Diego, CA, USA). Changes were considered statistically significant at $p < 0.05$.

Supplementary Materials: The following are available online at https://www.mdpi.com/article/10.3390/ijms222413258/s1.

Author Contributions: Conceptualization, G.K. (Gábor Katona), H.A., I.C. and S.V.; methodology, G.K. (Gábor Katona), H.A., M.M., A.S., I.G. and A.B.; software, G.K. (Gábor Katona), H.A. and I.G.; validation, G.K. (Gábor Katona), I.C., Z.K., S.V. and M.A.D.; formal analysis, I.C., Z.K., S.V. and M.A.D.; investigation, G.K. (Gábor Katona), H.A., R.A.; A.B., I.G., M.M., A.S., G.K. (Gábor Kozma) and S.V.; resources, I.C., M.A.D. and Z.K.; data curation, G.K. (Gábor Katona), H.A., I.G., S.V. and A.B.; writing—original draft preparation, H.A. and I.G.; writing—review and editing, G.K. (Gábor Katona), A.B., S.V. and M.A.D.; visualization, G.K. (Gábor Katona) and I.G.; supervision, I.C., A.B., S.V., M.A.D. and Z.K.; project administration, I.C., G.K. (Gábor Kozma), S.V. and M.A.D.; funding acquisition, I.C., M.A.D. and Z.K. All authors have read and agreed to the published version of the manuscript.

Funding: The publication was founded by the Ministry of Human Capacities, Hungary (Grant TKP-2020), and by the National Research, Development and Innovation Office, Hungary (GINOP-2.3.2-15-2016-00060) projects.

Institutional Review Board Statement: Not applicable.

Informed Consent Statement: Not applicable.

Data Availability Statement: Data are contained within the article and Supplementary Material.

Acknowledgments: The authors want to express their acknowledgment to the supporters. This study was supported by the National Research, Development and Innovation Office of Hungary, grant numbers NNE-29617 (M-ERA.NET2 nanoPD). S.V. was supported by the Hungarian Acad-emy of Sciences, Premium Postdoctoral Research Program (PREMIUM-2019-469). M.M. was sup-ported by the research grant (PD 138930) of the National Research, Development and Innovation Office, Hungary, the Gedeon Richter Plc Centenarial Foundation (H-1103 Budapest, Gyömröi str. 19-21., Hungary) and the "National Talent Program" with the financial aid of the Ministry of Human Resources (NTP-NFTÖ-21-B-0228). A.S. was supported by the ÚNKP-21-2-SZTE-364 New National Excellence Program of the Ministry for Innovation and Technology from the source of the National Research, Devel-opment and Innovation. G.K. (Gábor Kozma) gratefully acknowledges the support of the Bolyai János Research Fellowship (BO/00835/19/7).

Conflicts of Interest: The authors declare no conflict of interest. The funders had no role in the design of the study; in the collection, analyses, or interpretation of data; in the writing of the manuscript, or in the decision to publish the results.

References

1. Mayeux, R.; Stern, Y. Epidemiology of Alzheimer disease. *Cold Spring Harb. Perspect. Med.* **2012**, *2*, a006239. [CrossRef] [PubMed]
2. Reitz, C.; Brayne, C.; Mayeux, R. Epidemiology of Alzheimer disease. *Nat. Rev. Neurol.* **2011**, *7*, 137–152. [CrossRef] [PubMed]
3. Sosa-Ortiz, A.L.; Acosta-Castillo, I.; Prince, M.J. Epidemiology of dementias and Alzheimer's disease. *Arch. Med. Res.* **2012**, *43*, 600–608. [CrossRef]
4. Heron, M. Deaths: Leading Causes for 2016. *Natl. Vital. Stat. Rep.* **2018**, *67*, 1–77.
5. Casey, D.A.; Antimisiaris, D.; O'Brien, J. Drugs for Alzheimer's disease: Are they effective? *Pharm. Ther.* **2010**, *35*, 208–211.
6. Rivera, E.J.; Goldin, A.; Fulmer, N.; Tavares, R.; Wands, J.R.; de la Monte, S.M. Insulin and insulin-like growth factor expression and function deteriorate with progression of Alzheimer's disease: Link to brain reductions in acetylcholine. *J. Alzheimer's Dis.* **2005**, *8*, 247–268. [CrossRef] [PubMed]
7. Gasparini, L.; Gouras, G.K.; Wang, R.; Gross, R.S.; Beal, M.F.; Greengard, P.; Xu, H. Stimulation of β-amyloid precursor protein trafficking by insulin reduces intraneuronal β-amyloid and requires mitogen-activated protein kinase signaling. *J. Neurosci.* **2001**, *21*, 2561–2570. [CrossRef]
8. Craft, S.; Watson, G.S. Insulin and neurodegenerative disease: Shared and specific mechanisms. *Lancet Neurol.* **2004**, *3*, 169–178. [CrossRef]

9. Kellar, D.; Craft, S. Brain insulin resistance in Alzheimer's disease and related disorders: Mechanisms and therapeutic approaches. *Lancet. Neurol.* **2020**, *19*, 758–766. [CrossRef]
10. Reger, M.A.; Watson, G.S.; Green, P.S.; Baker, L.D.; Cholerton, B.; Fishel, M.A.; Plymate, S.R.; Cherrier, M.M.; Schellenberg, G.D.; Frey, W.H.; et al. Intranasal Insulin Administration Dose-Dependently Modulates Verbal Memory and Plasma Amyloid-β in Memory-Impaired Older Adults. *J. Alzheimer's Dis.* **2008**, *13*, 323–331. [CrossRef] [PubMed]
11. Craft, S.; Claxton, A.; Baker, L.D.; Hanson, A.J.; Cholerton, B.; Trittschuh, E.H.; Dahl, D.; Caulder, E.; Neth, B.; Montine, T.J.; et al. Effects of Regular and Long-Acting Insulin on Cognition and Alzheimer's Disease Biomarkers: A Pilot Clinical Trial. *J. Alzheimer's Dis.* **2017**, *57*, 1325–1334. [CrossRef] [PubMed]
12. Craft, S.; Baker, L.D.; Montine, T.J.; Minoshima, S.; Watson, G.S.; Claxton, A.; Arbuckle, M.; Callaghan, M.; Tsai, E.; Plymate, S.R.; et al. Intranasal Insulin Therapy for Alzheimer Disease and Amnestic Mild Cognitive Impairment: A Pilot Clinical Trial. *Arch. Neurol.* **2012**, *69*, 29–38. [CrossRef] [PubMed]
13. De la Monte, S.M.; Wands, J.R. Alzheimer's disease is type 3 diabetes—Evidence reviewed. *J. Diabetes Sci. Technol.* **2008**, *2*, 1101–1113. [CrossRef] [PubMed]
14. De la Monte, M.S. Brain insulin resistance and deficiency as therapeutic targets in Alzheimer's disease. *Curr. Alzheimer Res.* **2012**, *9*, 35–66. [CrossRef]
15. Talbot, K.; Wang, H.Y.; Kazi, H.; Han, L.Y.; Bakshi, K.P.; Stucky, A.; Fuino, R.L.; Kawaguchi, K.R.; Samoyedny, A.J.; Wilson, R.S.; et al. Demonstrated brain insulin resistance in Alzheimer's disease patients is associated with IGF-1 resistance, IRS-1 dysregulation, and cognitive decline. *J. Clin. Investig.* **2012**, *122*, 1316–1338. [CrossRef] [PubMed]
16. Bomfim, T.R.; Forny-Germano, L.; Sathler, L.B.; Brito-Moreira, J.; Houzel, J.C.; Decker, H.; Silverman, M.A.; Kazi, H.; Melo, H.M.; McClean, P.L.; et al. An anti-diabetes agent protects the mouse brain from defective insulin signaling caused by Alzheimer's disease–associated Aβ oligomers. *J. Clin. Investig.* **2012**, *122*, 1339–1353. [CrossRef]
17. Claxton, A.; Baker, L.D.; Hanson, A.; Trittschuh, E.H.; Cholerton, B.; Morgan, A.; Callaghan MArbuckle, M.; Behl, C.; Craft, S. Long-acting intranasal insulin detemir improves cognition for adults with mild cognitive impairment or early-stage Alzheimer's disease dementia. *J. Alzheimer's Dis.* **2015**, *44*, 897–906. [CrossRef]
18. Ruegsegger, G.N.; Manjunatha, S.; Summer, P.; Gopala, S.; Zabeilski, P.; Dasari, S.; Vanderboom, P.S.; Lanza, I.R.; Klaus, K.A.; Nair, K.S. Insulin deficiency and intranasal insulin alter brain mitochondrial function: A potential factor for dementia in diabetes. *FASEB J.* **2019**, *33*, 4458–4472. [CrossRef]
19. Bhowmik, A.; Khan, R.; Ghosh, M.K. Blood Brain Barrier: A Challenge for Effectual Therapy of Brain Tumors. *Biomed. Res. Int.* **2015**, *2015*, 320941. [CrossRef] [PubMed]
20. Keller, L.A.; Merkel, O.; Popp, A. Intranasal drug delivery: Opportunities and toxicologic challenges during drug development. *Drug Deliv. Transl. Res.* **2021**, 1–23. [CrossRef]
21. Vyas, T.K.; Shahiwala, A.; Marathe, S.; Misra, A. Intranasal drug delivery for brain targeting. *Curr. Drug Deliv.* **2005**, *2*, 165–175. [CrossRef]
22. Mustafa, G.; Alrohaimi, A.H.; Bhatnagar, A.; Baboota, S.; Ali, J.; Ahuja, A. Brain targeting by intranasal drug delivery (INDD): A combined effect of trans-neural and para-neuronal pathway. *Drug Deliv.* **2016**, *23*, 923–929. [CrossRef] [PubMed]
23. Lochhead, J.J.; Kellohen, K.L.; Ronaldson, P.T.; Davis, T.P. Distribution of insulin in trigeminal nerve and brain after intranasal administration. *Sci. Rep.* **2019**, *9*, 2621. [CrossRef] [PubMed]
24. Nyambura, B.K.; Kellaway, I.W.; Taylor, K.M.G. Insulin nanoparticles: Stability and aerosolization from pressurized metered dose inhalers. *Int. J. Pharm.* **2009**, *375*, 114–122. [CrossRef] [PubMed]
25. Picone, P.; Sabatino, M.A.; Ditta, L.A.; Amato, A.; San Biagio, P.L.; Mulè, F.; Giacomazza, D.; Dispenza, C.; Di Carlo, M. Nose-to-brain delivery of insulin enhanced by a nanogel carrier. *J. Control. Release* **2018**, *270*, 23–36. [CrossRef] [PubMed]
26. Alavian, F.; Shams, N. Oral and Intra-nasal Administration of Nanoparticles in the Cerebral Ischemia Treatment in Animal Experiments: Considering its Advantages and Disadvantages. *Curr. Clin. Pharmacol.* **2020**, *15*, 20–29. [CrossRef]
27. Fatouh, A.M.; Elshafeey, A.H.; Abdelbary, A. Intranasal agomelatine solid lipid nanoparticles to enhance brain delivery: Formulation, optimization and in vivo pharmacokinetics. *Drug Des. Dev. Ther.* **2017**, *11*, 1815–1825. [CrossRef]
28. Akel, H.; Ismail, R.; Katona, G.; Sabir, F.; Ambrus, R.; Csóka, I. A comparison study of lipid and polymeric nanoparticles in the nasal delivery of meloxicam: Formulation, characterization, and in vitro evaluation. *Int. J. Pharm.* **2021**, *604*, 120724. [CrossRef]
29. Sonvico, F.; Clementino, A.; Buttini, F.; Colombo, G.; Pescina, S.; Stanisçuaski Guterres, S.; Raffin Pohlmann, A.; Nicoli1, S. Surface-Modified Nanocarriers for Nose-to-Brain Delivery: From Bioadhesion to Targeting. *Pharmaceutics* **2018**, *10*, 34. [CrossRef]
30. Bruinsmann, F.A.; Pigana, S.; Aguirre, T.; Dadalt Souto, G.; Garrastazu Pereira, G.; Bianchera, A.; Tiozzo Fasiolo, L.; Colombo, G.; Marques, M.; Raffin Pohlmann, A.; et al. Chitosan-coated nanoparticles: Effect of chitosan molecular weight on nasal transmucosal delivery. *Pharmaceutics* **2019**, *11*, 86. [CrossRef] [PubMed]
31. Ravi, P.R.; Aditya, N.; Patil, S.; Cherian, L. Nasal in-situ gels for delivery of rasagiline mesylate: Improvement in bioavailability and brain localization. *Drug. Deliv.* **2015**, *22*, 903–910. [CrossRef] [PubMed]
32. Aderibigbe, B.A.; Naki, T. Chitosan-based nanocarriers for nose to brain delivery. *Appl. Sci.* **2019**, *9*, 2219. [CrossRef]
33. Gänger, S.; Schindowski, K. Tailoring Formulations for Intranasal Nose-to-Brain Delivery: A Review on Architecture, Physico-Chemical Characteristics and Mucociliary Clearance of the Nasal Olfactory Mucosa. *Pharmaceutics* **2018**, *10*, 116. [CrossRef] [PubMed]

34. Masserini, M. Nanoparticles for brain drug delivery. *ISRN Biochem.* **2013**, *2013*. [CrossRef]
35. Pires, P.C.; Santos, A.O. Nanosystems in nose-to-brain drug delivery: A review of non-clinical brain targeting studies. *J. Control. Release* **2018**, *270*, 89–100. [CrossRef] [PubMed]
36. Danaei, M.; Dehghankhold, M.; Ataei, S.; Hasanzadeh Davarani, F.; Javanmard, R.; Dokhani, A.; Khorasani, S.; Mozafari, M.R. Impact of particle size and polydispersity index on the clinical applications of lipidic nanocarrier systems. *Pharmaceutics* **2018**, *10*, 57. [CrossRef]
37. Zhou, Y.; Raphael, R.M. Solution pH alters mechanical and electrical properties of phosphatidylcholine membranes: Relation between interfacial electrostatics, intramembrane potential, and bending elasticity. *Biophys. J.* **2007**, *92*, 2451–2462. [CrossRef] [PubMed]
38. Vieira, A.C.; Chaves, L.L.; Pinheiro, S.; Pinto, S.; Pinheiro, M.; Lima, S.C.; Ferreira, D.; Sarmento, B.; Reis, S. Mucoadhesive chitosan-coated solid lipid nanoparticles for better management of tuberculosis. *Int. J. Pharm.* **2018**, *536*, 478–485. [CrossRef] [PubMed]
39. Barichello, J.M.; Morishita, M.; Takayama, K.; Nagai, T. Encapsulation of hydrophilic and lipophilic drugs in PLGA nanoparticles by the nanoprecipitation method. *Drug. Dev. Ind. Pharm.* **1999**, *25*, 471–476. [CrossRef]
40. Dyawanapelly, S.; Koli, U.; Dharamdasani, V.; Jain, R.; Dandekar, P. Improved mucoadhesion and cell uptake of chitosan and chitosan oligosaccharide surface-modified polymer nanoparticles for mucosal delivery of proteins. *Drug Deliv. Transl. Res.* **2016**, *6*, 365–379. [CrossRef]
41. Piazzini, V.; Landucci, E.; D'Ambrosio, M.; Tiozzo Fasiolo, L.; Cinci, L.; Colombo, G.; Pellegrini-Giampietro, D.E.; Bilia, A.R.; Luceri, C.; Bergonzi, M.C. Chitosan coated human serum albumin nanoparticles: A promising strategy for nose-to-brain drug delivery. *Int. J. Biol. Macromol.* **2019**, *129*, 267–280. [CrossRef]
42. Elnaggar, Y.S.R.; Etman, S.M.; Abdelmonsif, D.A.; Abdallah, O.Y. Intranasal Piperine-Loaded Chitosan Nanoparticles as Brain-Targeted Therapy in Alzheimer's Disease: Optimization, Biological Efficacy, and Potential Toxicity. *J. Pharm. Sci.* **2015**, *104*, 3544–3556. [CrossRef]
43. Li, Y.; Kröger, M.; Liu, W.K. Shape effect in cellular uptake of PEGylated nanoparticles: Comparison between sphere, rod, cube and disk. *Nanoscale* **2015**, *7*, 16631–16646. [CrossRef]
44. Mangialardo, S.; Piccirilli, F.; Perucchi, A.; Dore, P.; Postorino, P. Raman analysis of insulin denaturation induced by high-pressure and thermal treatments. *J. Raman Spectrosc.* **2012**, *43*, 692–700. [CrossRef]
45. Grenha, A.; Grainger, C.I.; Dailey, L.A.; Seijo, B.; Martin, G.P.; Remuñán-López, C.; Forbes, B. Chitosan nanoparticles are compatible with respiratory epithelial cells in vitro. *Eur. J. Pharm. Sci.* **2007**, *31*, 73–84. [CrossRef]
46. Nordgård, C.T.; Draget, K.I. Co association of mucus modulating agents and nanoparticles for mucosal drug delivery. *Adv. Drug Deliv. Rev.* **2018**, *124*, 175–183. [CrossRef] [PubMed]
47. Luo, Y.; Teng, Z.; Li, Y.; Wang, Q. Solid lipid nanoparticles for oral drug delivery: Chitosan coating improves stability, controlled delivery, mucoadhesion and cellular uptake. *Carbohydr. Polym.* **2015**, *122*, 221–229. [CrossRef] [PubMed]
48. Ismail, R.; Bocsik, A.; Katona, G.; Grof, I.; Deli, M.A.; Csoka, I. Encapsulation in Polymeric Nanoparticles Enhances the Enzymatic Stability and the Permeability of the GLP-1 Analog, Liraglutide, Across a Culture Model of Intestinal Permeability. *Pharmaceutics* **2019**, *11*, 599. [CrossRef] [PubMed]
49. Esim, O.; Savaser, A.; Ozkan, C.K.; Oztuna, A.; Goksel, B.A.; Ozler, M.; Tas, C.; Oskan, Y. Nose to brain delivery of eletriptan hydrobromide nanoparticles: Preparation, in vitro/in vivo evaluation and effect on trigeminal activation. *J. Drug. Deliv. Sci. Technol.* **2020**, *59*, 101919. [CrossRef]
50. Trotta, V.; Pavan, B.; Ferraro, L.; Beggiato, S.; Traini, D.; Des Reis, L.G.; Scalia, S.; Dalpiaz, A. Brain targeting of resveratrol by nasal administration of chitosan-coated lipid microparticles. *Eur. J. Pharm. Biopharm.* **2018**, *127*, 250–259. [CrossRef] [PubMed]
51. Brange, J. *Galenics of Insulin: The Physico-Chemical and Pharmaceutical Aspects of Insulin and Insulin Preparations*; Springer Science and Business Media: Berlin, Germany, 2012; pp. 1–30. [CrossRef]
52. Liu, J.; Zhang, S.M.; Chen, P.; Cheng, L.; Zhou, W.; Tang, W.X.; Chen, Z.W.; Ke, C.M. Controlled release of insulin from PLGA nanoparticles embedded within PVA hydrogels. *J. Mater. Sci. Mater. Med.* **2007**, *18*, 2205–2210. [CrossRef]
53. Patel, S.; Chavhan, S.; Soni, H.; Babbar, A.; Mathur, R.; Mishra, A.; Sawant, K. Brain targeting of risperidone-loaded solid lipid nanoparticles by intranasal route. *J. Drug Target.* **2011**, *19*, 468–474. [CrossRef]
54. Son, G.H.; Lee, B.J.; Cho, C.W. Mechanisms of drug release from advanced drug formulations such as polymeric-based drug-delivery systems and lipid nanoparticles. *J. Pharm. Investig.* **2017**, *47*, 287–296. [CrossRef]
55. Kravanja, G.; Primožič, M.; Knez, Ž.; Leitgeb, M. Chitosan-based (Nano) materials for novel biomedical applications. *Molecules* **2019**, *24*, 1960. [CrossRef] [PubMed]
56. Rhea, E.M.; Banks, W.A. A historical perspective on the interactions of insulin at the blood-brain barrier. *J. Neuroendocrinol.* **2021**, *33*, e12929. [CrossRef] [PubMed]
57. Ohtsuki, S.; Ikeda, C.; Uchida, Y.; Sakamoto, Y.; Miller, F.; Glacial, F.; Decleves, X.; Scherrmann, J.M.; Couraud, P.O.; Kubo, Y.; et al. Quantitative targeted absolute proteomic analysis of transporters, receptors and junction proteins for validation of human cerebral microvascular endothelial cell line hCMEC/D3 as a human blood–brain barrier model. *Mol. Pharm.* **2013**, *10*, 289–296. [CrossRef]
58. Jochum, W.; Hanggi, D.; Bruder, E.; Jeck, T.; Novotny, H.; Probst, A.; Tolnay, M. Inflammatory myofibroblastic tumour of the sella turcica. *Neuropathol. Appl. Neurobiol.* **2004**, *30*, 692–695. [CrossRef]

59. Musiek, E.S.; Holtzman, D.M. Three dimensions of the amyloid hypothesis: Time, space and 'wingmen'. *Nat. Neurosci.* **2015**, *18*, 800–806. [CrossRef] [PubMed]
60. Guzman-Martinez, L.; Maccioni, R.B.; Andrade, V.; Navarrete, L.P.; Pastor, M.G.; Ramos-Escobar, N. Neuroinflammation as a common feature of neurodegenerative disorders. *Front. Pharmacol.* **2019**, *10*, 1008. [CrossRef] [PubMed]
61. Orr, M.E.; Sullivan, A.C.; Frost, B. A brief overview of tauopathy: Causes, consequences, and therapeutic strategies. *Trends Pharmacol. Sci.* **2017**, *38*, 637–648. [CrossRef]
62. Fernández-Urrusuno, R.; Calvo, P.; Remuñán-López, C.; Vila-Jato, J.L.; Alonso, M.J. Enhancement of nasal absorption of insulin using chitosan nanoparticles. *Pharm. Res.* **1999**, *16*, 1576–1581. [CrossRef] [PubMed]
63. Thorne, R.G.; Pronk, G.J.; Padmanabhan, V.; Frey Ii, W.H. Delivery of insulin-like growth factor-I to the rat brain and spinal cord along olfactory and trigeminal pathways following intranasal administration. *Neuroscience* **2004**, *127*, 481–496. [CrossRef] [PubMed]
64. Barbosa, F.C.; Silva, M.C.D.; Silva, H.N.D.; Albuquerque, D.; Gomes, A.A.R.; Silva, S.M.D.L.; Fook, M.V.L. Progress in the Development of Chitosan Based Insulin Delivery Systems: A Systematic Literature Review. *Polymers* **2020**, *12*, 2499. [CrossRef] [PubMed]
65. Zhi, K.; Raji, B.; Nookala, A.R.; Khan, M.M.; Nguyen, X.H.; Sakshi, S.; Pourmotabbed, T.; Yallapu, M.M.; Kochat, H.; Tadrous, E.; et al. PLGA Nanoparticle-Based Formulations to Cross the Blood–Brain Barrier for Drug Delivery: From R&D to cGMP. *Pharmaceutics* **2021**, *13*, 500. [PubMed]
66. Walter, F.R.; Santa-Maria, A.R.; Mészáros, M.; Veszelka, S.; Dér, A.; Deli, M.A. Surface charge, glycocalyx, and blood-brain barrier function. *Tissue Barriers* **2021**, *9*, 1904773. [CrossRef] [PubMed]
67. Dyer, A.M.; Hinchcliffe, M.; Watts, P.; Castile, J.; Jabbal-Gill, I.; Nankervis, R.; Smith, A.; Illum, L. Nasal delivery of insulin using novel chitosan based formulations: A comparative study in two animal models between simple chitosan formulations and chitosan nanoparticles. *Pharm. Res.* **2002**, *19*, 998–1008. [CrossRef]
68. Xu, Y.; Zheng, Y.; Wu, L.; Zhu, X.; Zhang, Z.; Huang, Y. Novel solid lipid nanoparticle with endosomal escape function for oral delivery of insulin. *ACS Appl. Mater. Interfaces* **2018**, *10*, 9315–9324. [CrossRef]
69. Battaglia, L.; Trotta, M.; Gallarate, M.; Carlotti, M.E.; Zara, G.P.; Bargoni, A. Solid lipid nanoparticles formed by solvent-in-water emulsion-diffusion technique: Development and influence on insulin stability. *J. Microencapsul.* **2007**, *24*, 672–684. [CrossRef]
70. Yan, L.; Wang, H.; Jiang, Y.; Liu, J.; Wang, Z.; Yang, Y.; Huang, S.; Huang, Y. Cell-penetrating peptide-modified PLGA nanoparticles for enhanced nose-to-brain macromolecular delivery. *Macromol. Res.* **2013**, *21*, 435–441. [CrossRef]
71. Sarmento, B.; Martins, S.; Ferreira, D.; Souto, E.B. Oral insulin delivery by means of solid lipid nanoparticles. *Int. J. Nanomed.* **2007**, *2*, 743.
72. Haggag, Y.; Abdel-Wahab, Y.; Ojo, O.; Osman, M.; El-Gizawy, S.; El-Tanani, M.; Faheem, A.; McCarron, P. Preparation and in vivo evaluation of insulin-loaded biodegradable nanoparticles prepared from diblock copolymers of PLGA and PEG. *Int. J. Pharm.* **2016**, *499*, 236–246. [CrossRef]
73. Hecq, J.; Siepmann, F.; Siepmann, J.; Amighi, K.; Goole, J. Development and evaluation of chitosan and chitosan derivative nanoparticles containing insulin for oral administration. *Drug Dev. Ind. Pharm.* **2015**, *41*, 2037–2044. [CrossRef] [PubMed]
74. Devkar, T.B.; Tekade, A.R.; Khandelwal, K.R. Surface engineered nanostructured lipid carriers for efficient nose to brain delivery of ondansetron HCl using Delonix regia gum as a natural mucoadhesive polymer. *Colloids Surf. B Biointerfaces* **2014**, *122*, 143–150. [CrossRef] [PubMed]
75. Rençber, S.; Karavana, S.Y.; Yılmaz, F.F.; Eraç, B.; Nenni, M.; Özbal, S.; Pekçetin, C.; Gurer-Orhan, H.; Hoşgör-Limoncu, M.; Güneri, P.; et al. Development, characterization, and in vivo assessment of mucoadhesive nanoparticles containing fluconazole for the local treatment of oral candidiasis. *Int. J. Nanomed.* **2016**, *11*, 2641–2653. [CrossRef]
76. Bartos, C.; Ambrus, R.; Kovács, A.; Gáspár, R.; Sztojkov-Ivanov, A.; Márki, Á.; Janáky, T.; Tömösi, F.; Kecskeméti, G.; Szabó-Révész, P. Investigation of absorption routes of meloxicam and its salt form from intranasal delivery systems. *Molecules* **2018**, *23*, 784. [CrossRef] [PubMed]
77. Gieszinger, P.; Kiss, T.; Szabó-Révész, P.; Ambrus, R. The Development of an In Vitro Horizontal Diffusion Cell to Monitor Nasal Powder Penetration Inline. *Pharmaceutics* **2021**, *13*, 809. [CrossRef] [PubMed]
78. Yasir, M.; Sara, U.V.S.; Chauhan, I.; Gaur, P.K.; Singh, A.P.; Puri, D. Solid lipid nanoparticles for nose to brain delivery of donepezil: Formulation, optimization by Box–Behnken design, in vitro and in vivo evaluation. *Artif. Cells Nanomed. Biotechnol.* **2018**, *46*, 1838–1851. [CrossRef]
79. Joshi, A.S.; Patel, H.S.; Belgamwar, V.S.; Agrawal, A.; Tekade, A.R. Solid lipid nanoparticles of ondansetron HCl for intranasal delivery: Development, optimization and evaluation. *J. Mater. Sci. Mater. Med.* **2012**, *23*, 2163–2175. [CrossRef]
80. Dalpiaz, A.; Ferraro, L.; Perrone, D.; Leo, E.; Iannuccelli, V.; Pavan, B.; Paganetto, G.; Beggiato, S.; Scalia, S. Brain uptake of a Zidovudine prodrug after nasal administration of solid lipid microparticles. *Mol. Pharm.* **2014**, *11*, 1550–1561. [CrossRef]
81. Kürti, L.; Veszelka, S.; Bocsik, A.; Ozsvári, B.; Puskás, L.G.; Kittel, A.; Szabó-Révész, P.; Deli, M.A. Retinoic acid and hydrocortisone strengthen the barrier function of human RPMI 2650 cells, a model for nasal epithelial permeability. *Cytotechnology* **2013**, *65*, 395–406. [CrossRef] [PubMed]
82. Gróf, I.; Bocsik, A.; Harazin, A.; Santa-Maria, A.R.; Vizsnyiczai, G.; Barna, L.; Kiss, L.; Fűr, G.; Rakonczay, Z.; Ambrus, R.; et al. The Effect of Sodium Bicarbonate, a Beneficial Adjuvant Molecule in Cystic Fibrosis, on Bronchial Epithelial Cells Expressing a Wild-Type or Mutant CFTR Channel. *Int. J. Mol. Sci.* **2020**, *21*, 519. [CrossRef]

83. Katona, G.; Sipos, B.; Budai-Szűcs, M.; Balogh, G.T.; Veszelka, S.; Gróf, I.; Deli, M.A.; Volk, B.; Szabó-Révész, P.; Csóka, I. Development of In Situ Gelling Meloxicam-Human Serum Albumin Nanoparticle Formulation for Nose-to-Brain Application. *Pharmaceutics* **2021**, *13*, 646. [CrossRef] [PubMed]
84. Weksler, B.; Subileau, E.; Perriere, N.; Charneau, P.; Holloway, K.; Leveque, M.; Tricoire-Leignel, H.; Nicotra, A.; Bourdoulous, S.; Turowski, P.; et al. Blood-brain barrier-specific properties of a human adult brain endothelial cell line. *FASEB J.* **2005**, *19*, 1872–1874. [CrossRef]
85. Veszelka, S.; Tóth, A.; Walter, F.R.; Tóth, A.E.; Gróf, I.; Mészáros, M.; Bocsik, A.; Hellinger, É.; Vastag, M.; Rákhely, G.; et al. Comparison of a Rat Primary Cell-Based Blood-Brain Barrier Model with Epithelial and Brain Endothelial Cell Lines: Gene Expression and Drug Transport. *Front Mol. Neurosci.* **2018**, *11*, 166. [CrossRef] [PubMed]
86. Kürti, L.; Veszelka, S.; Bocsik, A.; Dung, N.T.K.; Ózsvári, B.; Puskás, L.G.; Kittel, A.; Szabó-Révész, P.; Deli, M.A. The effect of sucrose esters on a culture model of the nasal barrier. *Toxicol. In Vitro* **2012**, *26*, 445–454. [CrossRef] [PubMed]
87. Bocsik, A.; Walter, F.R.; Gyebrovszki, A.; Fülöp, L.; Blasig, I.; Dabrowski, S.; Ötvös, F.; Tóth, A.; Rákhely, G.; Veszelka, S.; et al. Reversible opening of intercellular junctions of intestinal epithelial and brain endothelial cells with tight junction modulator peptides. *J. Pharm. Sci.* **2016**, *105*, 754–765. [CrossRef]
88. Bocsik, A.; Gróf, I.; Kiss, L.; Ötvös, F.; Zsíros, O.; Daruka, L.; Fülöp, L.; Vastag, M.; Kittel, A.; Norbert, I.; et al. Dual action of the PN159/KLAL/MAP peptide: Increase of drug penetration across Caco-2 intestinal barrier model by modulation of tight junctions and plasma membrane permeability. *Pharmaceutics* **2019**, *11*, 73. [CrossRef] [PubMed]
89. Hellinger, É.; Veszelka, S.; Tóth, A.E.; Walter, F.; Kittel, Á.; Bakk, M.L.; Tihanyi, K.; Háda, V.; Nakagawa, S.; Dinh Ha Duy, T.; et al. Comparison of brain capillary endothelial cell-based and epithelial (MDCK-MDR1, Caco-2, and VB-Caco-2) cell-based surrogate blood–brain barrier penetration models. *Eur. J. Pharm. Biopharm.* **2012**, *82*, 340–351. [CrossRef] [PubMed]